UNIVERSITY OF SOUTHAMPTON

Electroweak Corrections to Hadronic Processes at TeV Energy Colliders

by

Martin Richard Nolten

A thesis submitted for the degree of

Doctor of Philosophy

School of Physics and Astronomy

February 2006

This thesis is dedicated to my parents

UNIVERSITY OF SOUTHAMPTON

ABSTRACT

FACULTY OF SCIENCE

SCHOOL OF PHYSICS AND ASTRONOMY

Doctor of Philosophy

Electroweak Corrections to Hadronic Processes at TeV Energy Colliders

Martin Richard Nolten

We study the next to leading order (NLO) weak corrections (order $\alpha_S^2\alpha_W$) to a number of hadronic processes. We discover the weak correction to $b\bar{b}$ production at Tevatron to be small (fractions of one percent) at inclusive level but potentially of some significance in the forward backward asymmetry. The correction to the total $b\bar{b}$ production cross-section at LHC is also found to be small (-2%) but possibly large enough to be significant following NNLO QCD calculations. We find the total cross-sections for two jet production at both Tevatron and LHC to be significantly larger - up to -3% at Tevatron and up to -30% at LHC. Calculations of polarised observables are also performed for both RHIC and a hypothetical polarised LHC. We find weak corrections to these observables to be typically tens or even hundreds of percent. A calculation of the $t\bar{t}$ production cross-section is also carried out. The corrections to a number of differential cross-sections for $gg \to t\bar{t}$ at LHC are found to be potentially significant - in the region of 5 to 10%. For $q\bar{q} \to t\bar{t}$ we find corrections of a similar magnitude.

Contents

List of Figures

List of Tables

Preface

The work presented in this thesis was carried out in collaboration with Professor D.A.Ross and Dr. S.Moretti of the University of Southampton. Work on the first calculation was also with E.Maina of the University of Turin.

The papers where the original work in this thesis was first presented are listed below:

- *One Loop Corrections To The b anti-b Cross-section At TeV Energy Colliders*
  E.Maina, S.Moretti, M.R.Nolten, D.A.Ross, Phys. Lett. B. **570**(2003) 205-214 [arXiv:hep-ph/0307091]

- *Weak Corrections And High E_T Jets At Tevatron*
  S.Moretti, M.R.Nolten, D.A.Ross, [arXiv:hep-ph/0503152]

- *Weak Effects In Proton Beam Asymmetries At Polarised RHIC And Beyond*
  S.Moretti, M.R.Nolten, D.A.Ross, [arXiv:hep-ph/0509254]

- *Weak Corrections To Gluon-induced top-antitop Hadro-production*
  S.Moretti, M.R.Nolten, D.A.Ross, [no hep-ph number at time of writing]

No claim of originality is made for chapters one to three which were compiled from a number of sources.

Acknowledgements

Firstly I would like to thank my supervisor Doug and collaborator Stefano for the advice, assistance and seemingly limitless patience that made this project possible. I'd also like to thank Ezio for his assistance in the early stages of the project and for an enjoyable and productive few weeks in Turin.

I've had a fantastic few years in Southampton and that is at least partly down to everyone in the group but in particular I'd like to thank the guys I've shared offices with over the last couple of years - Iain, Oli, the three Jons, Martin and Phil - it's been a lot of fun and I'll be sad to leave.

Finally, and most importantly, I would like to thank my family for their constant support and encouragement without which this work would have been impossible.

Chapter 1

Introduction

1.1 General Motivation

In this thesis we present a number of calculations of NLO ($\alpha_S^2\alpha_W$) weak corrections to hadronic processes. These calculations will be performed for the two TeV energy colliders, LHC (Large Hadron Collider) and Tevatron, as we expect to see large weak effects at high energy machines. We will also present some calculations for RHIC (Relativistic Heavy Ion Collider) where, as RHIC is a polarised machine, it is possible to define observables where weak corrections will be qualitatively distinct from QCD due to their parity violating nature.

Three calculations will be studied in detail - the $b\bar{b}$ production rate (assuming massless quarks), the full proton - (anti)proton to two jet rate (also assuming massless quarks) and the $t\bar{t}$ production rate (where the top mass is non zero.).

All of these calculations will be calculated for $gg \rightarrow$ final state and $qq \rightarrow$ final state (and, where appropriate, $qg \rightarrow$ final state). The processes with gluons in the initial state are IR finite at $\alpha_S^2\alpha_W$ order but the four quark processes will always contain infrared (IR) (soft and collinear) divergences. These will have to be cancelled using a

suitable subtraction method if we are to obtain matrix elements which are integrable via Monte Carlo methods.

1.1.1 Why Are Standard Model Calculations Important?

It is important and interesting to study weak corrections in a standard model calculation for a number of reasons. Firstly, via the calculation and measurement of asymmetries, we may examine weak effects even if the inclusive cross section is small. These asymmetries allow us to study qualitative effects that arise from weak physics and, in the case of entirely parity violating asymmetries, this means we can eliminate any errors associated with QCD (as pure QCD graphs will not contribute to these observables). Another reason we are interested in weak effects is that weak corrections are typically more significant than one would expect from a simple comparison of couplings with, for example, QCD. This is a consequence of potentially large non cancelling single and double logarithms which become significant at large centre of mass energies. The importance of weak corrections is discussed at length in Chapter 2.

It is also worth mentioning here why we are interested in standard model calculations at all. Calculations of this nature are important as part of the ongoing testing of the standard model. There are a number of discrepancies between current standard model predictions and experimental data that would potentially benefit from calculation of weak corrections.

Firstly the b jet excess detected at Tevatron. The transverse momentum (p_T) distribution of b-jet production at Tevatron shows a distinct disagreement with theoretical predictions [1] (currently calculated to NLO in QCD [2]). It is expected that comparison between b-jet production and predictions will continue at LHC at much higher accuracy [3]. Any improvement to the theoretical predictions here would clearly be of

some potential use. A calculation of the NLO weak contribution to $b\bar{b}$ production is presented in Chapter 4.

Another signal that should be considered is the high p_T jet excess discovered by the CDF collaboration at Run 1 of Tevatron [4]. Although it appears that this discrepancy may by solvable via a modification of the gluon Parton Distribution Functions (PDF's) [5] further theoretical examination of this region is likely to be of some interest.

Finally, a reliable standard model background is required for searches for physics beyond the standard model. A good example, and one where weak corrections are of particular importance, would be in searches for the exotic W and Z bosons described in (for example) [6]. In an attempt to detect physics of this nature it would be sensible to look for discrepancies between measurement and theoretical predictions of parity violating observables. As mentioned above this would eliminate any errors associated with QCD and these observables should be particularly sensitive to the existence of additional parity violating interactions.

1.2 The Colliders We Will Be Studying

The calculations presented here will be performed (where appropriate) for three different colliders - Tevatron, LHC and RHIC. Following is a brief discussion of the different machines properties:

Tevatron at Fermilab is the worlds highest energy currently operating collider. It is a proton-anti-proton collider with a centre of mass energy of around 2000GeV. Whilst this energy is above the threshold where the logarithmic corrections (see section(2.4)) to weak processes becomes large we need to remember that partonic energies will be scaled by the Bjorken x and as such will typically be in the region of the W mass - not high enough for us to see large weak logarithms.

LHC at CERN will become the worlds most powerful collider when it starts running within the next few years. It will be a proton-proton collider with a centre of mass energy of about 14TeV. This will result in partonic energies far above the W mass leading to potentially high significance for weak corrections.

RHIC at Brookhaven National Laboratories was designed as a heavy ion collider but has been used as a polarised proton proton collider. RHIC is a comparatively low energy collider when compared with LHC or Tevatron (at about 600GeV), however the fact that it can run with polarised beams means that it is an interesting machine from the point of view of weak physics. The asymmetries mentioned above (and described in section(2.2.1)) are defined for the case of polarised beams and as such, out of the three colliders considered, may only be measured at RHIC.

1.3 Outline Of Chapters

Below is a brief description of the contents of each chapter following this introduction:

- Chapter 2 - Why Weak Corrections Are Important:

  Presented here is a description of why we expect weak corrections to be important in what we would expect to be QCD dominated interactions. Discussed within are the parity sensitive observables that can be defined at a polarised collider and the forwards backwards asymmetry to which we expect to have a detectable weak contribution. We also consider the large non cancelling logarithms that appear in weak cross sections and which enhance them at high centre of mass energies.

- Chapter 3 - Methods For The Cancellation Of Soft And Collinear Divergences:

  Described in this chapter is the subtraction method of Catani & Seymour [7] that

we use to cancel IR divergences. This method is the one used in the calculations presented in Chapter 4 and Chapter 5 - those calculations where we make the assumption of massless external quarks.

- Chapter 4 - $b\bar{b}$ Production:

  The first calculation presented is an evaluation of the NLO weak correction to $b\bar{b}$ production at Tevatron and LHC (this calculation is not performed for RHIC as at that machine there is no capability to efficiently identify b jets). The total cross section will be calculated along with the forwards backwards asymmetry at Tevatron.

- Chapter 5 - Proton Proton To Two Jets:

  Following on from the $b\bar{b}$ production we extend the calculation to include all possible two jet final states with massless external particles. We will calculate the total cross section for both LHC and Tevatron and also the parity sensitive polarised observables for RHIC. Also presented will be an evaluation of the polarised observables at a hypothetical LHC with polarised proton beams.

- Chapter 6 - $t\bar{t}$ Production:

  Finally we will evaluate the NLO weak correction to $t\bar{t}$ production. This will be a very similar calculation to the case of $b\bar{b}$ production (in fact, topologically it is identical) but the necessary addition of the external top mass will complicate matters slightly. Here we use the subtraction method of Stefan Dittmaier [8] to render our results finite.

- Chapter 7 - Conclusions:

  Here we will briefly reiterate the implications of the results obtained during the course of this research and indicate where further work is required.

Chapter 2

Why Weak Corrections Are Important.

At the order where the calculations will be performed ($\alpha_s^2\alpha_W$) one would usually expect QCD effects to dominate by a factor of α_s/α_W however there are a number of reasons why weak corrections may be of some interest to calculate. There are qualitative differences between weak and QCD effects as a consequence of the parity violating nature of weak vertices which may be measurable at some colliders. There are also large non-cancelling logarithms that exist in the electroweak (EW) corrections that enhance them with respect to QCD.

2.1 Comparison To Two Loop QCD

Work is currently being done in an attempt to evaluate QCD corrections at two loop (NNLO) order [9]. A simple comparison of coupling constants,

$$\alpha_s^2\alpha_W > \alpha_s^4 \tag{2.1}$$

shows us that we can expect NLO weak effects to be at least of a comparable size to NNLO QCD effects. Clearly, if we are interested in improving theoretical predictions to the level of two loop QCD we will also need the one loop weak effects.

(It is worth mentioning that the simple comparison of couplings does not tell the whole story. The very large number of interferences that contribute to the two loop QCD will enhance the magnitude of that contribution compared to the NLO weak beyond what we may expect from comparing the couplings alone.[9])

2.2 Parity Violation

Another important justification of the value of calculating Weak corrections comes from the qualitative nature of the results generated by the parity violating nature of the weak vertices.

The Feynman rule for the Z-vertex is:

$$\frac{-ig}{\cos\theta_W}\gamma^\mu\left(\frac{1+\gamma^5}{2}c_R^f+\frac{1-\gamma^5}{2}c_L^f\right), \tag{2.2}$$

where f is the fermion flavour (although in most of what follows the Z vertex will be expressed in terms of vector and axial couplings rather than left and right handed couplings).

Clearly, assuming that $c_R \neq c_L$, we would obtain a different result from a left handed incoming state than a right handed incoming state - this is parity violation. We also generate parity violation from W boson interactions - a W boson does not couple to right handed particles at all.

(Note that the QCD vertex:

$$-ig_s\gamma^\mu t^a \tag{2.3}$$

does not have an axial part and that therefore purely QCD interferences will not contribute to any parity violating observables ie: the interferences will be insensitive to the incoming/outgoing helicities).

2.2.1 Polarised Observables

If we are performing calculations for a machine which has two polarised beams (for example RHIC) then one of the observables that can be examined is the *double helicity hadron asymmetry* [10] :-

$$A_{LL} = \frac{d\sigma_{++} - d\sigma_{+-} - d\sigma_{-+} + d\sigma_{--}}{d\sigma_{++} + d\sigma_{+-} + d\sigma_{-+} + d\sigma_{--}} \tag{2.4}$$

(where +/− refers to the helicity of the incoming particle(s))

If we have no parity violation (ie: $d\sigma_{++} = d\sigma_{--}$ and $d\sigma_{+-} = d\sigma_{-+}$) then this reduces to:-

$$A_{LL} = \frac{d\sigma_{++} - d\sigma_{+-}}{d\sigma_{++} + d\sigma_{+-}} \tag{2.5}$$

In general this is non-zero so, whilst A_{LL} will be sensitive to weak effects, we would expect it to be dominated by QCD effects in hadronic processes.

There are however a number of variables that can be defined which are *only* sensitive to parity violating effects. For example, again at a machine with both beams polarised, we have the parity violating asymmetry [10]:-

$$A_{LL}^{PV} = \frac{d\sigma_{++} - d\sigma_{--}}{2d\sigma_{TOT}} \tag{2.6}$$

(where $d\sigma_{TOT}$ is the cross-section summed over all helicity combinations)

or, for a single polarised beam we have the *single helicity hadron asymmetry* [10]:

$$A_L = \frac{d\sigma_{+} - d\sigma_{-}}{2d\sigma_{TOT}} \tag{2.7}$$

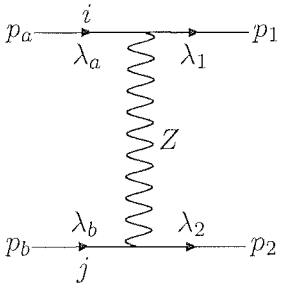

Figure 2.1: Tree level Z exchange in the t-channel. i and j are the incoming quark flavours and λ and p are the helicities and momenta of the external particles

Clearly, if the interaction is insensitive to the helicity of the external particles (as is the case for purely QCD processes), $d\sigma_{+(+)}$ will equal $d\sigma_{-(-)}$, meaning that both A_{LL}^{PV} and A_L will be zero.

These observables are only measurable at machines with polarised beam(s) and currently the only high energy polarised hadron collider is RHIC at Brookhaven. In principle LHC could be modified to incorporate polarised proton beams during a round of upgrades but this appears to be unlikely [11] [12]. Despite this A_{LL}, A_L and A_{LL}^{PV} are calculated for LHC to show the size of effect that would be measured at that machine. However, if we consider a top pair production process, we can study the polarisation structure of the *final* state quarks. In this way we can measure a variation on the polarised observables. This process is explained in more detail in chapter(6).

2.2.2 A Simple Example Of Parity Violation

A tree level diagram that violates parity is shown in fig(2.1)

Using the Feynman rule for the Z-vertex given in eq(2.2) the expression for this am-

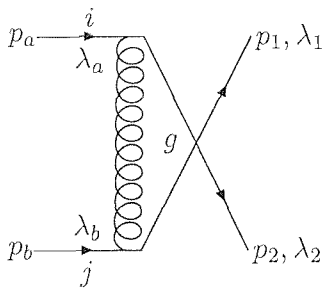

Figure 2.2: Tree level gluon exchange in the u-channel.

plitude is (dropping coupling constants):

$$\begin{aligned}
&\bar{u}(p_1)\gamma^\mu \left[\left(\frac{1+\gamma^5}{2}\right) c_R^i + \left(\frac{1-\gamma^5}{2}\right) c_L^i\right] \left(\frac{1+\lambda_a\gamma^5}{2}\right) u(p_a) \\
&\bar{u}(p_2)\gamma_\mu \left[\left(\frac{1+\gamma^5}{2}\right) c_R^j + \left(\frac{1-\gamma^5}{2}\right) c_L^j\right] \left(\frac{1+\lambda_b\gamma^5}{2}\right) u(p_b) \\
&\frac{1}{t-m_z^2}\delta_{\lambda_1\lambda_a}\delta_{\lambda_2\lambda_b}
\end{aligned} \tag{2.8}$$

So, if the helicity of incoming particle a is positive(negative), we pick up the term proportional to $c_R^i(c_L^i)$ and for particle b we pick up the term proportional to $c_R^j(c_L^j)$. This means that the $++$, $--$, $+-$ and $-+$ incoming helicity components will in general all be different.

The square of this diagram is an allowed interference but, since that would include two Z exchanges, it would be *very* small (proportional to α_W^2) compared to QCD corrections. With this in mind we will interfere the diagram shown in fig(2.1) with the QCD interference shown in fig(2.2). (The interference between the t-channel Z exchange and t-channel gluon exchange has a vanishing colour factor)

Note that the expression for the u-channel gluon exchange will include the helicity conserving δ-functions $\delta_{\lambda_1\lambda_b}\delta_{\lambda_2\lambda_a}$. If these are combined with the delta functions from eq(2.8) then we discover that only the $++$ and $--$ incoming helicity states will be non zero. Also, because we are interfering a t-channel diagram with a u-channel and have no flavour changing interactions (W-vertices for example) only the states with the same

incoming flavours will contribute.

If we evaluate this interference in the usual way then we obtain the two results:

$$d\sigma^{ii}_{++} = -8\mathrm{Tr}(t^a t^a)\frac{g^2 g_s^2}{\cos^2\theta_w}\left(\frac{s^2}{u(t-m_z^2)} + \frac{s^2}{t(u-m_z^2)}\right) c_R^{i\,2} \tag{2.9}$$

for incoming positive helicities and:

$$d\sigma^{ii}_{--} = -8\mathrm{Tr}(t^a t^a)\frac{g^2 g_s^2}{\cos^2\theta_w}\left(\frac{s^2}{u(t-m_z^2)} + \frac{s^2}{t(u-m_z^2)}\right) c_L^{i\,2} \tag{2.10}$$

for incoming negative helicities. Here we have included the contributions from two possible interferences, the one described above and then the same pair of amplitudes with the gluon and Z-boson interchanged (ie: t-channel gluon exchange interfering with u-channel Z exchange).

If we substitute these two expressions into eq(2.6) then we find that:

$$A_{LL}^{PV} = \frac{c_R^{i\,2} - c_L^{i\,2}}{2(c_R^{i\,2} + c_L^{i\,2})} \tag{2.11}$$

2.2.3 Tree Level Asymmetries

A discussion of the tree level asymmetries at RHIC may be found in [10]

Shown in fig(2.3), fig(2.4) and fig(2.5) are the tree level values for the A_{LL}, A_L and A_{LL}^{PV} (respectively) asymmetries at RHIC. A_{LL}^{PV} and A_L both only include the parity violating $\alpha_s\alpha_W$ and the α_W^2 contributions. A_{LL} also includes an α_s^2 contribution as it is not an exclusively parity violating observable. We can see that the absolute value of the A_{LL} asymmetry is the largest however, this observable is not exclusively parity violating and as such will have a contribution at all orders from pure QCD. The absolute values of A_L and A_{LL}^{PV} are a factor of ten smaller but, as they are entirely parity violating observables the only contribution will be from weak effects and as such the relative correction due to $\alpha_S^2\alpha_W$ should be larger.

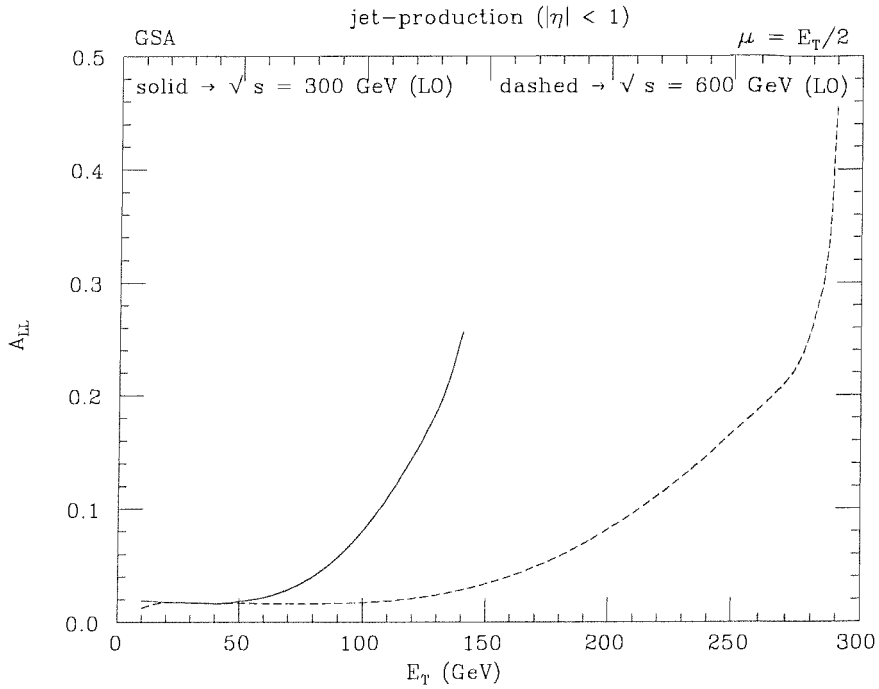

Figure 2.3: The tree level result for A_{LL} at RHIC (Solid line 300GeV, dashed 600GeV).

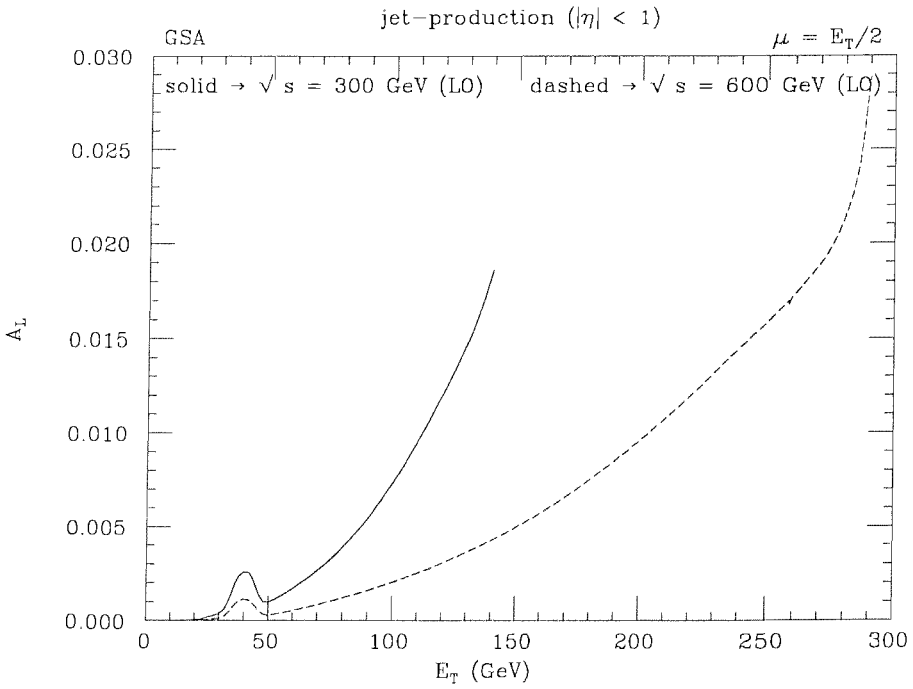

Figure 2.4: The tree level result for A_L at RHIC (Solid line 300GeV, dashed 600GeV).

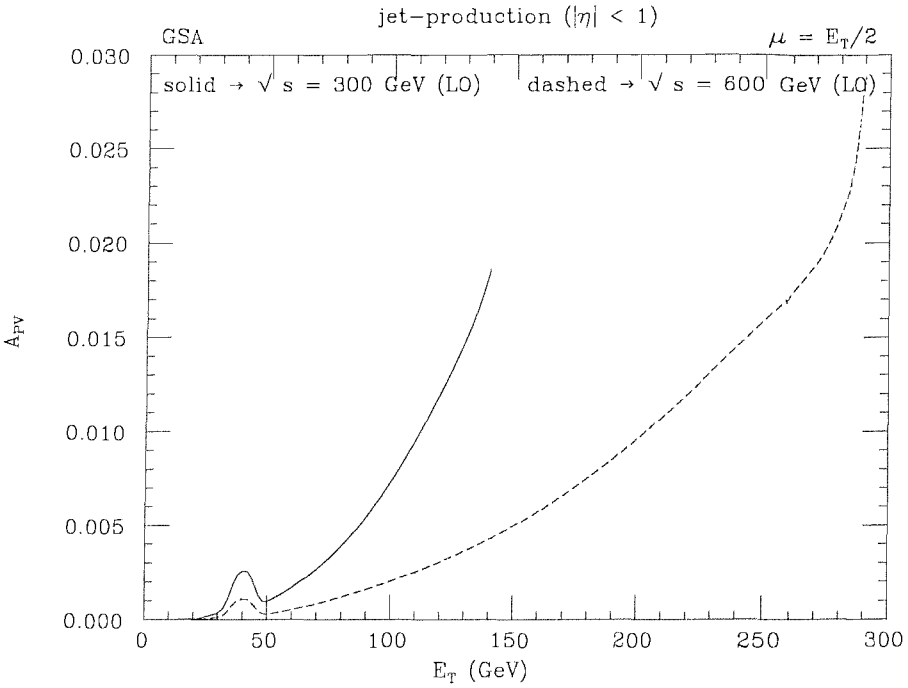

Figure 2.5: The tree level result for A_{LL}^{PV} at RHIC (Solid line 300GeV, dashed 600GeV).

2.3 Forward Backward Asymmetry

Another observable that can be studied is the forward/backward asymmetry. This observable is simplest to define if the initial state is a proton anti-proton pair and can *only* be defined for processes where the final state is a particle anti-particle pair. For example, the forward/backward asymmetry for $b\bar{b}$ production at a $p\bar{p}$ machine is:

$$\begin{aligned} A_{FB} &= \frac{\int_0^1 d\cos\theta \frac{d\sigma}{d\cos\theta} - \int_{-1}^0 d\cos\theta \frac{d\sigma}{d\cos\theta}}{\int_{-1}^1 d\cos\theta \frac{d\sigma}{d\cos\theta}} \\ &= \frac{\sigma_+^{b\bar{b}} - \sigma_-^{b\bar{b}}}{\sigma_+^{b\bar{b}} + \sigma_-^{b\bar{b}}} \end{aligned} \tag{2.12}$$

(Here $\sigma_+^{b\bar{b}}$ corresponds to the cross-section for events where the b is produced in the same direction as the p-beam and $\sigma_-^{b\bar{b}}$ corresponds to the cross-section for events where the b is produced in the opposite direction to the p-beam.)

In fact A_{FB} can only really be measured for heavy quark production due to the difficulty involved in accurately tagging light quark jets. Unlike A_{LL} and A_L we can

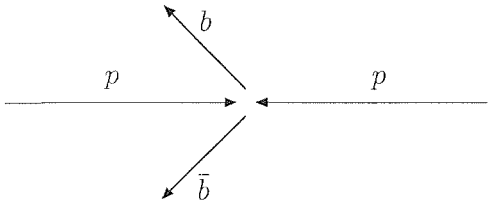

Figure 2.6: If we see a jet configuration like this at a pp collider then we can say, with reasonable assurance, that the quark was provided by the right hand beam and the anti-quark by the left hand beam.

measure the forward/backward asymmetry at machines where polarised beams are not available, for example at LHC and Tevatron. This is potentially quite important as the only currently available high energy polarised collider, RHIC, has a centre of mass energy of about the W-mass. This means that the logarithmic enhancement to weak effects (proportional to $ln^2\left(\frac{s}{m_W^2}\right)$, see section(2.4)) will be insignificant meaning that the one loop weak contributions will be significantly smaller than at the higher energy machines.

It is also interesting to note that it *is* possible to define the forwards/backwards asymmetry at colliders that do not have particle anti-particle beams (for example LHC) [13]. Each time a $b\bar{b}$ event is detected it is studied to see in which direction the system has to be boosted from the lab frame to make the jets back to back. From this one can deduce which proton beam provided the higher momentum parton to the interaction. The proton PDF's tell us that the higher momentum parton is more likely to be a quark than an anti-quark so with this knowledge we can define A_{FB} as follows:

$$A_{FB}^{pp} = \frac{\sigma_+^{b\bar{b}} - \sigma_-^{b\bar{b}}}{\sigma_+^{b\bar{b}} + \sigma_-^{b\bar{b}}} \tag{2.13}$$

Where $\sigma_+^{b\bar{b}}$ now refers to an event where the b jet is in the opposite direction to the boost and $\sigma_-^{b\bar{b}}$ to an event where the b jet is in the same direction as the boost.

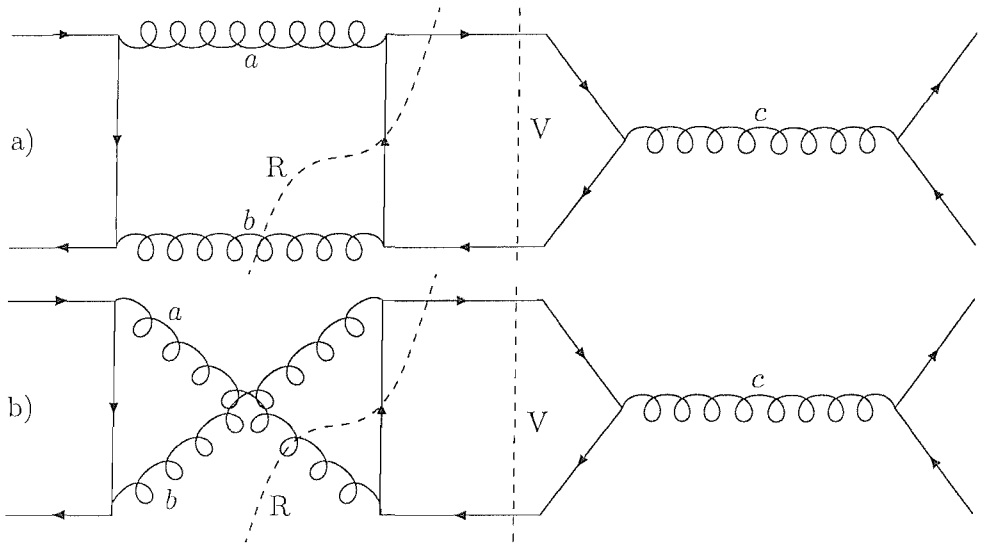

Figure 2.7: The QCD interferences that contribute to forwards/backwards asymmetry with *outgoing* quarks Q and $\bar{Q}$. The cut V corresponds to the virtual corrections and the cut R to the real corrections.

2.3.1 A_{FB} Without Parity Violation

When studying the forward/backward asymmetry it is important to consider the fact that (unlike A_{LL}^{PV} or A_L) it *is* possible to generate a contribution without parity violating vertices as shown in [14]. The effect appears in QCD and is briefly repeated here. The contribution originates when we interfere two diagrams in which gluons are exchanged in the s-channel (fig(2.7)) (Because we can only really measure A_{FB} for heavy quark production, and we assume that there are no heavy quarks in the initial state (anti)protons, all of the contributing diagrams must be in the s-channel for both α_s^3 and $\alpha_s^2\alpha_W$.). The colour factors for these two interferences are:

$$\mathrm{Col}_a = \mathrm{Tr}(t^a t^b t^c)\mathrm{Tr}(t^a t^c t^b) = \frac{1}{16}(f_{abc}^2 + d_{abc}^2) \tag{2.14}$$

$$\mathrm{Col}_b = \mathrm{Tr}(t^a t^c t^b)\mathrm{Tr}(t^a t^c t^b) = \frac{1}{16}(-f_{abc}^2 + d_{abc}^2) \tag{2.15}$$

Where $[t^a, t^b] = if_{abc}t^c$ and $\{t^a, t^b\} = id_{abc}t^c$.

If we drop the colour factors then we have the following relation.

$$d\sigma_a(Q, \bar{Q}) = -d\sigma_b(\bar{Q}, Q) \tag{2.16}$$

This holds true for both the real and virtual corrections (ie: both cuts in fig(2.7))

So, the total cross-section that contributes to the asymmetry is:

$$d\sigma_{A_{FB}}(Q, \bar{Q}) = \mathrm{Col}_a d\sigma_a(Q, \bar{Q}) + \mathrm{Col}_b d\sigma_b(Q, \bar{Q}) \tag{2.17}$$

and, if we exchange the outgoing quark and anti-quark:

$$\begin{aligned} d\sigma_{A_{FB}}(\bar{Q}, Q) &= \mathrm{Col}_a d\sigma_a(\bar{Q}, Q) + \mathrm{Col}_b d\sigma_b(\bar{Q}, Q) \\ (\text{From eq(2.16)}) &= -\mathrm{Col}_a d\sigma_b(Q, \bar{Q}) - \mathrm{Col}_b d\sigma_a(Q, \bar{Q}) \end{aligned} \tag{2.18}$$

So the charge asymmetry is:

$$\begin{aligned} & d\sigma_{A_{FB}}(Q, \bar{Q}) - d\sigma_{A_{FB}}(\bar{Q}, Q) \\ &= (\mathrm{Col}_a + \mathrm{Col}_b)(d\sigma_a(Q, \bar{Q}) + d\sigma_b(Q, \bar{Q})) \\ &= \frac{1}{8} d^2_{abc}(d\sigma_a(Q, \bar{Q}) + d\sigma_b(Q, \bar{Q})) \end{aligned} \tag{2.19}$$

(This result also shows that we can generate A_{FB} from QED since 'd_{abc}' is trivially non zero.)

This asymmetry relating to the exchange of final state quarks and anti-quarks is exactly equivalent to an asymmetry under the interchange of the final state momenta - ie: a transposition of the Mandelstam variables t and u (this is *only* true for the total cross-section, it is not true for individual interferences) - this asymmetry in the matrix element generates the forwards/backwards asymmetry in the final cross-section.

2.4 Sudakov Double Log Enhancement

It can be shown [15] [16] [17] (and references therein) that calculations of weak corrections tend to result in (potentially) large, non cancelling, Sudakov logarithms of the form $ln^2(\frac{s}{m^2})$ (where m is some weak mass in the diagram). The presence of these logs means that, at high energies, weak corrections will be enhanced relative to QCD corrections (where similar logarithms cancel).

It is worth pointing out that the s that appears in these logarithms is the partonic s and as such will be scaled by the Bjorken x. As a result of this the *machine* centre of mass energy must be well above the weak masses for the logarithms to be large.

If we consider as an example the graph pictured in fig(2.8) where we have a weak

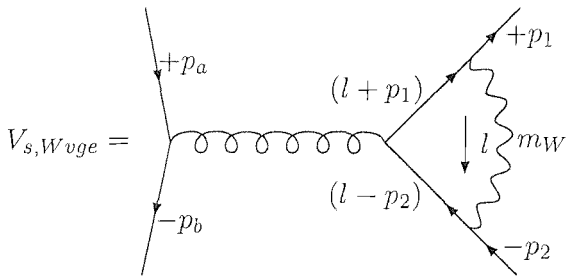

Figure 2.8: An example weak vertex correction to an s-channel gluon exchange.

boson vertex correction to s-channel gluon exchange (In what follows we will consider only light quarks and make the simplification that the weak boson has only a vector coupling to fermions. The double logarithms are still in evidence if we do not make these simplifications although the process involves somewhat more algebra.).

The expression for the amplitude shown in fig(2.8) is:

$$V_{s,Wvge} =$$
$$\int \frac{d^dl}{(2\pi)^d} \bar{u}(p_1) i g_W \gamma^\rho \frac{i(\not{l} + \not{p}_1)}{(l+p_1)^2} i g_S \gamma^\mu \frac{i(\not{l} - \not{p}_2)}{(l-p_2)^2} i g_W \gamma_\rho v(-p_2)$$
$$\frac{-i}{(l^2 - m_W^2)} \frac{-i}{s} \bar{v}(-p_b) i g_S \gamma_\mu u(p_a) \tag{2.20}$$

(Where the notation $s, Wvge$ denotes that we have a W vertex correction with a gluon exchange in the s channel)

If we go to the infrared (IR) ($l \to 0$) limit we obtain:

$$V_{s,Wvge} \to$$
$$\int \frac{d^dl}{(2\pi)^d} \frac{-1}{s} g_W^2 g_S^2 \frac{1}{(l^2 - m_W^2)(l+p_1)^2(l-p_2)^2}$$
$$\bar{u}(p_1) \gamma^\rho \not{p}_1 \gamma^\mu \not{p}_2 \gamma_\rho v(-p_2) \bar{v}(-p_b) \gamma_\mu u(p_a) \tag{2.21}$$

We now perform a little Dirac algebra and obtain:

$$p_{1\alpha} p_{2\beta} \gamma^\rho \gamma^\alpha \gamma^\mu \gamma^\beta \gamma_\rho$$
$$= 4 p_1 . p_2 \gamma^\mu \tag{2.22}$$

Substituting this back into eq(2.21) we obtain (in the limit):

$$V_{s,Wvge} \to$$
$$T_{s,g} \times \int \frac{d^dl}{(2\pi)^d} i g_W^2 \frac{4 p_1 . p_2}{(l^2 - m_W^2)(l+p_1)^2(l-p_2)^2} \tag{2.23}$$

Where $T_{s,g}$ is the tree level amplitude for a gluon exchanged in the s-channel. If we substitute in the scalar Veltman and Passarino function

$$C_0 = \int \frac{d^dl}{i\pi^2} \frac{1}{(l^2 - m_W^2)(l+p_1)^2(l-p_2)^2}$$

we obtain:

$$V_{s,Wvge} \to -T_{s,g} \times \frac{\alpha_W}{4\pi} 2 s C_0 \tag{2.24}$$

In the large s limit ($s >> m_W^2$) $C_0 \rightarrow \frac{1}{2s} ln^2\left(\frac{s}{m_w^2}\right)$. Therefore we can rewrite eq(2.24) in this limit as:

$$V_{s,Wvge} \rightarrow -T_{s,g} \times \frac{\alpha_W}{4\pi} ln^2\left(\frac{s}{m_w^2}\right) \tag{2.25}$$

An almost identical argument shows us that we also generate logs of a very similar form from box diagrams that include a massive internal boson.

We generate similar logarithms in pure QCD (although of course we do not include the weak mass scale) however they cancel during the subtraction procedure against the IR divergences generated by diagrams with real gluon emission.

In the weak case we need not consider diagrams with real W or Z boson emission as they will correspond to events which are experimentally distinguishable from those generated by virtual weak corrections (This is due to the real W/Z boson being unstable and typically decaying into high p_T leptons or jets which can be captured by the detectors). As a result these large Sudakov logs will remain in and enhance exclusive observables. We do not generate these Sudakov logarithms from the scalar corrections even though we are also ignoring the possibility of real scalar emission.

If we rewrite eq(2.21) for a scalar boson in the loop, again ignoring any pseudo scalar coupling but this time adding in a fermion mass m_f, we get:

$$\begin{aligned} & V_{s,\phi vge} \rightarrow \\ & \int \frac{d^d l}{(2\pi)^d} \frac{-1}{s} g_W^2 g_S^2 \frac{1}{(l^2 - m_\phi^2)[(l+p_1)^2 - m_f^2][(l-p_2)^2 - m_f^2]} \\ & \bar{u}(p_1)(\not{p}_1 + m_f)\gamma^\mu(\not{p}_2 + m_f)v(-p_2)\bar{v}(-p_b)\gamma_\mu u(p_a) \end{aligned} \tag{2.26}$$

Any term in the numerator that contains a $\not{p}_1$ or a $\not{p}_2$ is killed by the Dirac equation so the only terms that remain are those proportional to m_f^2 (so in the massless fermion case this diagram will vanish when the loop momentum goes soft). If we follow the

above argument through to eq(2.25) we obtain:

$$V_{s,\phi vge} \rightarrow -T_{s,g} \times \frac{\alpha_W}{4\pi} \frac{m_f^2}{2s} ln^2 \left(\frac{s}{m_w^2} \right) \tag{2.27}$$

So the log is suppressed by a factor of the fermion mass in the loop over s.

Nevertheless, the large logarithms generated by the W and Z boson graphs *will* enhance weak corrections relative to QCD corrections, amplifying their importance (especially at high energies).

Chapter 3

Methods For The Cancellation Of Soft And Collinear Divergences.

(The subtraction method described in this chapter was presented by S. Catani and M. Seymour in [7])

To calculate processes containing IR divergences (which in all the calculations presented here are four quark processes - at $\alpha_S^2\alpha_W$ $gg \to qq$ will not contain IR divergences as there are no possible bremsstrahlung diagrams) we need to follow some kind of subtraction algorithm to allow us to cancel these divergences in a fashion that will enable us to perform the phase space integral safely.

The Kinoshita, Lee, Nauenberg (KLN) theorem tells us that we expect there to be cancellations between the soft IR divergences arising from virtual loop corrections and real gluon emission when studying an IR safe observable. The remaining collinear divergences associated with initial state gluons are absorbed into the parton distribution functions.

3.1 General Motivation

All of the processes that will be calculated will be either two to two body processes or (when we have an external, real gluon) two to three body processes. The subtraction method used will be described below with this in mind.

The cross section to one loop order may be written:

$$\sigma^{TREE} + \sigma^{NLO} = \int_{[1,2]} d\sigma^{TREE} + \int_{[1,2,3]} d\sigma^{REAL} + \int_{[1,2]} d\sigma^{VIRTUAL} \tag{3.1}$$

Here $d\sigma^{TREE}$ is the tree level differential cross section (which is finite in four dimensions), $d\sigma^{REAL}$ is the cross section for diagrams with real gluon emission and $d\sigma^{VIRTUAL}$ is the cross section for interferences involving virtual corrections (both divergent in four dimensions). The subscripts $_{[1,2]}$ and $_{[1,2,3]}$ indicate terms where we are integrating over the phase space of the two final state quarks and over the phase space of the two final state quarks and an emitted real gluon respectively.

The divergences in $d\sigma^{REAL}$ will manifest themselves as terms proportional to $\frac{1}{p_i \cdot p_3}$ (where p_3 is the four momentum of the emitted gluon and p_i is the four momentum of the parton from which it is emitted) - this will diverge when p_3 is either soft or is collinear to p_i.

The divergences in $d\sigma^{VIRTUAL}$ will manifest themselves as $\frac{1}{\epsilon}$ or $\frac{1}{\epsilon^2}$ IR poles (working in $4 - 2\epsilon$ dimensions and having renormalised all UV poles).

Therefore if we wish to perform the phase space integrals we need to introduce a subtraction term in the following way:

$$d\sigma^{NLO} = [d\sigma^{REAL} - d\sigma^{A}] + d\sigma^{A} + d\sigma^{VIRTUAL}, \tag{3.2}$$

Where $d\sigma^{A}$ is the subtraction term, constructed to have the same singular behaviour as $d\sigma^{REAL}$ and to be analytically integrable over a single parton phase space (see below).

If this is the case then we can write:

$$\sigma^{NLO} = \int_{[1,2,3]} [d\sigma^{REAL} - d\sigma^{A}] + \int_{[1,2,3]} d\sigma^{A} + \int_{[1,2]} d\sigma^{VIRTUAL}, \tag{3.3}$$

where $[d\sigma^{REAL} - d\sigma^{A}]$ can be evaluated in four dimensions (by definition). If we can integrate $d\sigma^{A}$ over the phase space of the gluon then we have:

$$\sigma^{NLO} = \int_{[1,2,3]} [d\sigma^{REAL} - d\sigma^{A}] + \int_{[1,2]} [d\sigma^{VIRTUAL} + \int_{[3]} d\sigma^{A}] \tag{3.4}$$

(Actually, we also need to include the Altarelli-Parisi term in the integrand integrated over the two body phase space.)

$[d\sigma^{VIRTUAL} + \int_{[3]} d\sigma^{A}]$ can be integrated in four dimensions as the $\frac{1}{\epsilon}$ and $\frac{1}{\epsilon^2}$ poles should cancel between the two terms.

This cancellation does not exist in general but rather only for IR safe observables, that is observables that are defined so that they are insensitive to the number of soft or collinear partons in the final state. This restriction is not a problem in the calculation presented here as all observables considered are IR safe.

3.2 Evaluating the Dipole Terms

(In what follows we will label the incoming quark momenta as p_a and p_b and the outgoing quark momenta as p_1 and p_2. If we are looking at a bremsstrahlung diagram then the real gluon will be labelled with momentum p_3)

Also, the divergent contributions to the processes that will be evaluated in what follows will be QCD corrections to $\alpha_S\alpha_W$ tree level interferences. Therefore, the tree level contributions will look something like $\mathcal{M}_{weak} \times \mathcal{M}^{*}_{QCD}$ (up to some interference factor). However, for brevity, this will be written as $|\mathcal{M}|^2$ in what follows. Consider a bremsstrahlung matrix element with three QCD partons in the final state ($\mathcal{M}_{a,b,1,2,3}$). The dependence of the matrix element squared on the momentum of one final state

particle (p_j) is divergent in two regions of phase space - the region where p_j goes soft ($p_j = \lambda q$, $\lambda \to 0$ where q is any momentum) and the region where p_j goes collinear to any other parton in the interaction (denoted by p_i) - for later convenience this collinear region will be described by the limit $p_j \to (1-z)p_i/z$.

In both of these cases the matrix element squared will depend on a factor $1/(p_i p_j)$ as $p_i p_j$ tends to zero in the divergent regions.

It is important to note that one of the strengths of the dipole subtraction method from [7] is that the divergent structure of the matrix element squared is independent of the precise form of the matrix element. That is, (for a two to two body tree level process) we can factorise out the divergent part of $|\mathcal{M}_{a,b,1,2,3}|^2$ with respect to $|\mathcal{M}_{a,b,1,2}|^2$.

Therefore we can write:

$$d\sigma^A = \sum_{alldipoles} d\sigma^{TREE} \otimes dV_{dipole} \tag{3.5}$$

So we can also rewrite eq(3.4) as:

$$\sigma^{NLO} = \int_{[1,2,3]} \left[(d\sigma^{REAL})_{\epsilon=0} - \left(\sum_{alldipoles} d\sigma^{TREE} \otimes dV_{dipole} \right)_{\epsilon=0} \right]$$
$$+ \int_{[1,2]} [d\sigma^{VIRTUAL} + d\sigma^{TREE} \otimes I]_{\epsilon=0} \tag{3.6}$$

Where we have written:

$$\sum_{alldipoles} \int_{[3]} dV_{dipole} = I \tag{3.7}$$

Where $\otimes$ is a phase space convolution where we are summing over colour indices.

In the example of the LO matrix element $|\mathcal{M}_{a,b,1,2}|^2$ there are potentially 16 interferences between diagrams with real gluon emission from external particles - ie:

$$\sum_{i=a,b,1,2} \mathcal{M}^{i3}_{weak} \times \left[\sum_{j=a,b,1,2} \mathcal{M}^{j3}_{QCD} \right]^* \tag{3.8}$$

Where $\mathcal{M}^{i3}$ is the bremsstrahlung diagram where a gluon with momentum p_3 is emitted from particle i.

However, as mentioned above, the dipole structure is independent of the precise form of $|\mathcal{M}_{a,b,1,2}|^2$. Therefore, we simply have one dipole for each possible combination of emitter/emitted particles (p_i, p_j) and spectator particles (p_k). Symbolically this gives us, for the dipole counter-term to $|\mathcal{M}_{a,b,1,2,3}|^2$:

$$|\mathcal{M}_{a,b,1,2}|^2 \otimes V_{ij,k} \tag{3.9}$$

(Where $i, k = a, b, 1, 2$ and $j = 3$)

3.3 Constructing the Dipoles

To aid us in constructing the dipoles we need to study the behaviour of the bremsstrahlung interferences in the soft and collinear limits.

3.3.1 The Soft Limit

As stated above the soft limit is parameterised by $p_j = \lambda q$, $\lambda \to 0$ (where q is any momentum). In this limit the bremsstrahlung matrix element squared goes like: [18]

$$\begin{aligned} &|\mathcal{M}_{a,b,1,2,3}|^2 \to \\ &-\frac{1}{\lambda^2}\mu^{2\epsilon} g_{S\ 2,a}^2 < 1,2,3;a,b|[J^\mu(q)]^\dagger J_\mu(q)|1,2,3;a,b>_{2,a} \end{aligned} \tag{3.10}$$

Where $J^\mu(q)$ is the eikonal current defined in this case as:

$$J^\mu(q) = T_a \frac{p_a^\mu}{p_a.q} + T_b \frac{p_b^\mu}{p_b.q} + T_1 \frac{p_1^\mu}{p_1.q} + T_2 \frac{p_2^\mu}{p_2.q} \tag{3.11}$$

Where T_a are the generators of SU(3) up to a possible factor of minus one. We pick up a factor of minus one in $T_m.T_n$ if m and n correspond to a particle and an anti-particle or if they correspond to an incoming and an outgoing parton. For example, if we are

considering $q_a\bar{q}_b \rightarrow q_1\bar{q}_2$ then we would have:

$$T_a.T_b = (-1)t_a.t_b$$

$$T_1.T_2 = (-1)t_1.t_2$$

$$T_a.T_1 = (-1)t_a.t_1$$

$$T_a.T_2 = t_a.t_2 \text{ (here we pick up two factors of -1)} \tag{3.12}$$

And so on.

So the square of the eikonal current is:

$$[J^\mu(q)]^\dagger J_\mu(q) = \sum_{m,n=a,b,1,2} T_m.T_n \frac{p_m.p_n}{(p_m.q)(p_n.q)} \tag{3.13}$$

If we write:

$$\frac{p_m.p_n}{(p_m.q)(p_n.q)} = \frac{p_m.p_n}{(p_m.q)(p_m+p_n).q} + \frac{p_m.p_n}{(p_n.q)(p_m+p_n).q} \tag{3.14}$$

then we obtain, for the right hand side of eq(3.10):

$$-\frac{1}{\lambda^2} 2\mu^{2\epsilon} g_S^2 \sum_m \frac{1}{p_m.q} \sum_{n\neq m} \frac{p_m.p_n}{(p_m+p_n).q} T_m.T_n |\mathcal{M}_{a,b,1,2}|^2 \tag{3.15}$$

Where $|\mathcal{M}_{a,b,1,2}|^2$ is the LO interference with its colour factor removed.

If we extract a single combination of i and k we obtain:

$$-\frac{1}{\lambda^2}\frac{2g_S^2}{p_i.q}\mu^{2\epsilon} T_k.T_i \frac{p_k.p_i}{(p_i+p_k).q} \times |\mathcal{M}_{a,b,1,2}|^2 \tag{3.16}$$

(This will be useful for comparison later) Note that any particular combination of ij, k does not correspond directly a bremsstrahlung interference even though the sum over i, j and k does of course equal the sum over all interferences.

3.3.2 The Collinear Limit

To study the behaviour of the matrix element squared in the collinear limit we must be careful in defining that limit.

When p_i and p_j (two final state partons) go collinear we have:

$$
\begin{aligned}
p_i^\mu &= zp^\mu + k_\perp^\mu - \frac{k_\perp^2 n^\mu}{2zp.n} \\
p_j^\mu &= (1-z)p^\mu - k_\perp^\mu - \frac{k_\perp^2 n^\mu}{2(1-z)p.n} \\
2p_i.p_j &= -\frac{k_\perp^2}{z(1-z)}
\end{aligned}
\tag{3.17}
$$

Where p^μ is the direction of the two collinear vectors, $k_\perp^\mu$ is the direction along which the collinear limit is approached (the collinear limit is the $k_\perp^\mu \to 0$ limit) and n^μ is a vector forming a plane with p^μ that is perpendicular to $k_\perp^\mu$.

In the region described by these limits the bremsstrahlung matrix element squared becomes:

$$
\begin{aligned}
&|\mathcal{M}_{a,b,1,2,3}|^2 \to \\
&\frac{1}{p_i.p_j}\mu^{2\epsilon} g_S^2 \; {}_{2,a}\!<ij,k;a,b|\hat{P}_{(ij),i}(z,k_\perp;\epsilon)|ij,k;a,b>_{2,a}
\end{aligned}
\tag{3.18}
$$

Here the matrix element on the right is the tree level matrix element with parton j (parton 1 or parton 2 in practice) replaced by (ij). In practice this means that the interference will be equal to the normal tree level expression but with the emitter momentum replaced by p^μ.

Here $\hat{P}_{(ij),i}$ is the Altarelli-Parisi splitting function associated with the splitting parton $ij \to i+j$. In all the cases we are looking at this will be $q \to q+g$. In this case the splitting function (acting on the spin index of the (ij)) will be:

$$
<s|\hat{P}_{(ij),i}(z,f_\perp;\epsilon)|s'> = \delta_{ss'} c_F \left[\frac{1+z^2}{1-z} - \epsilon(1-z)\right]
\tag{3.19}
$$

Where ϵ is the dimensional regularisation parameter.

When we have p_a and p_i (one initial state parton and a final state parton) go collinear

we define the limit as:

$$p_i^\mu = (1-x)p_a^\mu + k_\perp^\mu - \frac{k_\perp^2}{1-x}\frac{n^\mu}{2p_a.n}$$
$$2p_i.p_a = -\frac{k_\perp^2}{1-x} \text{ as } k_\perp \to 0 \tag{3.20}$$

The splitting process here is $a \to (ai) + i$ $(q \to q + g)$. This time in the collinear limit we have:

$$|\mathcal{M}_{a,b,1,2,3}|^2 \to$$
$$\frac{1}{x}\frac{1}{p_i.p_a} 2\mu^{2\epsilon} g_S^2 \; {}_{2,a}\!<j,k;ai,b|\hat{P}_{a,(ai)}(x,k_\perp;\epsilon)|j,k;ai,b>_{2,a} \tag{3.21}$$

Again the matrix element on the right hand side is obtained by taking the tree level, this time replacing parton a (in practice a or b) with a parton (ai) - as dictated by the splitting described above. This means that parton a will have momentum xp_a^μ and we require an overall factor of $\frac{1}{x}$.

As in the case where two final state particles go collinear a and ai both correspond to quarks so the expression for $\hat{P}$ will be as in eq(3.19) (if we swap z for x).

3.3.3 Expressions for $d\sigma^A$

We now need to find an expression for $d\sigma^A$ (not integrated over the gluon phase space) in eq(3.4) which matches eq(3.15) and eq(3.18,3.21) in the soft and collinear limits respectively.

$d\sigma^A$ will be a sum of a number of different dipoles. There will be two dipoles associated with each possible bremsstrahlung interference - for example, for the interference between emission from particle 1 and emission from particle a there will be one dipole where particle 1 plays the role of emitter and a plays the role of spectator ($\mathcal{D}_{13}^a$) and one where a is the emitter and 1 the spectator ($\mathcal{D}_1^{a3}$).

If we look back at eq(3.14) we see how we break the different terms of the eikonal current squared into pairs of terms with the emitter and spectator particle defined. In the first term on the right hand side of eq(3.14) p_m is the emitter and p_n is the spectator - the reverse is true in the second term.

Note that this association does not mean that a particular dipole will necessarily cancel the divergences of a specific interference - in practice the sum of all dipoles including a factor of (for example) $1/p_1.p_3$ will cancel the sum of all interferences including the same factor. The cancellation does not always work on a diagram by diagram basis. This is because, in the soft limit, each dipole has a $1/\lambda^2$ pole which will cancel with the divergent part shown in eq(3.16) - however, as we will see below, each dipole also has a $1/\lambda$ pole. This is not required to cancel any divergence (and will in fact cancel between the sum of all dipoles) but rather is required to make the dipole tend to the correct form in the collinear limit. The consequence of this is that if we attempt to check that our dipole expression gives a finite answer in the soft limit we will not be able to do it on a diagram by diagram basis as the $1/\lambda$ poles will give us an erroneous divergence.

The expressions required to construct the various dipoles differ depending on whether our emitter and spectator particles are in the initial or final state. We will look at each combination individually below.

Final State Emitter and Final State Spectator ($\mathcal{D}_k^{ij}$)

We will first look at the case where we have both emitter and spectator in the final state. The expression for this dipole (ij emitter and k spectator) is:

$$\begin{aligned}
&\mathcal{D}_k^{ij} = \frac{-1}{2p_i.p_j}\frac{T_k.T_{ij}}{T_{ij}^2}V_{ij,k}|\mathcal{M}_{\tilde{ij},\tilde{k}}|^2 \\
&V_{ij,k} = 2g_S^2\mu^{2\epsilon}c_F\Big[-(1+\tilde{z}_i)-\epsilon(1-\tilde{z}_i)\Big] \\
&\mathcal{D}_k^{ij} = \\
&\frac{-2c_F g_S^2}{2p_i.p_j}\frac{T_k.T_{ij}}{T_{ij}^2}\left[\frac{2}{1-\tilde{z}_i(1-y_{ij,k})}-(1+\tilde{z}_i)\right] \\
&\times|\mathcal{M}_{\tilde{ij},\tilde{k}}|^2
\end{aligned} \tag{3.22}$$

Where $|\mathcal{M}_{\tilde{ij},\tilde{k}}|^2$ is the tree level interference with the colour factor removed and p_k replaced with $\tilde{p}_k$ and p_i replaced with $\tilde{p}_{ij}$.

$$\begin{aligned}
y_{ij,k} &= \frac{p_i.p_j}{p_i.p_j+p_j.p_k+p_k.p_i} \\
\tilde{z}_i &= \frac{p_i.p_k}{p_j.p_k+p_i.p_k} \\
\tilde{p}_k^\mu &= \frac{1}{1-y_{ij,k}}p_k^\mu \\
\tilde{p}_{ij}^\mu &= p_i^\mu+p_j^\mu-\frac{y_{ij,k}}{1-y_{ij,k}}p_k^\mu
\end{aligned} \tag{3.23}$$

$\mathcal{D}_k^{ij}$ in the Soft Limit

In the soft limit $p_j \to \lambda q$. In the limit characterised by this we will have:

$$\begin{aligned}
&y_{ij,k} \to 0 \ , \ \tilde{z}_i \to 1 \\
&\text{therefore, } \tilde{p}_k^\mu \to p_k^\mu \text{ and } \tilde{p}_{ij}^\mu \to p_i^\mu
\end{aligned} \tag{3.24}$$

Note that since the scaled momenta become the unscaled momenta in the soft limit the tree level interference in eq(3.22) will become the normal tree level interference expressed as a function of unscaled Mandelstam variables.

This means that in the soft limit eq(3.22) tends towards:

$$\mathcal{D}_k^{ij} = \frac{-2c_F g_S^2}{2\lambda p_i.q}\frac{T_k.T_{ij}}{T_{ij}^2}\left[\frac{1}{\lambda}\frac{2p_k.p_i}{(p_i+p_k).q} - 2\right] \times |\mathcal{M}|^2 \tag{3.25}$$

If we take the term proportional to $1/\lambda^2$ then we have:

$$-\frac{1}{\lambda^2}\frac{2g_S^2}{p_i.q}T_k.T_{ij}\frac{p_k.p_i}{(p_i+p_k).q} \times |\mathcal{M}_{i,k}|^2 \tag{3.26}$$

If we compare this with eq(3.16) (where we have extracted a single combination of i and k from the summations in the expression for the total soft limit eq(3.15)) we see that they are equal.

$\mathcal{D}_k^{ij}$ in the Collinear Limit

In the limit (defined in eq(3.17)) where two final state particles go collinear the variables in the dipole become:

$$y_{ij,k} \to \frac{-k_\perp^2}{2z(1-z)p.p_k}\ ,\ \tilde{z}_i \to z$$
$$\text{therefore, } \tilde{p}_k^\mu \to p_k^\mu \text{ and } \tilde{p}_{ij}^\mu \to p^\mu \tag{3.27}$$

(Where p, z and $k_\perp$ are as defined in eq(3.17))

Therefore the term in square brackets becomes:

$$\left[\frac{2}{1-z} - (1+z)\right] \tag{3.28}$$

Thus the expression for the dipole in the collinear limit is:

$$-2g_S^2 T_k.T_{ij}\frac{1}{p_i.p_j}\left[\frac{1+z^2}{1-z}\right] \times |\mathcal{M}(p_i^\mu \to p^\mu)|^2 \tag{3.29}$$

(Here the matrix element squared is equal to the normal LO tree level interference with the emitter quark's momentum changed to p^μ.)

Now we can see that eq(3.29) is equal to eq(3.18). This combined with the observation that the dipole also matches the bremsstrahlung interference in the soft limit means that this dipole expression fulfils the requirement of matching the singular behaviour of $d\sigma^{REAL}$.

Final State Emitter and Initial State Spectator ($\mathcal{D}_{ij}^{a}$)

We next consider the other case including a final state singularity, that with an initial state spectator. The expression for this dipole with emitter ij and spectator a is:

$$\begin{aligned}
&\mathcal{D}_{ij}^{a} = \frac{-1}{2p_i.p_j}\frac{1}{x_{ij,a}}V_{ij}^{a}\frac{T_a.T_{ij}}{T_{ij}^2}|\mathcal{M}_{\tilde{ij},\tilde{a}}|^2 \\
&V_{ij}^{a} = 2g_S^2\mu^{2\epsilon}c_F\left[\frac{2}{1-\tilde{z}_i+(1-x_{ij,a})} - (1+\tilde{z}_i) - \epsilon(1+\tilde{z}_i)\right] \\
&\mathcal{D}_{ij}^{a} = \\
&\frac{-2c_F g_S^2}{2p_i.p_j}\frac{T_a.T_{ij}}{T_{ij}^2}\frac{1}{x_{ij,a}}\left[\frac{2}{1-\tilde{z}_i+(1-x_{ij,a})} - (1+\tilde{z}_i)\right] \\
&\times|\mathcal{M}_{\tilde{ij},\tilde{a}}|^2
\end{aligned} \tag{3.30}$$

Where $|\mathcal{M}_{\tilde{ij},\tilde{a}}|^2$ is the tree level interference with the colour factor removed and p_a replaced with $\tilde{p}_a$ and p_i replaced with $\tilde{p}_{ij}$ and we also have:

$$\begin{aligned}
x_{ij,a} &= \frac{p_i.p_a + p_j.p_a - p_i.p_j}{p_i.p_a + p_j.p_a} \\
\tilde{z}_i &= \frac{p_i.p_a}{p_j.p_a + p_i.p_j} \\
\tilde{p}_a^{\mu} &= x_{ij,a}p_a^{\mu} \\
\tilde{p}_{ij}^{\mu} &= p_i^{\mu} + p_j^{\mu} - (1-x_{ij,a})p_a^{\mu}
\end{aligned} \tag{3.31}$$

$\mathcal{D}_{ij}^{a}$ in the Soft Limit

In the soft limit (defined by $p_j \to \lambda q$, $\lambda \to 0$) we have:

$$\begin{aligned} & x_{ij,a} \to 1 \\ & (1+\tilde{z}_i) \to 2 \\ & 1-\tilde{z}_i+1-x_{ij,a} = \frac{p_i.p_j+p_j.p_a}{p_i.p_a+p_j.p_a} \\ & \therefore \frac{2}{1-\tilde{z}_i+1-x_{ij,a}} \to \frac{2p_i.p_a}{\lambda q.(p_i+p_a)} \end{aligned} \tag{3.32}$$

So the part of $\mathcal{D}_{ij}^{a}$ proportional to $\frac{1}{\lambda^2}$ is:

$$-\frac{1}{\lambda^2}\frac{2g_S^2}{p_i.q}T_a.T_{ij}\frac{p_i.p_a}{q.(p_i+p_a)}|\mathcal{M}_{i,a}|^2 \tag{3.33}$$

Which cancels the divergence in eq(3.16).

$\mathcal{D}_{ij}^{a}$ in the Collinear Limit

Again we use the collinear limit as defined as in eq(3.17). In this case:

$$\begin{aligned} & \tilde{z}_i \to z \\ & 1-x_{ij,a} \to \frac{-k_\perp^2}{2z(1-z)p.p_a} \\ & x_{ij,a} \to 1 \\ & \tilde{p}_a^\mu \to p_a^\mu \\ & \tilde{p}_{ij}^\mu \to p_i^\mu + p_j^\mu = p^\mu \end{aligned} \tag{3.34}$$

Therefore, in the collinear limit the dipole becomes:

$$\begin{aligned} & \mathcal{D}_{ij}^{a} = \\ & -2g_S^2\frac{1}{2p_i.p_j}T_a.T_{ij}\left[\frac{2}{1-z}-(1+z)\right]\times|\mathcal{M}(p_i^\mu \to p^\mu)|^2 \end{aligned} \tag{3.35}$$

Which clearly cancels with the dipole interference in the collinear limit shown in eq(3.18).

Initial State Emitter and Final State Spectator ($\mathcal{D}_k^{ai}$)

For the dipole with an initial state singularity and a final state spectator (emitter ai, spectator k) we have the expression:

$$\begin{aligned}
&\mathcal{D}_k^{ai} = \frac{-1}{2p_a.p_i}\frac{1}{x_{ik,a}}\frac{T_k.T_{ai}}{T_{ai}}V_k^{ai}|\mathcal{M}_{\tilde{ai},\tilde{k}}|^2 \\
&V_k^{ai} = 2g_S^2\mu^{2\epsilon}c_F\left[\frac{2}{1-x_{ik,a}+u_i} - (1+x_{ik,a}) - \epsilon(1-x_{ik,a})\right] \\
&\mathcal{D}_k^{ai} = \\
&\frac{-2c_F g_S^2}{2p_a.p_i}\frac{T_k.T_{ai}}{T_{ai}^2}\frac{1}{x_{ik,a}}\left[\frac{2}{1-x_{ik,a}+u_i} - (1+x_{ik,a})\right] \\
&\times|\mathcal{M}_{\tilde{ai},\tilde{k}}|^2
\end{aligned} \tag{3.36}$$

Where we now have:

$$\begin{aligned}
x_{ik,a} &= \frac{p_k.p_a + p_i.p_a - p_i.p_k}{p_k.p_a + p_i.p_a} \\
u_i &= \frac{p_i.p_a}{p_i.p_a + p_k.p_a} \\
\tilde{p}_k^\mu &= p_k^\mu + p_i^\mu - (1-x_{ik,a})p_a^\mu \\
\tilde{p}_{ai}^\mu &= x_{ik,a}p_a^\mu
\end{aligned} \tag{3.37}$$

$\mathcal{D}_k^{ai}$ in the Soft Limit

In the soft limit ($p_i \to \lambda q$, $\lambda \to 0$) we have $x_{ik,a} \to 1$ and also:

$$\frac{2}{1-x_{ik,a}+u_i} \to \frac{1}{\lambda}\frac{2p_k.p_a}{(p_a+p_k).q}$$

S, in the soft limit, the divergent part of eq(3.36) becomes:

$$\begin{aligned}
&\mathcal{D}_k^{ai} = \\
&-\frac{1}{\lambda^2}\frac{1}{p_a.q}T_k.T_{ai}2g_S^2\mu^{2\epsilon}\left[\frac{2p_k.p_a}{(p_a+p_k).q}\right] \times |\mathcal{M}|^2
\end{aligned} \tag{3.38}$$

Again, in the soft limit, we can express the tree level interference as a function of unscaled Mandelstam variables.

This expression is equal to that given in eq(3.16) so again we can easily see that the soft divergences will cancel.

$\mathcal{D}_k^{ai}$ in the Collinear Limit

Because we are now looking at the case where the gluon goes collinear with an initial state particle we need to use the collinear limit as defined in eq(3.20). If we do this then we discover that, in that limit, we obtain:

$$x_{ik,a} \to x \ , \ u_i \to \frac{-k_\perp^2}{2p_k.p_a(1-x)}$$
$$\text{therefore, } \tilde{p}_k^\mu = p_k^\mu + p_i^\mu - (1-x)p_a^\mu \text{ and } \tilde{p}_{ai}^\mu = xp_a^\mu \tag{3.39}$$

So for the dipole in the collinear limit we have:

$$\mathcal{D}_k^{ai} =$$
$$\frac{1}{x}\frac{1}{p_i.p_a}2g_S^2\left[\frac{2}{1-x} - (1+x)\right] \times |\mathcal{M}(p_a^\mu \to xp_a^\mu)|^2 \tag{3.40}$$

This is equal to the bremsstrahlung interference in the collinear limit as given in eq(3.21).

Initial State Emitter and Initial State Spectator ($\mathcal{D}_b^{ai}$)

The final dipole we need is the one where we have an initial state emitter (aj) and an initial state spectator (b). In this case we have the expression:

$$\mathcal{D}_b^{ai} = \frac{-1}{2p_a.p_i}\frac{1}{x_{i,ab}}\frac{T_b.T_{ai}}{T_{ai}^2}V^{ai,b}|\mathcal{M}_{\tilde{ai},\tilde{b}}|^2$$
$$V^{ai,b} = 2g_S^2\mu^{2\epsilon}c_F\left[\frac{2}{1-x_{ia,b}} - (1+x_{ia,b}) - \epsilon(1-x_{ia,b})\right]$$
$$\mathcal{D}_b^{ai} =$$
$$\frac{-2c_F g_S^2}{2p_a.p_i}\frac{T_b.T_{ai}}{T_{ai}^2}\frac{1}{x_{i,ab}}\left[\frac{2}{1-x_{i,ab}} - (1+x_{i,ab})\right]$$
$$\times|\mathcal{M}_{\tilde{ai},\tilde{b}}|^2 \tag{3.41}$$

Where:

$$
\begin{aligned}
x_{i,ab} &= \frac{p_a.p_b - p_i.p_a - p_i.p_b}{p_a.p_b} \\
\tilde{p}^{\mu}_{ai} &= x_{i,ab} p^{\mu}_a \\
\tilde{k}^{\mu}_j &= k^{\mu}_j - \frac{2k_j.(K+\tilde{K})}{(K+\tilde{K})^2}(K+\tilde{K})^{\mu} + \frac{2k_j.K}{K^2}\tilde{K}^{\mu} \\
K^{\mu} &= p^{\mu}_a + p^{\mu}_b - p^{\mu}_i \\
\tilde{K}^{\mu} &= \tilde{p}^{\mu}_{ai} + p^{\mu}_b
\end{aligned}
\tag{3.42}
$$

Here $\tilde{k}^{\mu}_j$ are the modified momenta of all final state particles. This modification is required because we ideally want to be in a frame where p_b is unshifted - but we need to maintain the momentum conservation:

$$
\tilde{p}^{\mu}_{ai} + p^{\mu}_b - \sum k^{\mu}_j = 0 \tag{3.43}
$$

$\mathcal{D}^{ai}_b$ in the Soft Limit

In the soft limit

$$
\begin{aligned}
x_{i,ab} &\to 1 \\
1 - x_{i,ab} &\to \frac{p_i.(p_a+p_b)}{p_a.p_b}
\end{aligned}
\tag{3.44}
$$

In the soft limit $\tilde{p}^{\mu}_{ai} \to p^{\mu}_a$ and for the final state momenta we have:

$$
\begin{aligned}
K^{\mu}/\tilde{K}^{\mu} &\to p^{\mu}_a + p^{\mu}_b \\
\tilde{k}^{\mu}_j &\to k^{\mu}_j - \frac{2k_j.(2p_a+2p_b)}{(2p_a+2p_b)^2}(2p_a+2p_b)^{\mu} + \frac{2k_j.(p_a+p_b)}{(p_a+p_b)^2}(p_a+p_b)^{\mu} = k^{\mu}_j
\end{aligned}
\tag{3.45}
$$

Therefore, in the soft limit, the shifted tree level interference tends to the unshifted tree level interference as required.

So, in the soft limit the dipole becomes:

$$
-\frac{1}{\lambda^2}\frac{2g_S^2}{p_a.q}\mu^{2\epsilon} T_b.T_{aj}\frac{p_a.p_b}{(p_a+p_b).q} \times |\mathcal{M}|^2 \tag{3.46}
$$

Which is of the form required.

$\mathcal{D}_b^{ai}$ in the Collinear Limit

In the collinear limit $x_{i,ab} \to x$ so the dipole shown in eq(3.41) manifestly has approximately the correct form. $\tilde{p}_{ai}^{\mu} \to x p_a^{\mu}$ so, provided that the final state momenta tend to their unshifted values in the collinear limit the tree level interference will also have the correct form.

$$
\begin{aligned}
&K^{\mu} = p_a^{\mu} + p_b^{\mu} - p_i^{\mu} \to x p_a^{\mu} + p_b^{\mu} \\
&\tilde{K}^{\mu} \to x p_a^{\mu} + p_b^{\mu} \\
&\tilde{k}_j^{\mu} \to k_j^{\mu} - \frac{2k_j.(2xp_a + 2p_b)}{(2xp_a + 2p_b)^2}(2xp_a + 2p_b)^{\mu} + \frac{2k_j.(xp_a + p_b)}{(xp_a + p_b)^2}(xp_a + p_b)^{\mu} \\
&= k_j^{\mu}
\end{aligned}
\tag{3.47}
$$

Therefore the tree level interference in the dipole tends to the normal tree level expression with p_a replaced with xp_a meaning that the dipole matches with the expression given in eq(3.21).

3.3.4 Integrating the Dipole Terms

To obtain the terms needed in eq(3.3) we will need to be able to integrate the Dipole terms over the three body phase space.

Integrating $\mathcal{D}_k^{ij}$

The first term we will look at is the case with final state emitters and final state spectators. The three body phase space is:

$$
\begin{aligned}
&d\Phi(p_i, p_j, p_k; Q) = \frac{d^d p_i}{(2\pi)^{d-1}} \delta_+(p_i^2) \frac{d^d p_j}{(2\pi)^{d-1}} \delta_+(p_j^2) \\
&\frac{d^d p_k}{(2\pi)^{d-1}} \delta_+(p_k^2)(2\pi)^d \delta^d(Q - p_i - p_j - p_k)
\end{aligned}
\tag{3.48}
$$

If we rewrite this in terms of the shifted momenta then we have:

$$\begin{aligned} & d\Phi(p_i, p_j, p_k; Q) \\ & = d\Phi(\tilde{p}_{ij}, \tilde{p}_j; Q) \frac{d^d p_i}{(2\pi^{d-1})} \delta_+(p_i^2) \mathcal{J}(p_i; \tilde{p}_{ij}, \tilde{p}_j) \\ & \equiv d\Phi(\tilde{p}_{ij}, \tilde{p}_j; Q) \{dp_i(\tilde{p}_{ij}, \tilde{p}_k, \tilde{z}_i, y_{ij,k})\} \end{aligned} \tag{3.49}$$

Where $\mathcal{J}$, the Jacobian for this change of variables, is:

$$\mathcal{J}(p_i; \tilde{p}_{ij}, \tilde{p}_j) = \Theta(1 - \tilde{z}_i)\Theta(1 - y_{ij,k}) \frac{(1 - y_{ij,k})^{d-3}}{1 - \tilde{z}_i} \tag{3.50}$$

Where the $\tilde{z}_i$ and $y_{ij,k}$ variables are as defined in eq(3.23). We can now rewrite $\{dp_i(\tilde{p}_{ij}, \tilde{p}_k, \tilde{z}_i, y_{ij,k})\}$ in terms of these dipole variables as follows:

$$\begin{aligned} & \{dp_i(\tilde{p}_{ij}, \tilde{p}_k, \tilde{z}_i, y_{ij,k})\} = \\ & \frac{(2\tilde{p}_{ij}\tilde{p}_k)^{1-\epsilon}}{16\pi^2} \frac{d\Omega^{d-3}}{(2\pi)^{1-2\epsilon}} d\tilde{z}_i dy_{ij,k} \\ & \Theta(\tilde{z}_i(1 - \tilde{z}_i))\Theta(y_{ij,k}(1 - y_{ij,k}))(\tilde{z}_i(1 - \tilde{z}_i))^{-\epsilon}(1 - y_{ij,k})^{1-2\epsilon} y_{ij,k}^{-\epsilon} \end{aligned} \tag{3.51}$$

We can now, in principle, perform the integral:

$$\begin{aligned} & \int \{dp_i(\tilde{p}_{ij}, \tilde{p}_k, \tilde{z}_i, y_{ij,k})\} \mathcal{D}_k^{ij} = \\ & -\mathcal{V}_{ij,k} \frac{T_k . T_{ij}}{T_{ij}^2} |\mathcal{M}_{\tilde{ij},\tilde{k}}|^2 \end{aligned} \tag{3.52}$$

Here we have done the phase space integral over the emitted parton i leaving us with the two body phase space integral still to do. If we look at eq(3.49) we can see that the two body phase space left over is an integral over the shifted momenta. In eq(3.52) we see that the integrand's dependence on the shifted momenta is just the normal tree level interference with the shifted momenta as arguments. The consequence of this is that the two body phase space integral will be equal to the normal unshifted phase space integral of the normal, unshifted matrix element squared.

The $\mathcal{V}$ terms in eq(3.52) are:

$$\begin{aligned}
\mathcal{V}_{ij,k} &= \int \{dp_i(\tilde{p}_{ij}, \tilde{p}_k, \tilde{z}_i, y_{ij,k})\} \frac{1}{2p_i.p_j} V_{ij,k} \\
&= \frac{\alpha_S}{2\pi} \frac{1}{\Gamma(1-\epsilon)} \left(\frac{4\pi\mu^2}{2\tilde{p}_{ij}.\tilde{p}_k} \right)^{\epsilon} \mathcal{V}_{ij} \\
\mathcal{V}_{ij} &= c_F \left[\frac{1}{\epsilon^2} + \frac{3}{2\epsilon} + \frac{9}{2} - \frac{\pi^2}{2} + \mathcal{O}(\epsilon) \right] \quad (\text{as } \epsilon \to 0)
\end{aligned} \tag{3.53}$$

$V_{ij,k}$ is defined in eq(3.22).

Integrating $\mathcal{D}_{ij}^a$

In the case of an initial state spectator and a final state emitter the three body phase space is:

$$\begin{aligned}
&d\Phi(p_i, p_j; Q + p_a) = \\
&\frac{d^d p_i}{(2\pi)^{d-1}} \delta_+(p_i^2) \frac{d^d p_j}{(2\pi)^{d-1}} \delta_+(p_j^2) (2\pi)^d \delta^{(d)}(Q + p_a - p_i - p_j)
\end{aligned} \tag{3.54}$$

If we again split off the phase space of the single emitted parton we end up with the phase space convolution:

$$\begin{aligned}
&d\Phi(p_i, p_j; Q + p_a) = \int_0^1 dx d\Phi(\tilde{p}_{ij}; Q + x p_a) \times \\
&\left\{ \frac{d^d p_i}{(2\pi)^{d-1}} \delta_+(p_i^2) \Theta(x) \Theta(1-x) \delta(x - x_{ij,a}) \frac{1}{1 - \tilde{z}_i} \right\} \\
&\equiv \int_0^1 dx d\Phi(\tilde{p}_{ij}; Q + x p_a) \{dp_i(\tilde{p}_{ij}, p_a, x_{ij,a}, \tilde{z}_i; x)\}
\end{aligned} \tag{3.55}$$

Where the term in braces is the single particle phase space and the Jacobian for this change of variables.

Again we can re-express the Jacobian and the single body phase space (the term in braces) in terms of the dipole variables (and, in this case, also in terms of the convolution

variable x) as follows:

$$\{dp_i(\tilde{p}_{ij}, p_a, x_{ij,a}, \tilde{z}_i; x)\} =$$
$$\frac{(2\tilde{p}_{ij}p_a)^{1-\epsilon}}{16\pi^2}\frac{d\Omega^{d-3}}{(2\pi)^{1-2\epsilon}}d\tilde{z}_i dx_{ij,a}\Theta(\tilde{z}_i(1-\tilde{z}_i))\Theta(x(1-x))$$
$$(\tilde{z}_i(1-\tilde{z}_i))^{-\epsilon}\delta(x-x_{ij,a})(1-x)^{-\epsilon} \tag{3.56}$$

So for the integral of the dipole we will have:

$$\int\{dp_i(\tilde{p}_{ij}, p_a, x_{ij,a}, \tilde{z}_i; x)\}\mathcal{D}_{ij}^a =$$
$$\frac{\alpha_S}{2\pi}\frac{1}{\Gamma(1-\epsilon)}\left(\frac{4\pi\mu^2}{2\tilde{p}_{ij}p_a}\right)^{\epsilon}\mathcal{V}_{ij}(x;\epsilon)\frac{T_{ij}.T_a}{T_{ij}^2}|\mathcal{M}_{\tilde{ij},\tilde{a}}|^2 \tag{3.57}$$

Where $\mathcal{V}_{ij}(x;\epsilon)$ is defined similarly to before:

$$\int\{dp_i(\tilde{p}_{ij}, p_a, x_{ij,a}, \tilde{z}_i; x)\}V_{ij}^a =$$
$$\frac{\alpha_S}{2\pi}\frac{1}{\Gamma(1-\epsilon)}\left(\frac{4\pi\mu^2}{2\tilde{p}_{ij}p_a}\right)^{\epsilon}\mathcal{V}_{ij}(x;\epsilon) \tag{3.58}$$

We have to be a little more careful about the exact behaviour of $\mathcal{V}_{ij}(x;\epsilon)$ as ϵ approaches zero as we pick up a singularity in x at $x = 1$. To avoid this we introduce the + prescription. If we do this we obtain:

$$\mathcal{V}_{ij}(x;\epsilon) = [\mathcal{V}_{ij}(x;\epsilon)]_+ + \delta(1-x)\int_0^1 dz\mathcal{V}_{ij}(z;\epsilon) \tag{3.59}$$

where the 'plus prescription' part is defined (for some non plus prescription function f) as:

$$\int_0^1 dx f(x)[\mathcal{V}_{ij}(x;\epsilon)]_+ = \int_0^1 dx(f(x)-f(1))[\mathcal{V}_{ij}(x;\epsilon)] \tag{3.60}$$

If we perform the integral of V_{ij}^a then we obtain:

$$\mathcal{V}_{ij}(x;\epsilon) =$$
$$c_F\left[\left(\frac{2}{1-x}ln\frac{1}{1-x}\right)_+ - \frac{3}{2}\left(\frac{1}{1-x}\right)_+ + \frac{2}{1-x}ln(2-x)\right]$$
$$+\delta(1-x)\left[\mathcal{V}_{ij} - \frac{3}{2}c_F\right] + \mathcal{O}(\epsilon) \tag{3.61}$$

Where $\mathcal{V}_{ij}$ is the function given in eq(3.53).

Integrating $\mathcal{D}_k^{ai}$

We now consider the case with an initial state emitter and a final state spectator.

Again we split off the single particle part of the phase space and are left with the phase space convolution:

$$\begin{aligned} &d\Phi(p_i,p_k;Q+p_a) = \int_0^1 dx d\Phi(\tilde{p}_k;Q+xp_a) \\ &\frac{d^dp_i}{(2\pi)^{d-1}}\delta_+(p_i^2)\Theta(x)\Theta(1-x)\delta(x-x_{ik,a})\frac{1}{1-u_i} \\ &\equiv \int_0^1 dx d\Phi(\tilde{p}_k;Q+xp_a)\{dp_i(\tilde{p}_k,p_a,x_{ik,a},u_i;x)\} \end{aligned} \tag{3.62}$$

We now change variables to obtain an integral over the dipole variables u_i and $x_{ik,a}$:

$$\begin{aligned} &\{dp_i(\tilde{p}_k,p_a,x_{ik,a},u_i;x)\} = \\ &\frac{(2\tilde{p}_k p_a)^{1-\epsilon}}{16\pi^2}\frac{d\Omega^{(d-3)}}{(2\pi)^{1-2\epsilon}}du_i dx_{ik,a} \\ &\Theta(u_i(1-u_i))\Theta(x(1-x))(u_i(1-u_i))^{-\epsilon}\delta(x-x_{ik,a})(1-x)^{-\epsilon} \end{aligned} \tag{3.63}$$

(Note that we can easily perform the $x_{ik,a}$ integral due to the presence of the delta function)

We once again define a $\mathcal{V}$ term as the integral of the relevant V term:

$$\begin{aligned} &\int\{dp_i(\tilde{p}_k,p_a,x_{ik,a},u_i;x)\}\frac{1}{p_i.p_a}V_k^{ai}(x_{ik,a};u_i) = \\ &\frac{\alpha_S}{2\pi}\frac{1}{\Gamma(1-\epsilon)}\left(\frac{4\pi\mu^2}{2\tilde{p}_k p_a}\right)^{\epsilon}\mathcal{V}^{a,ai}(x;\epsilon) \end{aligned} \tag{3.64}$$

So the integral of the dipole over the single particle phase space will be:

$$\begin{aligned} &\int\{dp_i(\tilde{p}_k,p_a,x_{ik,a},u_i;x)\}\mathcal{D}_k^{ai} = \\ &\frac{\alpha_S}{2\pi}\frac{1}{\Gamma(1-\epsilon)}\left(\frac{4\pi\mu^2}{2\tilde{p}_k p_a}\right)^{\epsilon}\mathcal{V}^{a,ai}(x;\epsilon) \\ &\times\frac{T_k.T_{ai}}{T_{ai}^2}|\mathcal{M}_{\tilde{ai},\tilde{k}}|^2 \end{aligned} \tag{3.65}$$

The expression we obtain for $\mathcal{V}^{a,ai}(x;\epsilon)$ (when a and ai both correspond to quarks as is the case in the calculations presented here) is:

$$\mathcal{V}^{q,q}(x;\epsilon) = -\frac{1}{\epsilon}P^{qq}(x) + \delta(1-x)\left[\mathcal{V}_{qg}(\epsilon) + \left(\frac{2}{3}\pi^2 - 5\right)c_F\right]$$
$$+c_F\left[-\left(\frac{4}{1-x}ln\frac{1}{1-x}\right)_+ - \frac{2}{1-x}ln(2-x) + (1-x)\right.$$
$$\left.-(1+x)ln(1-x)\right] \tag{3.66}$$

Where P^{qq}, the Altarelli Parisi function for emission of a gluon from a quark, is:

$$P^{qq}(x) = c_F\left(\frac{1+x^2}{1-x}\right)_+ \tag{3.67}$$

Integrating $\mathcal{D}_b^{ai}$

We finally consider the second case with an initial state emitter, that with an initial state spectator. Splitting off the p_i part of the integral we obtain:

$$d\Phi(p_i, k_j ...; p_a + p_b)$$
$$= \int_0^1 dx d\Phi(\tilde{k}_j ...; xp_a + p_b)\frac{d^d p_i}{(2\pi)^{d-1}}\delta_+(p_i^2)\Theta(x)\Theta(1-x)\delta(x - x_{i,ab})$$
$$\equiv \int_0^1 dx d\Phi(\tilde{k}_j ...; xp_a + p_b)\{dp_i(p_a, p_b, x_{i,ab}; x)\} \tag{3.68}$$

Once again - this can be rewritten in terms of the dipole variables:

$$\{dp_i(p_a, p_b, x_{i,ab}; x)\} =$$
$$\frac{(2p_a p_b)^{1-\epsilon}}{16\pi^2}\frac{d\Omega^{d-3}}{(2\pi)^{1-2\epsilon}}d\tilde{\nu}_i dx_{i,ab}\Theta(x(1-x))\Theta(\tilde{\nu}_i)\theta\left(1 - \frac{\tilde{\nu}_i}{1-x}\right)$$
$$(1-x)^{-2\epsilon}\delta(x - x_{i,ab})\left(\frac{\tilde{\nu}_i}{1-x}\left(1 - \frac{\tilde{\nu}_i}{1-x}\right)\right) \tag{3.69}$$

(Where we have defined the new dipole variable $\tilde{\nu}_i = \frac{p_a.p_i}{p_a.p_b}$)

Once again we define the integral of the V term as:

$$\int\{dp_i(p_a, p_b, x_{i,ab}; x)\}\frac{1}{2p_a.p_i}V^{a,ib}(x_{i,ab}) =$$
$$\frac{\alpha_S}{2\pi}\frac{1}{\Gamma(1-\epsilon)}\left(\frac{4\pi\mu^2}{2p_a.p_b}\right)^{\epsilon}\tilde{\mathcal{V}}^{a,ai} \tag{3.70}$$

So the integral of the dipole over the single particle phase space will be:

$$\int \{dp_i(p_a, p_b, x_{i,ab}; x)\} \mathcal{D}_b^{ai} =$$
$$\frac{\alpha_S}{2\pi} \frac{1}{\Gamma(1-\epsilon)} \left(\frac{4\pi\mu^2}{2p_a.p_b}\right)^{\epsilon} \tilde{\mathcal{V}}^{a,ai}$$
$$\frac{T_b.T_{ai}}{T_{ai}^2} |\mathcal{M}_{\tilde{ai},\tilde{b}}|^2 \tag{3.71}$$

Where, after performing the integral, we obtain an expression for $\tilde{\mathcal{V}}^{a,ai}$ of the form:

$$\tilde{\mathcal{V}}^{a,ai} = \mathcal{V}^{a,ai} + T_a^2 \left[\left(\frac{2}{1-x} ln \frac{1}{1-x} \right)_+ + \frac{2}{1-x} ln(2-x) \right]$$
$$+\tilde{K}^{ab}(x) + \mathcal{O}(\epsilon)$$
$$\tilde{K}^{ab}(x) = P_{reg}^{qq}(x) ln(1-x) + T_a^2 \left[\left(\frac{2}{1-x} ln(1-x) \right)_+ - \frac{\pi^2}{3} \delta(1-x) \right] \tag{3.72}$$

$\mathcal{V}^{a,ai}$ is the same expression as given in eq(3.66) and $P_{reg}^{qq}(x) = -c_F(1+x)$

3.4 Constructing σ^{NLO}

The total expression for the NLO cross section is:

$$\sigma^{NLO} = \int_{[1,2,3]} (d\sigma^R - d\sigma^A) +$$
$$\left[\int_{[1,2,3]} d\sigma^A + \int_{[1,2]} d\sigma^V + \int_{[1,2]} d\sigma^C \right] \tag{3.73}$$

Where $d\sigma^C$ is the initial state collinear counter term:

$$d\sigma^C(p_a, p_b, \mu_F) =$$
$$-\frac{\alpha_S}{2\pi} \frac{1}{\Gamma(1-\epsilon)} \int_0^1 dy \int_0^1 dz d\sigma^{Born}(yp_a, zp_b)$$
$$\left\{ \delta(1-z) \left[-\frac{1}{\epsilon} \left(\frac{4\pi\mu^2}{\mu_F^2} \right)^{\epsilon} P^{aa}(y) \right] \right.$$
$$\left. +\delta(1-y) \left[-\frac{1}{\epsilon} \left(\frac{4\pi\mu^2}{\mu_F^2} \right)^{\epsilon} P^{bb}(z) \right] \right\} \tag{3.74}$$

Where:

$$d\sigma^{Born}(p_a, p_b) = \frac{\mathcal{N}_{in}}{n_s(a) n_s(b) \Phi(p_a p_b)} d\Phi(p_1, p_2; p_a, p_b) \frac{1}{S} F_J(p_1, p_2; p_a, p_b)$$
$$\times |\mathcal{M}_{p_a,p_b}|^2 \tag{3.75}$$

This is the Altarelli-Parisi subtraction term. This term arises to account for the IR divergences associated with the $3 \rightarrow 2$ body interactions that are absorbed into the PDF's.

We will now consider each term separately. The first term $(\int_{[1,2,3]}(d\sigma^R - d\sigma^A))$ can be integrated over the three body phase space as it is finite in both the soft and collinear regions (by construction, as shown above).

We now look at the $\int_{[1,2,3]} d\sigma^A$ term. In terms of the dipoles $d\sigma^A$ is (in the case of two to two quark scattering):

$$\begin{aligned}
&d\sigma^A(p_a,p_b) = \mathcal{N}_{in}\frac{1}{S}d\Phi(p_1,p_2,p_3)\times \\
&\{\mathcal{D}_{13,2}\times F_J(\tilde{p}_{13},\tilde{p}_2,p_a,p_b) + \mathcal{D}_{23,1}\times F_J(\tilde{p}_1,\tilde{p}_{23},p_a,p_b) \\
&+\mathcal{D}^a_{13}\times F_J(\tilde{p}_{13},p_2,\tilde{p}_a,p_b) + \mathcal{D}^a_{23}\times F_J(p_1,\tilde{p}_{23},\tilde{p}_a,p_b) \\
&+\mathcal{D}^b_{13}\times F_J(\tilde{p}_{13},p_2,p_a,\tilde{p}_b) + \mathcal{D}^b_{23}\times F_J(p_1,\tilde{p}_{23},p_a,\tilde{p}_b) \\
&+\mathcal{D}^{a3}_1\times F_J(\tilde{p}_1,p_2,\tilde{p}_{a3},p_b) + \mathcal{D}^{a3}_2\times F_J(p_1,\tilde{p}_2,\tilde{p}_{a3},p_b) \\
&+\mathcal{D}^{b3}_1\times F_J(\tilde{p}_1,p_2,p_a,\tilde{p}_{b3}) + \mathcal{D}^{b3}_2\times F_J(p_1,\tilde{p}_2,p_a,\tilde{p}_{b3}) \\
&+\mathcal{D}^{a3,b}\times F_J(\tilde{p}_1,\tilde{p}_2,\tilde{p}_{a3},p_b) + \mathcal{D}^{b3,a}\times F_J(\tilde{p}_1,\tilde{p}_2,p_a,\tilde{p}_{b3})\}
\end{aligned} \tag{3.76}$$

We split the dipole term into four parts:

$$d\sigma^A(p_a,p_b) = d\sigma^{A1}(p_a,p_b) + d\sigma^{A2}(p_a,p_b) + d\sigma^{A3}(p_a,p_b) + d\sigma^{A4}(p_a,p_b) \tag{3.77}$$

Each of these terms refers to the sum of a particular kind of dipole - specifically $A1$ is the sum of all final emitter - final spectator dipoles, $A2$ is the sum of all final emitter - initial spectator dipoles, $A3$ is the sum of all initial emitter - final spectator dipoles and $A4$ is the sum of all initial emitter - initial spectator dipoles. We will look at each of these in sequence:

The Expression for $d\sigma^{A1}$

Firstly we will consider the part of $d\sigma^A$ that contains the final state emitter - final state spectator dipoles ($\mathcal{D}_2^{13}$ and $\mathcal{D}_1^{23}$).

The expression for this sum of dipoles is built up from the expressions given in section(3.3.4).

$$\begin{aligned}
&\int_{[1,2,3]} d\sigma^{A1} = -\int_{[1,2]} \mathcal{N}_{in} \times \\
&\Bigg\{ d\Phi(\tilde{p}_{13},\tilde{p}_2;p_a,p_b)\frac{1}{S}F_J(\tilde{p}_{13},\tilde{p}_2;p_a,p_b) \\
&\frac{T_{13}.T_2}{T_{13}^2}|\mathcal{M}_{\tilde{13},\tilde{2}}|^2\frac{\alpha_S}{2\pi}\frac{1}{\Gamma(1-\epsilon)}\left(\frac{4\pi\mu^2}{2\tilde{p}_{13}.\tilde{p}_2}\right)^{\epsilon}\mathcal{V}_{13}(\epsilon) \\
&+d\Phi(\tilde{p}_1,\tilde{p}_{23};p_a,p_b)\frac{1}{S}F_J(\tilde{p}_1,\tilde{p}_{23};p_a,p_b) \\
&\frac{T_1.T_{23}}{T_{23}^2}|\mathcal{M}_{\tilde{1},\tilde{23}}|^2\frac{\alpha_S}{2\pi}\frac{1}{\Gamma(1-\epsilon)}\left(\frac{4\pi\mu^2}{2\tilde{p}_{13}.\tilde{p}_2}\right)^{\epsilon}\mathcal{V}_{23}(\epsilon)\Bigg\}
\end{aligned} \tag{3.78}$$

Where $\mathcal{N}_{in}$ is a catch all term for non QCD dependent quantities and the $\frac{1}{S}$ term is a symmetry factor. $\mathcal{V}_{ij}(\epsilon)$ is defined in eq(3.53)

If we change the variables of integration in both the first and second terms of eq(3.78) from the shifted to the unshifted momenta then we can gather the terms (noting that $\mathcal{V}_{13}=\mathcal{V}_{23}$) under a single phase space integral as follows:

$$\begin{aligned}
&\int_{[1,2,3]} d\sigma^{A1} = -\int_{[1,2]} 2\mathcal{N}_{in}d\Phi(p_1,p_2;p_a,p_b)\frac{1}{S}F_J(p_1,p_2;p_a,p_b) \\
&\frac{T_1.T_2}{c_F}|\mathcal{M}|^2\frac{\alpha_S}{2\pi}\frac{1}{\Gamma(1-\epsilon)}\left(\frac{4\pi\mu^2}{2p_1.p_2}\right)^{\epsilon}\mathcal{V}_{qg}(\epsilon)
\end{aligned} \tag{3.79}$$

For later convenience we will make the definition:

$$I(\epsilon,p_1,p_2) \equiv -\frac{T_1.T_2}{c_F}\frac{\alpha_S}{2\pi}\frac{1}{\Gamma(1-\epsilon)}\left(\frac{4\pi\mu^2}{2p_1.p_2}\right)^{\epsilon}\mathcal{V}_{qg}(\epsilon) \tag{3.80}$$

So:

$$\int_{[1,2,3]} d\sigma^{A1} = \int_{[1,2]} d\sigma^{Born} \times I(\epsilon,p_1,p_2) \tag{3.81}$$

The Expression for $d\sigma^{A2}$

This part of $d\sigma^{A}$ contains the four dipole terms with an initial state spectator and a final state emitter ($\mathcal{D}^{a}_{13}$, $\mathcal{D}^{a}_{23}$, $\mathcal{D}^{b}_{13}$ and $\mathcal{D}^{b}_{23}$).

Again, using the expressions shown in section(3.3.4) we obtain:

$$\begin{aligned}
&\int_{[1,2,3]} d\sigma^{A2} = -\int_{[1,2]} \mathcal{N}_{in} \int_0^1 dx \times \\
&\Bigg\{ d\Phi(\tilde{p}_{13}, p_2; xp_a, p_b) \frac{1}{S} F_J(\tilde{p}_{13}, p_2; xp_a, p_b) \\
&\frac{T_{13}.T_a}{T^2_{13}} |\mathcal{M}_{\tilde{13},xp_a}|^2 \frac{\alpha_S}{2\pi} \frac{1}{\Gamma(1-\epsilon)} \left(\frac{4\pi\mu^2}{2\tilde{p}_{13}.p_a} \right)^{\epsilon} \mathcal{V}_{13}(x,\epsilon) \\
&+ d\Phi(p_1, \tilde{p}_{23}; xp_a, p_b) \frac{1}{S} F_J(p_1, \tilde{p}_{23}; xp_a, p_b) \\
&\frac{T_{23}.T_a}{T^2_{23}} |\mathcal{M}_{\tilde{23},xp_a}|^2 \frac{\alpha_S}{2\pi} \frac{1}{\Gamma(1-\epsilon)} \left(\frac{4\pi\mu^2}{2\tilde{p}_{23}.p_a} \right)^{\epsilon} \mathcal{V}_{23}(x,\epsilon) + (a \to b) \Bigg\}
\end{aligned} \tag{3.82}$$

(Note that this expression depends on xp_a this is because we have used the delta function $\delta(x - x_{ij,a})$ in eq(3.55) to do the $x_{ij,a}$ integral) In a similar fashion to the final - final case we can rewrite this as:

$$\begin{aligned}
&\int_{[1,2,3]} d\sigma^{A2} = -\int_{[1,2]} \mathcal{N}_{in} \int_0^1 dx d\Phi(p_1, p_2; xp_a, p_b) \frac{1}{S} F_J(p_1, p_2; xp_a, p_b) \times \\
&|\mathcal{M}_{xp_a}|^2 \mathcal{V}_{qg}(x,\epsilon) \\
&\left\{ \frac{T_1.T_a}{c_F} \frac{\alpha_S}{2\pi} \frac{1}{\Gamma(1-\epsilon)} \left(\frac{4\pi\mu^2}{2p_1.p_a} \right)^{\epsilon} + \frac{T_2.T_a}{c_F} \frac{\alpha_S}{2\pi} \frac{1}{\Gamma(1-\epsilon)} \left(\frac{4\pi\mu^2}{2p_2.p_a} \right)^{\epsilon} \right\} \\
&+ (a \to b)
\end{aligned} \tag{3.83}$$

$\mathcal{V}_{qg}(x,\epsilon)$ is defined in eq(3.61) as:

$$\begin{aligned}
&\mathcal{V}_{qg}(x,\epsilon) = \\
&c_F \left[\left(\frac{2}{1-x} ln \frac{1}{1-x} \right)_+ - \frac{3}{2} \left(\frac{1}{1-x} \right)_+ + \frac{2}{1-x} ln(2-x) \right] \\
&+ \delta(1-x) \left[\mathcal{V}_{qg}(\epsilon) - \frac{3}{2} c_F \right]
\end{aligned}$$

If we plug this into eq(3.83) we obtain (using the delta function $\delta(1-x)$ to do the x integral in some terms) we obtain:

$$\int_{[1,2,3]} d\sigma^{A2} = -\int_{[1,2]} \mathcal{N}_{in} \int_0^1 dx d\Phi(p_1,p_2;xp_a,p_b)\frac{1}{S}F_J(p_1,p_2;xp_a,p_b)\times$$
$$|\mathcal{M}_{xp_a}|^2 c_F \left[\left(\frac{2}{1-x}ln\frac{1}{1-x}\right)_+ - \frac{3}{2}\left(\frac{1}{1-x}\right)_+ + \frac{2}{1-x}ln(2-x) - \delta(1-x)\frac{3}{2}\right]$$
$$\left\{\frac{T_1.T_a}{c_F}\frac{\alpha_S}{2\pi}\frac{1}{\Gamma(1-\epsilon)}\left(\frac{4\pi\mu^2}{2p_1.p_a}\right)^\epsilon + \frac{T_2.T_a}{c_F}\frac{\alpha_S}{2\pi}\frac{1}{\Gamma(1-\epsilon)}\left(\frac{4\pi\mu^2}{2p_2.p_a}\right)^\epsilon\right\}$$
$$+\left\{\int_{[1,2]} d\sigma^{Born}\times I(\epsilon,p_1,p_a) + \int_{[1,2]} d\sigma^{Born}\times I(\epsilon,p_2,p_a)\right\}$$
$$+(a\to b) \tag{3.84}$$

The Expression for $d\sigma^{A3}$

This part of $d\sigma^A$ contains the four dipole terms with a final state spectator and an initial state emitter ($\mathcal{D}_1^{a3}$, $\mathcal{D}_2^{a3}$, $\mathcal{D}_1^{b3}$ and $\mathcal{D}_2^{b3}$).

Again using the integrations shown in section(3.3.4) we have:

$$\int_{[1,2,3]} d\sigma^{A3} = -\int_{[1,2]} \mathcal{N}_{in}\int_0^1 dx$$
$$\left\{d\Phi(\tilde{p}_1,p_2;xp_a,p_b)\frac{1}{S}F_J(\tilde{p}_1,p_2;xp_a,p_b)\right.$$
$$\frac{T_{a3}.T_1}{T_{a3}^2}|\mathcal{M}_{\tilde{1},xp_a}|^2\frac{\alpha_S}{2\pi}\frac{1}{\Gamma(1-\epsilon)}\left(\frac{4\pi\mu^2}{2\tilde{p}_1.p_a}\right)^\epsilon \mathcal{V}^{a,ai}(x,\epsilon)$$
$$+d\Phi(p_1,\tilde{p}_2;xp_a,p_b)\frac{1}{S}F_J(p_1\tilde{p}_2;xp_a,p_b)$$
$$\left.\frac{T_{a3}.T_2}{T_{a3}^2}|\mathcal{M}_{\tilde{2},xp_a}|^2\frac{\alpha_S}{2\pi}\frac{1}{\Gamma(1-\epsilon)}\left(\frac{4\pi\mu^2}{2\tilde{p}_2.p_a}\right)^\epsilon \mathcal{V}^{a,ai}(x,\epsilon) + (a\to b)\right\} \tag{3.85}$$

Once again we may rewrite this as:

$$\int_{[1,2,3]} d\sigma^{A3} = -\int_{[1,2]} \mathcal{N}_{in}\int_0^1 dx d\Phi(p_1,p_2;xp_a,p_b)\frac{1}{S}F_J(p_1,p_2;xp_a,p_b)\times$$
$$|\mathcal{M}_{xp_a}|^2\mathcal{V}^{a,ai}(x,\epsilon)\times$$
$$\left\{\frac{T_a.T_1}{c_F}\frac{\alpha_S}{2\pi}\frac{1}{\Gamma(1-\epsilon)}\left(\frac{4\pi\mu^2}{2p_1.p_a}\right)^\epsilon + \frac{T_a.T_2}{c_F}\frac{\alpha_S}{2\pi}\frac{1}{\Gamma(1-\epsilon)}\left(\frac{4\pi\mu^2}{2p_2.p_a}\right)^\epsilon\right\}$$
$$+(a\to b) \tag{3.86}$$

$\mathcal{V}^{a,ai}(x,\epsilon)$ is defined in eq(3.66) - note that this term also includes an $I(\epsilon)$ term. So, separating out the x dependant and x independent terms we have:

$$\int_{[1,2,3]} d\sigma^{A3} = -\int_{[1,2]} \mathcal{N}_{in} \int_0^1 dx d\Phi(p_1,p_2;xp_a,p_b)\frac{1}{S}F_J(p_1,p_2;xp_a,p_b)\times$$
$$|\mathcal{M}_{xp_a}|^2(\mathcal{V}^{a,ai}(x,\epsilon)-\delta(1-x)\mathcal{V}_{qg}(\epsilon))\times$$
$$\left\{\frac{T_a.T_1}{c_F}\frac{\alpha_S}{2\pi}\frac{1}{\Gamma(1-\epsilon)}\left(\frac{4\pi\mu^2}{2p_1.p_a}\right)^{\epsilon}+\frac{T_a.T_2}{c_F}\frac{\alpha_S}{2\pi}\frac{1}{\Gamma(1-\epsilon)}\left(\frac{4\pi\mu^2}{2p_2.p_a}\right)^{\epsilon}\right\}$$
$$+\left\{\int_{[1,2]} d\sigma^{Born}\times I(\epsilon,p_1,p_a)+\int_{[1,2]} d\sigma^{Born}\times I(\epsilon,p_2,p_a)\right\}$$
$$+(a\to b) \tag{3.87}$$

The Expression for $d\sigma^{A4}$

This part of $d\sigma^A$ contains the two dipole terms with a final state spectator and final state emitter ($\mathcal{D}_b^{a3}$ and $\mathcal{D}_a^{b3}$).

$$\int_{[1,2,3]} d\sigma^{A4} = -\int_{[1,2]} \mathcal{N}_{in}\int_0^1 dx$$
$$d\Phi(p_1,p_2;xp_a,p_b)\frac{1}{S}F_J(p_1,p_2;xp_a,p_b)|\mathcal{M}_{xp_a}|^2$$
$$\frac{\alpha_S}{2\pi}\frac{1}{\Gamma(1-\epsilon)}\left(\frac{4\pi\mu^2}{2p_a.p_b}\right)^{\epsilon}\frac{T_{a3}.T_b}{T_{a3}^2}\tilde{\mathcal{V}}^{a3,a}(x,\epsilon)$$
$$+(a\to b) \tag{3.88}$$

Where $\tilde{\mathcal{V}}^{q,q}(x,\epsilon)$ is defined in eq(3.72). Again note that this expression will generate another $I(\epsilon)$ term as follows:

$$\begin{aligned}
&\int_{[1,2,3]} d\sigma^{A4} = -\int_{[1,2]} \mathcal{N}_{in} \int_0^1 dx \\
&d\Phi(p_1,p_2;xp_a,p_b)\frac{1}{S}F_J(p_1,p_2;xp_a,p_b)|\mathcal{M}_{xp_a}|^2 \\
&\frac{\alpha_S}{2\pi}\frac{1}{\Gamma(1-\epsilon)}\left(\frac{4\pi\mu^2}{2p_a.p_b}\right)^{\epsilon}\frac{T_{a3}.T_b}{T_{a3}^2}(\tilde{\mathcal{V}}^{a3,a}(x,\epsilon)-\delta(1-x)\mathcal{V}_{qg}(\epsilon)) \\
&+(a\rightarrow b) \\
&+\int_{[1,2]} d\sigma^{Born}\times I(\epsilon,p_a,p_b) \\
&+(a\rightarrow b)
\end{aligned} \tag{3.89}$$

3.4.1 The Total Expression for the Integrated Dipoles

The term proportional to $I(\epsilon)$, that is the term independent of x, will cancel the divergences in $d\sigma^V$. This is difficult to show in general but will be demonstrated in some detail in the specific case for each calculation.

If we factorise out a Born cross section that depends on (xp_a,p_b) then the x dependent parts of $d\sigma^{A2\rightarrow 4}$ can be written as (the term that depends on (p_a,xp_b) will have much the same form):

$$\begin{aligned}
&\int_{[1,2,3]} d\sigma_x^{A2} = -\int_0^1 dx \int d\sigma^{Born}(xp_a,p_b)\frac{\alpha_S}{2\pi}\frac{1}{\Gamma(1-\epsilon)} \\
&\left[\frac{T_1.T_a}{c_F}\left(\frac{4\pi\mu^2}{2p_1.p_a}\right)^{\epsilon}+\frac{T_2.T_a}{c_F}\left(\frac{4\pi\mu^2}{2p_2.p_a}\right)^{\epsilon}\right] \\
&\times(\mathcal{V}_{qg}(x,\epsilon)-\delta(1-x)\mathcal{V}_{qg}(\epsilon))
\end{aligned} \tag{3.90}$$

$$\begin{aligned}
&\int_{[1,2,3]} d\sigma_x^{A3} = -\int_0^1 dx \int d\sigma^{Born}(xp_a,p_b)\frac{\alpha_S}{2\pi}\frac{1}{\Gamma(1-\epsilon)} \\
&\left[\frac{T_1.T_a}{c_F}\left(\frac{4\pi\mu^2}{2p_1.p_a}\right)^{\epsilon}+\frac{T_2.T_a}{c_F}\left(\frac{4\pi\mu^2}{2p_2.p_a}\right)^{\epsilon}\right] \\
&\times(\mathcal{V}^{q,q}(x,\epsilon)-\delta(1-x)\mathcal{V}_{qg}(\epsilon))
\end{aligned} \tag{3.91}$$

$$\int_{[1,2,3]} d\sigma_x^{A4} = -\int_0^1 dx \int d\sigma^{Born}(xp_a, p_b) \frac{\alpha_S}{2\pi} \frac{1}{\Gamma(1-\epsilon)}$$
$$\left[\frac{T_1.T_a}{c_F}\left(\frac{4\pi\mu^2}{2p_1.p_a}\right)^{\epsilon} + \frac{T_2.T_a}{c_F}\left(\frac{4\pi\mu^2}{2p_2.p_a}\right)^{\epsilon}\right]$$
$$\times(\tilde{\mathcal{V}}^{q,q}(x,\epsilon) - \delta(1-x)\mathcal{V}_{qg}(\epsilon)) \tag{3.92}$$

We now collect these terms (along with the term in eq(3.74) proportional to $d\sigma^{Born}(xp_a, p_b)$) together:

$$\int_{[1,2,3]} d\sigma_x^A + \int_{[1,2]} d\sigma^C = \int_0^1 dx \int d\sigma^{Born}(xp_a, p_b) \times I_a(\epsilon, x, p_a, p_b) \tag{3.93}$$

Where:

$$I_a(\epsilon, x, p_a, p_b) =$$
$$\frac{\alpha_S}{2\pi}\frac{1}{\Gamma(1-\epsilon)}\Big\{$$
$$\left[\frac{T_1.T_a}{c_F}\left(\frac{4\pi\mu^2}{2p_1.p_a}\right)^{\epsilon} + \frac{T_2.T_a}{c_F}\left(\frac{4\pi\mu^2}{2p_2.p_a}\right)^{\epsilon}\right]$$
$$\times(\mathcal{V}_{qg}(x,\epsilon) - \delta(1-x)\mathcal{V}_{qg}(\epsilon))\Big\}$$
$$+\frac{\alpha_S}{2\pi}\frac{1}{\Gamma(1-\epsilon)}\Big\{$$
$$\left[\frac{T_1.T_a}{c_F}\left(\frac{4\pi\mu^2}{2p_1.p_a}\right)^{\epsilon} + \frac{T_2.T_a}{c_F}\left(\frac{4\pi\mu^2}{2p_2.p_a}\right)^{\epsilon}\right]$$
$$\times(\tilde{\mathcal{V}}^{q,q}(x,\epsilon) - \delta(1-x)\mathcal{V}_{qg}(\epsilon))$$
$$+\left[\frac{T_1.T_a}{c_F}\left(\frac{4\pi\mu^2}{2p_1.p_a}\right)^{\epsilon} + \frac{T_2.T_a}{c_F}\left(\frac{4\pi\mu^2}{2p_2.p_a}\right)^{\epsilon}\right]$$
$$\times(\tilde{\mathcal{V}}^{q,q}(x,\epsilon) - \delta(1-x)\mathcal{V}_{qg}(\epsilon))$$
$$+\left[-\frac{1}{\epsilon}\left(\frac{4\pi\mu^2}{\mu_F^2}\right)^{\epsilon} P^{qq}(x)\right]\Big\} \tag{3.94}$$

We can re-write the second term as follows:

$$
\begin{aligned}
&-\frac{\alpha_S}{2\pi}\frac{1}{\Gamma(1-\epsilon)}\Big\{ \\
&\left(\frac{T_1.T_a}{c_F}\left(\frac{4\pi\mu^2}{2p_1.p_a}\right)^{\epsilon}+\frac{T_2.T_a}{c_F}\left(\frac{4\pi\mu^2}{2p_2.p_a}\right)^{\epsilon}+\frac{T_a.T_b}{c_F}\left(\frac{4\pi\mu^2}{2p_a.p_b}\right)^{\epsilon}\right)\times \\
&\left[\mathcal{V}^{q,q}(x,\epsilon)+\frac{1}{\epsilon}P^{qq}(x)-\delta(1-x)\mathcal{V}_{qg}(\epsilon)\right] \\
&-\left(\frac{T_1.T_a}{c_F}\left(\frac{4\pi\mu^2}{2p_1.p_a}\right)^{\epsilon}+\frac{T_2.T_a}{c_F}\left(\frac{4\pi\mu^2}{2p_2.p_a}\right)^{\epsilon}+\frac{T_a.T_b}{c_F}\left(\frac{4\pi\mu^2}{2p_a.p_b}\right)^{\epsilon}+\left(\frac{4\pi\mu^2}{\mu_F^2}\right)^{\epsilon}\right)\times \\
&\frac{1}{\epsilon}P^{qq}(x) \\
&+\frac{T_a.T_b}{c_F}\left(\frac{4\pi\mu^2}{2p_a.p_b}\right)^{\epsilon}[\tilde{\mathcal{V}}^{q,q}(x,\epsilon)-\mathcal{V}^{q,q}(x,\epsilon)]\Big\}
\end{aligned}
\tag{3.95}
$$

We can simplify this expression if we notice that the term in square brackets is finite as $\epsilon \to 0$ and can be rewritten as follows:

$$
\begin{aligned}
&\mathcal{V}^{q,q}(x,\epsilon)+\frac{1}{\epsilon}P^{qq}(x)-\delta(1-x)\mathcal{V}_{qg}(\epsilon)= \\
&\bar{K}^{aa}(x)+P^{aa}(x)ln(x)-c_F\left[\left(\frac{2}{1-x}ln\frac{1}{1-x}\right)_+ +\frac{2}{1-x}ln(2-x)\right] \\
&\bar{K}^{qq}(x)= \\
&c_F\left[\left(\frac{2}{1-x}ln\frac{1-x}{x}\right)_+ -(1+x)ln\frac{1-x}{x}+(1-x)-\delta(1-x)(5-\pi^2)\right]
\end{aligned}
\tag{3.96}
$$

Given that this term has no $1/\epsilon$ poles when we make the expansion $(X)^{\epsilon} \to 1+\epsilon ln(X)+$ ... we only keep the first terms as $\epsilon \to 0$. This means that the first term in parentheses will be:

$$
\begin{aligned}
&\left(\frac{T_1.T_a}{c_F}\left(\frac{4\pi\mu^2}{2p_1.p_a}\right)^{\epsilon}+\frac{T_2.T_a}{c_F}\left(\frac{4\pi\mu^2}{2p_2.p_a}\right)^{\epsilon}+\frac{T_a.T_b}{c_F}\left(\frac{4\pi\mu^2}{2p_a.p_b}\right)^{\epsilon}\right)= \\
&\frac{(T_1+T_2+T_b).T_a}{c_F}=-1
\end{aligned}
\tag{3.97}
$$

So the entirety of the first term in eq(3.95) is:

$$
-\bar{K}^{aa}(x)-P^{aa}(x)ln(x)+c_F\left[\left(\frac{2}{1-x}ln\frac{1}{1-x}\right)_+ +\frac{2}{1-x}ln(2-x)\right] \tag{3.98}
$$

We now rewrite the second term in eq(3.95) (the term proportional to $\frac{1}{\epsilon}P^{qq}(x)$):

$$
\begin{aligned}
&-\left[\frac{T_1.T_a}{c_F}\left(\frac{4\pi\mu^2}{2p_1.p_a}\right)^{\epsilon}+\frac{T_2.T_a}{c_F}\left(\frac{4\pi\mu^2}{2p_2.p_a}\right)^{\epsilon}+\frac{T_a.T_b}{c_F}\left(\frac{4\pi\mu^2}{2p_a.p_b}\right)^{\epsilon}+\left(\frac{4\pi\mu^2}{\mu_F^2}\right)^{\epsilon}\right]\times\\
&\frac{1}{\epsilon}P^{qq}(x)\\
&=-\left[\frac{T_1.T_a}{c_F}\left(1+\epsilon ln\left(\frac{4\pi\mu^2}{2p_1.p_a}\right)\right)+\frac{T_2.T_a}{c_F}\left(1+\epsilon ln\left(\frac{4\pi\mu^2}{2p_2.p_a}\right)\right)\right.\\
&\left.\frac{T_a.T_b}{c_F}\left(1+\epsilon ln\left(\frac{4\pi\mu^2}{2p_a.p_b}\right)\right)+\left(1+\epsilon ln\left(\frac{4\pi\mu^2}{\mu_F^2}\right)\right)\right]\frac{1}{\epsilon}P^{qq}(x)\\
&=-\left[\frac{T_1.T_a}{c_F}ln\left(\frac{4\pi\mu^2}{2p_1.p_a}\right)+\frac{T_2.T_a}{c_F}ln\left(\frac{4\pi\mu^2}{2p_2.p_a}\right)+\frac{T_a.T_b}{c_F}ln\left(\frac{4\pi\mu^2}{2p_a.p_b}\right)\right.\\
&\left.+ln\left(\frac{4\pi\mu^2}{\mu_F^2}\right)+\left(\frac{(T_1+T_2+T_b).T_a}{c_F}+1\right)\frac{1}{\epsilon}\right]P^{aa}(x)
\end{aligned}
\tag{3.99}
$$

Note that by colour charge conservation the $1/\epsilon$ term will cancel and if we rewrite $ln\left(\frac{4\pi\mu^2}{\mu_F^2}\right)$ as $-\frac{(T_1+T_2+T_b).T_a}{c_F}ln\left(\frac{4\pi\mu^2}{\mu_F^2}\right)$ then we obtain:

$$
-\left[\frac{T_1.T_a}{c_F}ln\left(\frac{\mu_F^2}{2p_1.p_a}\right)+\frac{T_2.T_a}{c_F}ln\left(\frac{\mu_F^2}{2p_2.p_a}\right)+\frac{T_a.T_b}{c_F}ln\left(\frac{\mu_F^2}{2p_a.p_b}\right)\right]P^{aa}(x)
\tag{3.100}
$$

Finally we can rewrite the last term in eq(3.95) as:

$$
\frac{T_a.T_b}{c_F}\tilde{K}^{aa}(x)+T_a.T_b\left[\left(\frac{2}{1-x}ln\frac{1}{1-x}\right)+\frac{2}{1-x}ln(2-x)\right]
\tag{3.101}
$$

If we gather together eq(3.98), eq(3.100) and eq(3.101) and insert them into eq(3.94) we obtain (for $\epsilon\to 0$):

$$
\begin{aligned}
&I_a(\epsilon,x,p_a,p_b)=\\
&\frac{\alpha_S}{2\pi}\left\{\left[\frac{T_1.T_a}{c_F}\left(\frac{4\pi\mu^2}{2p_1.p_a}\right)^{\epsilon}+\frac{T_2.T_a}{c_F}\left(\frac{4\pi\mu^2}{2p_2.p_a}\right)^{\epsilon}\right]\right.\\
&\left.\times(\mathcal{V}_{qg}(x,\epsilon)-\delta(1-x)\mathcal{V}_{qg}(\epsilon))\right\}\\
&-\frac{\alpha_S}{2\pi}\left\{-\bar{K}^{aa}(x)-P^{aa}(x)ln(x)+c_F\left[\left(\frac{2}{1-x}ln\frac{1}{1-x}\right)_+\right.\right.+\frac{2}{1-x}ln(2-x)\Big]\\
&-\left[\frac{T_1.T_a}{c_F}ln\left(\frac{\mu_F^2}{2p_1.p_a}\right)+\frac{T_2.T_a}{c_F}ln\left(\frac{\mu_F^2}{2p_2.p_a}\right)+\frac{T_a.T_b}{c_F}ln\left(\frac{\mu_F^2}{2p_a.p_b}\right)\right]P^{aa}(x)\\
&\left.+\frac{T_a.T_b}{c_F}\tilde{K}^{aa}(x)+T_a.T_b\left[\left(\frac{2}{1-x}ln\frac{1}{1-x}\right)+\frac{2}{1-x}ln(2-x)\right]\right\}
\end{aligned}
\tag{3.102}
$$

So, the final expression we have collecting together both the $I(\epsilon)$ term and the x dependant part is:

$$\begin{aligned}
&\int_{[1,2,3]} d\sigma^A + \int_{[1,2]} d\sigma^C = \\
&\int_{[1,2]} [d\sigma^{Born}(p_a, p_b) \times I(\epsilon, p_a, p_b)] \\
&+ \int_{[1,2]} \int_0^1 dx [d\sigma^{Born}(xp_a, p_b) \times I_a(\epsilon, x, p_a, p_b)] \\
&+ \int_{[1,2]} \int_0^1 dx [d\sigma^{Born}(p_a, xp_b) \times I_b(\epsilon, x, p_a, p_b)]
\end{aligned} \tag{3.103}$$

We can re-express eq(3.103) as in [7] to obtain:

$$\begin{aligned}
&\int_{[1,2,3]} d\sigma^A + \int_{[1,2]} d\sigma^C = \\
&\int_{[1,2]} [d\sigma^{Born}(p_a, p_b) \times I(\epsilon, p_a, p_b)] \\
&+ \int_{[1,2]} \int_0^1 dx [d\sigma^{Born}(xp_a, p_b) \times K^{a,a}(x)] \\
&+ \int_{[1,2]} \int_0^1 dx [d\sigma^{Born}(p_a, xp_b) \times K^{b,b}(x)] \\
&+ \int_{[1,2]} \int_0^1 dx [d\sigma^{Born}(xp_a, p_b) \times P^{a,a}(x, xp_a)] \\
&+ \int_{[1,2]} \int_0^1 dx [d\sigma^{Born}(p_a, xp_b) \times P^{b,b}(x, xp_b)] \\
&\equiv \int_{[1,2]} [d\sigma^{Born}(p_a, p_b) \times I(\epsilon, p_a, p_b)] + \\
&+ \int_{[1,2]} \int_0^1 dx [\hat{\sigma}^{NLO\{1,2\}}(x; xp_a, p_b) + \hat{\sigma}^{NLO\{1,2\}}(x; p_a, xp_b)]
\end{aligned} \tag{3.104}$$

Where:

$$\begin{aligned}
&P^{a,a}(x, xp_a) = -\frac{\alpha_S}{2\pi} \left(\frac{1+x^2}{1-x} \right)_+ \frac{c_F}{T_a^2} \\
&\left[T_1.T_a ln \left(\frac{2xp_a.p_1}{\mu^2} \right) + T_2.T_a ln \left(\frac{2xp_a.p_2}{\mu^2} \right) + T_a.T_b ln \left(\frac{2xp_a.p_b}{\mu^2} \right) \right]
\end{aligned} \tag{3.105}$$

and

$$K^{a,a}(x) = \frac{\alpha_S}{2\pi}$$
$$\left[\delta^{aa}\left(T_1.T_a\frac{\gamma_1}{T_a^2} + T_2.T_a\frac{\gamma_2}{T_a^2}\right)\left(\left(\frac{1}{1-x}\right)_+ + \delta(1-x)\right)\right.$$
$$\bar{K}^{a,a}(x) - K_{FS}^{a,a}$$
$$\left.-T_a.T_b\frac{1}{T_a^2}\tilde{K}^{a,a}(x)\right], \tag{3.106}$$

where $\gamma_1/2 = \frac{3}{2}c_F$.

Following this method we are able to cancel IR divergences between the real and virtual parts of the calculations in such a way as to allow for numerical integration over the remaining phase space. The equations derived here will be used in the next two chapters where we perform calculations where we assume massless external quarks.

The subtraction method is slightly different when we allow for massive external particles (as we must for the $t\bar{t}$ calculation) and is described in chapter(6)

Chapter 4

b b-bar Production.

4.1 Introduction

The first calculation we will perform will be the one loop corrections to the $b\bar{b}$ production rate. This calculation is actually two processes ($gg \rightarrow b\bar{b}$ and four quark process nine, as designated in the following chapter) of the full four-quark calculation.

The observables that will be calculated are the total cross-section and forwards-backwards asymmetry for LHC and Tevatron. None of the polarised observables (A_{LL} etc.) will be studied for this process as RHIC (the only available polarised collider) is unable to positively identify b quarks in the final state (for a general discussion of RHIC's capabilities see [19]). Should a polarised collider become available which can tag b-jets then the appropriate calculations could easily be performed.

This calculation is potentially of some interest due to the observed discrepancy between theory and experiment at Tevatron where an excess of $b/\bar{b}$ jets has been observed [1]. Any improvement in the theoretical prediction of $b\bar{b}$ production rates at Tevatron could perhaps help to explain this observation.

Since the calculation is being performed for hadron colliders we can make the assump-

tion that we have no bottom or top quarks in the initial state. This is a reasonable assumption since we know that the Parton Distribution Functions (PDF's) for b and t quarks in the proton are very small [20] [21] [22]. This means that, in general terms, we can describe the $b\bar{b}$ productions rate as the sum of two processes:

$$gg \rightarrow q\bar{q}$$

$$q\bar{q} \rightarrow q'\bar{q}'(+\text{real gluon})$$

That is, two gluons going to quark-anti-quark pair and quark-anti-quark pair going to a quark-anti-quark pair of a different generation (none of the initial state particles will be of the same generation as the b-quark) with a possible emission of a real gluon. This means that the number of contributing interferences will be quite limited.

For the $gg \rightarrow q\bar{q}$ we will have the diagrams shown in fig(4.1). An interference between any of the tree level diagrams and one of the one loop diagrams will give an allowed interference at the order we are interested in $(\alpha_S^2\alpha_W)$. We know that the sum of these interferences will not contain any IR divergences as there are no possible gluon bremsstrahlung diagrams that we could draw to the same order for $gg \rightarrow q\bar{q}$. This means that we can safely evaluate this contribution using numerical methods. We will use similar reduction methods to those described below to simplify the box diagrams (see also the very similar processes in $t\bar{t}$).

The virtual interferences for $q\bar{q} \rightarrow q'\bar{q}'$ will be only those shown in fig(4.2) - all other interferences will have vanishing colours factors or, in the case of diagrams including W-boson exchange, will be subject to Cabibbo suppression. The $q\bar{q} \rightarrow q'\bar{q}' + g$ interferences that will cancel the IR divergences of the virtual corrections will be those shown in fig(4.3) - again, all other combinations will have vanishing colour factors.

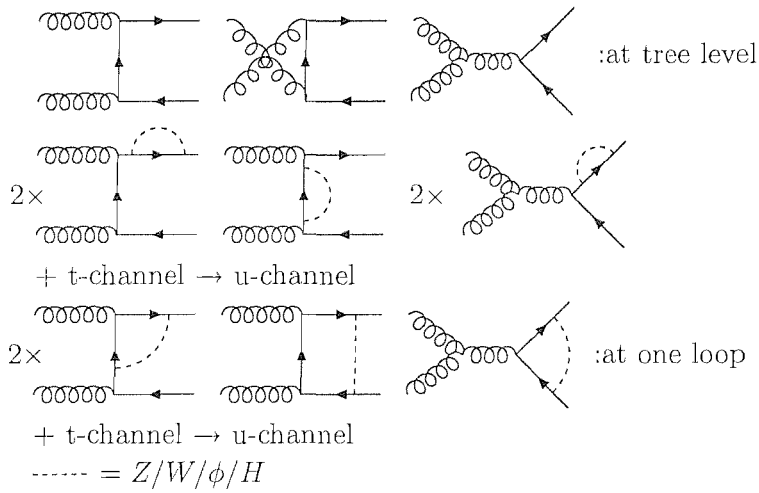

Figure 4.1: The interferences that contribute to $gg \to q\bar{q}$ at $\alpha_S^2\alpha_W$ order

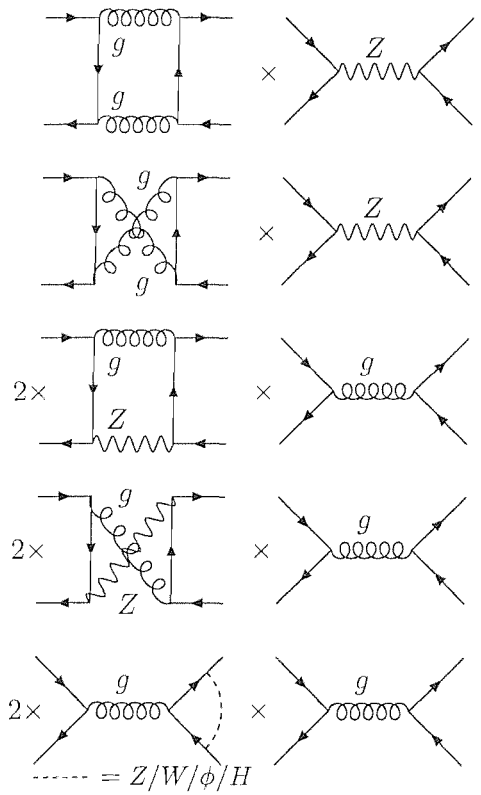

Figure 4.2: The interferences that contribute to $q\bar{q} \to q'\bar{q}'$ at $\alpha_S^2\alpha_W$ order. The factors of two attached to the box diagrams are associated with an interchange of the gluon and the Z-boson. The factor of two attached to the vertex correction diagram is associated with putting the triangle on either the initial or final state particles.

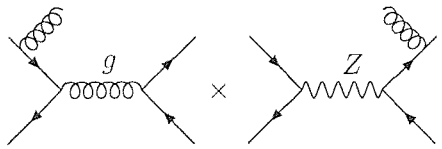

+ All permutations where we interfere initial state radiation with final state radiation

Figure 4.3: The interferences that contribute to $q\bar{q} \to q'\bar{q}' + g$ at $\alpha_S^2\alpha_W$ order

4.2 Evaluating The Virtual Corrections

The virtual correction amplitudes (here and in the full two jet calculation and $t\bar{t}$ calculation) are calculated using the following method and FORM [23].

4.2.1 Helicity Amplitudes For Massless Quarks

To evaluate the virtual corrections in the $b\bar{b}$ (and indeed for the 4-quark and $t\bar{t}$ case) case we will use the Helicity amplitudes method. This method has a number of advantages - firstly, since we are calculating amplitudes rather that interferences we expect that each expression we use will be comparatively simple (this isn't particularly important in the calculations with massless quarks but the expressions for interferences in the $t\bar{t}$ rate would be very large, potentially thousands of terms)

If we take an example of a general t-channel amplitude then we would have a diagram as described in fig(4.4). As mentioned above, all of the virtual corrections required for the $b\bar{b}$ production rate are actually in the s-channel however, we can easily cross the t-channel amplitudes generated by this method to the s-channel as is required.

For example, we will look at a box diagram with two internal gluons (fig(4.5)). This will include a box integral which we will define from the scalar Veltman & Passarino

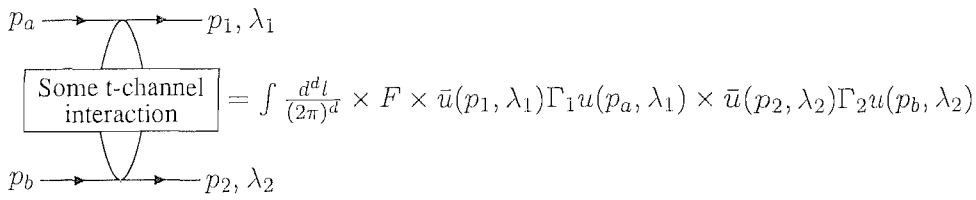

Figure 4.4: The expression for a general t-channel diagram will be of the form shown here. F is some overall factor including couplings, colour factors and internal propagators, $\Gamma_{1,2}$ are strings of gamma matrices and momenta (including loop momenta). We will also have an integration over any loop momenta present (this calculation is to one loop order only so there will only ever be at most one loop momentum to be integrated over).

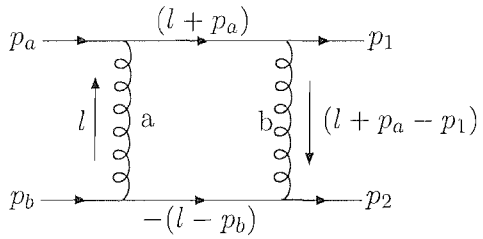

Figure 4.5: A t-channel massless box diagram

function as follows:

$$D_0 = \int \frac{d^d l}{i\pi^2} \frac{1}{l^2(l+p_a)^2(l+p_a-p_1)^2(l-p_b)^2} \equiv \int \frac{d^d l}{i\pi^2} d_0 \tag{4.1}$$

The expression for the diagram in fig(4.5) will be:

Amplitude =

$$C \times g_S^4 \int \frac{d^d l}{(2\pi)^d} \frac{-1}{l^2(l+p_a)^2(l+p_a-p_1)^2(l-p_b)^2}$$

$$\bar{u}(p_1, \lambda_1)\gamma^\mu(\not{l} + \not{p}_a)\gamma^\nu u(p_a, \lambda_1)\bar{u}(p_2, \lambda_2)\gamma^\mu(\not{l} - \not{p}_b)\gamma^\nu u(p_b, \lambda_2)$$

So the terms in fig(4.4) will be:

$$F = C \times g_S^4(-d_0)$$

$$\Gamma_1 = \gamma^\mu(\not{l} + \not{p}_a)\gamma^\nu$$

$$\Gamma_2 = \gamma^\mu(\not{l} - \not{p}_b)\gamma^\nu \tag{4.2}$$

Where C is some colour factor. In practice this factor will only be evaluated at the interference level and can therefore be dropped until that point. Also note that the terms including $\Gamma_{1,2}$ are under the loop integral.

First let's look at the p_a/p_1 line. A general form of Γ_1 is:

$$\Gamma_1 = \sum_{i=1}^{4} \gamma^\mu (a_i + b_i \gamma^5) v_{i\mu}$$
$$v_{1\mu} = p_{a\mu}, v_{2\mu} = p_{1\mu}, v_{3\mu} = p_{2\mu}, v_{4\mu} = n_\mu \tag{4.3}$$

Where n_μ is a vector of length $\sqrt{s}$ that is normal to the scattering plane.

However, from the Dirac equation for spinors, we know that:

$$\bar{u}(p_1)\not{p}_a u(p_a) = \bar{u}(p_1)\not{p}_1 u(p_a) = 0 \tag{4.4}$$

so we are only interested in the terms $a_{3,4}$ and $b_{3,4}$.

$$\begin{aligned}
&\bar{u}(p_1, \lambda_1)\Gamma_1 u(p_a, \lambda_1) = \\
&\bar{u}(p_1, \lambda_1)(a_3\not{p}_2 + b_3\not{p}_2\gamma^5)u(p_a, \lambda_1) + \bar{u}(p_1, \lambda_1)(a_4\not{n} + b_4\not{n}\gamma^5)u(p_a, \lambda_1) \\
&= (a_3 + b_3\lambda_1)\bar{u}(p_1)\left(\frac{1 - \lambda_1\gamma^5}{2}\right)\not{p}_2\, u(p_a) \\
&+(a_4 + b_4\lambda_1)\bar{u}(p_1)\left(\frac{1 - \lambda_1\gamma^5}{2}\right)\not{n} u(p_a) \\
&\equiv A_3 + A_4
\end{aligned} \tag{4.5}$$

Take the mod-square of the term including a_3/b_3 (A_3).

$$\begin{aligned}
&(a_3 + b_3\lambda_1)^2 \mathrm{Tr}\left(\not{p}_1\left(\frac{1 - \lambda_1\gamma^5}{2}\right)\not{p}_2\,\not{p}_a\,\not{p}_2\right) \\
&= (a_3 + b_3\lambda_1)^2 4(p_a.p_2)(p_1.p_2)
\end{aligned}$$

The square root of this is (we will fix the phase later):

$$A_3 = (a_3 + b_3\lambda_1)\sqrt{-su} \tag{4.6}$$

Similarly, for the term including a_4/b_4 (A_4), we obtain:

$$A_4 = (a_4 + b_4\lambda_1)\bar{u}(p_1)\left(\frac{1 - \lambda_1\gamma^5}{2}\right)\not{n} u(p_a) \to (a_4 + b_4\lambda_1)\sqrt{-ts} \tag{4.7}$$

In this process of squaring and square-rooting we have lost any information about phases. Since this amplitude will eventually be squared we don't need to worry about the absolute phase merely the relative phase between the two terms. We can extract this relative phase by evaluating the product of A_3 and A_4. Assume that the A_4 term has some phase P_4 attached to it. From eq(4.6) and eq(4.7) the product of the two terms will be:

$$A_3 A_4^* = (a_3 + b_3\lambda_1)(a_4 + b_4\lambda_1)\sqrt{-su}\sqrt{-ts} \times P_4^* \tag{4.8}$$

Where we know that $\sqrt{-su}\sqrt{-ts}$ must be positive. We also know that:

$$\begin{aligned} A_3 A_4^* &= (a_3 + b_3\lambda_1)(a_4 + b_4\lambda_1)\mathrm{Tr}\left(\not{p}_1 \left(\frac{1-\lambda_1\gamma^5}{2}\right)\not{p}_2\not{p}_a\not{n}\right) \\ &= (a_3 + b_3\lambda_1)(a_4 + b_4\lambda_1)\left\{\frac{1}{2}p_{1\mu}p_{2\nu}p_{a\rho}n_\sigma \mathrm{Tr}(\gamma^\mu\gamma^\nu\gamma^\rho\gamma^\sigma)\right. \\ &\left. + \frac{\lambda_1}{2}p_{1\mu}p_{2\nu}p_{a\rho}n_\sigma \mathrm{Tr}(\gamma^\mu\gamma^\nu\gamma^\rho\gamma^\sigma\gamma^5)\right\} \end{aligned} \tag{4.9}$$

The first term will be a sum of scalar products which will vanish since n dotted into any of the momenta is zero. So, from the second term we get:

$$A_3 A_4^* = 2(a_3 + b_3\lambda_1)(a_4 + b_4\lambda_1)p_{1\mu}p_{a\nu}p_{2\rho}n_\sigma\epsilon^{\mu\nu\rho\sigma}(i\lambda_1) \tag{4.10}$$

We now define $p_{1\mu}p_{a\nu}p_{2\rho}n_\sigma\epsilon^{\mu\nu\rho\sigma}$ to be positive (we have this freedom because n^μ can be either in or out of the scattering plane) - this means that P_4^* must be equal to $(i\lambda_1)$. ie: $P_4 = (-i\lambda_1)$.

Therefore:

$$\begin{aligned} &\bar{u}(p_1,\lambda_1)\Gamma_1 u(p_a,\lambda_1) = \\ &(a_3 + b_3\lambda_1)\sqrt{-su} - i\lambda_1(a_4 + b_4\lambda_1)\sqrt{-ts} \end{aligned} \tag{4.11}$$

We now need to find expressions for $a_{3,4}$ and $b_{3,4}$ in terms of Γ_1. From above we had:

$$\Gamma_1 = \gamma^\mu a_3 p_{2\mu} + \gamma^\mu b_3\gamma^5 p_{2\mu} + \gamma^\mu a_4 n_\mu + \gamma^\mu b_4\gamma^5 n_\mu \tag{4.12}$$

We need to define a vector w^μ such that $w.p_a = w.p_1 = w.n = 0$ and $w.p_2 = 1$.

$$w^\mu = \left[\frac{p_a^\mu}{-u} + \frac{p_1^\mu}{s} - p_2^\mu\left(\frac{t}{su}\right)\right] \tag{4.13}$$

So we have:

$$\Gamma_1\gamma^\nu w_\nu = \gamma^\mu a_3 p_{2\mu}\gamma^\nu w_\nu + \gamma^\mu b_3\gamma^5 p_{2\mu}\gamma^\nu w_\nu + \gamma^\mu a_4 n_\mu\gamma^\nu w_\nu + \gamma^\mu b_4\gamma^5 n_\mu\gamma^\nu w_\nu \tag{4.14}$$

Therefore:

$$\mathrm{Tr}(\Gamma_1\gamma^\nu w_\nu) = 4a_3 p_2^\mu w_\mu = 4a_3 \tag{4.15}$$

[Using $\mathrm{Tr}(\gamma.a\gamma.b) = 4a.b$] So, if we substitute in for w_μ we have:

$$a_3 = -\frac{1}{4su}(s\mathrm{Tr}(\Gamma_1\not{p}_a\,) - u\mathrm{Tr}(\Gamma_1\not{p}_1\,) + t\mathrm{Tr}(\Gamma_1\not{p}_2\,)) \tag{4.16}$$

Similarly if we evaluate $\mathrm{Tr}(\Gamma_1\gamma^5\gamma^\nu w_\nu)$ we obtain:

$$b_3 = -\frac{1}{4su}(s\mathrm{Tr}(\Gamma_1\gamma^5\not{p}_a\,) - u\mathrm{Tr}(\Gamma_1\gamma^5\not{p}_1\,) + t\mathrm{Tr}(\Gamma_1\gamma^5\not{p}_2\,)) \tag{4.17}$$

To find a_4 and b_4 in the same way we will need a vector that satisfies $w'.p_a = w'.p_1 = w'.p_2 = 0$ and $w'.n = 1$. $w'^\mu = -\frac{1}{s}n^\mu$ will work. From this we can discover:

$$\begin{aligned} a_4 &= -\frac{1}{4s}\mathrm{Tr}(\Gamma_1\not{n}\,) \\ b_4 &= -\frac{1}{4s}\mathrm{Tr}(\Gamma_1\gamma^5\not{n}\,) \end{aligned} \tag{4.18}$$

If we use the same method to express the Γ_2 line we obtain:

$$\bar{u}(p_2,\lambda_2)\Gamma_2 u(p_b,\lambda_2) =$$

$$(c_3 + \lambda_2 d_3)\sqrt{-su} - (i\lambda_2)(c_4 + \lambda_2 d_4)\sqrt{-st}$$

Where:

$$\begin{aligned} c_3 &= \frac{-1}{4su}(s\mathrm{Tr}(\Gamma_2\not{p}_b\,) - u\mathrm{Tr}(\Gamma_2\not{p}_2\,) + t\mathrm{Tr}(\Gamma_2\not{p}_1\,)) \\ d_3 &= \frac{-1}{4su}(s\mathrm{Tr}(\Gamma_2\gamma^5\not{p}_b\,) - u\mathrm{Tr}(\Gamma_2\gamma^5\not{p}_2\,) + t\mathrm{Tr}(\Gamma_2\gamma^5\not{p}_1\,)) \\ c_4 &= \frac{-1}{4s}\mathrm{Tr}(\Gamma_2\not{n}\,) \\ d_4 &= \frac{-1}{4s}\mathrm{Tr}(\Gamma_2\gamma^5\not{n}\,) \end{aligned} \tag{4.19}$$

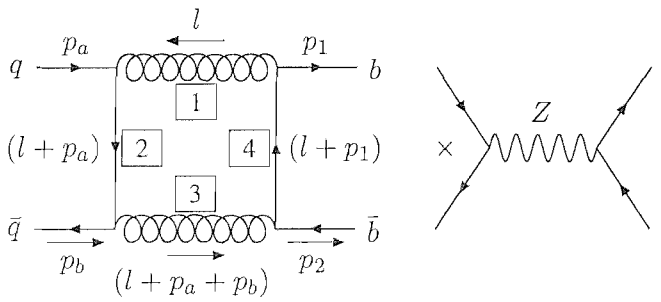

Figure 4.6: Interference between a one loop diagram with two gluons exchanged in the s-channel and a tree level diagram with a single Z-boson exchanged in the s-channel

(Note that when we extracted the relative phase between the '3' and '4' terms in this case we *must* use the convention that $p_{1\mu}p_{a\nu}p_{2\rho}n_\sigma\epsilon^{\mu\nu\rho\sigma}$ is positive as in the Γ_1 case.) So, we finally have:

$$\begin{aligned}
&\text{Amplitude} = \\
&F \times [(a_3 + \lambda_1 b_3)(c_3 + \lambda_2 d_3)(-su) \\
&-\lambda_1\lambda_2(a_4 + \lambda_1 b_4)(c_4 + \lambda_2 d_4)(-st) \\
&-i\lambda_2(a_3 + \lambda_1 b_3)(c_4 + \lambda_2 d_4)\sqrt{-su}\sqrt{-st} \\
&-i\lambda_1(a_4 + \lambda_1 b_4)(c_3 + \lambda_2 d_3)\sqrt{-su}\sqrt{-st}]
\end{aligned} \tag{4.20}$$

With $a_{3,4}$, $b_{3,4}$, $c_{3,4}$ and $d_{3,4}$ defined as above.

4.2.2 Structuring The Loop Integrals

We will deal with the loop integrals using the prescription described in the paper by Veltman & Passerino [24]. We take the example of one of the interferences that contributes to the $b\bar{b}$ rate - interference between a diagram with two gluons exchanged in the s-channel and a tree level diagram with a single Z-boson exchanged in the s-channel (fig(4.6)). The expression for this interference from the Feynman rules will

be:

$$\text{(couplings/colour)} \times \frac{1}{s}\frac{i}{16\pi^2} D_0$$

$$\mathrm{Tr}(u(p_1,\lambda_1)\bar{u}(p_1,\lambda_1)\gamma^\mu(l\!\!\!/ + p\!\!\!/_1)\gamma^\nu v(p_2,\lambda_2)\bar{v}(p_2,\lambda_2)(c_V + c_A\gamma^5)\gamma^\rho)$$

$$\mathrm{Tr}(v(p_b,\lambda_b)\bar{v}(p_b,\lambda_b)\gamma_\nu(l\!\!\!/ + p\!\!\!/_a)\gamma_\mu u(p_a,\lambda_a)\bar{u}(p_a,\lambda_a)(c_V + c_A\gamma^5)\gamma_\rho)$$

Where the scalar box integral is:

$$D_0 = \int \frac{d^d l}{i\pi^2} \frac{1}{l^2(l+p_a)^2(l+p_1)^2(l+p_a+p_b)^2} \tag{4.21}$$

To avoid having to evaluate tensor box integrals we will reduce the box diagram down to a sum of simpler triangle integrals.

From eq(4.21) we can see that we should only get at most two powers of the loop momentum in the numerator. This means that the reductions shown in eq(4.24→4.27) and eq(4.30→4.33) will be sufficient to express the interference in terms of more simple integrals.

If we again use the definition:

$$D_0 = \int \frac{d^d l}{i\pi^2} \frac{1}{l^2(l+p_a)^2(l+p_a-p_1)^2(l-p_b)^2} \equiv \int \frac{d^d l}{i\pi^2} d_0 \tag{4.22}$$

then we obtain:

$$\int \frac{d^dl}{i\pi^2} l^2 d_0 = \int \frac{d^dl}{i\pi^2} \frac{1}{(l+p_a)^2(l+p_1)^2(l+p_a+p_b)^2} \equiv C_{0(1)} \tag{4.23}$$

$$\int \frac{d^dl}{i\pi^2}(l+p_a)^2 d_0 = \int \frac{d^dl}{i\pi^2}(l^2 d_0 + 2l.p_a d_0)$$

$$= \int \frac{d^dl}{i\pi^2} \frac{1}{l^2(l+p_1)^2(l+p_a+p_b)^2} \equiv C_{0(2)}$$

$$\therefore \int \frac{d^dl}{i\pi^2} l.p_a d_0 = \frac{1}{2}(C_{0(2)} - C_{0(1)}) \tag{4.24}$$

$$\int \frac{d^dl}{i\pi^2}(l+p_1)^2 d_0 = \int \frac{d^dl}{i\pi^2}(l^2 d_0 + 2l.p_1 d_0)$$

$$= \int \frac{d^dl}{i\pi^2} \frac{1}{l^2(l+p_a)^2(l+p_a+p_b)^2} \equiv C_{0(4)}$$

$$\therefore \int \frac{d^dl}{i\pi^2} l.p_1 d_0 = \frac{1}{2}(C_{0(4)} - C_{0(1)}) \tag{4.25}$$

$$\int \frac{d^dl}{i\pi^2}(l+p_a+p_b)^2 d_0 = \int \frac{d^dl}{i\pi^2}(l^2 d_0 + 2l.p_a d_0 + 2l.p_b d_0 + s d_0)$$

$$= \int \frac{d^dl}{i\pi^2} \frac{1}{l^2(l+p_a)^2(l+p_1)^2} \equiv C_{0(3)}$$

$$\therefore \int \frac{d^dl}{i\pi^2} l.p_b d_0 = \frac{1}{2}(C_{0(3)} - l^2 \times D_0 - 2l.p_a \times D_0 - s \times D_0)$$

$$= \frac{1}{2}(C_{0(3)} - C_{0(2)} - sD_0) \tag{4.26}$$

$$p_1 + p_2 = p_a + p_b$$

$$\therefore \int \frac{d^dl}{i\pi^2} l.p_2 d_0 = \int \frac{d^dl}{i\pi^2}(l.p_a d_0 + l.p_b d_0 - l.p_1 d_0)$$

$$= \frac{1}{2}(C_{0(3)} - C_{0(4)} - sD_0) \tag{4.27}$$

Here $C_{0(a)}$ are triangle diagrams generated by 'pinching off' the propagator labelled a from fig(4.6). These triangle diagrams are shown in fig(4.7). Massless scalar and tensor triangles are comparatively easy to deal with so we can now use the methods described in [24] to simplify express the interference in terms of Veltman-Passarino (triangle)

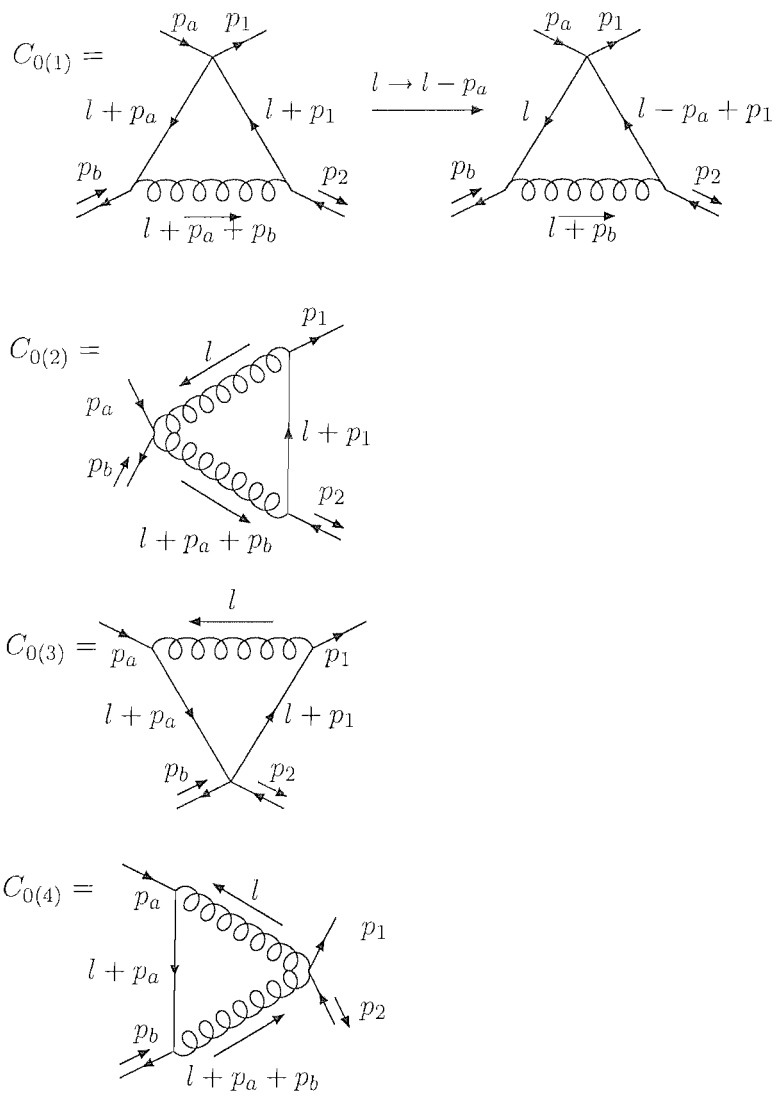

Figure 4.7: The pinched box diagrams $C_{0(1\to4)}$. Note that in $C_{0(1)}$ we have pinched off the propagator with momentum l - however it is easier to manipulate the loop integrals (using the VP methods) if we still have a $\frac{1}{l^2}$ propagator. With this in mind we will shift the loop momentum in all terms proportional to $C_{0(1)}$ (as we are free to do) such that $l \to l - p_a$ leaving us with the triangle integral shown.

functions. The general form is:

$$C_0; C_\mu; C_{\mu\nu}(p_1, p_2, m_1, m_2, m_3) =$$
$$= \frac{1}{i\pi^2}\int d^d l \frac{1; l_\mu; l_\mu l_\nu}{(l^2 - m_1^2)((l+p_1)^2 - m_2^2)((l+p_1+p_2)^2 - m_3^2)}$$
$$C_\mu = p_1^\mu C_{11} + p_2^\mu C_{12}$$
$$C_{\mu\nu} = p_1^\mu p_1^\nu C_{21} + p_2^\mu p_2^\nu C_{22} + (p_1^\mu p_2^\nu + p_2^\mu p_1^\nu) C_{23} + g_{\mu\nu} C_{24} \tag{4.28}$$

If we define:

$$C_{0(i)} \equiv \int \frac{d^d l}{i\pi^2} c_{0(i)} \tag{4.29}$$

then for the shifted $C_{0(1)}$ we have:

$$\int \frac{d^d l}{i\pi^2} c_{0(1)} l.q_1 = C_{11(1)}(p_a - p_1).q_1 - C_{12(1)} p_2.q_1$$
$$\int \frac{d^d l}{i\pi^2} c_{0(1)} l.q_1 l.q_2 = (p_a - p_1).q_1 (p_a - p_1).q_2 C_{21(1)} + p_2.q_1 p_2.q_2 C_{22(1)}$$
$$-((p_a - p_1).q_1 p_2.q_2 + (p_a - p_1).q_2 p_2.q_1) C_{23(1)} - (p_a - p_1).p_2 C_{24(1)} \tag{4.30}$$

For $C_{0(2)}$ we have:

$$\int \frac{d^d l}{i\pi^2} c_{0(2)} l.q_1 = C_{11(2)}(p_a + p_b).q_1 - C_{12(2)} p_2.q_1$$
$$\int \frac{d^d l}{i\pi^2} c_{0(2)} l.q_1 l.q_2 = (p_a + p_b).q_1 (p_a + p_b).q_2 C_{21(2)} + p_2.q_1 p_2.q_2 C_{22(2)}$$
$$-((p_a + p_b).q_1 p_2.q_2 + (p_a + p_b).q_2 p_2.q_1) C_{23(2)} - (p_a + p_b).p_2 C_{24(2)} \tag{4.31}$$

For $C_{0(3)}$ we have:

$$\int \frac{d^d l}{i\pi^2} c_{0(3)} l.q_1 = C_{11(3)} p_a.q_1 + C_{12(3)}(p_b - p_2).q_1$$
$$\int \frac{d^d l}{i\pi^2} c_{0(3)} l.q_1 l.q_2 = p_a.q_1 p_a.q_2 C_{21(3)} + (p_b - p_2).q_1 (p_b - p_2).q_2 C_{22(3)}$$
$$+(p_a.q_1 (p_b - p_2).q_2 + p_a.q_2 (p_b - p_2).q_1) C_{23(3)} + p_a.(p_b - p_2) C_{24(3)} \tag{4.32}$$

And for $C_{0(4)}$ we have:

$$\int \frac{d^d l}{i\pi^2} c_{0(4)} l.q_1 = C_{11(4)} p_a.q_1 + C_{12(4)} p_b.q_1$$
$$\int \frac{d^d l}{i\pi^2} c_{0(4)} l.q_1 l.q_2 = p_a.q_1 p_a.q_2 C_{21(4)} + p_b.q_1 p_b.q_2 C_{22(4)}$$
$$+(p_a.q_1 p_b.q_2 + p_a.q_2 p_b.q_1) C_{23(4)} + p_a.p_b C_{24(4)} \tag{4.33}$$

Although this process was described for only the box diagram with two gluons exchanged in the s-channel (as shown in fig(4.6)) however it is simple to extend it to the other box diagrams required. The box diagram with a Z-boson and a gluon exchanged in the s-channel (the first interference shown in eq(4.2)) can be dealt with as follows: We need to redefine the scalar box integral to include the Z-mass on one of the propagators, ie:

$$D_0 = \int \frac{d^d l}{i\pi^2} \frac{1}{(l^2 - m_z^2)(l + p_a)^2 (l + p_1)^2 (l + p_a + p_b)^2} \tag{4.34}$$

Here we have (compared to fig(4.6)) replaced the gluon with momentum l with a Z-boson (we could have also replaced the $l + p_a + p_b$ propagator however this choice will manifest itself as an overall factor of two on this diagram.). We also need to evaluate the contributions from the two crossed boxes (the second and fourth interferences from

fig(4.2)). These can be evaluated by using the following crossing relation:

Let:

$$B_{s,gg} = \text{masslessbox}(s, t, \lambda_1, \lambda_b)$$

and

$$B_{s,gZ} = \text{massivebox}(s, t, \lambda_1, \lambda_b, m_z)$$

Crossing gives:

$$B_{s,gg,X} = \text{masslessbox}(s, u, \lambda_1, -\lambda_b)$$

and

$$B_{s,gZ,X} = \text{massivebox}(s, u, \lambda_1, -\lambda_b, m_z) \tag{4.35}$$

Where (with all exchanges in the s-channel) $B_{s,gg}$ is the uncrossed gluon-gluon box, $B_{s,gZ}$ is the uncrossed gluon-Z box, $B_{s,gg,X}$ is the crossed gluon-gluon box and $B_{s,gZ,X}$ is the crossed gluon-Z box.

These are all of the box diagrams required for the IR divergent virtual corrections. We can now interfere these amplitudes with appropriate tree level diagrams (a Z in the s-channel for the double gluon boxes and a gluon in the s-channel for the gluon-Z boxes), calculate the relevant colour factors and thus find the interferences.

To complete the calculation of the virtual corrections for this process we also need to evaluate the one-loop weak corrections to the pure QCD tree level interferences.

These will include all of the corrections to $gg \to b\bar{b}$ (shown in fig(4.1)) and the corrections to the interference between two s-channel gluon exchanges (the last interference in fig(4.2)).

We know that the virtual corrections to $gg \to b\bar{b}$ must at least sum to being IR finite - this is because there are no possible gluon bremsstrahlung corrections to this process at $\alpha_S^2\alpha_W$ (the tree level $gg \to b\bar{b}$ is order α_S^2 so we only have weak corrections to this -

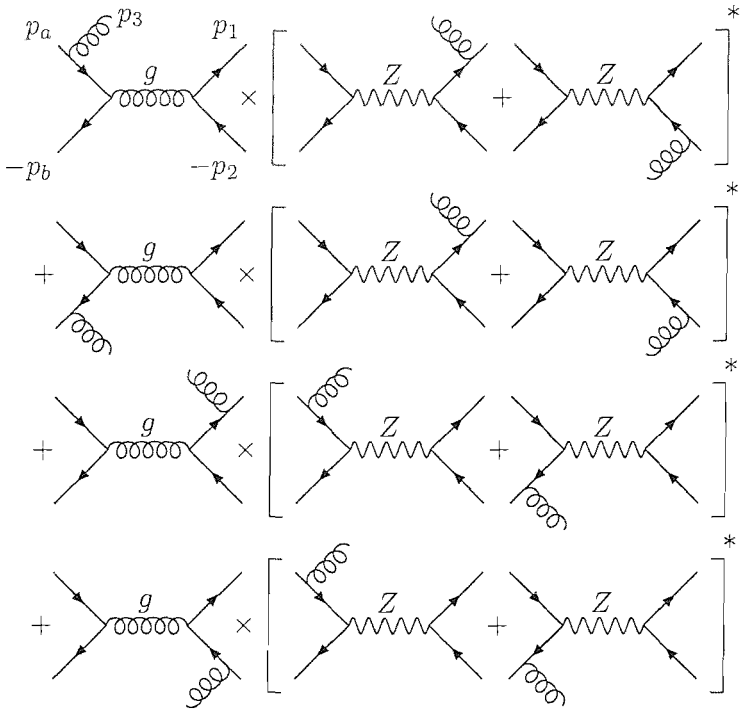

Figure 4.8: All of the real gluon emission diagrams that contribute to the $b\bar{b}$ production rate at order $\alpha_S^2\alpha_W$.

not QCD corrections) and therefore there are no collinear or soft divergences to cancel any divergences in the virtual interferences. In fact, in Feynman gauge, all of the interference graphs that contribute to the gg process are individually finite. This means that we can easily do this part of the calculation using numerical methods.

The weak vertex corrections to $q\bar{q} \rightarrow b\bar{b}$ are also individually finite so, again, we may evaluate them simply using numerical methods.

4.3 Evaluating The Real Corrections

Having evaluated all of the virtual corrections that contribute to the process we need to calculate the contribution from diagrams including real gluon emission. These interferences are those shown in fig(4.8) For example, the expression for the first interference

on the first line of fig(4.8) is:

$$\begin{aligned}
&\text{colour} \times g_s^4 \frac{g^2}{\cos^2\theta_W} \frac{1}{16} \frac{1}{2p_1.p_2} \frac{1}{2p_a.p_b} \frac{1}{-2p_a.p_3} \frac{1}{2p_1.p_3} \\
&\times \{\bar{u}(1-\lambda_1\gamma^5)\gamma^\mu v(p_2)\bar{v}(1+\lambda_b\gamma^5)\gamma_\mu(\not{p}_a - \not{p}_3\ )\gamma^\nu \epsilon_\nu(p_3)u(p_a)\} \\
&\times \{\bar{u}(p_1)(1-\lambda_1\gamma^5)\gamma^\rho \epsilon_\rho(p_3)(\not{p}_1 + \not{p}_3\ )\gamma^\sigma(c_V + c_A\gamma^5) \\
&v(p_2)\bar{v}(p_b)(1+\lambda_b\gamma^5)\gamma_\sigma(c_V + c_A\gamma^5)u(p_a)\}^* \\
&= -\frac{c_F c_A}{2} \times g_s^4 \frac{g^2}{\cos^2\theta_W} \frac{1}{16} \frac{1}{2p_1.p_2} \frac{1}{2p_a.p_b} \frac{1}{2p_a.p_3} \frac{1}{2p_1.p_3} \\
&\times \text{Tr}(\not{p}_1\ (1-\lambda_1\gamma^5)\gamma^\mu \not{p}_2\ \gamma^\sigma(\not{p}_1 + \not{p}_3\ )\gamma^\rho \epsilon^*_\rho(p_3)) \\
&\times \text{Tr}(\not{p}_b\ (1+\lambda_b\gamma^5)\gamma_\mu(\not{p}_a - \not{p}_3\ )\gamma^\nu \epsilon_\nu(p_3)\not{p}_a\ \gamma_\sigma)
\end{aligned} \tag{4.36}$$

When the traces are evaluated this expression will yield terms proportional to $1/p_1.p_3$ and $1/p_a.p_3$; these are the terms that will diverge in the soft ($p_3 \to 0$) and collinear ($p_1.p_3, p_a.p_3 \to 0$) limits. The other interferences will give terms proportional to the inverse of p_3 dotted into the other external momenta - this means that the contribution from the real corrections will go infinite when p_3 is either soft or collinear with any of the external momenta.

In the case of the $b\bar{b}$ production rate the collinear divergences will actually cancel amongst themselves.

We look at the interference between real gluon emission from particle a (where the emitted gluon has momentum xp_a. ie: the emitted gluon is collinear to particle a) and the two diagrams with real gluon emission from the two final state particles (fig(4.9)).

If we look at the expression for the gluon exchange diagram we have:

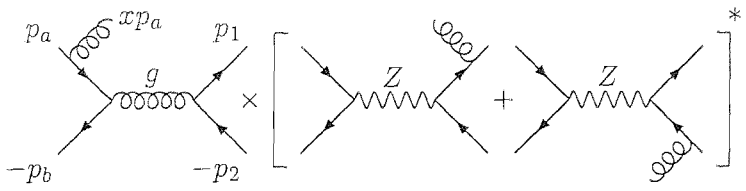

Figure 4.9: A set of cancelling diagrams in the collinear limit.

$$\begin{aligned}
&\bar{v}(p_b) i g_S \gamma^\rho \frac{i\not{p}_a}{(1-x)p_a.p_3} i g_S \gamma^\sigma \epsilon_\sigma(xp_a) u(p_a) \\
&\frac{-i}{s} \bar{u}(p_1) i g_S \gamma_\rho v(p_2) \\
&= \frac{-g_S}{(1-x)p_a.p_3} \bar{v}(p_b) i g_S \gamma^\rho [\not{p}_a \gamma^\sigma \epsilon_\sigma(xp_a)] u(p_a) \\
&\frac{-i}{s} \bar{u}(p_1) i g_S \gamma_\rho v(p_2) \\
&= \frac{-g_S}{(1-x)p_a.p_3} \bar{v}(p_b) i g_S \gamma^\rho [2p_a.\epsilon(xp_a) - \gamma^\sigma \epsilon_\sigma(xp_a) \not{p}_a] u(p_a) \\
&\frac{-i}{s} \bar{u}(p_1) i g_S \gamma_\rho v(p_2) \\
&= \frac{-2g_S p_a.\epsilon(xp_a)}{(1-x)p_a.p_3} \bar{v}(p_b) i g_S \gamma^\rho u(p_a) \frac{-i}{s} \bar{u}(p_1) i g_S \gamma_\rho v(p_2)
\end{aligned} \tag{4.37}$$

So the amplitude for the diagram with bremsstrahlung of particle a is:

$$\frac{-2g_S p_a.\epsilon(xp_a)}{(1-x)p_a.p_3} \times T_{s,g} \tag{4.38}$$

Where $T_{s,g}$ is the tree level amplitude for gluon exchange in the s-channel.

If we perform a similar manipulation for the two diagrams on the right hand side we obtain an expression for the total interference of (we have dropped the axial part of the Z-boson coupling. This will not affect the cancellation but will make the equations easier to read.):

$$\begin{aligned}
&2 \times \frac{-2g_S p_a.\epsilon(xp_a)}{(1-x)p_a.p_3} \times T_{s,g} \times \bar{u}(p_a) i g \gamma_\alpha v(p_b) \frac{i}{s} \times \\
&[\frac{-g_S}{2xp_1.p_a} \bar{v}(p_2) i g \gamma^\alpha [2\epsilon^*(xp_a).(p_1 + xp_a) - \gamma^\mu \epsilon^*_\mu(xp_a) x\not{p}_a] u(p_1) \\
&- \frac{-g_S}{2xp_2.p_a} \bar{v}(p_2) [2\epsilon^*(xp_a).(p_2 + xp_a) - \gamma^\mu \epsilon^*_\mu(xp_a) x\not{p}_a] i g \gamma^\alpha u(p_1)]
\end{aligned} \tag{4.39}$$

If we now explicitly multiply the $p_a.\epsilon(xp_a)$ on the left hand side into the right hand side we obtain (using the relation $\sum \epsilon^{\mu}\epsilon^{\nu *} \rightarrow -g^{\mu\nu}$ as we are in Feynman gauge. Note that only in this gauge can we obtain a diagram by diagram correspondence with the IR divergences):

$$\begin{aligned}
&2 \times \frac{2g_S^2}{2x(1-x)p_a.p_3} \times T_{s,g} \times \bar{u}(p_a) ig\gamma_\alpha v(p_b) \frac{i}{s} \times \\
&[\frac{1}{p_1.p_a} \bar{v}(p_2) ig\gamma^\alpha [-2p_a.(p_1 + xp_a) + x\not{p}_a \not{p}_a] u(p_1) \\
&-\frac{1}{p_2.p_a} \bar{v}(p_2)[-2p_a.(p_2 + xp_a) + x\not{p}_a \not{p}_a] ig\gamma^\alpha u(p_1)
\end{aligned} \tag{4.40}$$

Dropping terms proportional to $p_a^2 (= 0)$ gives us:

$$\begin{aligned}
&2 \times \frac{2g_S^2}{2x(1-x)p_a.p_3} \times T_{s,g} \times \bar{u}(p_a) ig\gamma_\alpha v(p_b) \frac{i}{s} \times \\
&[\frac{1}{p_1.p_a} \bar{v}(p_2) ig\gamma^\alpha (-2p_1.p_a) u(p_1) \\
&-\frac{1}{p_2.p_a} \bar{v}(p_2)(-2p_2.p_a) ig\gamma^\alpha u(p_1)
\end{aligned} \tag{4.41}$$

Which clearly cancels. A similar cancellation exists for all of the possible combinations of diagrams.

Note that the soft divergences remain and will need to be dealt with via the subtraction method. Also note that this cancellation does not work in general and that in the full $pp \rightarrow$ two jets calculation we will have collinear divergences.

4.4 Evaluating The Dipole Terms

We now need to evaluate the dipole terms according to the prescription described earlier.

Because the only bremsstrahlung diagrams that contribute to the $b\bar{b}$ production rate are the ones shown in fig(4.8) we will only need the four initial state emitter/final state spectator dipoles and the four initial state spectator/final state emitter dipoles (ie: no

final/final or initial/initial terms).

All of the dipoles needed will be proportional to the interference between tree level gluon exchange in the s-channel and tree level Z exchange in the s-channel. The expression for this tree level interference is:

$$2T_{s,g}T_{s,Z}(\tilde{s},\tilde{t},\lambda_1,\lambda_b) =$$
$$\frac{1}{2}\frac{g_s^2 g^2}{\cos^2\theta_W}\frac{1}{\tilde{s}(\tilde{s}-m_Z^2)}(c_V^b+\lambda_1 c_A^b)(c_V^q-\lambda_b c_A^q)[2\tilde{t}+(1-\lambda_1\lambda_b)\tilde{s}]^2 \qquad (4.42)$$

Where $c_{V/A}^b$ are the vector and axial couplings to the bottom quark and $c_{V/A}^q$ are the vector and axial couplings of the incoming quark flavour, $\tilde{s}$, $\tilde{t}$ and $\tilde{u}$ are the Mandelstam variables constructed (where necessary) from the shifted momenta, λ_1 is the helicity of the outgoing quark and λ_b is the helicity of the incoming anti quark.

So, the dipoles will be:

For the case of particle 1 emitter, particle a spectator:

$$D_{13}^a = \frac{-1}{2p_1.p_3}\frac{1}{x_{13,a}}2g_s^2 c_F\left[\frac{2}{1-\tilde{z}_1+(1-x_{13,a})}-(1+\tilde{z}_1)\right]$$
$$\times 2T_{s,g}T_{s,Z}(\tilde{s},\tilde{t},\lambda_1,\lambda_b)$$

where:

$$\tilde{s} = 2\tilde{p_a}.p_b, \quad \tilde{p_a} = x_{13,a}p_a$$

$$\tilde{t} = -2p_b.p_2 (\neq -2p_a.p_1)$$

$$x_{13,a} = \frac{p_1.p_a+p_3.p_a-p_1.p_3}{p_1.p_a+p_3.p_a}$$

$$\tilde{z}_1 = \frac{p_1.p_a}{p_1.p_a+p_3.p_a}$$

In the collinear limit this becomes:

$$\frac{-1}{2p_1.p_3}2g_s^2 c_F\left[\frac{2}{1-\tilde{z}_1}-(1+\tilde{z}_1)\right]\times 2T_{s,g}T_{s,Z}(2p_a.p_b,-2p_a.p_1,\lambda_1,\lambda_b) \quad (4.43)$$

(The overall minus sign here is from the colour factor used in [7] (see eq(3.12)) as we have an outgoing quark and an incoming quark.)

For the case of particle 1 emitter, particle b spectator:

$$D_{13}^{b} = \frac{+1}{2p_1.p_3}\frac{1}{x_{13,b}}2g_s^2 c_F \left[\frac{2}{1-\tilde{z}_1+(1-x_{13,b})} - (1+\tilde{z}_1)\right]$$
$$\times 2T_{s,g}T_{s,Z}(\tilde{s},\tilde{t},\lambda_1,\lambda_b)$$

where:

$$\tilde{s} = 2p_a.\tilde{p}_b, \quad \tilde{p}_b = x_{13,b}p_b$$

$$\tilde{t} = -2\tilde{p}_b.p_2$$

$$x_{13,b} = \frac{p_1.p_b + p_3.p_b - p_1.p_3}{p_1.p_b + p_3.p_b}$$

$$\tilde{z}_1 = \frac{p_1.p_b}{p_1.p_b + p_3.p_b}$$

In the collinear limit this becomes:

$$\frac{1}{2p_1.p_3}2g_s^2 c_F \left[\frac{2}{1-\tilde{z}_1} - (1+\tilde{z}_1)\right] \times 2T_{s,g}T_{s,Z}(2p_a.p_b, -2p_a.p_1, \lambda_1, \lambda_b) \quad (4.44)$$

(The overall plus sign here is again from the colour factors used in the subtraction process as we have an outgoing quark and an incoming anti-quark.)

So in the limit where p_3 is collinear with p_1 the contributions from D_{13}^a and D_{13}^b cancel. This is what we would expect to happen given we know that the collinear divergences cancel in the bremsstrahlung interferences.

Similarly, for the dipoles D_{23}^a and D_{23}^b in the limit where p_2 goes collinear with p_3 we have:

$$D_{23}^{a} = \frac{-1}{2p_2.p_3}2g_s^2 c_F \left[\frac{2}{1-\tilde{z}_2} - (1+\tilde{z}_2)\right] \times 2T_{s,g}T_{s,Z}(2p_a.p_b, -2p_a.p_1, \lambda_1, \lambda_b)$$
$$D_{23}^{b} = \frac{+1}{2p_2.p_3}2g_s^2 c_F \left[\frac{2}{1-\tilde{z}_2} - (1+\tilde{z}_2)\right] \times 2T_{s,g}T_{s,Z}(2p_a.p_b, -2p_a.p_1, \lambda_1, \lambda_b)$$
$$\text{Where:} \quad \tilde{z}_2 = \frac{p_2.p_{a/b}}{p_2.p_{a/b} + p_3.p_{a/b}} \quad (4.45)$$

Again the contribution with particle a as spectator cancels with the contribution where particle b is the spectator (in the collinear limit only).

The dipoles for initial state emitter and final state spectator are of a slightly different

form.

For the case of particle a emitter and particle 1 spectator:

$$D_1^{a3} = \frac{-1}{2p_a.p_3}\frac{1}{x_{31,a}}2g_s^2 c_F \left[\frac{2}{1-x_{31,a}+u_3} - (1+x_{31,a})\right]$$
$$\times 2T_{s,g}T_{s,Z}(\tilde{s},\tilde{t},\lambda_1,\lambda_b)$$

where:

$$\tilde{s} = 2\tilde{p_1}.p_2, \quad \tilde{p_1} = x_{31,a}p_1$$

$$\tilde{t} = -2p_b.p_2$$

$$x_{31,a} = \frac{p_1.p_a + p_3.p_a - p_1.p_3}{p_1.p_a + p_3.p_a}$$

$$u_3 = \frac{p_3.p_a}{p_1.p_a + p_3.p_a} \tag{4.46}$$

And for the case of particle a emitter and particle 2 spectator:

$$D_2^{a3} = \frac{+1}{2p_a.p_3}\frac{1}{x_{32,a}}2g_s^2 c_F \left[\frac{2}{1-x_{32,a}+u_3} - (1+x_{32,a})\right]$$
$$\times 2T_{s,g}T_{s,Z}(\tilde{s},\tilde{t},\lambda_1,\lambda_b)$$

where:

$$\tilde{s} = 2p_1.\tilde{p_2}, \quad \tilde{p_2} = x_{32,a}p_2$$

$$\tilde{t} = -2p_b.\tilde{p_2}$$

$$x_{32,a} = \frac{p_3.p_a + p_2.p_a - p_2.p_3}{p_3.p_a + p_2.p_a}$$

$$u_3 = \frac{p_3.p_a}{p_3.p_a + p_2.p_a} \tag{4.47}$$

For the case of particle b emitter and particle 1 spectator:

$$D_1^{b3} = \frac{+1}{2p_b.p_3}\frac{1}{x_{31,b}}2g_s^2 c_F \left[\frac{2}{1-x_{31,b}+u_3} - (1+x_{31,b})\right]$$
$$\times 2T_{s,g}T_{s,Z}(\tilde{s},\tilde{t},\lambda_1,\lambda_b)$$

where:

$$\tilde{s} = 2\tilde{p_1}.p_2, \quad \tilde{p_1} = x_{31,b}p_1$$

$$\tilde{t} = -2p_a.\tilde{p_1}$$

$$x_{31,b} = \frac{p_1.p_b + p_3.p_b - p_1.p_3}{p_1.p_b + p_3.p_b}$$

$$u_3 = \frac{p_3.p_b}{p_1.p_b + p_3.p_b}$$

(4.48)

And for the case of particle b emitter and particle 2 spectator:

$$D_2^{b3} = \frac{-1}{2p_b.p_3}\frac{1}{x_{32,b}}2g_s^2 c_F \left[\frac{2}{1-x_{32,b}+u_3} - (1+x_{32,b})\right]$$
$$\times 2T_{s,g}T_{s,Z}(\tilde{s},\tilde{t},\lambda_1,\lambda_b)$$

where:

$$\tilde{s} = 2p_1.\tilde{p_2}, \quad \tilde{p_2} = x_{32,b}p_2$$

$$\tilde{t} = -2p_a.p_1$$

$$x_{32,b} = \frac{p_3.p_b + p_2.p_b - p_2.p_3}{p_3.p_b + p_2.p_b}$$

$$u_3 = \frac{p_3.p_b}{p_3.p_b + p_2.p_b}$$

(4.49)

As in the case with final state emitter and initial state spectator these dipoles also all cancel amongst themselves in the collinear limits $p_a.p_3 \to 0$ and $p_b.p_3 \to 0$.

The remaining dipoles ($\mathcal{D}_{23}^1$, $\mathcal{D}_{13}^2$, $\mathcal{D}_{b3}^a$ and $\mathcal{D}_{a3}^b$) do not contribute as they all have vanishing colour factors (typically $Tr(t^A)Tr(t^B t^A t^B)$) - this is not true in general and

these dipoles will be needed for the two jet calculation.

If we now sum all of the non zero dipole terms and add them to the sum of all real correction interferences then we will obtain a result that is finite in the soft limit (This cancellation is shown in some detail in chapter(3)). This means that we can safely perform the integration over the two to three body phase space to find the $q\bar{q} \to b\bar{b} + g$ cross section.

4.5 The Integrated Dipole Subtractions

The insertion term will be proportional to the $\alpha_S \alpha_W$ order tree level interference. From [7] and eq(3.80) the general expression for the integrated dipole for a two to two body interaction is:

$$
\begin{aligned}
&I(p_a, p_b, p_1, p_2, \epsilon, \mu^2) = \\
&-\frac{g_S^2}{8\pi^2}\frac{1}{\Gamma(1-\epsilon)} \\
&\left\{ \frac{1}{T_1^2}\nu_1(\epsilon)\left[T_1.T_a \left(\frac{4\pi\mu^2}{2p_1.p_a}\right)^{\epsilon} + T_1.T_b \left(\frac{4\pi\mu^2}{2p_1.p_b}\right)^{\epsilon} + T_1.T_2 \left(\frac{4\pi\mu^2}{2p_1.p_2}\right)^{\epsilon} \right] \right. \\
&+\frac{1}{T_2^2}\nu_2(\epsilon)\left[T_2.T_a \left(\frac{4\pi\mu^2}{2p_2.p_a}\right)^{\epsilon} + T_2.T_b \left(\frac{4\pi\mu^2}{2p_2.p_b}\right)^{\epsilon} + T_1.T_2 \left(\frac{4\pi\mu^2}{2p_1.p_2}\right)^{\epsilon} \right] \\
&+\frac{1}{T_a^2}\nu_a(\epsilon)\left[T_1.T_a \left(\frac{4\pi\mu^2}{2p_1.p_a}\right)^{\epsilon} + T_2.T_a \left(\frac{4\pi\mu^2}{2p_2.p_a}\right)^{\epsilon} + T_a.T_b \left(\frac{4\pi\mu^2}{2p_a.p_b}\right)^{\epsilon} \right] \\
&\left. +\frac{1}{T_b^2}\nu_b(\epsilon)\left[T_1.T_b \left(\frac{4\pi\mu^2}{2p_1.p_b}\right)^{\epsilon} + T_2.T_b \left(\frac{4\pi\mu^2}{2p_2.p_b}\right)^{\epsilon} + T_a.T_b \left(\frac{4\pi\mu^2}{2p_a.p_b}\right)^{\epsilon} \right] \right\} \quad (4.50)
\end{aligned}
$$

For the process we are studying here we know that the colour factor associated with initial-initial and final-final interferences will vanish. As a consequence of this we can set $T_a.T_b$ and $T_1.T_2$ to zero. The other colour factors will be:

$$
\begin{aligned}
&\frac{1}{T_1^2} = \frac{1}{T_2^2} = \frac{1}{T_a^2} = \frac{1}{T_b^2} = \frac{1}{c_F} \\
&T_1.T_a = T_2.T_b = -\frac{c_F c_A}{2} \\
&T_1.T_b = T_2.T_a = \frac{c_F c_A}{2} \quad (4.51)
\end{aligned}
$$

For gluon emission from a quark or anti-quark we have [7]:

$$\nu_{1,2,a,b}(\epsilon) = c_F \left[\frac{1}{\epsilon^2} + \frac{3}{2\epsilon} + \frac{9}{2} - \frac{\pi^2}{2} + \mathcal{O}(\epsilon) \right] \tag{4.52}$$

Substituting this in (and dropping the overall factor of $\frac{(4\pi)^\epsilon}{\Gamma(1-\epsilon)}$) gives:

$$\begin{aligned} &I(p_a, p_b, p_1, p_2, \epsilon, \mu^2) = \\ &-\frac{g_S^2}{8\pi^2} \left[\frac{1}{\epsilon^2} + \frac{3}{2\epsilon} + \frac{9}{2} - \frac{\pi^2}{2} + \mathcal{O}(\epsilon) \right] \frac{c_F c_A}{2} \\ &2 \times \left\{ \left[\left(\frac{\mu^2}{2p_1.p_b} \right)^\epsilon - \left(\frac{\mu^2}{2p_1.p_a} \right)^\epsilon + \left(\frac{\mu^2}{2p_2.p_a} \right)^\epsilon - \left(\frac{\mu^2}{2p_2.p_b} \right)^\epsilon \right] \right\} \end{aligned} \tag{4.53}$$

If we now replace $(x)^\epsilon$ with $1 - (\epsilon) ln(1/x) + (\epsilon^2/2) ln^2(1/x)$ we obtain:

$$\begin{aligned} &I(p_a, p_b, p_1, p_2, \epsilon, \mu^2) = \\ &\left\{ \left[\frac{1}{\epsilon^2} + \frac{3}{2\epsilon} + \frac{9}{2} - \frac{\pi^2}{2} - \frac{1}{\epsilon} ln \left(\frac{2p_a.p_2}{\mu^2} \right) + \frac{1}{2} ln^2 \left(\frac{2p_a.p_2}{\mu^2} \right) - \frac{3}{2} ln \left(\frac{2p_a.p_2}{\mu^2} \right) \right] \right. \\ &+ \left[\frac{1}{\epsilon^2} + \frac{3}{2\epsilon} + \frac{9}{2} - \frac{\pi^2}{2} - \frac{1}{\epsilon} ln \left(\frac{2p_b.p_1}{\mu^2} \right) + \frac{1}{2} ln^2 \left(\frac{2p_b.p_1}{\mu^2} \right) - \frac{3}{2} ln \left(\frac{2p_b.p_1}{\mu^2} \right) \right] \\ &- \left[\frac{1}{\epsilon^2} + \frac{3}{2\epsilon} + \frac{9}{2} - \frac{\pi^2}{2} - \frac{1}{\epsilon} ln \left(\frac{2p_a.p_1}{\mu^2} \right) + \frac{1}{2} ln^2 \left(\frac{2p_a.p_1}{\mu^2} \right) - \frac{3}{2} ln \left(\frac{2p_a.p_1}{\mu^2} \right) \right] \\ &\left. - \left[\frac{1}{\epsilon^2} + \frac{3}{2\epsilon} + \frac{9}{2} - \frac{\pi^2}{2} - \frac{1}{\epsilon} ln \left(\frac{2p_b.p_2}{\mu^2} \right) + \frac{1}{2} ln^2 \left(\frac{2p_b.p_2}{\mu^2} \right) - \frac{3}{2} ln \left(\frac{2p_b.p_2}{\mu^2} \right) \right] \right\} \\ &\times - \frac{g_S^2}{4\pi^2} \frac{c_F c_A}{2} \end{aligned} \tag{4.54}$$

Here we have left the four contributions from the four possible combinations of emitter and spectator separate. So, the divergent part of the integrated dipoles for the combination emitter i and spectator j is:

$$I(2p_i.p_j, \epsilon, \mu^2) = \pm \frac{-1}{16\pi^2} g_S^2 \frac{c_F c_A}{2} \left(\frac{4}{\epsilon^2} + \frac{6}{\epsilon} - \frac{4}{\epsilon} ln \left(\frac{2p_i.p_j}{\mu^2} \right) \right) \tag{4.55}$$

Therefore, including the tree level interference, the total insertion term for the $b\bar{b}$ production rate is:

$$(-I(-t,\epsilon,\mu^2)+I(-u,\epsilon,\mu^2)+I(-u,\epsilon,\mu^2)-I(-t,\epsilon,\mu^2))\times$$

$$(T_{s,g}T_{s,Z})$$

$$=\frac{1}{16\pi^2}\frac{g^2g_S^4}{4\cos^2\theta_W}c_Fc_A(c_V^b+\lambda_1c_A^b)(c_V^q-\lambda_bc_A^q)\times$$

$$\left[-\frac{4}{\epsilon}ln\left(\frac{|t|}{\mu^2}\right)+\frac{4}{\epsilon}ln\left(\frac{|u|}{\mu^2}\right)\right]\frac{1}{s(s-m_Z^2)}(s+2t-s\lambda_1\lambda_b)^2 \qquad (4.56)$$

(Where the $T_{s,g}T_{s,Z}$ is the interference between tree level, s-channel Z and gluon exchange with the colour factor removed.)

$$(T_{s,g}T_{s,Z})=$$

$$\frac{g^2g_S^2}{4\cos^2\theta_W}(c_V^b+\lambda_1c_A^b)(c_V^q-\lambda_bc_A^q)\frac{1}{s(s-m_Z^2)}(s+2t-s\lambda_1\lambda_b)^2 \qquad (4.57)$$

In an interference between two s-channel diagrams we actually need to sum over any outgoing helicities since, in these topologies, they are unconstrained. Here however all helicities have been left completely general as the cancellation of divergences should work helicity by helicity. We have also omitted a factor of two for interference, a factor of 1/9 for averaging over colours and a factor of $\delta_{\lambda_a,-\lambda_b}$ ensuring that the incoming particles are in an allowed (ie: opposite) helicity combination. These factors have been omitted since they are trivially common to both the integrated dipole and the virtual corrections.

The virtual corrections that will contain an IR divergence will be the first four interferences shown in fig(4.2).

The first interference will be $B_{s,gg}$ (the amplitude for a box diagram with two uncrossed gluons exchanged in the s-channel) $\times$ $T_{s,Z}$ (the amplitude for a tree diagram with one Z exchanged in the s-channel) $\times$ $\frac{c_Fc_A}{2}$ (the colour factor associated with this interference).

Evaluating these amplitudes using the methods described earlier and then dropping all non divergent parts yields:

$$\begin{aligned}
&B_{s,gg} \times T_{s,Z} \times \frac{c_F c_A}{2} \\
&= \frac{c_F c_A}{2} \frac{g^2 g_S^4}{4 \cos\theta_W} (c_V^b + \lambda_1 c_A^b)(c_V^q - \lambda_b c_A^q) \frac{1}{16\pi^2} \\
&\left[-\frac{4}{\epsilon^2} + \frac{4}{\epsilon} ln\left(\frac{|t|}{\mu^2}\right) \right] \frac{1}{s(s-m_Z^2)} (s + 2t - s\lambda_1\lambda_b)^2
\end{aligned} \tag{4.58}$$

Note that this is proportional to $T_{s,g} T_{s,Z}$ as the divergent part of $B_{s,gg}$ is proportional to the gluon tree level diagram (this is not true for the non divergent parts however). The second interference will be $B_{s,gg,X}$ (the amplitude for a box diagram with two crossed gluons exchanged in the s-channel) $\times\ T_{s,Z} \times \frac{c_F c_A}{2}$.

$$\begin{aligned}
&B_{s,gg,X} \times T_{s,Z} \times \frac{c_F c_A}{2} \\
&= -\frac{c_F c_A}{2} \frac{g^2 g_S^4}{4 \cos\theta_W} (c_V^b + \lambda_1 c_A^b)(c_V^q - \lambda_b c_A^q) \frac{1}{16\pi^2} \\
&\left[-\frac{4}{\epsilon^2} + \frac{4}{\epsilon} ln\left(\frac{|u|}{\mu^2}\right) \right] \frac{1}{s(s-m_Z^2)} (s + 2t - s\lambda_1\lambda_b)^2
\end{aligned} \tag{4.59}$$

The double $(\frac{1}{\epsilon^2})$ poles will cancel between the box and crossed box diagrams.

The third interference will be $T_{s,g}$ (the amplitude for a tree diagram with one g exchanged in the s-channel) $\times\ B_{s,gZ}$ (the amplitude for a box diagram with an uncrossed gluon and Z exchanged in the s-channel) $\times\ \frac{c_F c_A}{2}\ \times\ 2$ (we have an extra factor of 2 associated with exchanging the gluon and Z)

$$\begin{aligned}
&2 \times B_{s,gZ} \times T_{s,g} \times \frac{c_F c_A}{2} \\
&= c_F c_A \frac{g^2 g_S^4}{4 \cos\theta_W} (c_V^b + \lambda_1 c_A^b)(c_V^q - \lambda_b c_A^q) \frac{1}{16\pi^2} \\
&\left[-\frac{2}{\epsilon^2} + \frac{2}{\epsilon} ln\left(\frac{|t|}{\mu^2}\right) + \frac{4}{\epsilon} ln\left(\left|1 - \frac{s}{m_z^2}\right|\right) \right] \frac{1}{s(s-m_Z^2)} (s + 2t - s\lambda_1\lambda_b)^2
\end{aligned} \tag{4.60}$$

The fourth and final contributing virtual interference will be $T_{s,g} \times B_{s,gZ,X}$ (the amplitude for a box diagram with a crossed gluon and Z exchanged in the s-channel) $\times$

$\frac{c_F c_A}{2} \times 2.$

$$
\begin{aligned}
& 2 \times B_{s,gZ,X} \times T_{s,g} \times \frac{c_F c_A}{2} \\
& = -c_F c_A \frac{g^2 g_S^4}{4 \cos\theta_W} (c_V^b + \lambda_1 c_A^b)(c_V^q - \lambda_b c_A^q) \frac{1}{16\pi^2} \\
& \left[-\frac{2}{\epsilon^2} + \frac{2}{\epsilon} ln\left(\frac{|u|}{\mu^2}\right) + \frac{4}{\epsilon} ln\left(\left|1 - \frac{s}{m_z^2}\right|\right) \right] \frac{1}{s(s-m_Z^2)} (s + 2t - s\lambda_1\lambda_b)^2 \quad (4.61)
\end{aligned}
$$

Here the double poles and the $ln\left(\left|1 - \frac{s}{m_z^2}\right|\right)$ terms both cancel between the crossed and uncrossed boxes.

If we sum these four contributions together we obtain for the total IR divergence from the virtual corrections:

$$
\begin{aligned}
& c_F c_A \frac{g^2 g_S^4}{4 \cos\theta_W} (c_V^b + \lambda_1 c_A^b)(c_V^q - \lambda_b c_A^q) \frac{1}{16\pi^2} \\
& \left[\frac{4}{\epsilon} ln\left(\frac{|t|}{\mu^2}\right) - \frac{4}{\epsilon} ln\left(\frac{|u|}{\mu^2}\right) \right] \frac{1}{s(s-m_Z^2)} (s + 2t - s\lambda_1\lambda_b)^2 \quad (4.62)
\end{aligned}
$$

This is equal and opposite to the divergent part of the integrated dipole (fig(4.56)) so we can confirm that the final answer will be finite.

4.6 The x Dependent Integrated Dipoles And Phase Space Integration

The remaining integrated dipoles will be a subset of those for the full four quark case and, unlike the x independent part there is little to be gained by looking at them separately. For a full description of the 'K' and 'P' terms see section(5.5).

The Monte Carlo integration over the phase space will be essentially identical to that performed in the full four quark case. For a description of this see section(5.6).

4.7 Results For $b\bar{b}$ Production

The results presented below were first published in [25].

The NLO QCD corrections to $b\bar{b}$ production may be found in [26].

4.7.1 Total Cross Sections

Tevatron

Presented in fig(4.10) are the results for the total $b\bar{b}$ production cross section at the Tevatron. The centre of mass energy of the $p\bar{p}$ pair used was $2TeV$ and the rapidity range integrated over was -2 to +2 (This is actually a somewhat larger range than can be observed at Tevatron, $0.1 < |\eta| < 0.7$ would be more realistic, but the results have only a very small dependence on η). The $\alpha_S^2\alpha_W$ contribution is split up into $gg \rightarrow b\bar{b}$ and $q\bar{q} \rightarrow b\bar{b}$ parts. Also presented for comparison are the tree level weak and QCD contributions and the one loop QCD corrections.

Fig(4.11) shows the ratio of the NLO weak corrections calculated here to the LO QCD cross section.

The QCD contribution is absolutely dominant across the entire spectrum of transverse momentum with the weak corrections being limited to a fraction of one percent. The weak corrections are nowhere near large enough to explain the current theory vs. data differences at Tevatron [1]. This is a result of the fact that at Tevatron the parton energies are typically small enough (not significantly larger than the W or Z mass) that the contribution to the weak corrections from the Sudakov logarithms is not large. The LO weak corrections are some three orders of magnitude smaller than the QCD rates (away from the Z resonance at any rate). Note that both LO and NLO QCD are of similar magnitudes - this is indicative of the fact that the QCD results have

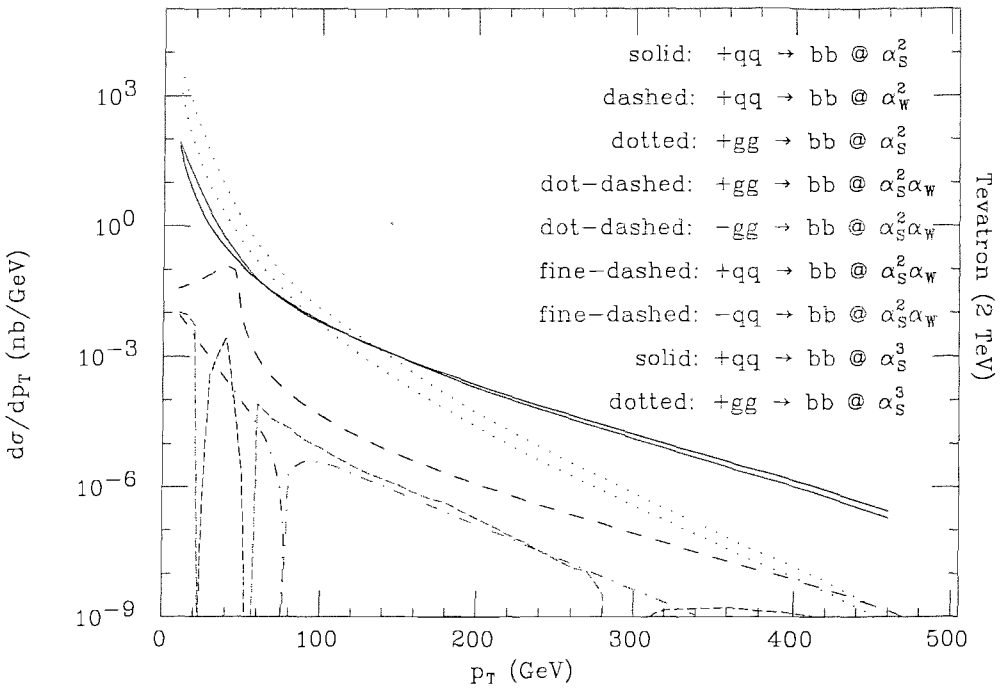

Figure 4.10: The total cross section contributions to $b\bar{b}$ production at Tevatron ($E_{cm} = 2TeV$) plotted against the transverse momentum of the b-jet.

significant K factors (defined as $\frac{\sigma(\alpha_S^3)}{\sigma(\alpha_S^2)}$), about 2, for the gg rate and 1 for the $q\bar{q}$ rate. These large K factors suggest that the QCD results are not entirely perturbatively safe at this order.

The NLO weak corrections are generally up to a further order of magnitude smaller than the LO weak cross section although the structure is more complicated. The $q\bar{q} \rightarrow b\bar{b}$ at $\alpha_S^2\alpha_W$ begins negative at low p_T briefly becoming positive at the Z resonance and becoming positive again at higher p_T (300GeV). The $gg \rightarrow b\bar{b}$ starts positive but becomes negative at a p_T of about 400GeV (note that the gg rate does not show any particular structure around the Z resonance as there are no contributing diagrams with a Z boson in the s-channel as there are in the $q\bar{q}$ rate).

Fig(4.11) clearly shows how small the $\alpha_S^2\alpha_W$ corrections are when compared with the QCD corrections.

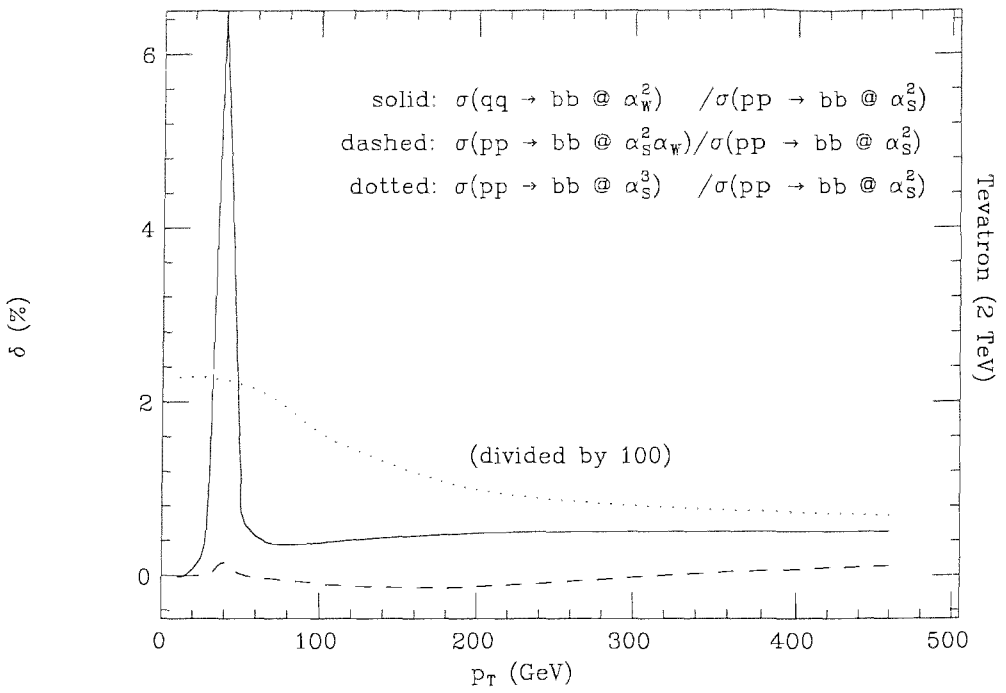

Figure 4.11: Ratio of the one loop weak result ($\alpha_S^2\alpha_W$) to the tree level QCD (α_S^2) $b\bar{b}$ production rate. Also presented for comparison are the tree level weak corrections (α_W^2) and the one loop QCD corrections (α_S^3).

LHC

Fig(4.12) shows the results for $b\bar{b}$ production at LHC. The rapidity range is again restricted to $|\eta| < 2$ (reasonably realistic for LHC) but this time the centre of mass energy for the initial pp pair is set at 14TeV - this should be high enough such that the partonic energies are large enough that the Sudakov logs begin to contribute significantly. As in the Tevatron plot we split the $\alpha_S^2\alpha_W$ cross section into both the gg and $q\bar{q}$ terms and also show the LO QCD and pure weak corrections along with the NLO QCD corrections.

Firstly it can clearly be seen that the NLO weak corrections are indeed relatively larger when compared to the QCD cross sections than they were at Tevatron - $1-2\%$ (see fig(4.13)) of the LO QCD.

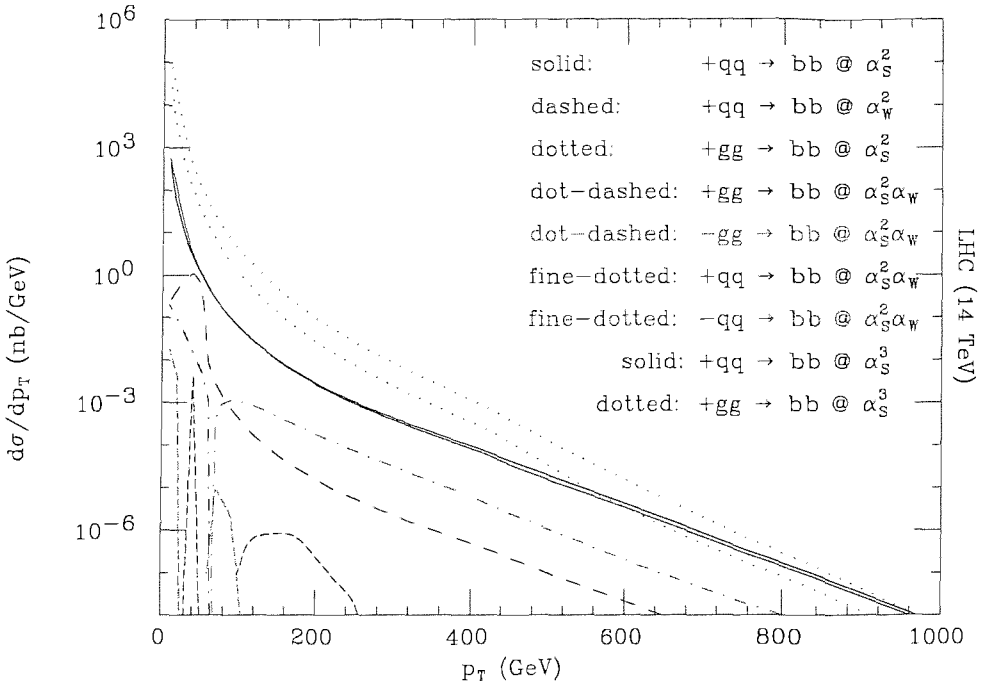

Figure 4.12: The total cross section contributions to $b\bar{b}$ production at LHC ($E_{cm} = 14TeV$) plotted against the transverse momentum of the b-jet.

Other characteristics worth noting are that the $gg \rightarrow b\bar{b}$ processes are significantly larger than the $q\bar{q}$ process both at LO and NLO QCD and NLO weak at LHC whereas they were of comparable size at Tevatron. This is as would be expected due to the preponderance of gluons in the initial state protons at LHC energies. In fact, it can be seen that the $\alpha_S^2\alpha_W$ gg corrections are somewhat larger than the LO (α_W^2) due to the tree level weak calculation not including any gg diagrams.

The qualitative structure of the NLO weak corrections is the same as at Tevatron with the two contributions fluctuating between positive and negative corrections and with a peak in the $q\bar{q}$ curve at the Z resonance. In fig(4.13) we can see clearly the significance of the weak corrections to the total cross section. The correction rises to as high as 2% of the tree level QCD cross section. As things stand this correction is swamped by the uncertainty in the higher order QCD corrections (estimated to be of the order of 10% [26] - as can be seen in fig(4.12) the K factors for QCD at LHC are somewhat

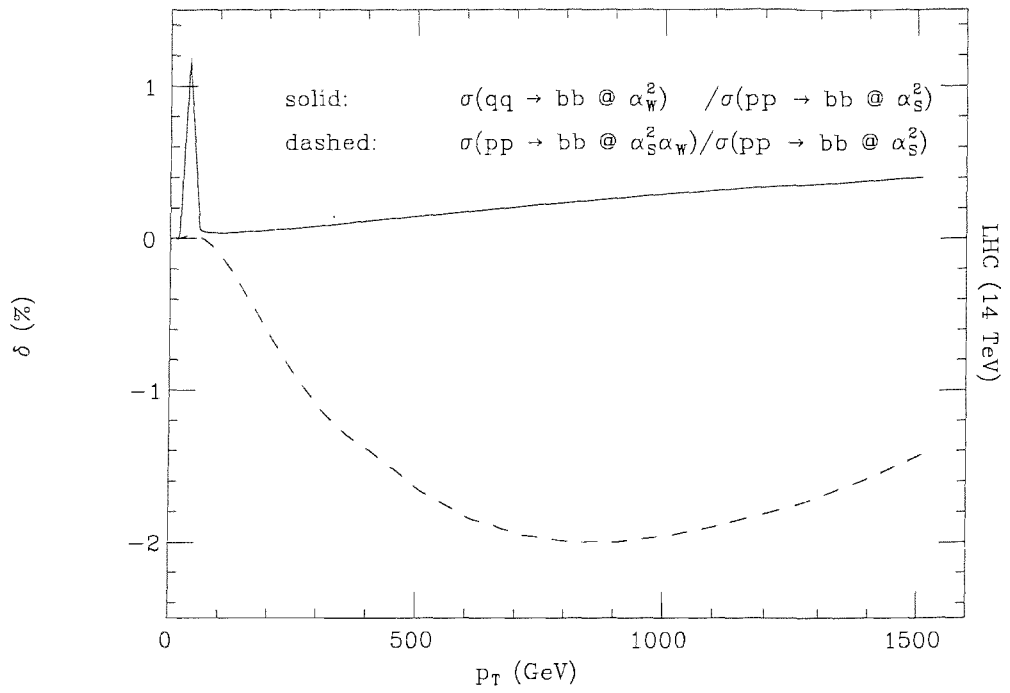

Figure 4.13: Ratio of the one loop weak result ($\alpha_S^2\alpha_W$) to the tree level QCD (α_S^2) $b\bar{b}$ production rate. Also presented for comparison are the tree level weak corrections (α_W^2). Here the one loop QCD results have been omitted as they are currently perturbatively unreliable [26]

higher than at Tevatron, as much as 4 for the gg cross section, indicating a large degree of perturbative uncertainty). However [9] work is being carried out to obtain the α_S^4 (NNLO) QCD corrections. Once these calculations are complete it is likely that a -2% correction will be of some significance - probably detectable at LHC owing to the very high luminosity, and hence, statistics at that machine.

4.7.2 Asymmetries

Fig(4.14) shows the calculated forward backwards asymmetry for $b\bar{b}$ production at Tevatron. The one loop correction can be seen to be both larger and of the opposite sign to the tree level weak contribution with an absolute asymmetry of approximately 0.5%. In principle this should be detectable at Tevatron Run 2.

It is important to note that, as mentioned in section(2.3.1), NLO QCD also generates a

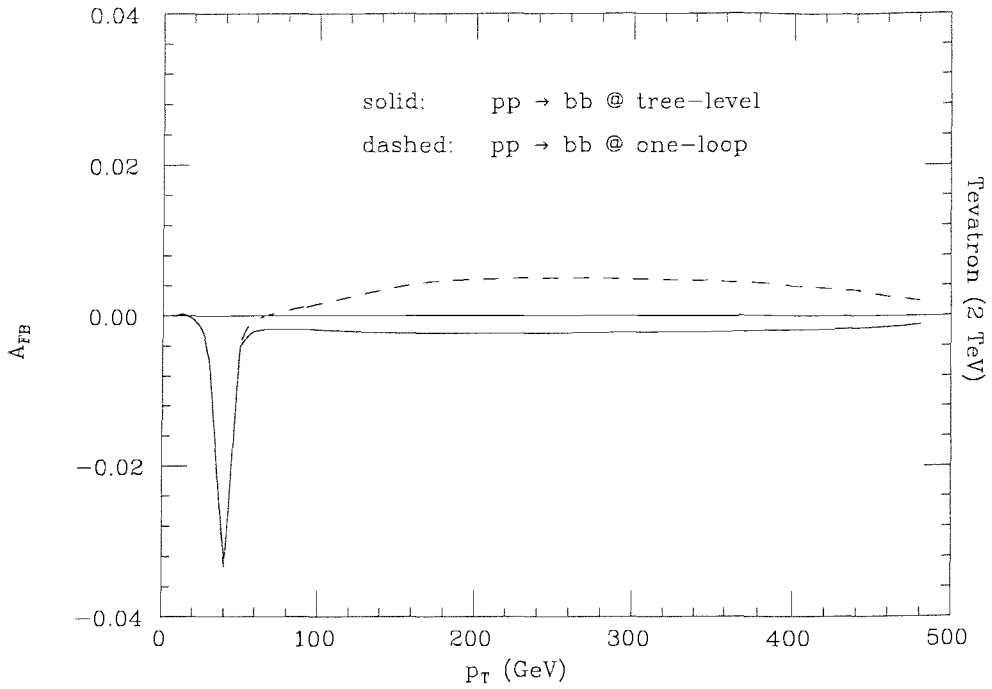

Figure 4.14: The forwards backwards asymmetry at the Tevatron ($2TeV$) plotting the contribution from both $\alpha_S^2\alpha_W$ and α_W^2 orders. The dominant contribution to A_{FB} however will come from α_S^3 order (see fig(4.15)).

contribution to the forwards backwards asymmetry [14]. Fig(4.15) shows the variation of the QCD contribution to A_{FB} with both $cos(\theta)$ and centre of mass energy. As can be seen from the first plot the QCD contribution is largest at high $cos(\theta)$ (and therefore low p_T and high η) - however, as mentioned above, in practice we should restrict the rapidity range such that we ignore events strongly along the beam pipe.

A realistic maximum rapidity of 0.7 corresponds to a $cos\theta$ of about 0.6 ($\eta = -ln(tan(\theta/2))$). Across the reasonable $cos(\theta)$ range the absolute asymmetry is at most 5%. Given this we see that the weak correction to A_{FB} will generally be about 10% of the total asymmety. (Note that the helicity dependent observables have not been calculated for $b\bar{b}$ production as RHIC is the only currently available high energy polarised machine and does not have the capability to tag b jets [19]. These results would be of interest were it to become possible for polarised beams to be used at LHC.)

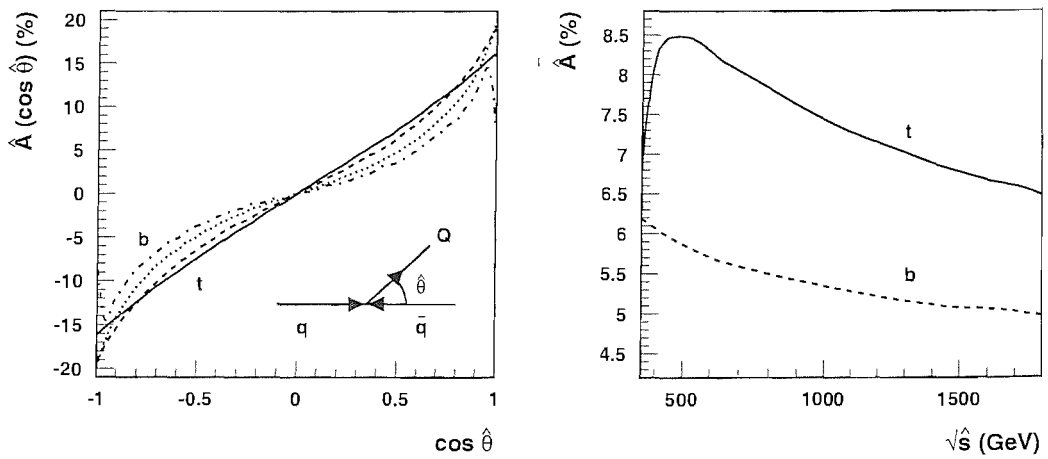

Figure 4.15: [14] The forward backwards asymmetry generated by one loop QCD presented against $cos\theta$ and E_{cm}.

Chapter 5

Proton - Proton To Two Jets.

We will now extend the $b\bar{b}$ calculation to a general calculation of all proton (anti)proton to two jet processes. We will make similar assumptions to in the earlier calculation - there are no b or t quarks in the initial states, we still consider only massless external quarks and we drop any suppressed W exchange diagrams (ones where the W emission changes quark generation).

5.1 The Virtual Corrections in the 4-Quark Case

There are eleven different four quark processes that contribute to the $pp \rightarrow$ two jets rate:

- Process 1) - $qq \rightarrow qq$
- Process 2) - $\bar{q}\bar{q} \rightarrow \bar{q}\bar{q}$
- Process 3) - $qq' \rightarrow qq'$ (same generation)
- Process 4) - $\bar{q}\bar{q}' \rightarrow \bar{q}\bar{q}'$ (same generation)
- Process 5) - $qq' \rightarrow qq'$ (different generation)

- Process 6) - $\bar{q}\bar{q}' \rightarrow \bar{q}\bar{q}'$ (different generation)
- Process 7) - $q\bar{q} \rightarrow q\bar{q}$
- Process 8) - $q\bar{q} \rightarrow q'\bar{q}'$ (same generation)
- Process 9) - $q\bar{q} \rightarrow q'\bar{q}'$ (different generation)
- Process 10) - $q\bar{q}' \rightarrow q\bar{q}'$ (same generation)
- Process 11) - $q\bar{q}' \rightarrow q\bar{q}'$ (different generation)

(Note that process 9 is the same process as considered in the $b\bar{b}$ production calculation.)

5.2 The Bremsstrahlung Corrections to the 4-Quark Case

The tree level interferences shown in fig(5.13) form the basis of all the possible bremsstrahlung corrections to $qq/\bar{q}\bar{q} \rightarrow qq/\bar{q}\bar{q}$ processes (that is processes one to six).

In principle there will be twenty bremsstrahlung interferences associated with each tree level topology - the four possible bremsstrahlung diagrams involving s,t or u channel Z/W boson exchange (real gluon emission from external leg a,b,1 and 2) interfered with the five possible bremsstrahlung diagrams involving s,t or u channel gluon exchange (real gluon emission from external quark a,b,1 and 2 and real gluon emission from the internal virtual gluon). Not all of these twenty interferences will contribute for a given topology due to possible vanishing colour factors.

Note that not all of the tree level interferences shown actually contribute at tree level due to having vanishing colour factors. For example the $gtZt$ interference in fig(5.13) will have zero colour factor - $\mathrm{Tr}(t^A)\mathrm{Tr}(t^A) = 0$. However when we add soft gluon

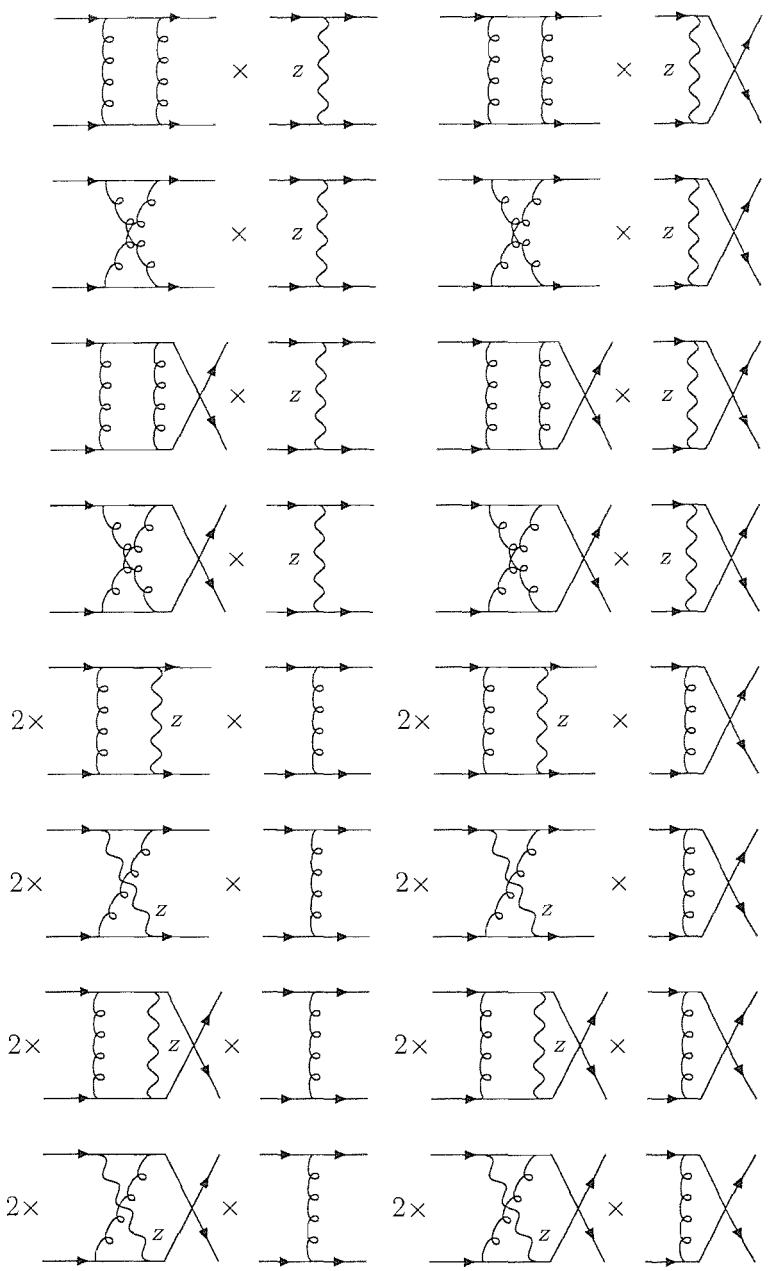

Figure 5.1: The set of interferences that contributes to process one ($qq \to qq$) and two ($\bar{q}\bar{q} \to \bar{q}\bar{q}$), the latter obtained by reversing the arrows on all fermion lines of the former.

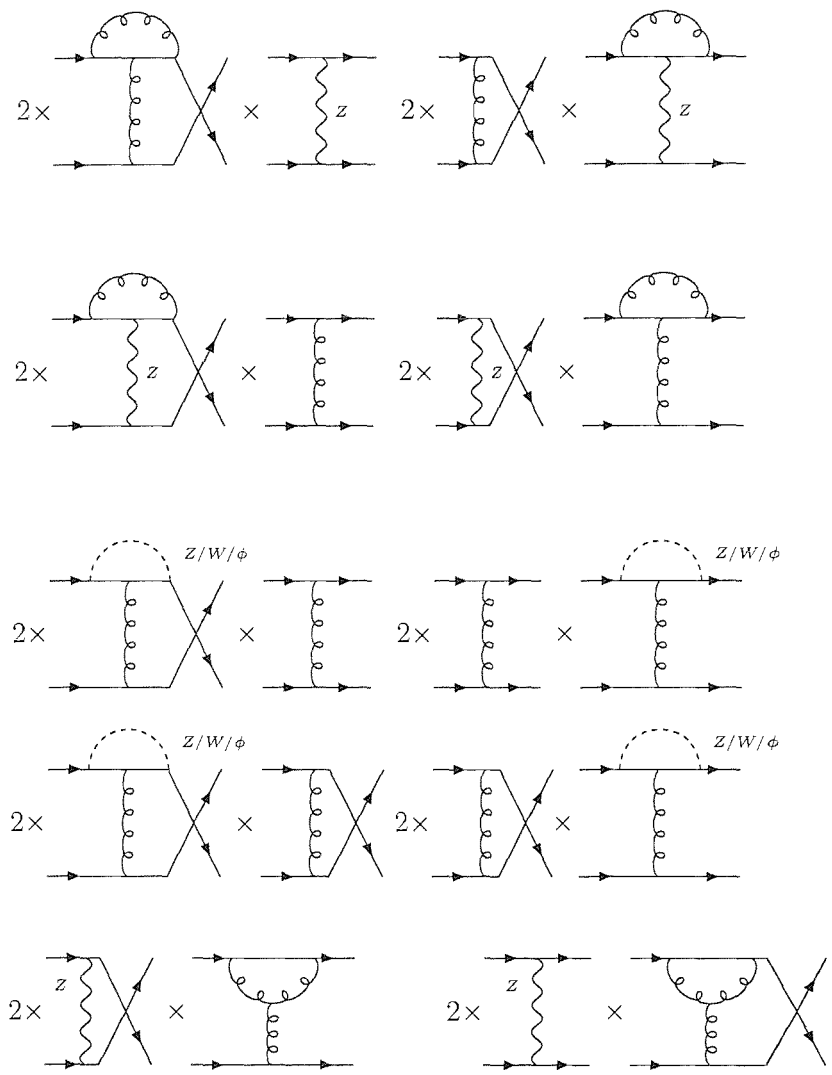

Figure 5.2: Continuing the set of interferences that contributes to process one ($qq \to qq$) and two ($\bar{q}\bar{q} \to \bar{q}\bar{q}$), the latter obtained by reversing the arrows on all fermion lines of the former.

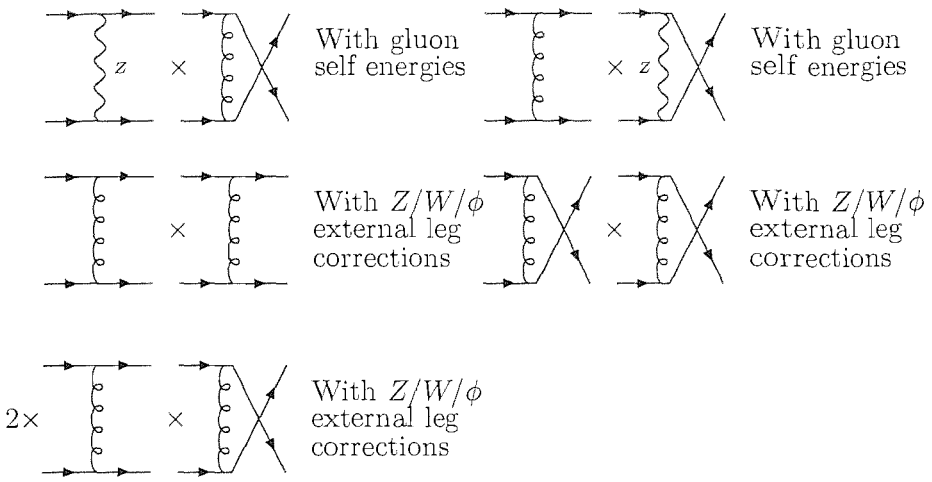

Figure 5.3: Continuing the set of interferences that contributes to process one ($qq \to qq$) and two ($\bar{q}\bar{q} \to \bar{q}\bar{q}$), the latter obtained by reversing the arrows on all fermion lines of the former.

emission to both diagrams in the interference we will change the colour factor, potentially rendering it non zero. For example, again looking at the $gtZt$ interference in fig(5.13) - if we add gluon emission from particle one on the left hand diagram and from particle two on the right hand diagram then the colour factor will become $\mathrm{Tr}(t^A t^B)\mathrm{Tr}(t^A t^B) = c_F c_A/2$. If, on the other hand, we interfere two diagrams with emission from particle one then the colour factor will be $\mathrm{Tr}(t^A t^B t^B)\mathrm{Tr}(t^A)$ which is still zero.

The tree level interferences that provide the basis for the bremsstrahlung corrections

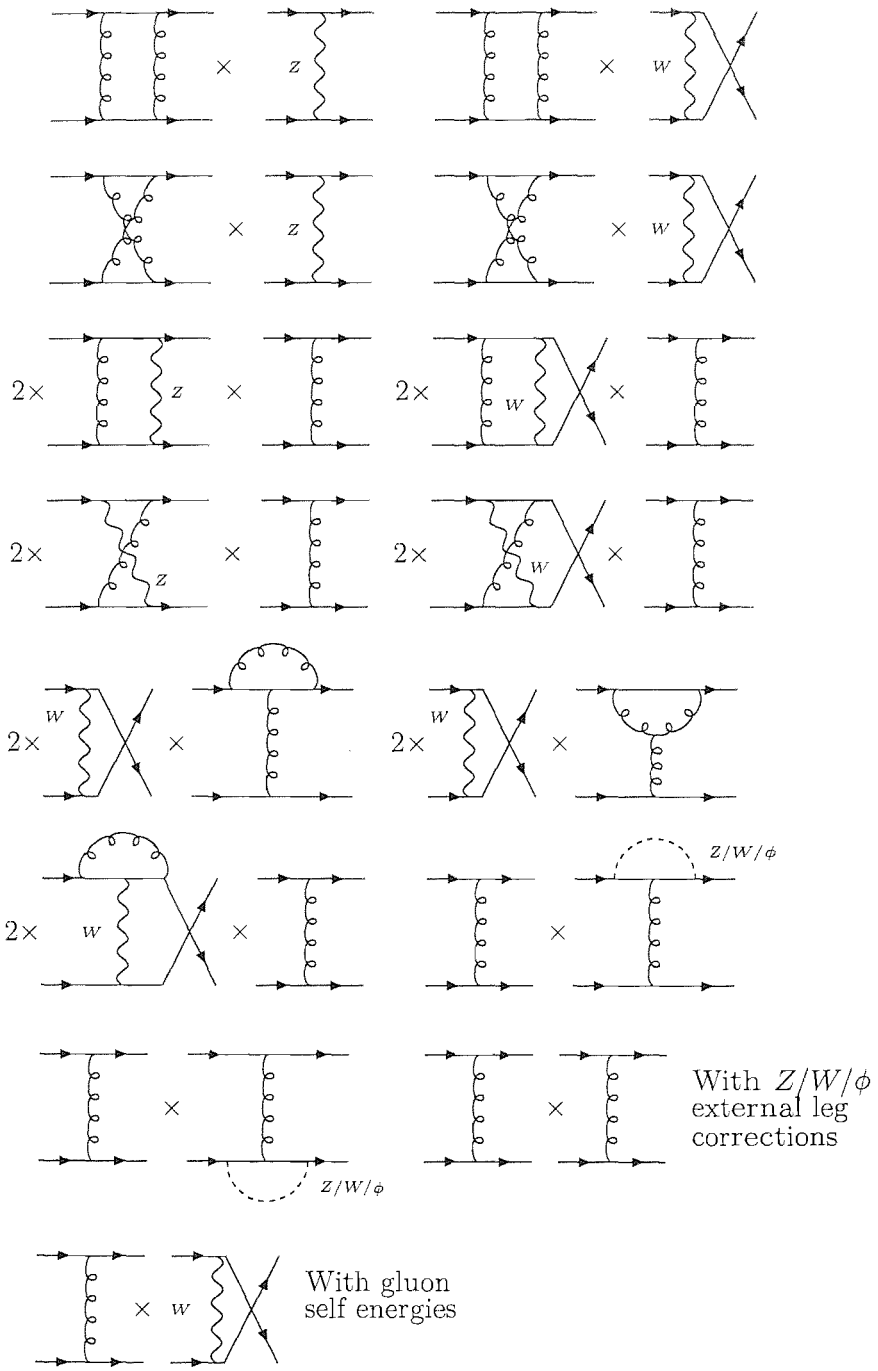

Figure 5.4: The set of interferences that contributes to process three ($qQ \to qQ$ (same generation)) and four ($\bar{q}\bar{Q} \to \bar{q}\bar{Q}$ (same generation)), the latter obtained by reversing the arrows on all fermion lines of the former. Here, the weak couplings to the two fermion lines will be different, this means we cannot implement the last two interferences as a factor of 2 as we could in Figs. 5.1, 5.2.

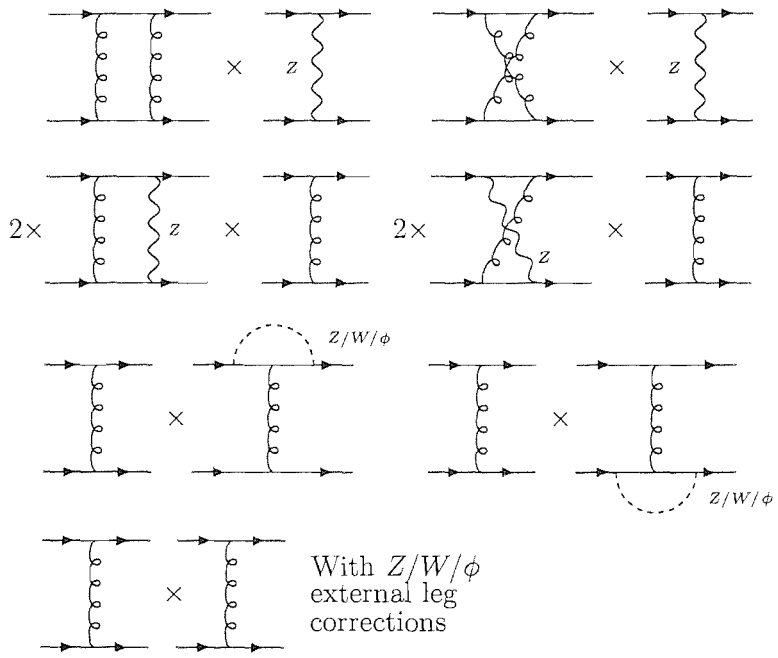

Figure 5.5: The set of interferences that contributes to process five ($qQ \to qQ$ (different generation)) and six ($\bar{q}\bar{Q} \to \bar{q}\bar{Q}$ (different generation)), the latter obtained by reversing the arrows on all fermion lines of the former. Here, the weak couplings to the two fermion lines will be different, this means we cannot implement the last two interferences as a factor of 2 as we could in Figs. 5.1, 5.2.

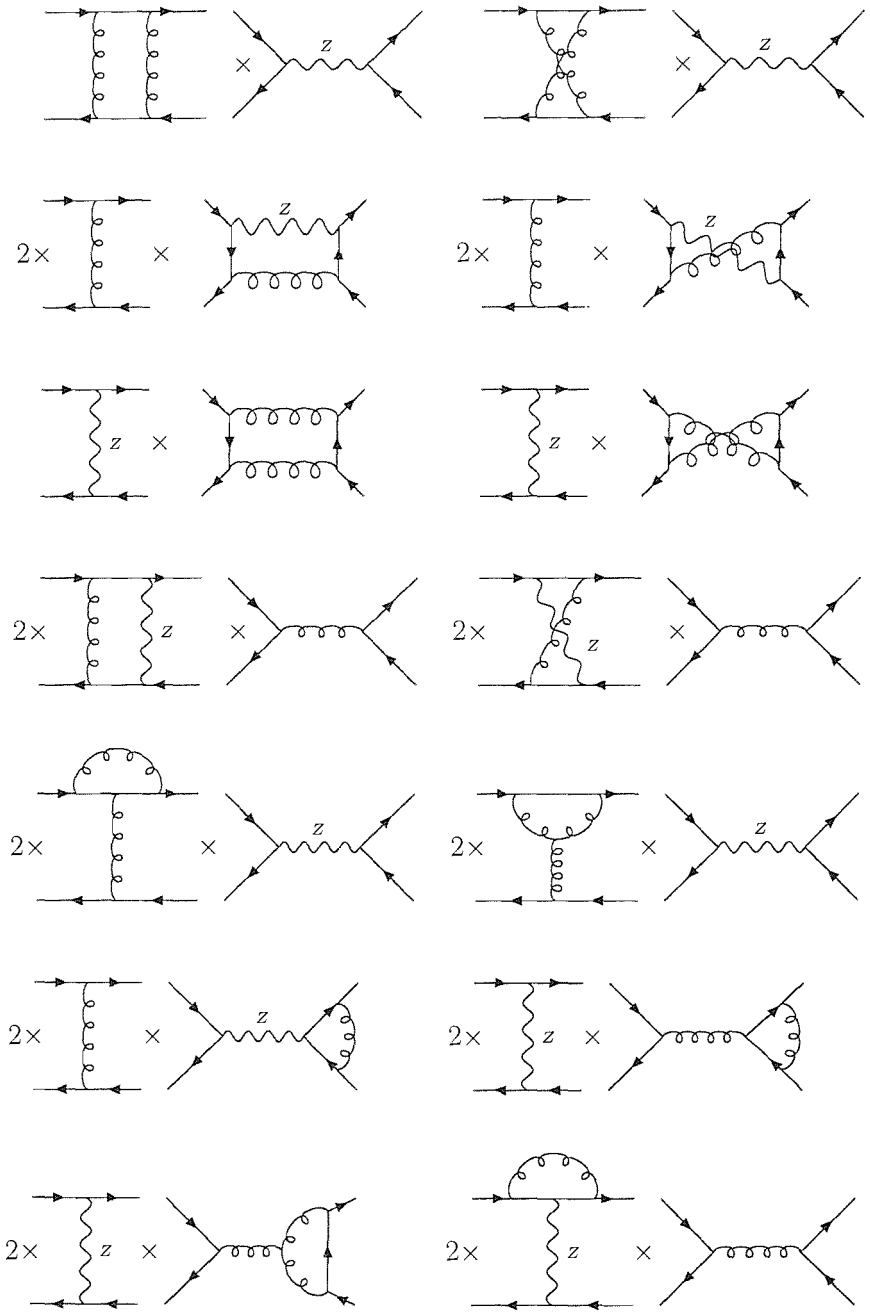

Figure 5.6: The set of interferences that contributes to process seven ($q\bar{q} \rightarrow q\bar{q}$).

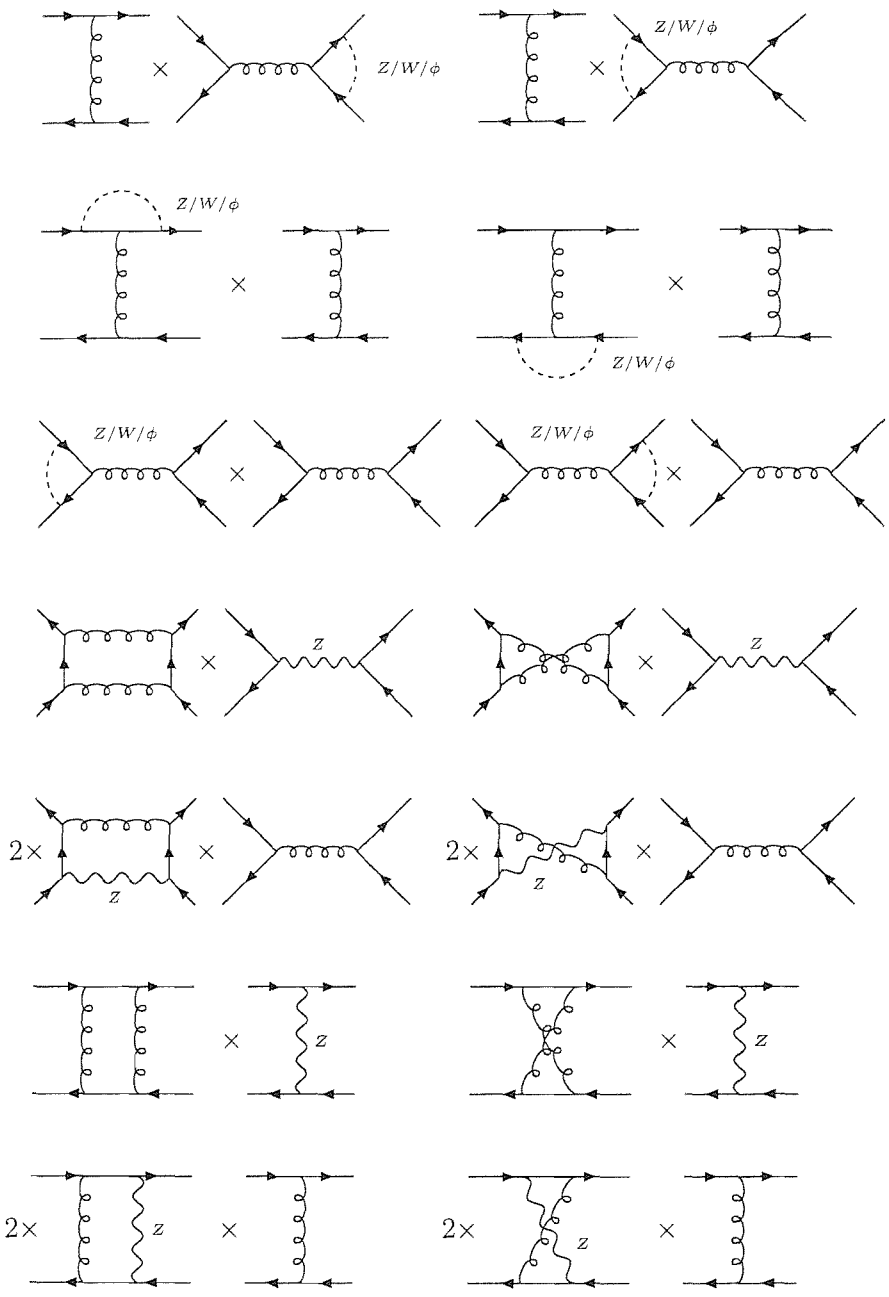

Figure 5.7: The set of interferences that contributes to process seven ($q\bar{q} \rightarrow q\bar{q}$): continued from Fig. 5.6.

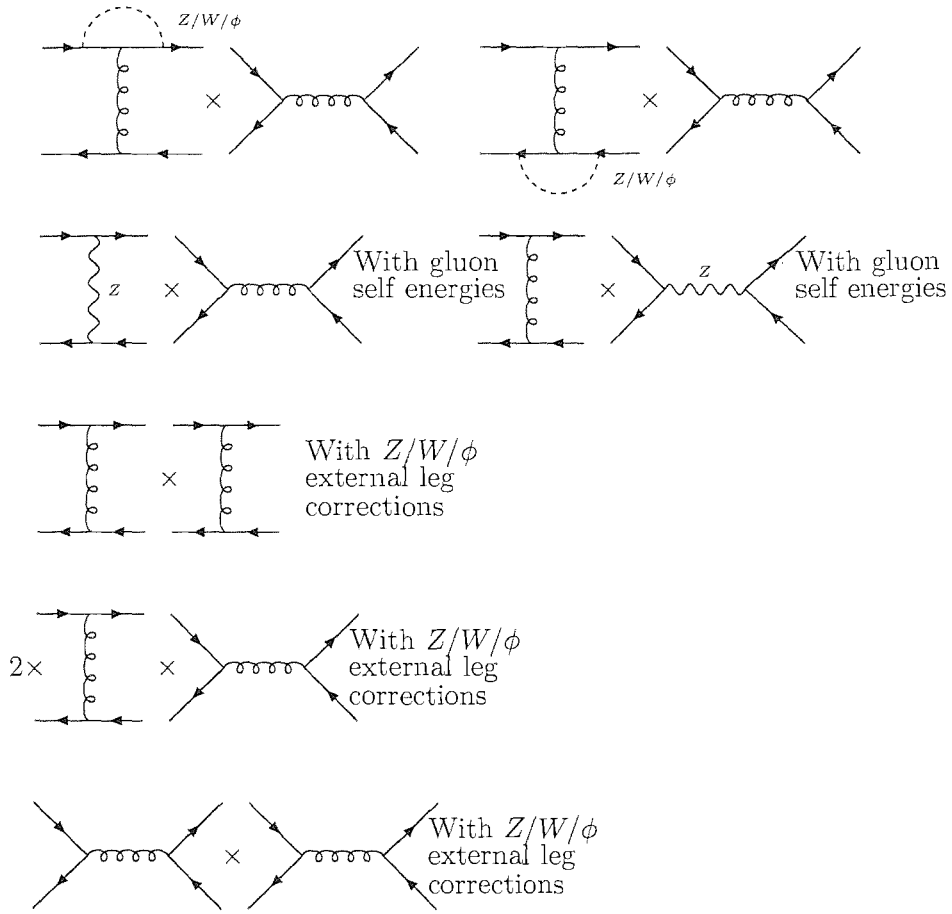

Figure 5.8: The set of interferences that contributes to process seven ($q\bar{q} \rightarrow q\bar{q}$): continued from Figs. 5.6 and 5.7.

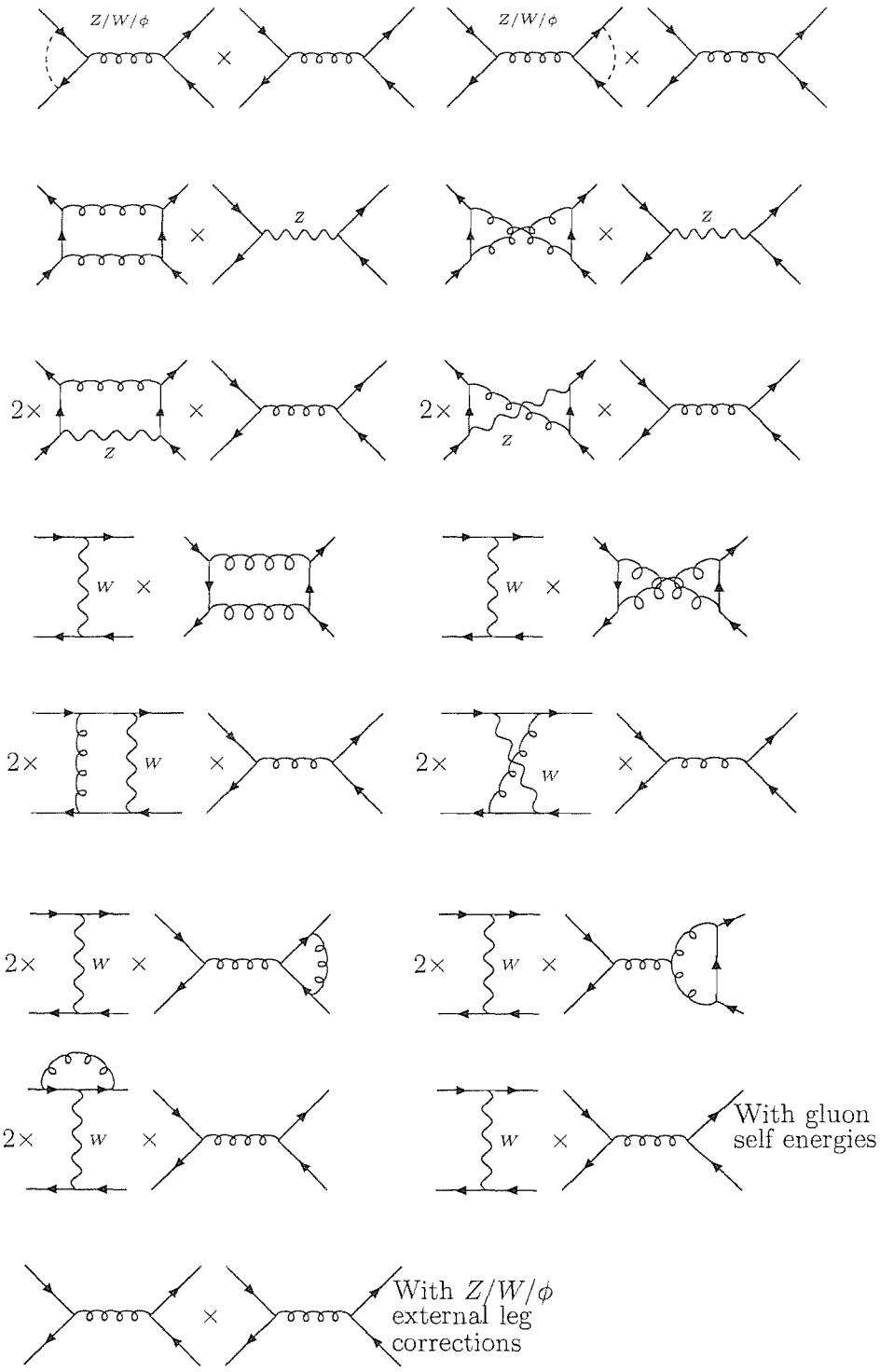

Figure 5.9: The set of interferences that contributes to process eight ($q\bar{q} \rightarrow Q\bar{Q}$ (same generation)).

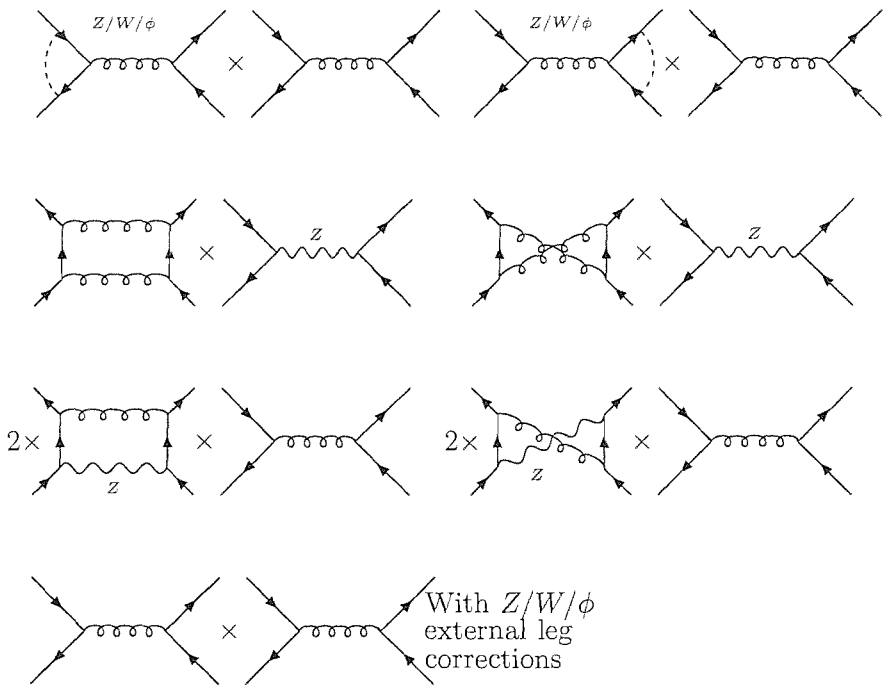

Figure 5.10: The set of interferences that contributes to process nine ($q\bar{q} \rightarrow Q\bar{Q}$ (different generation)).

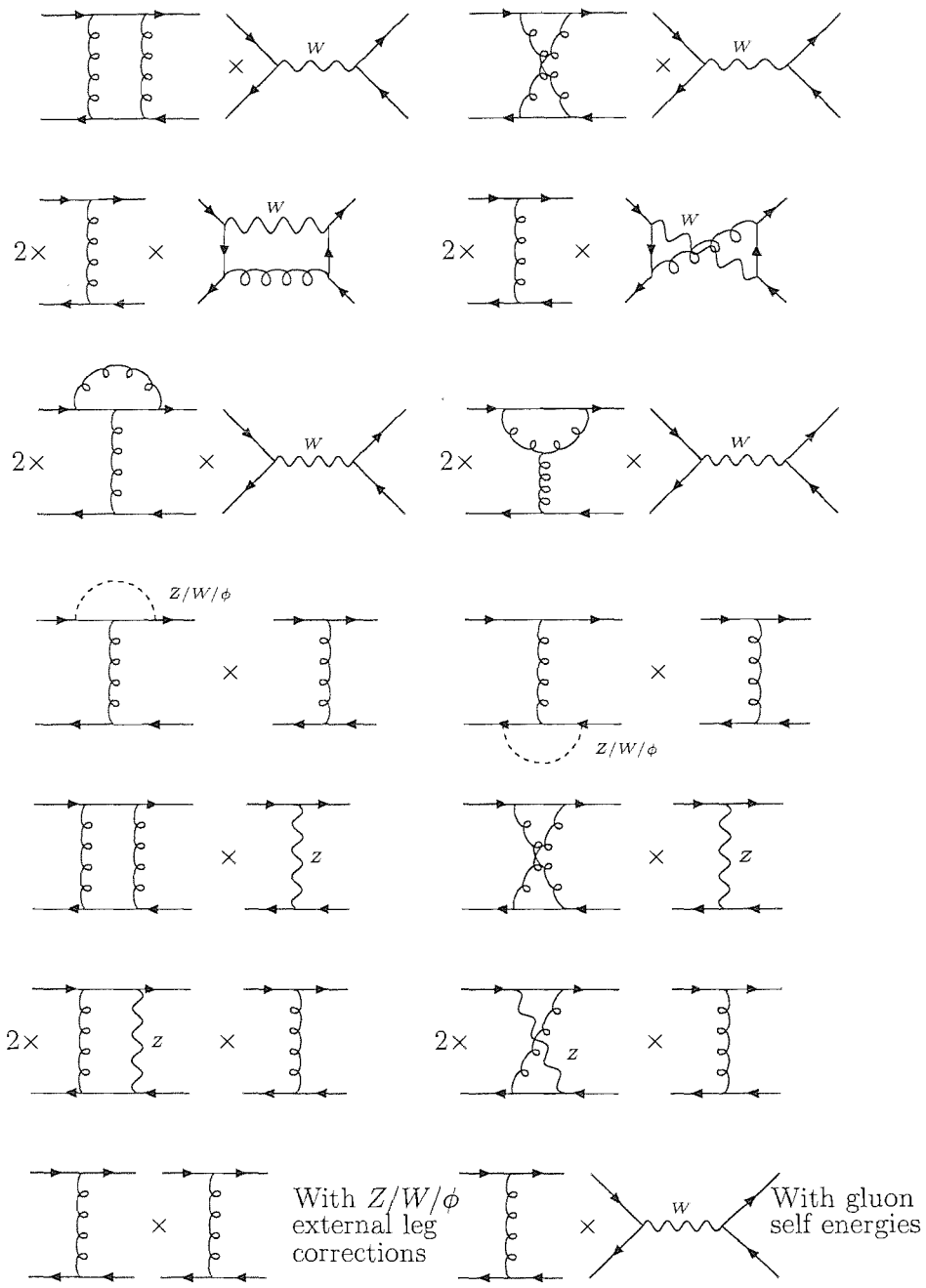

Figure 5.11: The set of interferences that contributes to process ten ($q\bar{Q} \rightarrow q\bar{Q}$ (same generation)).

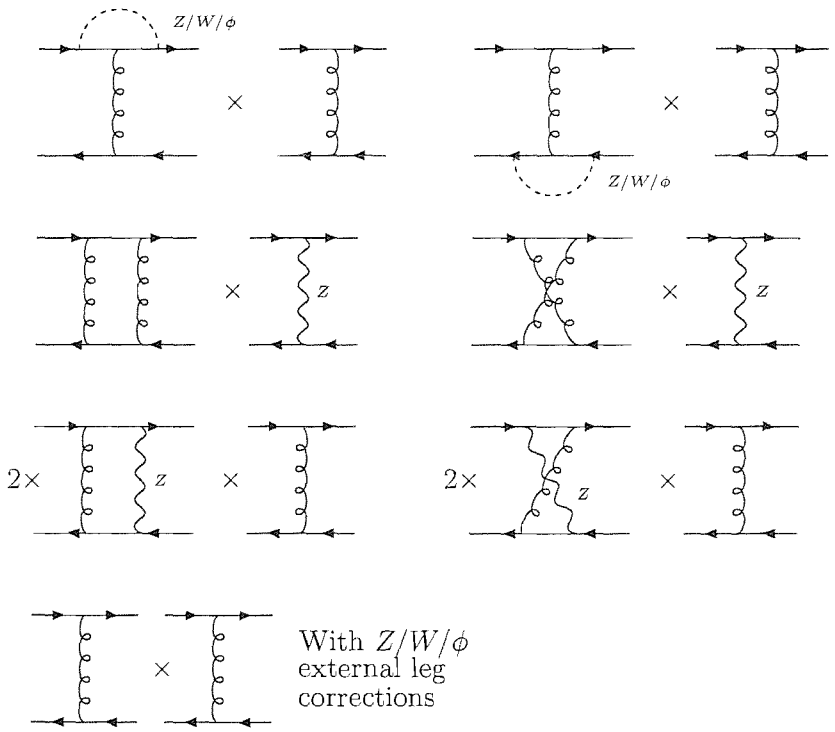

Figure 5.12: The set of interferences that contributes to process eleven ($q\bar{Q} \rightarrow q\bar{Q}$ (different generation)).

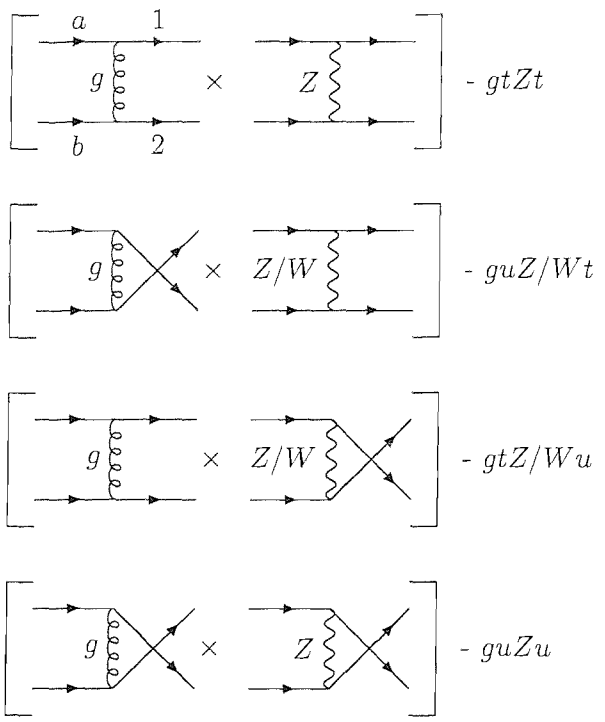

Figure 5.13: The tree level topologies that, following the addition of soft gluon emission, form the basis of the bremsstrahlung corrections to $qq \rightarrow qq$ and $\bar{q}\bar{q} \rightarrow \bar{q}\bar{q}$.

to processes one to six are:

- Process 1) - $gtZt$, $guZu$, $gtZu$, $guZt$

- Process 2) - $gtZt$, $guZu$, $gtZu$, $guZt$

- Process 3) - $gtZt$, $gtWu$, $guWt$

- Process 4) - $gtZt$, $gtWu$, $guWt$

- Process 5) - $gtZt$

- Process 6) - $gtZt$ (5.1)

The tree level interferences shown in fig(5.14) form the basis of the bremsstrahlung corrections to $q\bar{q} \rightarrow q\bar{q}$ processes (that is, processes seven to eleven).

The tree level interferences that provide the basis for the bremsstrahlung corrections

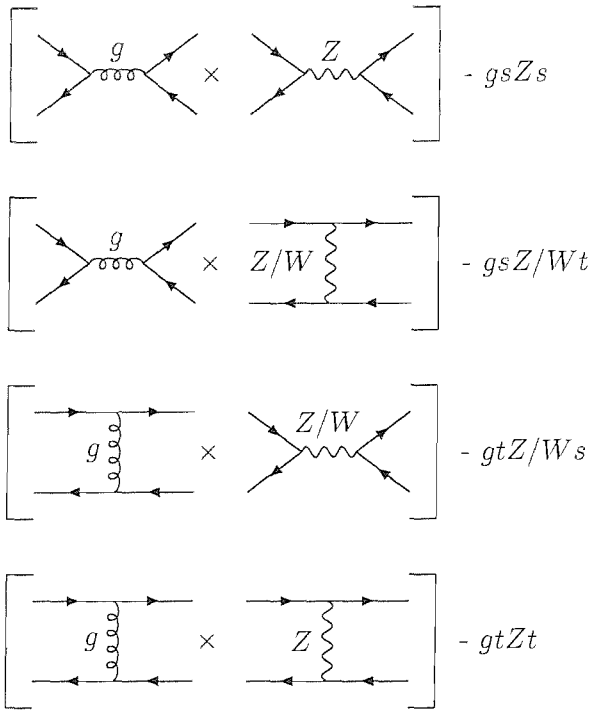

Figure 5.14: The tree level topologies that, following the addition of soft gluon emission, form the basis of the bremsstrahlung corrections to $q\bar{q} \rightarrow q\bar{q}$.

to processes seven to eleven are:

- Process 7) - $gsZs$, $gtZt$, $gsZt$, $gtZs$

- Process 8) - $gsZs$, $gsWt$

- Process 9) - $gsZs$

- Process 10) - $gtZt$, $gtWs$

- Process 11) - $gtZt$ (5.2)

If we have an expression for the sum of all bremsstrahlung interferences based on the tree level interference $gtZs$ of the form:

$$gtZs_{brem} = (g_V^1 + \lambda_1 g_A^1)(g_V^b - \lambda_b g_A^b) f(p_a, p_b, p_1, p_2, p_3, m_Z, \Gamma_Z)$$

and an expression for the sum of all bremsstrahlung interferences based on the tree level interference $gsZs$ of the form:

$$gsZs_{brem} = (g_V^1 + \lambda_1 g_A^1)(g_V^b - \lambda_b g_A^b) g(p_a, p_b, p_1, p_2, p_3, m_Z, \Gamma_Z)$$

then for the other topologies we have:

$$\begin{aligned}
gtZt_{brem} &= -(g_V^1 - \lambda_1 g_A^1)(g_V^2 - \lambda_2 g_A^2) g(-p_2, p_b, p_1, -p_a, p_3, m_Z, \Gamma_Z) \\
guZt_{brem} &= -(g_V^1 + \lambda_1 g_A^1)(g_V^2 + \lambda_2 g_A^2) f(p_b, -p_2, p_1, -p_a, p_3, m_Z, \Gamma_Z) \\
guWt_{brem} &= -(1 + \lambda_1)(1 + \lambda_2)\frac{\cos^2(\theta_W)}{2} f(p_b, -p_2, p_1, -p_a, p_3, m_w, \Gamma_W) \\
gtZu_{brem} &= -(g_V^1 - \lambda_1 g_A^1)(g_V^2 - \lambda_2 g_A^2) f(p_a, -p_2, p_1, -p_b, p_3, m_Z, \Gamma_Z) \\
gtWu_{brem} &= (1 + \lambda_1)(1 + \lambda_2)\frac{\cos^2(\theta_W)}{2} f(p_a, -p_2, p_1, -p_b, p_3, m_W, \Gamma_W) \\
guZu_{brem} &= (g_V^1 - \lambda_1 g_A^1)(g_V^2 - \lambda_2 g_A^2) g(p_a, -p_2, p_1, -p_b, p_3, m_Z, \Gamma_Z) \\
gsZt_{brem} &= (g_V^1 + \lambda_1 g_A^1)(g_V^b - \lambda_b g_A^b) f(-p_2, p_b, p_1, -p_a, p_3, m_Z, \Gamma_Z) \\
gsWt_{brem} &= (1 + \lambda_1)(1 - \lambda_b)\frac{\cos^2(\theta_W)}{2} f(-p_2, p_b, p_1, -p_a, p_3, m_W, \Gamma_W) \\
gtWs_{brem} &= (1 + \lambda_1)(1 - \lambda_b)\frac{\cos^2(\theta_W)}{2} f(p_a, p_b, p_1, p_2, p_3, m_W, \Gamma_W)
\end{aligned} \tag{5.3}$$

(the factor of $\frac{\cos^2(\theta_W)}{2}$ is to compensate for the difference between the Z and W couplings.)

5.3 The Dipole Subtraction Terms in the 4-Quark Case

If we first consider process one ($q\bar{q} \to q\bar{q}$ of the same flavour) we have four topologies at $\alpha_S \alpha_W$ order - interference between two t-channel tree level diagrams (one with a Z boson exchanged and one with a gluon exchanged) - $gtZt$, interference between two u-channel diagrams (again one Z and one gluon) - $guZu$ and the two possible interferences between t-channel and u-channel exchanges (one with the gluon in the t-channel and the Z in the u-channel and vice versa) - $gtZu$ and $guZt$.

Note that not all of these topologies actually contribute at leading order, specifically $gtZt$ and $guZu$ both have vanishing colour factors. However we will have gluon bremsstrahlung corrections to all four topologies as the additional gluon will change the colour factor, therefore we will have dipole subtraction terms proportional to each of the four tree level interferences (up to colour factors)(as usual, the incoming quarks will have momenta p_a and p_b and the final state quarks will have momenta p_1 and p_2 with the emitted gluon having momentum p_3).

If we start by looking at the case of $gtZt$ there will be eight dipoles that contribute:

- Interference between emission from particle a and particle 2. One case where a is the emitter and 2 the spectator and one case the other way round.
- Interference between emission from particle b and particle 1. Again with either particle playing the role of emitter.
- Interference between emission from particle 1 and particle 2.
- Interference between emission from particle a and particle b.

The dipoles associated with interference between particle a and particle 1 and the interference between particle b and particle 2 both have vanishing colour factors.

All of these dipoles will be proportional to the tree level interference:

$$T_{t,g}T_{t,Z}(\tilde{s},\tilde{t},\lambda_1,\lambda_2) =$$
$$\frac{g^2 g_S^2}{4\cos^2\theta_W}(c_V^1+\lambda_1 c_A^1)(c_V^2+\lambda_2 c_A^2)\frac{1}{\tilde{t}(\tilde{t}-m_Z^2)}(\tilde{t}+2\tilde{s}+\tilde{t}\lambda_1\lambda_2)^2 \qquad (5.4)$$

This is simply the tree level matrix element squared with the colour factor omitted (which, in this case, is zero). $\tilde{s}$ and $\tilde{t}$ are the usual Mandelstam variables but potentially rescaled by the x factor from [7].

For the term where we interfere emission from particle a with emission from particle 2 we have:

$$x = \frac{p_2.p_a + p_3.p_a - p_2.p_3}{p_2.p_a + p_3.p_a}$$

$$z = \frac{p_2.p_a}{p_2.p_a + p_3.p_a}$$

$$u = \frac{p_3.p_a}{p_2.p_a + p_3.p_a}$$

$$\tilde{t} = 2p_1.p_b - 2xp_a.p_b$$

$$\tilde{s} = xs$$

$$p_{23} = p_2.p_3$$

$$p_{a3} = p_a.p_3$$

$$\text{colourfactor} = -\frac{C_F C_A}{2} \tag{5.5}$$

For the term where we interfere emission from particle b with emission from particle 1 we have:

$$x = \frac{p_1.p_b + p_3.p_b - p_1.p_3}{p_1.p_b + p_3.p_b}$$

$$z = \frac{p_1.p_b}{p_1.p_b + p_3.p_b}$$

$$u = \frac{p_3.p_b}{p_1.p_b + p_3.p_b}$$

$$\tilde{t} = 2p_2.p_a - 2xp_a.p_b$$

$$\tilde{s} = xs$$

$$p_{13} = p_1.p_3$$

$$p_{b3} = p_b.p_3$$

$$\text{colourfactor} = -\frac{C_F C_A}{2} \tag{5.6}$$

In either of these two cases the dipoles for a final state emitter and initial state spectator will be:

$$D_{ij}^{a/b} = -\frac{\text{colourfactor}}{2p_{i3}} \frac{V_{ij}^{a/b}(z,x)}{x} \times T_{t,g} T_{t,Z}(\tilde{s},\tilde{t},\lambda_1,\lambda_2)$$
$$V_{ij}^{a/b}(z,x) = \frac{4}{2-z-x} - 2(1+z) \tag{5.7}$$

And for the case with an initial state emitter and final state spectator:

$$D_{j}^{ia/b} = -\frac{\text{colourfactor}}{2p_{a/b3}} \frac{V_{i}^{ja/b}(x,u)}{x} \times T_{t,g} T_{t,Z}(\tilde{s},\tilde{t},\lambda_1,\lambda_2)$$
$$V_{i}^{ja/b}(z,x) = \frac{4}{1-x+u} - 2(1+x) \tag{5.8}$$

For the two cases with final state emitters and final state spectators (interference between emission from particle 1 and emission from particle 2) we have:

$$D_{j}^{ik} = -\frac{\text{colourfactor}}{2p_{i3}} V_{jk}^{i}(z,y) T_{t,g} T_{t,Z}(\tilde{s},\tilde{t},\lambda_1,\lambda_2)$$
$$V_{jk}^{i}(z,y) = \frac{4}{1-z+zy} - 2(1+z) \tag{5.9}$$

If the emitter is particle 1 (and the spectator is particle 2):

$$z = \frac{p_1 \cdot p_2}{p_1 \cdot p_2 + p_2 \cdot p_3}$$
$$y = \frac{p_1 \cdot p_3}{p_a \cdot p_b}$$
$$\tilde{t} = -2\left[p_1 \cdot p_a + p_3 \cdot p_a - \frac{y}{(1-y)} p_2 \cdot p_a\right]$$
$$\tilde{s} = p_a \cdot p_b$$
$$p_{13} = p_1 \cdot p_3$$
$$\text{colourfactor} = \frac{c_F c_A}{2} \tag{5.10}$$

If the emitter is particle 2:

$$
\begin{aligned}
z &= \frac{p_1.p_2}{p_1.p_2 + p_1.p_3} \\
y &= \frac{p_2.p_3}{p_a.p_b} \\
\tilde{t} &= -2\frac{p_1.p_a}{1-y} \\
\tilde{s} &= p_a.p_b \\
p_{23} &= p_2.p_3 \\
\text{colourfactor} &= \frac{c_F c_A}{2}
\end{aligned}
\tag{5.11}
$$

Finally, for the two cases where we have initial state emitters and initial state spectators (interference between emission from particle a and emission from particle b) we have:

$$
\begin{aligned}
D_{a/b}^{3b/a} &= -\frac{\text{colourfactor}}{2p_{a/b3}} V_{b/a}^{a/bi}(x) T_{t,g} T_{t,Z}(\tilde{s}, \tilde{t}, \lambda_1, \lambda_2) \\
V_{b/a}^{a/bi}(x) &= \frac{4}{1-x} - 2(1+x)
\end{aligned}
\tag{5.12}
$$

If the emitter is particle a (and the spectator is particle b):

$$
\begin{aligned}
x &= 1 - \frac{p_3.p_a + p_3.p_b}{p_a.p_b} \\
\tilde{t} &= -2\left((1+x)p_1.p_a + p_1.p_b - p_1.p_3\right. \\
&\left. -(2p_1.p_b + (1+x)p_1.p_a - p_1.p_3)x\frac{2p_a.p_b - p_3.p_a}{4xp_a.p_b + (1-x)p_3.p_a)}\right) \\
\tilde{s} &= p_1.p_2 \\
p_{a3} &= p_a.p_3 \\
\text{colourfactor} &= \frac{c_F c_A}{2}
\end{aligned}
\tag{5.13}
$$

If the emitter is particle b:

$$
\begin{aligned}
x &= 1 - \frac{p_3.p_a + p_3.p_b}{p_a.p_b} \\
\tilde{t} &= -2\,(2p_1.p_a + p_1.p_b - p_1.p_3 \\
&-(2p_1.p_a + (1+x)p_1.p_b - p_1.p_3)\frac{(1+x)p_a.p_b - p_3.p_a}{4xp_a.p_b + (1-x)p_3.p_b)}) \\
\tilde{s} &= p_1.p_2 \\
p_{b3} &= p_b.p_3 \\
\text{colourfactor} &= \frac{c_F c_A}{2}
\end{aligned}
\tag{5.14}
$$

For completeness it is also worth noting that in the case where we have interference between emission from particle 1 and particle a we have:

$$
\begin{aligned}
x &= \frac{p_1.p_a + p_3.p_a - p_1.p_3}{p_1.p_a + p_3.p_a} \\
z &= \frac{p_1.p_a}{p_1.p_a + p_3.p_a} \\
u &= \frac{p_3.p_a}{p_1.p_a + p_3.p_a} \\
\tilde{t} &= -2p_2.p_b \\
\tilde{s} &= xs \\
p_{13} &= p_1.p_3 \\
p_{a3} &= p_3.p_a \\
\text{colourfactor} &= 0
\end{aligned}
\tag{5.15}
$$

For interference between emission from particle 2 and particle b:

$$x = \frac{p_2.p_b + p_3.p_b - p_2.p_3}{p_2.p_b + p_3.p_b}$$

$$z = \frac{p_2.p_b}{p_2.p_b + p_3.p_b}$$

$$u = \frac{p_3.p_b}{p_2.p_b + p_3.p_b}$$

$$\tilde{t} = -2p_1.p_a$$

$$\tilde{s} = xs$$

$$p_{23} = p_2.p_3$$

$$p_{b3} = p_3.p_b$$

$$\text{colourfactor} = 0 \tag{5.16}$$

(Although the colour factors for these pairs of particles for this topology vanish they won't for every topology. The expressions for the dipole variables given above are independent of topology.)

Depending on which particle is the emitter and which is the spectator the dipoles can be evaluated using eq(5.7) and eq(5.8). Eq(5.7) for a final state emitter and eq(5.8) for an initial state emitter.

In the case where we are evaluating dipoles for corrections to interference between two t-channel exchanges the colour factors come out to be zero and as such these terms do not contribute - they will, however, contribute to other topologies.

For the other topologies (see above) the values of x, z, u, $\tilde{s}$, $\tilde{t}$, p_{i3} and p_{a3} and the expressions we use to obtain the dipole for a particular interference remain the same - the only things that change are the colour factors and (of course) the tree level interference.

For the $guZu$ topology we have:

$$\begin{aligned}
\text{colourfactor}_{a,1} &= -\frac{c_F c_A}{2} \\
\text{colourfactor}_{a,2} &= 0 \\
\text{colourfactor}_{b,1} &= 0 \\
\text{colourfactor}_{b,2} &= -\frac{c_F c_A}{2} \\
\text{colourfactor}_{1,2} &= \frac{c_F c_A}{2} \\
\text{colourfactor}_{a,b} &= \frac{c_F c_A}{2}
\end{aligned} \tag{5.17}$$

Where (for example) $\text{colourfactor}_{a,1}$ is the colour factor for interference between emission from particle a and particle 1.

The tree level interference for $guZu$ is:

$$\begin{aligned}
&T_{u,g}T_{u,Z}(\tilde{u},\tilde{t},\lambda_1,\lambda_2) = \\
&\frac{g^2 g_S^2}{4\cos^2\theta_W}(c_V^1+\lambda_1 c_A^1)(c_V^2+\lambda_2 c_A^2)\frac{2\tilde{u}}{\tilde{u}-m_Z^2}\left(1+2\frac{\tilde{t}}{\tilde{u}}-\lambda_1\lambda_2\right)
\end{aligned} \tag{5.18}$$

Where $\tilde{u} = -\tilde{s}-\tilde{t}$. We obtain expressions for x, z, u, $\tilde{s}$, $\tilde{t}$, p_{i3} and p_{a3} from the equations given below:

$$\begin{aligned}
&\text{interference}_{a,1} \rightarrow \text{eq(5.15)} \\
&\text{interference}_{a,2} \rightarrow \text{eq(5.5)} \\
&\text{interference}_{b,1} \rightarrow \text{eq(5.6)} \\
&\text{interference}_{b,2} \rightarrow \text{eq(5.16)} \\
&\text{interference}_{1,2} \rightarrow \text{eq(5.10) or eq(5.11)} \\
&\text{interference}_{a,b} \rightarrow \text{eq(5.13) or eq(5.14)} \\
&\text{[depending on which is the emitter and which is the spectator]}
\end{aligned} \tag{5.19}$$

For the $gtZu$ topology we have:

$$\begin{aligned}
\text{colourfactor}_{a,1} &= -c_F c_A (c_F - c_A/2) \\
\text{colourfactor}_{a,2} &= -c_F^2 c_A \\
\text{colourfactor}_{b,1} &= -c_F^2 c_A \\
\text{colourfactor}_{b,2} &= -c_F c_A (c_F - c_A/2) \\
\text{colourfactor}_{1,2} &= c_F c_A (c_F - c_A/2) \\
\text{colourfactor}_{a,b} &= c_F c_A (c_F - c_A/2)
\end{aligned} \tag{5.20}$$

With a tree level interference of:

$$\begin{aligned}
&T_{t,g} T_{u,Z}(\tilde{u}, \tilde{t}, \lambda_1, \lambda_2) = \\
&-\frac{g^2 g_S^2}{4\cos^2\theta_W}(c_V^1 + \lambda_1 c_A^1)(c_V^2 + \lambda_2 c_A^2)\frac{8\tilde{u}}{\tilde{u} - m_Z^2}\left(2 + \frac{\tilde{t}}{\tilde{u}} + \frac{\tilde{u}}{\tilde{t}}\right)
\end{aligned} \tag{5.21}$$

For the $guZt$ topology we have:

$$\begin{aligned}
\text{colourfactor}_{a,1} &= -c_F^2 c_A \\
\text{colourfactor}_{a,2} &= -c_F c_A (c_F - c_A/2) \\
\text{colourfactor}_{b,1} &= -c_F c_A (c_F - c_A/2) \\
\text{colourfactor}_{b,2} &= -c_F^2 c_A \\
\text{colourfactor}_{1,2} &= c_F c_A (c_F - c_A/2) \\
\text{colourfactor}_{a,b} &= c_F c_A (c_F - c_A/2)
\end{aligned} \tag{5.22}$$

With a tree level interference of:

$$\begin{aligned}
&T_{u,g} T_{t,Z}(\tilde{u}, \tilde{t}, \lambda_1, \lambda_2) = \\
&-\frac{g^2 g_S^2}{4\cos^2\theta_W}(c_V^1 + \lambda_1 c_A^1)(c_V^2 + \lambda_2 c_A^2)\frac{8\tilde{t}}{\tilde{t} - m_Z^2}\left(2 + \frac{\tilde{t}}{\tilde{u}} + \frac{\tilde{u}}{\tilde{t}}\right)
\end{aligned} \tag{5.23}$$

These are in fact all of the possible topologies for quark-quark (or anti-quark-anti-quark) scattering, for quark-anti-quark scattering we will have:

$gsZs$:

$$\begin{aligned}
\text{colourfactor}_{a,1} &= -\frac{c_F c_A}{2} \\
\text{colourfactor}_{a,2} &= \frac{c_F c_A}{2} \\
\text{colourfactor}_{b,1} &= \frac{c_F c_A}{2} \\
\text{colourfactor}_{b,2} &= -\frac{c_F c_A}{2} \\
\text{colourfactor}_{1,2} &= 0 \\
\text{colourfactor}_{a,b} &= 0
\end{aligned} \tag{5.24}$$

$gtZt$ (quark-anti-quark) this will differ from the quark-quark case due to the colour factor (see eq(3.12)):

$$\begin{aligned}
\text{colourfactor}_{a,1} &= 0 \\
\text{colourfactor}_{a,2} &= \frac{c_F c_A}{2} \\
\text{colourfactor}_{b,1} &= \frac{c_F c_A}{2} \\
\text{colourfactor}_{b,2} &= 0 \\
\text{colourfactor}_{1,2} &= -\frac{c_F c_A}{2} \\
\text{colourfactor}_{a,b} &= -\frac{c_F c_A}{2}
\end{aligned} \tag{5.25}$$

$gtZs$:

$$\begin{aligned}
\text{colourfactor}_{a,1} &= -c_F c_A (c_F - c_A/2) \\
\text{colourfactor}_{a,2} &= c_F c_A (c_F - c_A/2) \\
\text{colourfactor}_{b,1} &= c_F c_A (c_F - c_A/2) \\
\text{colourfactor}_{b,2} &= -c_F c_A (c_F - c_A/2) \\
\text{colourfactor}_{1,2} &= -c_F^2 c_A \\
\text{colourfactor}_{a,b} &= -c_F^2 c_A
\end{aligned} \tag{5.26}$$

$gsZt$:

$$\begin{aligned}
\text{colourfactor}_{a,1} &= -c_F^2 c_A \\
\text{colourfactor}_{a,2} &= c_F c_A (c_F - c_A/2) \\
\text{colourfactor}_{b,1} &= c_F c_A (c_F - c_A/2) \\
\text{colourfactor}_{b,2} &= -c_F^2 c_A \\
\text{colourfactor}_{1,2} &= -c_F c_A (c_F - c_A/2) \\
\text{colourfactor}_{a,b} &= -c_F c_A (c_F - c_A/2)
\end{aligned} \tag{5.27}$$

5.4 The Integrated Dipole Subtractions

Shown below is a demonstration of the cancellation of the IR divergences coming from the one loop corrections to the interference between a t-channel gluon exchange and an s-channel Z exchange. These poles will cancel with an integrated dipole term that is proportional to the same tree level interference.

In practice this will be one part of process seven ($q\bar{q} \to q\bar{q}$ shown in fig(5.6, 5.7 and 5.8)) - for the complete process we would also need corrections to t-channel Z and s-channel gluon, t-channel Z and gluon and s-channel Z and gluon. The IR poles generated by corrections to each of these interferences will cancel individually with their own integrated dipole term.

The s-channel graph squared part will be mechanically very similar to the case for $b\bar{b}$ production (shown in eq(4.55 - 4.62)) and the t-channel squared part can be obtained by crossing this result.

The full expressions for all of the prototype diagrams needed for this calculation are given in Appendix B.

5.4.1 The Pole Parts of The Virtual Corrections

The Box Diagrams

There will be two interferences including two gluon box diagrams. Firstly we have the interference between a t-channel, uncrossed two gluon box ($B_{t,gg}$) and s-channel, tree level Z exchange ($T_{s,Z}$). Keeping only the pole parts of this interference we have:

$$
\begin{aligned}
&2 \times B_{t,gg} \times T_{s,Z} \times c_F^2 c_A = \\
&\\
&\delta_{\lambda_a,-\lambda_b}\delta_{\lambda_a,\lambda_1}\delta_{\lambda_b,\lambda_2} \times \\
&2c_F^2 c_A \frac{g^2 g_s^4}{4\cos^2\theta_W}(g_V+\lambda_1 g_A)(g_V-\lambda_b g_A)\frac{1}{16\pi^2} \\
&\left(-\frac{4}{\epsilon^2}+\frac{4}{\epsilon}ln\left(\frac{|s|}{\mu^2}\right)\right) \\
&\frac{1}{t(s-m_Z^2)}(2s+t(1-\lambda_1\lambda_2))(2t+s(1-\lambda_1\lambda_b))
\end{aligned}
\tag{5.28}
$$

Where we have a factor of two for interference and the colour factor is $c_F c_A = \mathrm{tr}(t^A t^B t^B t^A)$ (note there will be an overall factor of $\delta_{\lambda_a,-\lambda_b}\delta_{\lambda_a,\lambda_1}\delta_{\lambda_b,\lambda_2}$ attached to every interference to ensure helicity conservation - for convenience this will be omitted from this calculation from here on).

Secondly we will have the interference between a t-channel, crossed two gluon box ($B_{t,gg,X}$) and s-channel, tree level Z exchange ($T_{s,Z}$). From this we will obtain:

$$
\begin{aligned}
&2 \times B_{t,gg,X} \times T_{s,Z} \times c_F c_A(c_F - c_a/2) = \\
&2c_F c_A(c_F - c_A/2)\frac{g^2 g_s^4}{4\cos^2\theta_W}(g_V+\lambda_1 g_A)(g_V-\lambda_b g_A)\frac{1}{16\pi^2} \\
&\left(\frac{4}{\epsilon^2}-\frac{4}{\epsilon}ln\left(\frac{|u|}{\mu^2}\right)\right) \\
&\frac{1}{t(s-m_Z^2)}(2s+t(1-\lambda_1\lambda_2))(2t+s(1-\lambda_1\lambda_b))
\end{aligned}
\tag{5.29}
$$

Here the colour factor is $\mathrm{tr}(t^A t^B t^A t^B) = c_F c_A(c_F - c_A/2)$.

There will also be two interferences including the gluon-Z box. Firstly the interference

between a t-channel, tree level gluon exchange ($T_{t,g}$) and the s-channel gluon-Z box ($B_{s,gZ}$):

$$
\begin{aligned}
&4 \times T_{t,g} \times B_{s,gZ} \times c_F c_A (c_F - c_a/2) = \\
&4 c_F c_A (c_F - c_A/2) \frac{g^2 g_s^4}{4 \cos^2 \theta_W} (g_V + \lambda_1 g_A)(g_V - \lambda_b g_A) \frac{1}{16\pi^2} \\
&\left(-\frac{2}{\epsilon^2} + \frac{2}{\epsilon} ln \left(\frac{|t|}{\mu^2} \right) + \frac{4}{\epsilon} \frac{m_z^2}{s} ln \left(\left| 1 - \frac{s}{m_z^2} \right| \right) \right) \\
&\frac{1}{t(s - m_Z^2)} (2s + t(1 - \lambda_1 \lambda_2))(2t + s(1 - \lambda_1 \lambda_b))
\end{aligned}
\tag{5.30}
$$

Here we have a factor of two for interference and a factor of two associated with interchanging the gluon and the Z.

Secondly we will have the interference between a t-channel, tree level gluon exchange ($T_{t,g}$) and the s-channel gluon-Z crossed box ($B_{s,gZ,X}$):

$$
\begin{aligned}
&4 \times T_{t,g} \times B_{s,gZ,X} \times c_F c_A (c_F - c_a/2) = \\
&4 c_F c_A (c_F - c_A/2) \frac{g^2 g_s^4}{4 \cos^2 \theta_W} (g_V + \lambda_1 g_A)(g_V - \lambda_b g_A) \frac{1}{16\pi^2} \\
&\left(\frac{2}{\epsilon^2} - \frac{2}{\epsilon} ln \left(\frac{|u|}{\mu^2} \right) - \frac{4}{\epsilon} \frac{m_z^2}{s} ln \left(\left| 1 - \frac{s}{m_z^2} \right| \right) \right) \\
&\frac{1}{t(s - m_Z^2)} (2s + t(1 - \lambda_1 \lambda_2))(2t + s(1 - \lambda_1 \lambda_b))
\end{aligned}
\tag{5.31}
$$

So the sum of the contributions from all of the box diagrams will be:

$$
\begin{aligned}
&2 B_{t,gg} T_{s,Z} c_F^2 c_A + (2 B_{t,gg,X} T_{s,Z} + 4 T_{t,g} B_{s,gZ} + 4 T_{t,g} B_{s,gZ,X}) c_F c_A (c_F - c_a/2) = \\
&\frac{g^2 g_s^4}{4 \cos^2 \theta_W} (g_V + \lambda_1 g_A)(g_V - \lambda_b g_A) \frac{1}{t(s - m_z^2)} (2s + t(1 - \lambda_1 \lambda_2))(2t + s(1 - \lambda_1 \lambda_b)) \\
&\frac{1}{16\pi^2} \left[2 c_F^2 c_A \frac{4}{\epsilon} ln \left(\frac{|s|}{\mu^2} \right) - c_F c_A^2 \frac{4}{\epsilon^2} - 2 c_F c_A (c_F - c_A/2) \frac{4}{\epsilon} ln \left(\frac{|u|}{\mu^2} \right) \right. \\
&\left. 2 c_F c_A (c_F - c_A/2) \left(\frac{4}{\epsilon} ln \left(\frac{|t|}{\mu^2} \right) - \frac{4}{\epsilon} ln \left(\frac{|u|}{\mu^2} \right) \right) \right]
\end{aligned}
\tag{5.32}
$$

The Vertex Corrections

We will also have contributions from a number of interferences including triangle diagrams. Firstly the interference between a QED-type gluon vertex correction to a

t-channel gluon exchange ($V^{qed}_{t,gvge}$) and the s-channel, tree level Z exchange ($T_{s,Z}$).

$$
\begin{aligned}
&4 \times V^{qed}_{t,gvge} \times T_{s,Z} \times c_F c_A (c_F - c_A/2) = \\
&4 c_F c_A (c_F - c_A/2) \frac{g^2 g_s^4}{4\cos^2\theta_W} (g_V + \lambda_1 g_A)(g_V - \lambda_b g_A) \frac{1}{16\pi^2} \\
&\left(-\frac{2}{\epsilon^2} - \frac{3}{\epsilon} + \frac{2}{\epsilon} ln\left(\frac{|t|}{\mu^2}\right)\right) \\
&\frac{1}{t(s-m_z^2)} (2s + t(1-\lambda_1\lambda_2))(2t + s(1-\lambda_1\lambda_b))
\end{aligned}
\tag{5.33}
$$

Here we have two factors of two, one for the interference and one to account for the fact that we can have the vertex correction on either of the two quark lines.

Secondly we will have the interference between a QCD-type gluon vertex correction to a t-channel gluon exchange ($V^{qcd}_{t,gvge}$) and the s-channel, tree level Z exchange ($T_{s,Z}$).

$$
\begin{aligned}
&4 \times V^{qcd}_{t,gvge} \times T_{s,Z} \times \frac{c_F c_A^2}{2} = \\
&4 \frac{c_F c_A^2}{2} \frac{g^2 g_s^4}{4\cos^2\theta_W} (g_V + \lambda_1 g_A)(g_V - \lambda_b g_A) \frac{1}{16\pi^2} \\
&\left(-\frac{1}{\epsilon}\right) \\
&\frac{1}{t(s-m_z^2)} (2s + t(1-\lambda_1\lambda_2))(2t + s(1-\lambda_1\lambda_b))
\end{aligned}
\tag{5.34}
$$

Finally we have the interference between a QED-type gluon vertex correction to an s-channel Z exchange ($V^{qed}_{s,gvZe}$) (in this case we cannot have a QCD-type vertex) and a tree level t-channel gluon exchange.

$$
\begin{aligned}
&4 \times V^{qed}_{s,gvZe} \times T_{t,g} \times c_F^2 c_A = \\
&4 c_F^2 c_A \frac{g^2 g_s^4}{4\cos^2\theta_W} (g_V + \lambda_1 g_A)(g_V - \lambda_b g_A) \frac{1}{16\pi^2} \\
&\left(-\frac{2}{\epsilon} - \frac{3}{\epsilon} + \frac{2}{\epsilon} ln\left(\frac{|s|}{\mu^2}\right)\right) \\
&\frac{1}{t(s-m_z^2)} (2s + t(1-\lambda_1\lambda_2))(2t + s(1-\lambda_1\lambda_b))
\end{aligned}
\tag{5.35}
$$

If we combine the triangle results we obtain:

$$
\begin{aligned}
&4V^{qed}_{t,gvge}T_{s,Z}c_Fc_A(c_F-c_A/2)+4V^{qcd}_{t,gvge}T_{s,Z}\frac{c_Fc_A^2}{2}+4V^{qed}_{s,gvZe}T_{t,g}c_F^2c_A= \\
&\frac{g^2g_s^4}{4\cos^2\theta_W}(g_V+\lambda_1 g_A)(g_V-\lambda_b g_A) \\
&\frac{1}{t(s-m_z^2)}(2s+t(1-\lambda_1\lambda_2))(2t+s(1-\lambda_1\lambda_b)) \\
&\frac{1}{16\pi^2}\left[4c_F^2c_A\left(-\frac{2}{\epsilon^2}-\frac{3}{\epsilon}+\frac{2}{\epsilon}ln\left(\frac{|t|}{\mu^2}\right)\right)\right. \\
&-2c_Fc_A^2\left(-\frac{2}{\epsilon^2}-\frac{3}{\epsilon}+\frac{2}{\epsilon}ln\left(\frac{|t|}{\mu^2}\right)\right) \\
&\left.+2c_Fc_A^2\left(\frac{-1}{\epsilon}\right)+4c_F^2c_A\left(-\frac{2}{\epsilon^2}-\frac{3}{\epsilon}+\frac{2}{\epsilon}ln\left(\frac{|s|}{\mu^2}\right)\right)\right]
\end{aligned}
\tag{5.36}
$$

The $I(\epsilon)$ Term

Using the formulae presented in Chapter 3 we have, for the integrated dipole term:

$$
\begin{aligned}
&2\times I(\epsilon)= \\
&\frac{g^2g_s^4}{4\cos^2\theta_W}(g_V+\lambda_1 g_A)(g_V-\lambda_b g_A) \\
&\frac{1}{t(s-m_z^2)}(2s+t(1-\lambda_1\lambda_2))(2t+s(1-\lambda_1\lambda_b)) \\
&\frac{1}{16\pi^2}\left[4c_F^2c_A\left(\frac{4}{\epsilon^2}+\frac{6}{\epsilon}-\frac{4}{\epsilon}ln\left(\frac{|s|}{\mu^2}\right)\right)\right. \\
&-4c_Fc_A(c_F-c_A/2)\frac{4}{\epsilon}ln\left(\frac{|t|}{\mu^2}\right) \\
&\left.+4c_Fc_A(c_F-c_A/2)\frac{4}{\epsilon}ln\left(\frac{|u|}{\mu^2}\right)\right]
\end{aligned}
\tag{5.37}
$$

If we sum the contributions from eq(5.32, 5.36 and 5.37) we obtain a complete cancellation of all the log terms and all of the double poles. We are however left with the single pole:

$$
\begin{aligned}
&\frac{g^2g_s^4}{4\cos^2\theta_W}(g_V+\lambda_1 g_A)(g_V-\lambda_b g_A) \\
&\frac{1}{t(s-m_z^2)}(2s+t(1-\lambda_1\lambda_2))(2t+s(1-\lambda_1\lambda_b)) \\
&c_Fc_A^2\frac{1}{16\pi^2}\frac{4}{\epsilon}
\end{aligned}
\tag{5.38}
$$

This left over pole will be cancelled by the IR divergent part of the external quark self energies. These diagrams have thus far been ignored as they do not have a finite contribution to the matrix element (This was not required in the $b\bar{b}$ case as there the interferences including external quark self energies have vanishing colour factors).

Given this proof that the IR poles cancel we can safely drop the poles in both the virtual corrections and in $I(\epsilon)$ when we code the process. Note that unlike in the $b\bar{b}$ case we do have collinear divergences (from initial-initial and final-final interferences that are no longer forbidden by colour) as well as soft poles.

5.5 The x Dependent Parts Of The Integrated Dipoles

We recall, from Chapter(3), that the expression for the total next to leading order cross section is:

$$\begin{aligned}
&\sigma^{NLO}(p_a, p_b) = \\
&\sigma^{NLO\{1,2\}}(p_a, p_b) + \sigma^{NLO\{1,2,3\}}(p_a, p_b) \\
&+ \int_0^1 dx [\hat{\sigma}^{NLO\{1,2\}}(x; xp_a, p_b) + \hat{\sigma}^{NLO\{1,2\}}(x; p_a, xp_b)]
\end{aligned} \tag{5.39}$$

Where $\{1,2\}$ indicates a term that has been integrated over the phase space of the two final state quarks and $\{1,2,3\}$ indicates a term integrated over the phase space of the two final state quarks and an emitted final state real gluon.

The first two terms have already been evaluated ($\sigma^{NLO\{1,2\}}(p_a, p_b)$ is the sum of all virtual corrections rendered finite by the $I(\epsilon)$ term and $\sigma^{NLO\{1,2,3\}}(p_a, p_b)$ is the sum of all bremsstrahlung corrections rendered finite by the dipole terms) but we still need to deal with the third term.

From Chapter(3), eq(3.104) we have:

$$\int_0^1 dx[\hat{\sigma}^{NLO\{1,2\}}(x;xp_a,p_b)+\hat{\sigma}^{NLO\{1,2\}}(x;p_a,xp_b)]$$
$$=\int_0^1 dx\int_{[1,2]}[d\sigma_{a,b}^{TREE}(xp_a,p_b)\otimes(K+P)^{a,a}(x)]_{\epsilon=0}+$$
$$\int_0^1 dx\int_{[1,2]}[d\sigma_{a,b}^{TREE}(p_a,xp_b)\otimes(K+P)^{b,b}(x)]_{\epsilon=0}$$
$$=\int_0^1 dx\int d\Phi^{(1,2)}(xp_a,p_b)F_J^{(1,2)}(p_1,p_2;xp_a,p_b)$$
$$<p_1,p_2,xp_a,p_b|(K^{a,a}(x)+P^{a,a}(xp_a,x))|p_1,p_2,xp_a,p_b>$$
$$+\int_0^1 dx\int d\Phi^{(1,2)}(p_a,xp_b)F_J^{(1,2)}(p_1,p_2;p_a,xp_b)$$
$$<p_1,p_2,p_a,xp_b|(K^{b,b}(x)+P^{b,b}(xp_b,x))|p_1,p_2,p_a,xp_b> \qquad (5.40)$$

Where the function $F_J^{(1,2)}$ defines the particular observable we are intending to compute. Here we are again integrating over the phase space of the two final state quarks.

As for both the virtual and real corrections (and their respective dipole parts) we need to break the calculation down into the eleven sub-processes defined at the start of this chapter. The topologies that contribute to the insertion terms for a given process are the same as those that contribute to the $I(\epsilon)$, dipole terms and bremsstrahlung interferences - those given in eq(5.1) and eq(5.2). We have a $\hat{\sigma}$ term for each individual topology (denoted by *top*) in a given process.

From [7] and eq(3.105) we have (in the case of soft gluon emission from a quark):

$$P^{a,a}(x,xp_a)=-\frac{\alpha_S}{2\pi}\left(\frac{1+x^2}{1-x}\right)_+\frac{c_F}{T_a^2}$$
$$\left[T_1.T_a ln\left(\frac{2xp_a.p_1}{\mu^2}\right)+T_2.T_a ln\left(\frac{2xp_a.p_2}{\mu^2}\right)+T_a.T_b ln\left(\frac{2xp_a.p_b}{\mu^2}\right)\right]$$
$$P^{b,b}(x,xp_b)=-\frac{\alpha_S}{2\pi}\left(\frac{1+x^2}{1-x}\right)_+\frac{c_F}{T_b^2}$$
$$\left[T_1.T_b ln\left(\frac{2xp_b.p_1}{\mu^2}\right)+T_2.T_b ln\left(\frac{2xp_b.p_2}{\mu^2}\right)+T_a.T_b ln\left(\frac{2xp_a.p_b}{\mu^2}\right)\right] \qquad (5.41)$$

(T_a^2 and $T_b^2=c_F$).

This term is proportional to a 'plus prescription' part and as such the integral over x

is treated as a convolution of the form:

$$(\text{plus prescription part})_+ \times [f(x) - f(1)] \tag{5.42}$$

This means that the terms proportional to $P^{a,a/b,b}$ will be:

$$\begin{aligned}
&\left(\frac{1+x^2}{1-x}\right)\frac{\alpha_S}{2\pi} \times C(top) \\
&\Bigg[\left(2T_a.T_b ln\left(\frac{s}{\mu^2}\right) + (T_a.T_1 + T_b.T_2) ln\left(\frac{-t}{\mu^2}\right) + (T_a.T_2 + T_b.T_1) ln\left(\frac{-u}{\mu^2}\right)\right) \\
&\times \mathcal{M}^2_{tree}(s,t,top) \\
&- \left(2T_a.T_b ln\left(\frac{\hat{s}}{\mu^2}\right) + (T_a.T_1 + T_b.T_2) ln\left(\frac{-\hat{t}}{\mu^2}\right) + (T_a.T_2 + T_b.T_1) ln\left(\frac{-\hat{u}}{\mu^2}\right)\right) \\
&\times \frac{1}{x}\mathcal{M}^2_{tree}(\hat{s},\hat{t},top)\Bigg]
\end{aligned} \tag{5.43}$$

Where $C(top)$ is the tree level coupling of the particular topology we are dealing with (see below).

For the 'K' part we have:

$$\begin{aligned}
&K^{a,a}(x) = \frac{\alpha_S}{2\pi} \\
&\Bigg[\delta^{aa}\left(T_1.T_a\frac{\gamma_1}{T_a^2} + T_2.T_a\frac{\gamma_2}{T_a^2}\right)\left(\left(\frac{1}{1-x}\right)_+ + \delta(1-x)\right) \\
&+\bar{K}^{a,a}(x) - K^{a,a}_{FS} \\
&-T_a.T_b\frac{1}{T_a^2}\tilde{K}^{a,a}(x)\Bigg]
\end{aligned} \tag{5.44}$$

(Clearly $\delta^{a,a}$ in this case will be one since the two particles are both quarks but it has been included for completeness. Again $T_a^2 = c_F$)

$$\bar{K}^{a,a} =$$

$$c_F col_{tree}\left[\frac{2}{1-x}ln\left(\frac{1-x}{x}\right)_+ - (1+x)ln\left(\frac{1-x}{x}\right) + (1-x)\right]$$

$$-c_F col_{tree}\delta(1-x)(5-\pi^2)$$

$$\bar{K}^{a,a}(x) =$$

$$-(1+x)ln(1-x) + \delta^{aa}T_a^2\left[\left(\frac{2}{1-x}ln(1-x)\right)_+ - \frac{\pi^2}{3}\delta(1-x)\right] \tag{5.45}$$

The scheme dependent part, $K_{FS}^{a,a}$, is zero in the $\bar{MS}/\bar{DR}$ schemes.

Therefore we have for the total part proportional to $K^{a,a/b,b}$:

$$C(top)\frac{\alpha_S}{2\pi}\left[\frac{1}{x}\mathcal{M}^2_{tree}(\hat{s},\hat{t},top) - \mathcal{M}^2_{tree}(s,t,top)\right] \times$$

$$\left[\left(\frac{1}{1-x}\right)\frac{3}{2}(T_1.T_a + T_2.T_a + T_1.T_b + T_2.T_b)\right.$$

$$\left.-c_F col_{tree}\frac{2}{1-x}ln\left(\frac{1-x}{x}\right) - T_a.T_b\left(\frac{2}{1-x}ln(1-x)\right)\right]$$

$$+C(top)\frac{\alpha_S}{2\pi}\mathcal{M}^2_{tree}(\hat{s},\hat{t},top) \times$$

$$\left[-c_F col_{tree}\left[(1+x)ln\left(\frac{1-x}{x}\right) + (1-x)\right]\right.$$

$$\left.+T_a.T_b\frac{1}{c_F}(1+x)ln(1-x)\right]$$

$$+C(top)\frac{\alpha_S}{2\pi}\mathcal{M}^2_{tree}(s,t,top) \times$$

$$\left[\frac{3}{2}(T_1.T_a + T_2.T_a + T_1.T_b + T_2.T_b) - 2c_F col_{tree}(5-\pi^2) + T_a.T_b\frac{2\pi^2}{3}\right] \tag{5.46}$$

Where we have used the definition $\gamma_{1/2} = \frac{3}{2}c_F$.

In the term proportional to $\mathcal{M}^2_{tree}(s,t,top)$ we have used the delta functions to perform the x integral - therefore this term will not appear underneath the integral.

So, the total term for a particular topology will be:

$$\int d\Phi^{\{1,2\}} F_J^{(1,2)} \frac{C(top)\alpha_S}{2\pi} \mathcal{M}^2_{tree}(s,t,top) \times$$
$$\left[\frac{3}{2}\left(T_1.T_a + T_2.T_a + T_1.T_b + T_2.T_b\right) - 2c_F col_{tree}(5-\pi^2) + T_a.T_b\frac{2\pi^2}{3}\right.$$
$$+\left(\frac{1+x^2}{1-x}\right)2T_a.T_b ln\left(\frac{s}{\mu^2}\right) + \left(\frac{1+x^2}{1-x}\right)(T_a.T_1 + T_b.T_2) ln\left(\frac{-t}{\mu^2}\right)$$
$$\left.+\left(\frac{1+x^2}{1-x}\right)(T_a.T_2 + T_b.T_1) ln\left(\frac{-u}{\mu^2}\right)\right]$$

$$+\int_0^1 dx \int d\hat{\Phi}^{\{1,2\}} \hat{F}_J^{(1,2)} \frac{C(top)\alpha_S}{2\pi}\left[\frac{1}{x}\mathcal{M}^2_{tree}(\hat{s},\hat{t},top) - \mathcal{M}^2_{tree}(s,t,top)\right] \times$$
$$\left[\left(\frac{1}{1-x}\right)\frac{3}{2}\left(T_1.T_a + T_2.T_a + T_1.T_b + T_2.T_b\right)\right.$$
$$\left.-c_F col_{tree}\frac{2}{1-x} ln\left(\frac{1-x}{x}\right) - T_a.T_b\left(\frac{2}{1-x} ln(1-x)\right)\right]$$

$$+\int_0^1 dx \int d\hat{\Phi}^{\{1,2\}} \hat{F}_J^{(1,2)} \frac{C(top)\alpha_S}{2\pi} \mathcal{M}^2_{tree}(\hat{s},\hat{t},top) \times$$
$$\left[\frac{3}{2}\left(T_1.T_a + T_2.T_a + T_1.T_b + T_2.T_b\right) - 2c_F col_{tree}(5-\pi^2) + T_a.T_b\frac{2\pi^2}{3}\right.$$
$$-\left(\frac{1+x^2}{1-x}\right)\frac{1}{x}2T_a.T_b ln\left(\frac{\hat{s}}{\mu^2}\right) - \left(\frac{1+x^2}{1-x}\right)\frac{1}{x}(T_a.T_1 + T_b.T_2) ln\left(\frac{-\hat{t}}{\mu^2}\right)$$
$$\left.-\left(\frac{1+x^2}{1-x}\right)\frac{1}{x}(T_a.T_2 + T_b.T_1) ln\left(\frac{-\hat{u}}{\mu^2}\right)\right] \tag{5.47}$$

Where:

$$d\hat{\Phi}^{\{1,2\}} = d\Phi^{\{1,2\}}(xp_a, p_b) = d\Phi^{\{1,2\}}(p_a, xp_b)$$
$$d\Phi^{\{1,2\}} = d\Phi^{\{1,2\}}(p_a, p_b) \tag{5.48}$$

The equality in the first line is true in all cases as the phase space is Lorentz invariant.

$$\hat{F}_J^{(1,2)} = F_J^{(1,2)}(xp_a, p_b; p_1, p_2) = F_J^{(1,2)}(p_a, xp_b; p_1, p_2)$$
$$F_J^{(1,2)} = F_J^{(1,2)}(p_a, p_b; p_1, p_2) \tag{5.49}$$

Here the equality in the first line only holds in cases where the observable being examined is Lorentz invariant. If we were studying (for example) the scattering angle then

Topology	$T_a.T_b/T_1.T_2$	$T_1.T_a/T_2.T_b$	$T_1.T_b/T_2.T_a$	col_{tree}
$gtZt(qq)$	$\frac{c_F c_A}{2}$	0	$-\frac{c_F c_A}{2}$	0
$guZu$	$\frac{c_F c_A}{2}$	$-\frac{c_F c_A}{2}$	0	0
$guZt$	$(c_F - c_A/2)c_F c_A$	$-c_F^2 c_A$	$-(c_F - c_A/2)c_F c_A$	$c_F c_A$
$gtZu$	$(c_F - c_A/2)c_F c_A$	$-(c_F - c_A/2)c_F c_A$	$-c_F^2 c_A$	$c_F c_A$
$gtZt(q\bar{q})$	$-\frac{c_F c_A}{2}$	0	$\frac{c_F c_A}{2}$	0
$gsZs$	0	$-\frac{c_F c_A}{2}$	$\frac{c_F c_A}{2}$	0
$gsZt$	$-(c_F - c_A/2)c_F c_A$	$-c_F^2 c_A$	$(c_F - c_A/2)c_F c_A$	$c_F c_A$
$gtZs$	$-c_F^2 c_A$	$-(c_F - c_A/2)c_F c_A$	$c_F^2 c_A$	$c_F c_A$

Table 5.1: Colour factors for the various topologies.

we would have to split up the function into two parts.

The colour factors $(T_i.T_j)$ will vary depending on which topology we are considering. Note that again these are colour factors as defined in [7] and as such will potentially differ from the normal colour factor by a factor of -1 (we pick up a factor of -1 if we interfere emission from a particle and emission from an antiparticle similarly if we interfere emission from an initial state particle and emission from a final state particle). The colour factors associated with each topology are given in table(5.1). Note that the colour factors for the topologies including a W will be the same as for the corresponding Z topology.

The coupling factors $(C(top))$ are given in table(5.5):

top	$C(top)$
$gtZt$	$g^2 g_S^2/cos^2(\theta_W)\frac{1}{4}(g_V^1 - \lambda_1 g_A^1)(g_V^2 - \lambda_2 g_A^2)$
$gtZu$	$g^2 g_S^2/cos^2(\theta_W)\frac{1}{4}(g_V^1 - \lambda_1 g_A^1)(g_V^2 - \lambda_2 g_A^2)$
$guZt$	$g^2 g_S^2/cos^2(\theta_W)\frac{1}{4}(g_V^1 + \lambda_1 g_A^1)(g_V^2 + \lambda_2 g_A^2)$
$guZu$	$g^2 g_S^2/cos^2(\theta_W)\frac{1}{4}(g_V^1 - \lambda_1 g_A^1)(g_V^2 - \lambda_2 g_A^2)$
$gsZs$	$g^2 g_S^2/cos^2(\theta_W)\frac{1}{4}(g_V^1 + \lambda_1 g_A^1)(g_V^b - \lambda_b g_A^b)$
$gtZs$	$g^2 g_S^2/cos^2(\theta_W)\frac{1}{4}(g_V^1 + \lambda_1 g_A^1)(g_V^b - \lambda_b g_A^b)$
$gsZt$	$g^2 g_S^2/cos^2(\theta_W)\frac{1}{4}(g_V^1 + \lambda_1 g_A^1)(g_V^b - \lambda_b g_A^b)$
$guWt$	$g^2 g_S^2 \frac{1}{8}(1+\lambda_1)(1+\lambda_2)$
$gtWu$	$g^2 g_S^2 \frac{1}{8}(1+\lambda_1)(1+\lambda_2)$
$gtWs$	$g^2 g_S^2 \frac{1}{8}(1+\lambda_1)(1-\lambda_b)$
$gsWt$	$g^2 g_S^2 \frac{1}{8}(1+\lambda_1)(1-\lambda_b)$

Table 5.2: The couplings for the various topologies.

5.6 Integrating Over The Phase Space

To perform the integral over the phase space (and also over the dipole variable x) we use a Monte Carlo type method - specifically the VEGAS [27] code.

5.6.1 How Does VEGAS work?

Because the phase space integral is multidimensional it is significantly faster to use a Monte Carlo type approach rather than a trapezium rule inspired method.

In the simplest terms a Monte Carlo integral works as follows. For some observable $\mathcal{O}(x)$ the mean value can be calculated as:

$$< \mathcal{O} >_w \equiv \frac{\int dx \mathcal{O}(x) w(x)}{\int dx w(x)} = \lim_{N \to \infty} \frac{\sum_i^N \mathcal{O}(x_i)}{N} \tag{5.50}$$

Where each x_i corresponds to a particular phase space point and where $w(x)$ is some weighting function for each point in phase space.

We can, with reasonable ease, use numerical methods to evaluate the last term in eq(5.50) for large values of N which therefore allows us to get a handle on the integral in the second term.

A value for p_T is calculated for each phase space point - the result for that point is then binned according to this value. This allows us to evaluate observables as a function of p_T.

We restrict the integral over rapidity (or, equivalently, the scattering angle) to the region that can be measured at the experiment we are calculating for. This allowed rapidity range is dependent on the detectors ability to pick up events with the jets oriented along, or close to, the beam axis. This range is machine dependent - the exact values are given in section(5.7).

VEGAS uses so called 'adaptive sampling'. On the first iteration of the Monte Carlo

the phase space points are selected at random across the entire phase space volume. On second and subsequent iterations a weighting is implemented that ensures that more phase space points are sampled in the regions where the cross section is large. This 'importance sampling' results in enhanced accuracy where it is most important. VEGAS also increases the weighting in regions of phase space that contribute most to the error ('stratified sampling') - the combination of these two weightings makes VEGAS the most popular algorithm for this kind of calculation.

5.6.2 The Two to Two Body Part of the Phase Space

The two body phase space is:

$$d\sigma = \frac{1}{4E_a E_b |v_a - v_b|} \frac{d^3p_1}{(2\pi)^3 2E_1} \frac{d^3p_2}{(2\pi)^3 2E_2} |\bar{\mathcal{M}}|^2 (2\pi)^4 \delta^4(p_a + p_b - p_1 - p_2) \tag{5.51}$$

The Lorentz invariant part is:

$$d\Pi |\bar{\mathcal{M}}|^2 = \frac{d^3p_1}{(2\pi)^3 2E_1} \frac{d^3p_2}{(2\pi)^3 2E_2} (2\pi)^4 \delta^4(p_a + p_b - p_1 - p_2) |\bar{\mathcal{M}}|^2 \tag{5.52}$$

Following some changes of variable and using the delta function to do some of the integrals we obtain:

$$\begin{aligned} d\Pi |\bar{\mathcal{M}}|^2 &= d\Omega \frac{p_1^2}{16\pi^2 E_1 E_2} \left(\frac{p_1}{E_1} + \frac{p_1}{E_2} \right)^{-1} |\bar{\mathcal{M}}|^2 \\ &= d\Omega \frac{1}{16\pi^2} \frac{|p_1|}{E_{cm}} |\bar{\mathcal{M}}|^2 \end{aligned} \tag{5.53}$$

Substitute this back into the equation for $d\sigma$ and we obtain:

$$d\sigma = d\Omega \frac{1}{2E_A 2E_B |v_a - v_b|} \frac{|p_1|}{(2\pi)^2 4E_{cm}} |\bar{\mathcal{M}}|^2 \tag{5.54}$$

In the case where all external masses are negligible (in fact, in the the case where all external masses are equal):

$$d\sigma = d\Omega \frac{|\bar{\mathcal{M}}|^2}{64\pi^2 E_{cm}^2} \tag{5.55}$$

If we modify this to account for the integration over the PDF's ($f_i^b(x_b)$) then we have:

$$d\sigma = \sum_{ij} f_i^1(x_1) f_j^2(x_2) \frac{1}{64\pi^2 \hat{s}} |\bar{\mathcal{M}}|_{ij}^2 dx_1 dx_2 d\phi d\cos\theta \tag{5.56}$$

$\hat{s} = x_1 x_2 s$, (note that $|\bar{\mathcal{M}}|_{ij}^2$ is a function of $\hat{s}$). The indices '1' and '2' correspond to the two incoming hadrons (pp for LHC and $p\bar{p}$ for Tevatron) and the summation over i and j corresponds to a summation over all possible combinations of incoming partons. The PDF's also depend on an energy scale - in this case we use the renormalisation scale μ (we set the renormalisation scale to be either E_{cm} or E_T depending on which PDF's we are using) to match up with the prescription we use for the cancellation of IR divergences.

When calculating unpolarised observables we use the CTEQ PDF's [20] and when calculating polarised observables we use the Gehrmann-Stirling set A (GSA) PDF's [21]. The dependence of the results on the exact PDF's used is discussed in section(5.6.4).

Ideally we want the limits of the integrals in the phase space to be fixed as this is easier for the integration programs (in this case 'VEGAS' [27]) to deal with. To change the variables of integration so that this is the case we first multiply through by $\frac{x_1}{x_1}$:

$$d\sigma = \sum_{ij} f_i^1(x_1) f_j^2(x_2) \frac{1}{64\pi^2 \hat{s}} |\bar{\mathcal{M}}|_{ij}^2 \frac{dx_1}{x_1} dx_2 x_1 d\phi d\cos\theta \tag{5.57}$$

Change variables from x_1 to $ln(x_1)$ ($\frac{dln(x_1)}{dx_1} = \frac{1}{x_1}$) and from x_2 to p_q ($\hat{s} = x_1 x_2 s = E_{cm}^2 = 4E_q^2 = 4p_q^2$).

$$d\sigma = \sum_{ij} f_i^1(x_1) f_j^2(x_2) \frac{1}{8\pi^2 \hat{s} s} |\bar{\mathcal{M}}|_{ij}^2 |p_q| dln(x_1) dp_q d\phi sin\theta d\theta \tag{5.58}$$

We would now like to change variables from θ to η, the rapidity.

$$\eta = -ln\left[tan\frac{\theta}{2}\right] \tag{5.59}$$

In practice we will constrain the rapidity integral to only include events that can actually be detected at whatever experiment we are performing the calculation for. Typically this means we only integrate up to some maximum rapidity (corresponding to a minimum value of θ).

$$d\sigma = \sum_{ij} f_i^1(x_1) f_j^2(x_2) \frac{1}{8\pi^2 \hat{s} s} |\bar{\mathcal{M}}|_{ij}^2 |p_q| dln(x_1) dp_q d\phi sin^2\theta d\eta \tag{5.60}$$

Finally we will exchange p_q for the transverse momentum, p_T. $p_T = sin\theta p_q$ so $\frac{dp_T}{dp_q} = sin\theta$.

$$d\sigma = \sum_{ij} f_i^1(x_1) f_j^2(x_2) \frac{1}{8\pi^2 \hat{s} s} |\bar{\mathcal{M}}|_{ij}^2 p_T dln(x_1) dp_T d\phi d\eta \tag{5.61}$$

This is the final form of the two body phase space measure that is used in the Monte Carlo calculations for the massless cases (both pp to two jets and $b\bar{b}$ production).

5.6.3 The Two to Three Body Part of the Phase Space

The integration over the two to three body phase space is somewhat less complicated than the two to two as there is no x dependent part of the unintegrated dipoles. The phase space used in the massless case is:

$$d\sigma = \frac{1}{(2\pi)^5} \frac{1}{16\hat{s}} |\mathcal{M}|^2 \frac{m_{12}}{2} \frac{\hat{s} - m_{12}^2}{2\hat{s}} dm_{12} d\Omega_1 d\Omega_3 \tag{5.62}$$

Where $\hat{s}$ is s scaled by the Bjorken x's, and m_{12}^2 is the invariant mass squared of the two final state quarks, $(p_a + p_b - p_3)^2$. $d\Omega_1$ is the scattering angle of particle 1 in the centre of mass frame and $d\Omega_3$ is the scattering angle of particle 3, the gluon, also in the centre of mass frame.

Note that once again we have had to define a phase space where the limits on the integrals are constant - this is because this is what VEGAS requires.

5.6.4 Dependence Of Results On The PDF's

The polarised PDF's are less accurately known than the unpolarised and are also only valid up to a maximum value of μ^2 of about 1TeV - therefore the maximum p_T that can be studied is 500GeV.

We compare our results using two possible options for our PDF's - GSA and Glück-Reya-Stratmann-Vogelsang standard set (GRSV-STN) [21] [22]. Fig(5.15) shows that

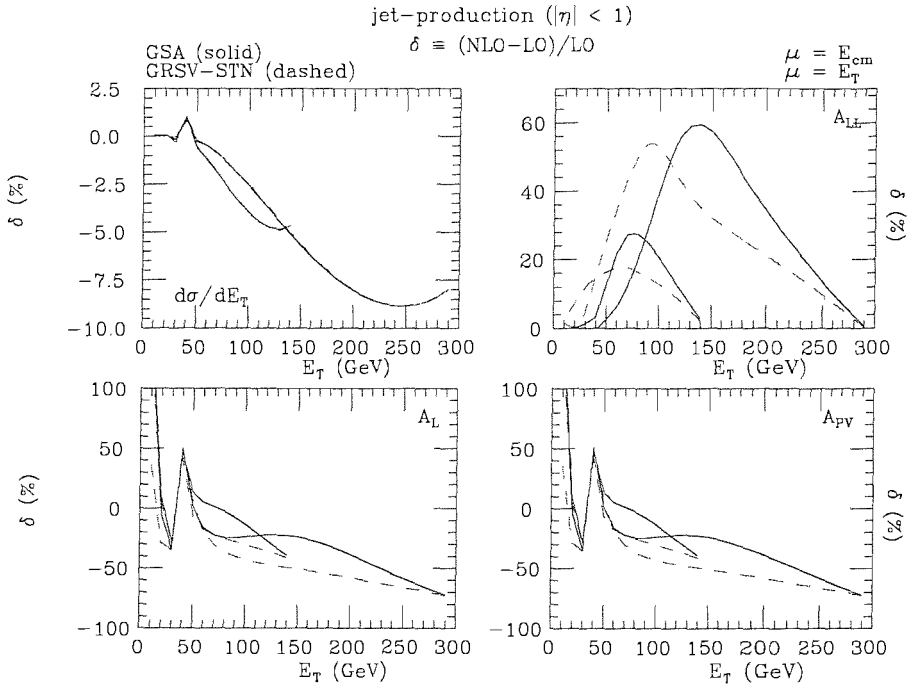

Figure 5.15: The dependence of both the total cross section and the beam asymmetries on the choice of PDF's (GSA and GRSV-STN). The results both both RHIC-spin energies are plotted.

the dependence of the total cross section at RHIC on the (polarised) PDF used is insignificant.

However, there does appear to be some effect on the asymmetries. The A_{LL} correction remains at a very similar magnitude although where the peak of the correction lies on the p_T scale is dependent of the PDF used (140GeV for GSA and 80Gev for GSRV-STN). For A_L the GSRV-STN result generates a larger correction at low p_T (above the

Z resonance) but which tends to the GSA result near the p_T limit.

In fig(5.16) we can see that, at LHC, there is a very small variation on the total cross

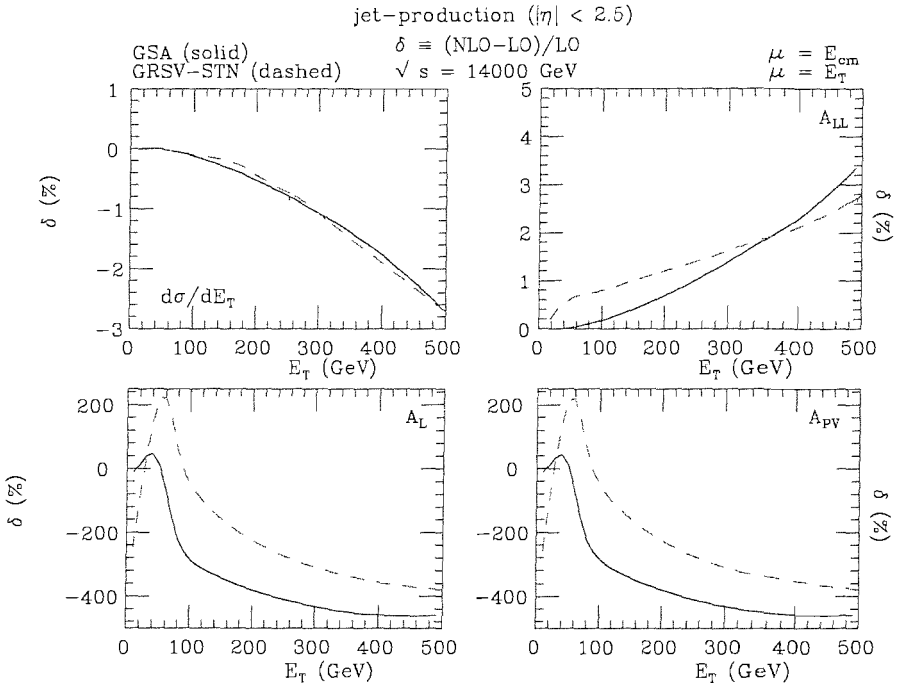

Figure 5.16: The dependence of both the total cross section and the beam asymmetries at a polarised LHC on the choice of PDF's (GSA and GRSV-STN).

section depending on which PDF is used (a larger variation than at RHIC but still insignificant).

In the polarised observables we see only a small variation in the results for the correction to A_{LL} but the correction to A_L varies greatly depending on the PDF used. At low p_T the GSRV-STN PDF's give corrections that are large and positive (+200% compared with +40% for GSA) but at high p_T, when both corrections become negative, the GSA result is somewhat larger (-440% compared with -360%).

It is potentially of some interest that there seems to be a variation in the results for these asymmetries with choice of PDF. One of the purposes of a polarised experiment (such as RHIC-spin) is to reduce the uncertainty inherent in polarised PDF's. If we measure an observable that has a strong dependence on choice of PDF and compare it

with theoretical predictions that make use of varying PDF's then in principle we may be able to shed some light on the polarisation structure of the proton.

Note that here the variation in A_L is of most interest as it is entirely parity violating and as such will have no contribution from pure QCD. A_{LL} is not a parity violating observable and as such we would need to include NLO QCD to obtain a reliable NLO result.

5.7 Results For The Full Four Quark Calculation

5.7.1 Total Cross-sections

Tevatron

The results presented below were first published in [28].

Presented in fig(5.17) are the total results for two jet production at Tevatron - here they have been integrated over a rapidity of $0.1 < |\eta| < 0.7$ to match the CDF detector coverage. The correction here is significantly larger than in the case of the $b\bar{b}$ production rate - of the order of 3% compared with a small fraction of 1%. The partonic energies are still not however, in general, high enough to make the Sudakov logarithms large. The correction is enhanced due to the fact that we have many more diagrams contributing to the one loop correction (a factor of ten or more than in the $b\bar{b}$ case, see section(5.1)) than we did in the $b\bar{b}$ calculation, whereas the number of diagrams contributing to the QCD tree level has only increased by a factor of three or so.

It is interesting to compare these results with the Run 1 results from the CDF experiment [4]. We can see from fig(5.18) that a large positive correction would help to explain this experimental result using only the standard model (it is worth mentioning that work has been done to explain this disagreement by modifying the gluon PDF's,

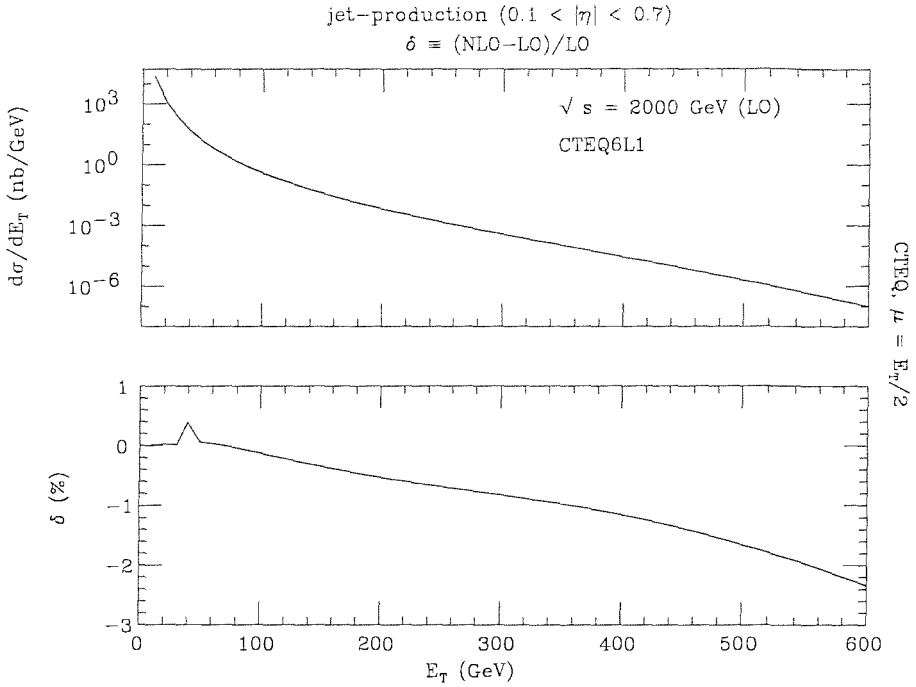

Figure 5.17: Presented here is the total two jet production rate at the Tevatron (2TeV) plotted against p_T. The lower plot gives the percentage correction of the $\alpha_S^2\alpha_W$ term relative to the sum of all tree level processes (α_W^2, $\alpha_W\alpha_S$ and α_S^2).

see [5]. Also, preliminary data from Run 2 indicates that the discrepancy between data and theory may not be significant [29]). However the result obtained from the NLO weak corrections is negative meaning that the agreement between theory and experiment is actually worse. However, at 500GeV the weak correction is only between 1 and 2% which is small compared with the statistical errors.

LHC

At LHC we integrate the rapidity over a range of -2.5 to 2.5 - this is reasonable for the LHC detectors. Fig(5.19) shows the total cross section for two jet production plotted against E_T. Once again δ is the correction to the LO cross section (α_S^2, $\alpha_S\alpha_W$ and α_W^2) from the NLO weak correction.

As can easily be seen in the figure the corrections are again greatly enhanced when

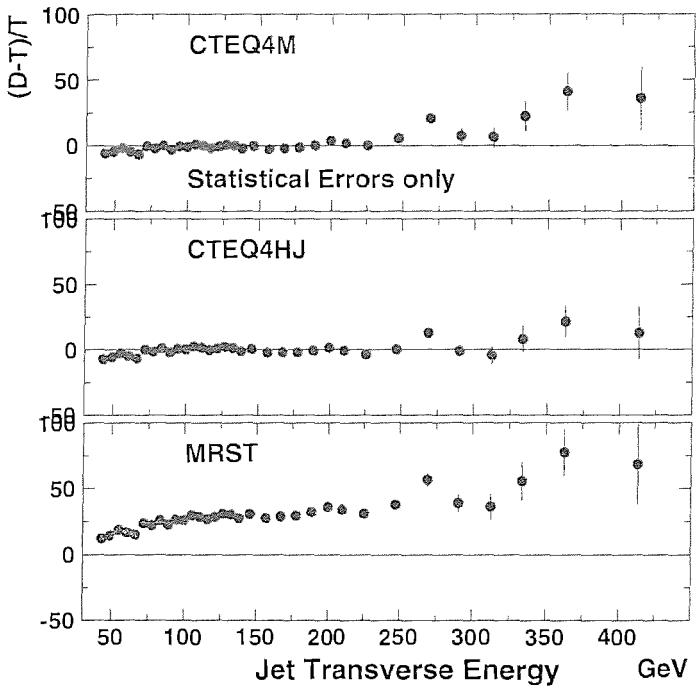

Figure 5.18: [4] Shown above are are plots showing the discrepancy between theory and experiment at Tevatron [(Data-Theory)/Theory] for several different PDF's.

compared to the $b\bar{b}$ production cross section (an increase from 2% to as much as 30%). Once again this is a result of the significantly larger number of diagrams that contribute to the correction. At LHC the NLO weak corrections are large across the majority of the p_T spectrum rising to 10% and above at anything over 1000GeV this means that the weak correction to the total two jet cross section is significant even when compared to the current uncertainties associated with the NLO QCD results [30] [31] [32].

In fig(5.20) the various contributing parts of the two jet cross section are shown as in comparison to the LO QCD (both gg and qq to 2 jets). We can clearly see that at low p_T the gg contributions are dominant but that the qq contributions become comparable and eventually larger between 1000 and 2000 GeV.

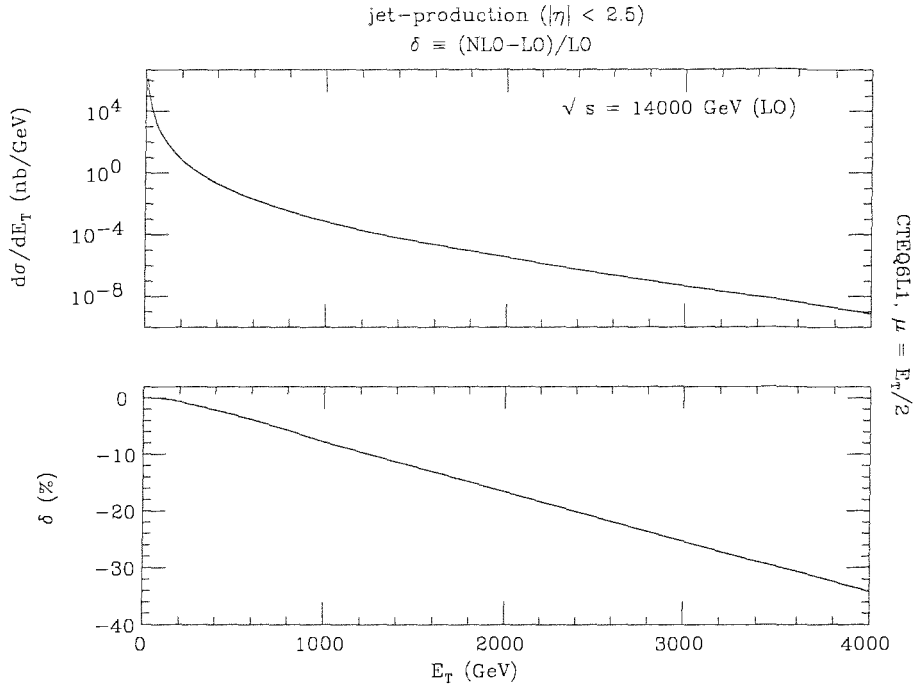

Figure 5.19: Presented above is the total two jet production rate at LHC (14TeV) plotted against p_T. The lower plot gives the percentage correction of the $\alpha_S^2\alpha_W$ term relative to the sum of all tree level processes (α_W^2, $\alpha_w\alpha_S$ and α_S^2).

5.7.2 Polarised Observables

The results presented below were first published in [33].

RHIC

In fig(5.21) we present the total cross section at RHIC as well as the three polarised beam asymmetries (A_L, A_{LL} and A_{LL}^{PV} all defined in section(2.2.1)). We integrate over a rapidity $|\eta| < 1$ and at the two RHIC-spin energies (300 and 600GeV). The first result it is interesting to observe is that the correction to the total cross section is somewhat larger than at Tevatron (see fig(5.17)); 8% at 300GeV compared with about 1% at Tevatron. This is perhaps surprising given that the centre of mass energy at RHIC is significantly smaller than at Tevatron meaning that the Sudakov logs will be even less significant.

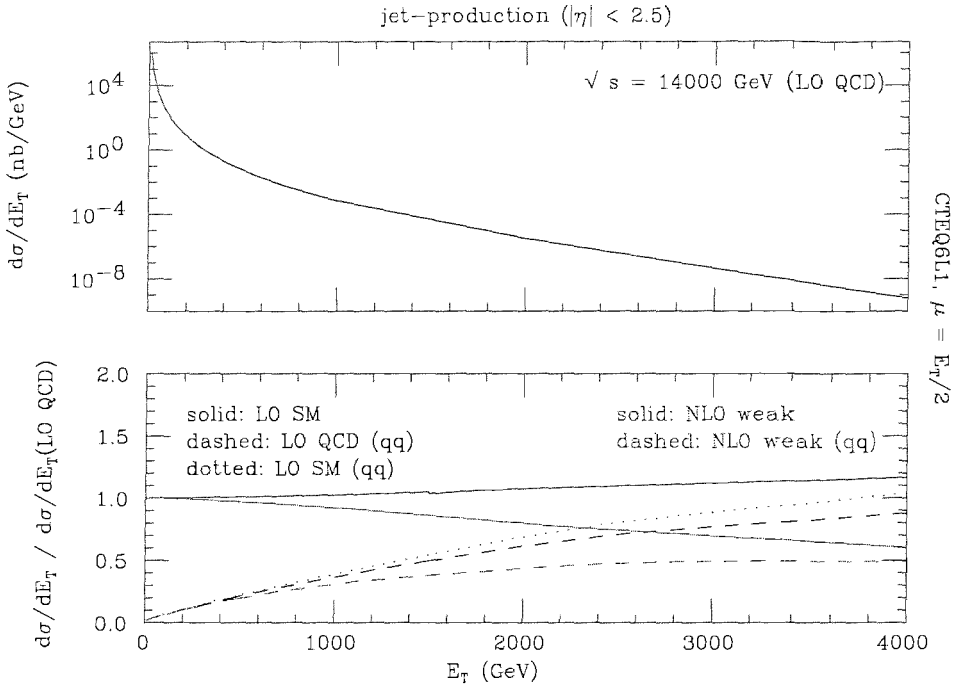

Figure 5.20: The relative sizes of the LO and NLO corrections compared with the tree level QCD results.

The explanation for this large correction can be discovered if we break the correction down and look at the contributions from the subprocesses. This breakdown is shown in Table(5.3). If we look at the contribution to the LO cross section from the different processes we see that the dominant four quark processes are $qq \rightarrow qq$ and $qq' \rightarrow qq'$. These two processes also have not insignificant corrections to them from the one loop weak effects and are therefore the dominant contribution to the total δ. These largest corrections will be suppressed at Tevatron due to the initial state being a $p\bar{p}$ resulting in the correction to the total cross section being smaller at that machine.

Looking at the asymmetries we see that the effects are very significant. For A_{LL} we have, for the 300(600)GeV machine, a maximum of some 25(60)% at an E_T of 70(140)GeV. A_L and A_{PV} both rise to as high as -70% corrections at high E_T (140GeV for $\sqrt{s}$=300GeV and 300GeV for $\sqrt{s}$=600GeV) and to +100% at low E_T (away from the resonance effects at the Z mass).

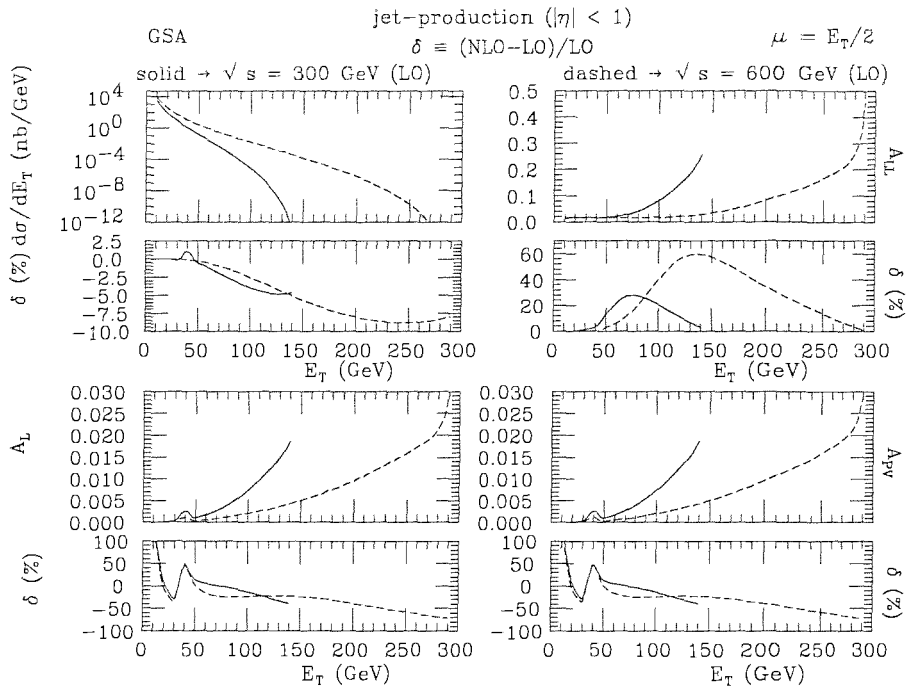

Figure 5.21: The total cross section, A_{LL}, A_L and A_{PV} calculated for RHIC at a centre of mass energy of both 300 and 600 GeV plotted against E_T. Each observable is also presented as a correction to the total tree level contribution.

All of these results should be observable at RHIC.

A Hypothetical Polarised LHC

The results for the polarised asymmetries at a hypothetic polarised LHC are shown in fig(5.22). Here we use the standard LHC energy of 14TeV and $|\eta| < 2.5$. The plot of the total cross section is the same as that given in fig(5.19) but over a restricted E_T. This restriction is in place because the polarised PDF's used (GSA) to evaluate the polarised observables are only valid up to an E_T of about 500GeV.

The behaviour of the asymmetries at LHC compared to those at RHIC could benefit from some explanation. Both of the LHC asymmetries are somewhat smaller than those at RHIC on an absolute scale. The one loop weak correction relative to the tree level asymmetry is smaller at LHC than RHIC for A_{LL} (the non parity violating asymmetry)

Subprocess	$\sqrt{s} = 300,\ E_T = 70$ (GeV)		$\sqrt{s} = 600,\ E_T = 140$ (GeV)	
	LO (%)	Corr (%)	LO (%)	Corr (%)
$gg \to gg$	1.35		1.17	
$gg \to q\bar{q}$	0.065	0.027	0.057	–0.18
$q\bar{q} \to gg$	0.19	0.025	0.18	–0.18
$qg \to qg,\ gg \to qg$	24.7	–0.06	23.0	–0.26
$qq \to qq,\ \bar{q}\bar{q} \to \bar{q}\bar{q}$	46.1	–0.90	47.1	–3.0
$qq' \to qq',\ \bar{q}\bar{q}' \to \bar{q}\bar{q}'$(same gen.)	23.8	–6.64	24.6	–14.7
$qq' \to qq',\ \bar{q}\bar{q}' \to \bar{q}\bar{q}'$(diff. gen.)	0.72	0.055	0.7	–0.84
$q\bar{q} \to q\bar{q}$	0.95	–0.25	0.93	–0.71
$q\bar{q} \to q'\bar{q}'$(same gen.)	0.06	10.9	0.057	25.5
$q\bar{q} \to q'\bar{q}'$(diff. gen.)	0.18	1.23	0.17	1.17
$q\bar{q}' \to q\bar{q}'$(same gen.)	1.28	3.2	1.25	2.24
$q\bar{q}' \to q\bar{q}'$(diff. gen.)	0.72	0.05	0.71	–0.8

Table 5.3: A breakdown of the contribution to the RHIC total cross section from each possible sub-process. The column labelled 'LO' shows the percentage of the total leading order cross section associated with each process and the column labelled 'Corr' shows the percentage NLO weak correction to that process.

but larger for the parity violating A_L.

At RHIC energies the proton PDF's are dominated by qq pairs so we can say, to

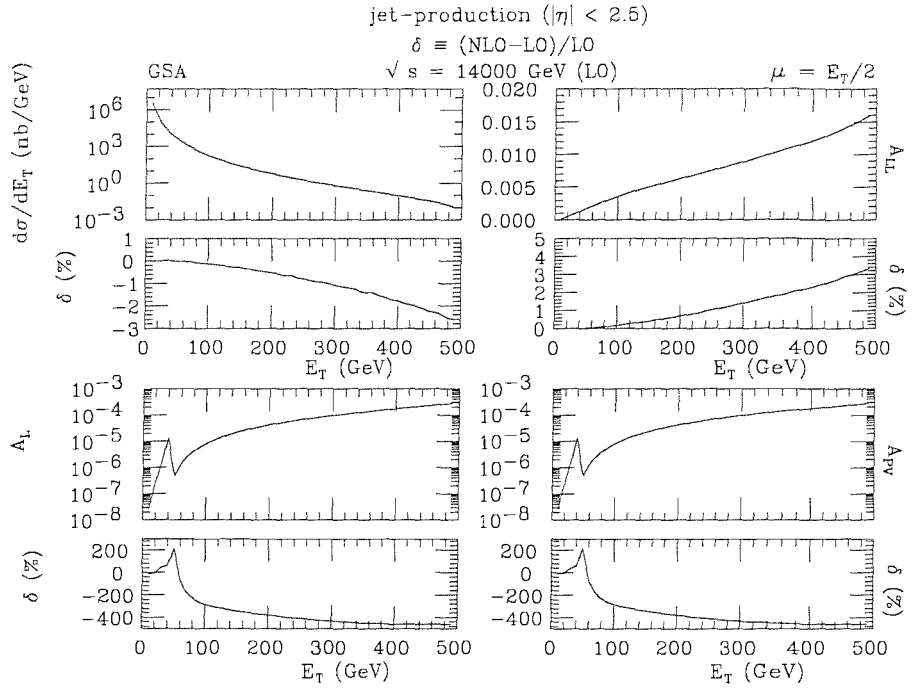

Figure 5.22: The total cross section, A_{LL}, A_L and A_{PV} calculated for LHC at a centre of mass energy of 14 TeV plotted against E_T. Note that the asymmetries are only measurable at a collider with polarised beams which is currently not the case at LHC - these results are presented to show what would be visible at a hypothetical polarised LHC. Each observable is also presented as a correction to the total tree level contribution.

reasonable degree of accuracy, that:

$$A_{LL}^{RHIC} = \frac{\Delta_{LL}\sigma(qq)}{d\sigma(qq)}$$
$$A_{L}^{RHIC} = \frac{\Delta_{L}\sigma(qg)}{d\sigma(qq)}$$
$$\Delta_{LL}\sigma = d\sigma_{++} + d\sigma_{--} - d\sigma_{+-} - d\sigma_{-+}$$
$$\Delta_{L}\sigma = d\sigma_{+} - d\sigma_{-} \tag{5.63}$$

This is true at both tree level and NLO.

However, at LHC the PDF's are generally dominated by gg (this is true across the

entire p_T spectrum accessible to the polarised PDF's) so we should write:

$$A_{LL}^{LHC} = \frac{\Delta_{LL}\sigma(qq) + \Delta_{LL}\sigma(qg) + \Delta_{LL}\sigma(gg)}{d\sigma(qq) + d\sigma(qg) + d\sigma(gg)}$$
$$A_{L}^{LHC} = \frac{\Delta_{L}\sigma(qq) + \Delta_{L}\sigma(qg) + \Delta_{L}\sigma(gg)}{d\sigma(qq) + d\sigma(qg) + d\sigma(gg)} \tag{5.64}$$

At leading order, the contribution to A_L at LHC reduces to:

$$A_{L}^{LHC}(LO) = \frac{\Delta_{L}\sigma(qq)}{d\sigma(qq) + d\sigma(qg) + d\sigma(gg)} \tag{5.65}$$

This is because, at tree level, quark-gluon and gluon-gluon scattering do not have any parity violating terms (they must be pure QCD interferences). As a result the LO A_L is very small (the numerator is suppressed by the PDF's relative to the denominator). This argument does not apply at NLO where we do have $\alpha_S^2\alpha_W$, parity violating contributions to both gg and qg scattering. This means that the NLO will be enhanced relative to the LO leading to a larger correction. This argument does not apply at RHIC as the preferred qq scattering contributes both at LO and NLO.

The absolute asymmetries are reduced at LHC due to the gg dominance of the PDF's we would therefore expect them to rise with increasing p_T as we move into regions with higher incidences of qq initial states however this is difficult to test at present due to the restrictions associated with polarised PDF's.

Chapter 6

t t-bar Production.

The final calculation we will look at is the proton-(anti)proton to $t\bar{t}$ rate. This calculation will be very similar to that for the $b\bar{b}$ rate however due to the large top mass we may no longer make the approximation that all external masses are zero. We may still assume that there are no b or t quarks in the initial state so the topologies of the diagrams we consider will be restricted to those we had in the $b\bar{b}$ calculation.

A calculation of the top production rate will be of interest at the LHC due to the enormous number of tops expected to be created at that machine. Weak contributions to the top production process are of particular interest as, if we can study parity violating observables, then we effectively remove any uncertainty in our predictions resulting from QCD (unknown higher order corrections for example). As described in chapter(2) it is simple to define parity violating observables when we have polarised beams, but these are not available at LHC. However, as it is possible to get a handle on the helicity of a produced top quark we can define similar helicity dependent observables despite the lack of polarised beams. Rather than being dependent on the helicity of the incoming particles these observables will depend on the helicity of the outgoing tops.

The lifetime of a top (anti)quark is too short to measure the helicity directly but it is

possible to do so indirectly by studying the top decay products [34].

6.1 Studying The Helicity Of $t\bar{t}$ Pairs

When we have calculated the matrix element for top anti-top pair production (with helicities λ_1 and λ_2 respectively) we have the helicity matrix element:

$$R^{\lambda_1'\lambda_2'}_{\lambda_1\lambda_2} = \mathcal{M}_{\lambda_1\lambda_2}\mathcal{M}^{*\lambda_1'\lambda_2'} \tag{6.1}$$

(Note that there is interference between $\lambda_i = +1$ and $\lambda_i = -1$)

To calculate real observables we need to generate a $pp \rightarrow$ top decay products cross section rather than simply a $pp \rightarrow t\bar{t}$ cross section.

In the narrow width approximation ($m_t \gg \Gamma$ and $E_{cm} - m_t \gg \Gamma$) this cross section is proportional to:

$$\sum_{\lambda' s} R^{\lambda_1'\lambda_2'}_{\lambda_1\lambda_2}\rho^{(\alpha)\lambda_1}_{\lambda_1'}\bar{\rho}^{(\bar{\alpha})\lambda_2}_{\lambda_2'} \tag{6.2}$$

Where:

$$\begin{aligned}\rho^{(\alpha)\lambda_1}_{\lambda_1'} &= \mu^{(\alpha)}_{\lambda_1'}\mu^{*(\alpha)\lambda_1} \\ \bar{\rho}^{(\bar{\alpha})\lambda_2}_{\lambda_2'} &= \bar{\mu}^{(\bar{\alpha})}_{\lambda_2'}\bar{\mu}^{*(\bar{\alpha})\lambda_2}\end{aligned} \tag{6.3}$$

and $\mu^{(\alpha)}_{\lambda}(\bar{\mu}^{(\alpha)}_{\lambda})$ is the matrix element for the decay of a top (anti)quark of helicity λ into a particular state $\alpha(\bar{\alpha})$.

If we integrate $\rho^{(\alpha)\lambda_1}_{\lambda_1'}$ over all phase space except for the angle of one of the decay products (I) we obtain something of the form:

$$B^{(\alpha)}\frac{(1 + h^I\hat{q}_I.\underline{\sigma})}{4\pi} \tag{6.4}$$

and for $\bar{\rho}^{(\bar{\alpha})\lambda_2}_{\lambda_2'}$ integrated over all phase space bar the angle of decay product J:

$$B^{(\bar{\alpha})}\frac{(1 + h^J\hat{q}_J.\underline{\sigma})}{4\pi} \tag{6.5}$$

Where $B^{(\alpha)/(\bar{\alpha})}$ is the branching ratio of $t/\bar{t}$ into channel $\alpha/\bar{\alpha}$ and $\hat{q}_I$ and $\hat{q}_J$ are unit vectors in the rest frame of the quark and anti-quark respectively.

We choose two vectors, $\underline{b}_3$ and $\underline{\bar{b}}_3$, to be polar vectors in the rest frame of the quark and anti-quark. If we integrate eq(6.2) over all phase space excepting the polar angle of decay product I (the angle between $\underline{b}_3$ and $\hat{q}_I$, θ_I) and the polar angle of decay product J (the angle between $\underline{\bar{b}}_3$ and $\hat{q}_J$, θ_J) then we obtain the differential cross section:

$$\frac{d^3\sigma}{dcos\theta_{cm}dcos\theta_I dcos\theta_J} \propto$$
$$[4A + 2B_3 h^I cos\theta_I + 2\bar{B}_3 h^J + C_{33} cos\theta_I cos\theta_J] \tag{6.6}$$

where:

$$A = \frac{1}{4} R^{\lambda_1 \lambda_2}_{\lambda_1 \lambda_2}$$
$$B_3 = \frac{1}{2} (\underline{b}_3 . \underline{\sigma})^{\lambda_1}_{\lambda_1'} R^{\lambda_1' \lambda_2}_{\lambda_1 \lambda_2}$$
$$\bar{B}_3 = \frac{1}{2} (\underline{\bar{b}}_3 . \sigma)^{\lambda_2}_{\lambda_2'} R^{\lambda_1 \lambda_2'}_{\lambda_1 \lambda_2}$$
$$C_{33} = (\underline{b}_3 . \underline{\sigma})^{\lambda_1}_{\lambda_1'} (\underline{b}_3 . \sigma)^{\lambda_2}_{\lambda_2'} R^{\lambda_1' \lambda_2'}_{\lambda_1 \lambda_2} \tag{6.7}$$

Thus we can extract the helicity structure of the production matrix element from study of the angular distribution of the decay products.

This analysis of the results obtained here has not yet been performed. Presented in section(6.8) along with the total top production cross sections (where this analysis is not necessary) are the observables A_{LL}, A_L and A_{LL}^{PV} calculated as if we could measure the helicity of the top quarks directly. These are not realistic observables but do give some indication of the maximum significance of realistic study of polarised observables.

6.2 gg to $t\bar{t}$

The first contribution to the $t\bar{t}$ production cross section that we will look at is the gluon-gluon goes to top-anti-top process. At order $\alpha_S^2\alpha_W$ these contributions will be bubble, vertex and box corrections to the tree level $gg \rightarrow t\bar{t}$. As was the case for gluon-gluon to massless quarks we know that the total cross section for these virtual corrections must be IR finite (since there are no gluon bremsstrahlung diagrams at this order to cancel any divergences).

6.2.1 Helicity Amplitudes For gg To $t\bar{t}$

Consider the case where we have incoming gluons with momenta p_a and p_b and outgoing massive quarks with momenta p_1 and p_2. The axes are set up (for convenience) such that:

$$\begin{aligned}
p_1^\mu &= \left(\frac{\sqrt{s}}{2}, 0, 0, \frac{\sqrt{s-4m_t^2}}{2}\right) \\
p_2^\mu &= \left(\frac{\sqrt{s}}{2}, 0, 0, -\frac{\sqrt{s-4m_t^2}}{2}\right) \\
p_a^\mu &= \left(\frac{\sqrt{s}}{2}, -\frac{\sqrt{s}}{2}\sin\theta, 0, \frac{\sqrt{s}}{2}cos\theta\right) \\
p_b^\mu &= \left(\frac{\sqrt{s}}{2}, \frac{\sqrt{s}}{2}\sin\theta, 0, -\frac{\sqrt{s}}{2}cos\theta\right)
\end{aligned} \tag{6.8}$$

The gluon polarisations may be taken to be:

$$\begin{aligned}
\epsilon_a^\mu &= \frac{1}{\sqrt{2}}(0, cos\theta, i\lambda_a, \sin\theta) \\
\epsilon_b^\mu &= \frac{1}{\sqrt{2}}(0, -cos\theta, -i\lambda_b, -\sin\theta)
\end{aligned} \tag{6.9}$$

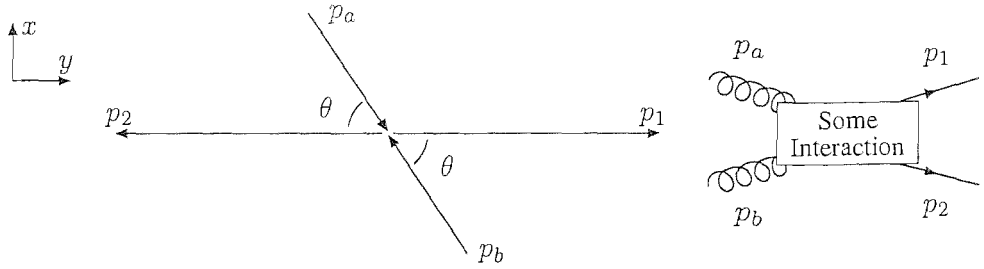

Figure 6.1: The incoming gluons are in the x-z plane with angle θ to the z-axis and the outgoing quarks are emitted in the positive and negative z-direction

The spinors are:

$$u(p_1,\lambda_1) = \sqrt{E+m_t}\begin{pmatrix} \chi(\lambda_1) \\ \frac{\lambda_1 p}{E+m_t}\chi(\lambda_1) \end{pmatrix}$$

$$v(p_2,\lambda_2) = \sqrt{E+m_t}\begin{pmatrix} \frac{-\lambda_2 p}{E+m_t}\chi(\lambda_2) \\ \chi(\lambda_2) \end{pmatrix}$$

$$\bar{u}(p_1,\lambda_1) = \gamma^0 u^\dagger(p_1,\lambda_1) = \sqrt{E+m_t}\left(\chi^\dagger(\lambda_1), -\frac{\lambda_1 p}{E+m_t}\chi^\dagger(\lambda)\right)$$

$$\bar{v}(p_2,\lambda_2) = \gamma^0 v^\dagger(p_2,\lambda_2) = \sqrt{E+m_t}\left(-\frac{\lambda_2 p}{E+m_t}, -\chi^\dagger(\lambda_2)\right) \tag{6.10}$$

Where $p = \frac{\sqrt{s-4m_t^2}}{2}$ and $E = \frac{\sqrt{s}}{2}$. In general the expression for the interaction shown in fig(6.1) will be:

$$\bar{u}(p_1,\lambda_1)\{\Gamma\}v(p_2,\lambda_2) \tag{6.11}$$

(Here Γ is a string of gamma matrices depending on $p_a, p_b, p_1, p_2, \epsilon_a, \epsilon_b$ and any loop momenta (l).) This can then be split into vector, axial and tensor parts:

$$\begin{aligned} &\bar{u}(p_1,\lambda_1)\{\Gamma\}v(p_2,\lambda_2) = \\ &V_\mu \bar{u}(p_1,\lambda_1)\gamma^\mu v(p_2,\lambda_2) + \\ &A_\mu \bar{u}(p_1,\lambda_1)\gamma^\mu\gamma^5 v(p_2,\lambda_2) + \\ &T_{\mu\nu}\bar{u}(p_1,\lambda_1)\sigma^{\mu\nu}v(p_2,\lambda_2) \end{aligned} \tag{6.12}$$

where $\sigma^{\mu\nu} = \frac{i}{2}(\gamma^\mu\gamma^\nu - \gamma^\nu\gamma^\mu)$.

This statement is equivalent to saying:

$$\Gamma = v_\mu\gamma^\mu + a_\mu\gamma^\mu\gamma^5 + \frac{i}{2}T_{\mu\nu}(\gamma^\mu\gamma^\nu - \gamma^\nu\gamma^\mu) + S1 + P1\gamma^5 \tag{6.13}$$

where S is a scalar term and P is a pseudoscalar term. V_μ will be a combination of S and v_μ and A_μ will be a combination of P and a_μ.

So we have:

$$\begin{aligned}
&\mathrm{Tr}(\Gamma\gamma^\rho) = v_\mu\mathrm{Tr}(\gamma^\mu\gamma^\rho) = 4v^\rho \\
&\therefore v^\rho = \frac{1}{4}\mathrm{Tr}(\Gamma\gamma^\rho) \\
&\mathrm{Tr}(\Gamma p_1^\rho) = Sp_1^\rho\mathrm{Tr}(\mathbf{1}) = 4Sp_1^\rho \\
&\therefore Sp_1^\rho = \frac{1}{4}\mathrm{Tr}(\Gamma p_1^\rho) \\
&\mathrm{Tr}(\Gamma\gamma^\rho\gamma^5) = a_\mu\mathrm{Tr}(\gamma^\mu\gamma^\rho(\gamma^5)^2) = 4a^\rho \\
&\therefore a^\rho = \frac{1}{4}\mathrm{Tr}(\Gamma\gamma^\rho\gamma^5) \\
&\mathrm{Tr}(\Gamma p_1^\rho\gamma^5) = Pp_1^\rho\mathrm{Tr}(1(\gamma^5)^2) = 4Pp_1^\rho \\
&\therefore Pp_1^\rho = \frac{1}{4}\mathrm{Tr}(\Gamma p_1^\rho\gamma^5)
\end{aligned} \tag{6.14}$$

All other terms trace to zero.

The Dirac Equation for spinors is:

$$\begin{aligned}
&\bar{v}(p_2,\lambda_2)(\gamma^\mu p_{1\mu} - 1m_t)u(p_1,\lambda_1) = 0 \\
&\therefore \bar{u}(p_1,\lambda_1)(\gamma^\mu p_{1\mu} - 1m_t)v(p_2,\lambda_2) = 0 \\
&\bar{u}(p_1,\lambda_1)\left(\frac{\gamma^\mu p_{1\mu}}{m_t}\right)v(p_2,\lambda_2) = \bar{u}(p_1,\lambda_1)(\mathbf{1})v(p_2,\lambda_2)
\end{aligned} \tag{6.15}$$

So when we sandwich Γ between spinors we can write:

$$\begin{aligned}
\bar{u}(p_1,\lambda_1)\{\Gamma\}v(p_2,\lambda_2) &= \left(v_\mu + \frac{p_{1\mu}S}{m_t}\right)\bar{u}(p_1,\lambda_1)\gamma^\mu v(p_2,\lambda_2) \\
&+ \left(-a_\mu + \frac{p_{1\mu}P}{m_t}\right)\bar{u}(p_1,\lambda_1)\gamma^\mu\gamma^5 v(p_2,\lambda_2) + \frac{i}{2}T_{\mu\nu}\bar{u}(p_1,\lambda_1)\sigma^{\mu\nu}v(p_2,\lambda_2)
\end{aligned} \tag{6.16}$$

So, if we substitute in from eq(6.14), then we discover:

$$V_\mu = \frac{1}{4}\mathrm{Tr}(\Gamma\gamma_\mu) + \frac{1}{4m_t}\mathrm{Tr}(\Gamma p_{1\mu})$$
$$A_\mu = -\frac{1}{4}\mathrm{Tr}(\Gamma\gamma_\mu\gamma^5) + \frac{1}{4m_t}\mathrm{Tr}(\Gamma p_{1\mu}\gamma^5) \tag{6.17}$$

We can also calculate that:

$$\mathrm{Tr}(\Gamma\sigma_{\rho\sigma}) = -\frac{1}{4}T_{\mu\nu}\mathrm{Tr}((\gamma^\mu\gamma^\nu - \gamma^\nu\gamma^\mu)(\gamma^\rho\gamma^\sigma - \gamma^\sigma\gamma^\rho)) = 4(T_{\rho\sigma} - T_{\sigma\rho}) \tag{6.18}$$

All of the other traces vanish.

We know that the left hand side is antisymmetric under the interchange $\sigma \leftrightarrow \rho$ and that therefore $T_{\rho\sigma} = -T_{\sigma\rho}$. So we now have:

$$T_{\mu\nu} = \frac{1}{8}\mathrm{Tr}(\Gamma\sigma_{\mu\nu}) \tag{6.19}$$

We now define l^μ and n^ν to be unit vectors in the 1 and 2 (x and y) directions. This means that we have $\frac{(p_1+p_2)^\mu}{\sqrt{s}}, l^\mu, n^\mu, \frac{(p_1-p_2)^\mu}{\sqrt{s-4m_t^2}}$ as unit vectors in the 0,1,2 & 3 directions. So, for the vector part, we can say:

$$\bar{u}(p_1,\lambda_1)\gamma^\mu v(p_2,\lambda_2) = al^\mu + bm^\mu + c\frac{(p_1-p_2)^\mu}{\sqrt{s-4m_t^2}} + d\frac{(p_1+p_2)^\mu}{\sqrt{s}}$$
$$\times\frac{(p_1-p_2)^\mu}{\sqrt{s-4m_t^2}}(\text{unit vector in the 3 direction}) \rightarrow$$
$$-\bar{u}(p_1,\lambda_1)\gamma^3 v(p_2,\lambda_2) = -c \tag{6.20}$$

If we write this out in detail then we get:

$$c = (E+m_t)\left(\chi^\dagger(\lambda_1), -\frac{\lambda_1 p}{E+m_t}\right)\begin{pmatrix} 0 & \sigma^3 \\ -\sigma^3 & 0 \end{pmatrix}\begin{pmatrix} -\frac{\lambda_2 p}{E+m_t}\chi(\lambda_2) \\ \chi(\lambda_2) \end{pmatrix}$$

$$= (E+m_t)\left(-\lambda_1\lambda_2\frac{p^2}{(E+m_t)^2}+1\right)\chi^\dagger(\lambda_1)\sigma^3\chi(\lambda_2)$$

If $\lambda_1 = \lambda_2 = 1$ then: $\chi^\dagger(\lambda_1)\sigma^3\chi(\lambda_2) = 1$

If $\lambda_1 = \lambda_2 = -1$ then: $\chi^\dagger(\lambda_1)\sigma^3\chi(\lambda_2) = -1$

If $\lambda_1 \neq \lambda_2$ then: $\chi^\dagger(\lambda_1)\sigma^3\chi(\lambda_2) = 0$

Therefore: $\chi^\dagger(\lambda_1)\sigma^3\chi(\lambda_2) = \lambda_1\delta_{\lambda_1\lambda_2}$

Thus: $c = 2m_t\lambda_1\delta_{\lambda_1\lambda_2}$ (6.21)

The expressions for $\chi^\dagger\sigma^i\chi$ will be needed later on and are:

$$\chi^\dagger(\lambda_1)\sigma^1\chi(\lambda_2) = \delta_{\lambda_1,-\lambda_2}$$

$$\chi^\dagger(\lambda_1)\sigma^2\chi(\lambda_2) = -\lambda_1 i\delta_{\lambda_1,-\lambda_2}$$

$$\chi^\dagger(\lambda_1)\sigma^3\chi(\lambda_2) = \lambda_1\delta_{\lambda_1\lambda_2} \quad (6.22)$$

Similarly if we multiply through by a unit vector in the 2 direction (n^μ) we can obtain:

$$b = (E+m_t)\left(-\frac{\lambda_1\lambda_2 p^2}{(E+m_t)^2}+1\right)\chi^\dagger(\lambda_1)\sigma^2\chi(\lambda_2)$$

$$= -2i\lambda_1 E\delta_{\lambda_1,-\lambda_2} \quad (6.23)$$

If we repeat this process for the other two directions we end up with:

$$a = 2E\delta_{\lambda_1,-\lambda_2}$$

$$b = -2i\lambda_1 E\delta_{\lambda_1,-\lambda_2}$$

$$c = 2m_t\lambda_1\delta_{\lambda_1\lambda_2}$$

$$d = 0 \quad (6.24)$$

Therefore:

$$\bar{u}(p_1,\lambda_1)\gamma^\mu v(p_2,\lambda_2) = 2E\delta_{\lambda_1,-\lambda_2}v_1^\mu - 2i\lambda_1 E\delta_{\lambda_1,-\lambda_2}v_2^\mu + 2m_t\lambda_1\delta_{\lambda_1\lambda_2}v_3^\mu \tag{6.25}$$

where $v_0^\mu, v_1^\mu, v_2^\mu, v_3^\mu$ are a set of basis vectors.

We can perform the same analysis on the axial part. If:

$$\bar{u}(p_1,\lambda_1)\gamma^\mu\gamma^5 v(p_2,\lambda_2) = \bar{a}v_1^\mu + \bar{b}v_2^\mu + \bar{c}v_3^\mu + \bar{d}v_0^\mu \tag{6.26}$$

then we end up with:

$$\bar{u}(p_1,\lambda_1)\gamma^\mu\gamma^5 v(p_2,\lambda_2) = 2p\lambda_1\delta_{\lambda_1,-\lambda_2}v_1^\mu - 2ip\delta_{\lambda_1,-\lambda_2}v_2^\mu + 2m_t\delta_{\lambda_1\lambda_2}v_0^\mu \tag{6.27}$$

The process for extracting an expression for the tensor structure is a little different and is worth explaining in some detail. We are trying to express:

$$\bar{u}(p1,\lambda_1)\sigma^{\mu\nu}v(p_2,\lambda_2) \tag{6.28}$$

in are more convenient form so we need to break $\sigma^{\mu\nu}$ into its component parts. Beginning with the purely spatial components.

$$\begin{aligned}
\sigma^{ij} &= \frac{i}{2}(\gamma^i\gamma^j - \gamma^j\gamma^i) \\
&= \frac{i}{2}\left[\begin{pmatrix} 0 & \sigma^i \\ -\sigma^i & 0 \end{pmatrix}, \begin{pmatrix} 0 & \sigma^j \\ -\sigma^j & 0 \end{pmatrix}\right] \\
&= -\frac{i}{2}\begin{pmatrix} [\sigma_i,\sigma_j] & 0 \\ 0 & [\sigma_i,\sigma_j] \end{pmatrix}
\end{aligned}$$

Then, since $[\sigma_i,\sigma_j] = 2i\epsilon_{ijk}\sigma_k$, we have:

$$\sigma^{ij} = \epsilon_{ijk}\begin{pmatrix} \sigma_k & 0 \\ 0 & \sigma_k \end{pmatrix} \tag{6.29}$$

So we have:

$$\bar{u}(p1,\lambda_1)\sigma^{ij}v(p_2,\lambda_2) = \bar{u}(p1,\lambda_1)\epsilon_{ijk}\begin{pmatrix}\sigma_k & 0\\ 0 & \sigma_k\end{pmatrix}v(p_2,\lambda_2)$$

$$= \epsilon_{ijk}(E+m_t)\left(\chi^\dagger(\lambda_1)\sigma_k, \frac{-\lambda_1 p}{E+m_t}\chi^\dagger(\lambda_1)\sigma_k\right)\begin{pmatrix}\frac{-\lambda_2 p}{E+m_t}\chi(\lambda_2)\\ \chi(\lambda_2)\end{pmatrix}$$

$$= -\epsilon_{ijk}p(\lambda_1+\lambda_2)\chi^\dagger(\lambda_1)\sigma_k\chi(\lambda_2) \tag{6.30}$$

Clearly this will only be non-zero when $\lambda_1 = \lambda_2$ so (according to eq(6.22)) the only term that will contribute will be the term including σ_3. Therefore:

$$\bar{u}(p1,\lambda_1)\sigma^{12}v(p_2,\lambda_2) = -2p\delta_{\lambda_1\lambda_2} \tag{6.31}$$

We also need to look at components with one time index:

$$\sigma^{0k} = \frac{i}{2}(\gamma^0\gamma^k - \gamma^k\gamma^0)$$

$$= \frac{i}{2}\left[\begin{pmatrix}1 & 0\\ 0 & -1\end{pmatrix}, \begin{pmatrix}0 & \sigma_k\\ -\sigma_k & 0\end{pmatrix}\right]$$

$$= \frac{i}{2}\begin{pmatrix}0 & 2\sigma_k\\ 2\sigma_k & 0\end{pmatrix} (= i\sigma_k\gamma^5) \tag{6.32}$$

So, if we sandwich this between spinors we get:

$$\bar{u}(p1,\lambda_1)\sigma^{0k}v(p_2,\lambda_2) = \bar{u}(p1,\lambda_1)i\begin{pmatrix}0 & \sigma_k\\ \sigma_k & 0\end{pmatrix}v(p_2,\lambda_2)$$

$$= i(E+m_t)\left(-\frac{\lambda_1 p}{E+m_t}\chi^\dagger(\lambda_1)\sigma_k, \chi^\dagger(\lambda_1)\sigma_k\right)\begin{pmatrix}-\frac{\lambda_2 p}{E+m_t}\chi(\lambda_2)\\ \chi(\lambda_2)\end{pmatrix}$$

$$= i(E+m_t)\left(\frac{\lambda_1\lambda_2 p^2}{(E+m_t)^2}+1\right)\chi^\dagger(\lambda_1)\sigma_k\chi(\lambda_2) \tag{6.33}$$

This does not vanish for any helicity combination and therefore the terms including σ_1, σ_2 & σ_3 will all contribute. Using the expressions from eq(6.22) we obtain:

$$\bar{u}(p1,\lambda_1)\sigma^{01}v(p_2,\lambda_2) = i2m_t\delta_{\lambda_1,-\lambda_2} \tag{6.34}$$

$$\bar{u}(p1,\lambda_1)\sigma^{02}v(p_2,\lambda_2) = 2\lambda_1 m_t \delta_{\lambda_1,-\lambda_2} \tag{6.35}$$

$$\bar{u}(p1,\lambda_1)\sigma^{03}v(p_2,\lambda_2) = 2iE\lambda_1\delta_{\lambda_1\lambda_2} \tag{6.36}$$

Combining the results from eq(6.31) and eq(6.34→6.36) eventually yields:

$$\begin{aligned}
&\bar{u}(p_1,\lambda_1)\sigma^{\mu\nu}v(p_2,\lambda_2) = \\
&-2p\delta\lambda_1\lambda_2(v_1^\mu v_2^\nu - v_2^\mu v_1^\nu) + i2m_t\delta_{\lambda_1,-\lambda_2}(v_0^\mu v_1^\nu - v_1^\mu v_0^\nu) \\
&+2\lambda_1 m_t\delta_{\lambda_1,-\lambda_2}(v_0^\mu v_2^\nu - v_2^\mu v_0^\nu) - 2iE\lambda_1\delta\lambda_1\lambda_2(v_3^\mu v_0^\nu - v_0^\mu v_3^\nu)
\end{aligned} \tag{6.37}$$

So we have, from eq(6.12), eq(6.17), eq(6.19), eq(6.25), eq(6.27) and eq(6.37), an expression for the $gg \to t\bar{t}$ amplitude:

$$\begin{aligned}
&\bar{u}(p_1,\lambda_1)\{\Gamma\}v(p_2,\lambda_2) = \\
&\left[\frac{1}{4}\mathrm{Tr}(\Gamma\gamma_\mu) + \frac{1}{4m_t}\mathrm{Tr}(\Gamma p_1^\mu)\right]\times \\
&[2E\delta_{\lambda_1,-\lambda_2}v_1^\mu - 2i\lambda_1 E\delta_{\lambda_1,-\lambda_2}v_2^\mu + 2m_t\lambda_1\delta_{\lambda_1\lambda_2}v_3^\mu] - \\
&\left[\frac{1}{4}\mathrm{Tr}(\Gamma\gamma_\mu\gamma^5) + \frac{1}{4m_t}\mathrm{Tr}(\Gamma p_1^\mu\gamma^5)\right]\times \\
&[2p\lambda_1\delta_{\lambda_1,-\lambda_2}v_1^\mu - 2ip\delta_{\lambda_1,-\lambda_2}v_2^\mu + 2m_t\delta_{\lambda_1\lambda_2}v_0^\mu] + \\
&\left[\frac{1}{8}\mathrm{Tr}(\Gamma\sigma_{\mu\nu})\right]\times \\
&[-2p\delta\lambda_1\lambda_2(v_1^\mu v_2^\nu - v_2^\mu v_1^\nu) + i2m_t\delta_{\lambda_1,-\lambda_2}(v_0^\mu v_1^\nu - v_1^\mu v_0^\nu) \\
&+2\lambda_1 m_t\delta_{\lambda_1,-\lambda_2}(v_0^\mu v_2^\nu - v_2^\mu v_0^\nu) - 2iE\lambda_1\delta\lambda_1\lambda_2(v_3^\mu v_0^\nu - v_0^\mu v_3^\nu)]
\end{aligned} \tag{6.38}$$

If we wish to extract a similar expression for the $q\bar{q} \to t\bar{t}$ amplitude then we simply multiply the expression above by a second term of the form $\bar{u}\Gamma v$ this time referring to the initial quark line. If the initial state quarks are massive then this expression will have the same form as given above, however in the calculation presented here the initial state quarks are always considered to be light. The method for expressing $\bar{u}\Gamma v$ for massless quarks is presented in some detail in the chapter on $q\bar{q} \to b\bar{b}$.

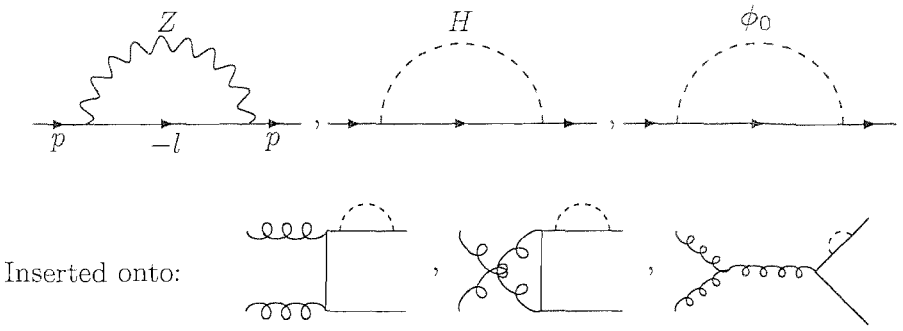

Figure 6.2: Bubble Diagrams with neutral bosons

6.2.2 One Loop Corrections To gg To $t\bar{t}$

External Leg Self Energy Corrections

For the neutral particle loops (Higgs, Z and ϕ_0) we have bubble diagrams like those shown in fig(6.2). The external particle will be a top quark and both of the internal lines will have masses associated with them (since the flavour of the top will be unchanged by the emission of a neutral boson): The expression for a general bubble diagram of this form (with boson mass $m_{Z/H}$) is:

$$\int \frac{d^d l}{(2\pi)^d} \bar{u}(p)[\gamma^\mu(A+B\gamma^5)] \frac{(-\not{l}+m_t)}{(l^2-m_t^2)} [\gamma_\mu(A+B\gamma^5)]u(p) \frac{1}{(l+p)^2-m_{Z/H}}$$

$$= B_0\{[\bar{u}(p)[\gamma^\mu(A+B\gamma^5)](-\not{l})[\gamma_\mu(A+B\gamma^5)]u(p)]$$

$$+[\bar{u}(p)[\gamma^\mu(A+B\gamma^5)]m_t[\gamma_\mu(A+B\gamma^5)]u(p)]\}$$

$$= B_1[\bar{u}(p)[\gamma^\mu(A+B\gamma^5)](-\not{p})[\gamma_\mu(A+B\gamma^5)]u(p)]$$

$$+B_1 m_t[\bar{u}(p)[\gamma^\mu(A+B\gamma^5)][\gamma_\mu(A+B\gamma^5)]u(p)] \qquad (6.39)$$

Here A and B are the vector and axial couplings of whichever neutral particle is in the loop. B_0 and B_1 are two point Veltman & Passarino [24] functions:

$$\frac{i}{16\pi^2}B_0 = \int \frac{d^dl}{(2\pi)^d}\frac{1}{(l^2-m_t^2)((l+p)^2-m_{Z/H}^2)}$$
$$\frac{i}{16\pi^2}p^\mu B_1 = \int \frac{d^dl}{(2\pi)^d}\frac{l^\mu}{(l^2-m_t^2)((l+p)^2-m_{Z/H}^2)} \tag{6.40}$$

We can rewrite eq(6.39) as:

$$\alpha B_1(m_t^2, m_{Z/H}^2, p^2)\not{p} + \beta m_t B_0(m_t^2, m_{Z/H}^2, p^2) \tag{6.41}$$

(Both α and β could have an axial part so $\alpha = \alpha_V + \alpha_A\gamma^5$ and $\beta = \beta_V + \beta_A\gamma^5$)

Now expand $B_{0,1}$ in p^2 around m_t^2

$$\begin{aligned}
&\alpha[B_1(m_t^2, m_{Z/H}^2, p^2) + B_1'(m_t^2, m_{Z/H}^2, p^2)(p^2-m_t^2)](\not{p}-m_t)\\
&+\alpha[B_1(m_t^2, m_{Z/H}^2, p^2) + B_1'(m_t^2, m_{Z/H}^2, p^2)(p^2-m_t^2)]m_t\\
&+\beta m_t[B_0(m_t^2, m_{Z/H}^2, p^2) + B_0'(m_t^2, m_{Z/H}^2, p^2)(p^2-m_t^2)]
\end{aligned} \tag{6.42}$$

where $B_{0/1}' = \frac{\partial}{\partial p^2}B_{0/1}$. Now use $(p^2-m_t^2) = (\not{p}-m_t)(\not{p}+m_t) = (\not{p}-m_t)(\not{p}-m_t+2m_t)$:

$$\begin{aligned}
&\alpha[B_1(m_t^2, m_{Z/H}^2, m_t^2)](\not{p}-m_t)\\
&+\alpha[B_1(m_t^2, m_{Z/H}^2, m_t^2)^{(*)} + B_1'(m_t^2, m_{Z/H}^2, m_t^2)2m_t(\not{p}-m_t)]m_t\\
&+\beta[B_0(m_t^2, m_{Z/H}^2, m_t^2)^{(*)} + B_0'(m_t^2, m_{Z/H}^2, m_t^2)2m_t(\not{p}-m_t)]m_t\\
&+\mathcal{O}(\not{p}-m_t)^{2(**)}
\end{aligned} \tag{6.43}$$

The terms marked $^{(*)}$ are removed by renormalisation and the terms marked $^{(**)}$ vanish due to the on-shell condition.

So at the level of Feynman rules the expression for a tree level diagram with a neutral

external leg correction will be:

$$[\alpha B_1(m_t^2, m_{Z/H}^2, m_t^2) + 2\alpha m_t^2 B_1'(m_t^2, m_{Z/H}^2, m_t^2)$$
$$+2\beta m_t^2 B_0'(m_t^2, m_{Z/H}^2, m_t^2)]$$
$$\times(\text{Tree level } |\mathcal{M}|)$$

(6.44)

remembering that α and β both contain axial parts and as such need to be included in the trace. Performing a similar manipulation for the case of a charged boson ($W^{+/-}$ or $\phi^{+/-}$) in the loop we obtain:

$$[\alpha B_1(0, m_W^2, m_t^2) + 2\alpha m_t^2 B_1'(0, m_W^2, m_t^2)] \times$$
$$\times(\text{Tree level } |\mathcal{M}|)$$

(6.45)

(In this case the internal quark will be a bottom and can therefore be treated as massless, this means that the propagator in eq(6.39) would have the form $\frac{(-\not{l})}{(l^2-m_t^2)}$. As a consequence of this we would lose the term proportional to m_t meaning that there would be no dependence on B_0.)

So, for example, in the case of the external Z self energy inserted onto the t-channel diagram (the left most diagram in fig(6.2)) we would have:

$$\Gamma = \frac{-ig_s^2}{t - m_t^2}(A + B\gamma^5)\gamma^\mu \epsilon_\mu^a(p_a)(\not{p}_b - \not{p}_2 + m_t)\gamma^\nu \epsilon^b(p_b) \tag{6.46}$$

Where Γ is the string of gamma matrices between the Dirac spinors in the t-channel amplitude - as used in eq(6.38). $A = \alpha_V^Z B_1 + 2m_t^2 \alpha_V^Z B_1' + 2m_t^2 \beta_V^Z B_0'$ and $B = \alpha_A^Z B_1 + 2m_t^2 \alpha_A^Z B_1' + 2m_t^2 \beta_A^Z B_0'$.

Finding α And β For The Five Self Energy Diagrams

If we now obtain an expression for the 1PI function for the five different bubble diagrams in a form similar to eq(6.41) then we will be able to extract values for α and β for each of the corrections. For example, the 1PI function for the Z-boson bubble has the form:

$$\begin{aligned}
&-\frac{i}{4}\left(\frac{g}{\cos\theta_W}\right)^2\int\frac{d^dl}{(2\pi)^d}\frac{\gamma^\mu(c_V^t-c_A^t\gamma^5)(m_t-\not{l})\gamma_\mu(c_V^t-c_A^t\gamma^5)}{(l^2-m_t^2)((l+p)^2-m_z^2)}\\
&=-\frac{i}{4}\left(\frac{g}{\cos\theta_W}\right)^2\frac{i}{16\pi^2}\left\{\gamma^\mu(c_V^t-c_A^t\gamma^5)\gamma_\mu(c_V^t-c_A^t\gamma^5)m_tB_0\right.\\
&\left.-\gamma^\mu(c_V^t-c_A^t\gamma^5)\not{p}\gamma_\mu(c_V^t-c_A^t\gamma^5)B_1\right\} \qquad (6.47)
\end{aligned}$$

If we look at the term proportional to m_tB_0 and multiply out the brackets then we get:

$$\begin{aligned}
&(c_V^t)^2\gamma_\mu\gamma^\mu-(c_V^tc_A^t)\gamma^\mu\gamma_\mu\gamma^5-(c_V^tc_A^t)\gamma^\mu\gamma^5\gamma_\mu-(c_A^t)^2\gamma_\mu\gamma^\mu\\
&=4((c_V^t)^2-(c_A^t)^2) \qquad (6.48)
\end{aligned}$$

Similarly, for the term proportional to B_1:

$$\{[-2((c_V^t)^2+(c_A^t)^2)]-[4(c_V^tc_A^t)]\gamma^5\}\not{p} \qquad (6.49)$$

So, substituting these into eq(6.47), we have:

$$\frac{1}{4}\frac{1}{16\pi^2}\left(\frac{g}{\cos\theta_W}\right)^2\{m_tB_0(4((c_V^t)^2-(c_A^t)^2))+B_1(2((c_V^t)^2+(c_A^t)^2)+4(c_V^tc_A^t)\gamma^5)\}\not{p} \qquad (6.50)$$

Comparing this with eq(6.41) we find:

$$\begin{aligned}
\alpha_V^Z&=\frac{1}{4}\frac{1}{16\pi^2}\left(\frac{g}{\cos\theta_W}\right)^2 2((c_V^t)^2+(c_A^t)^2))\\
\alpha_A^Z&=\frac{1}{4}\frac{1}{16\pi^2}\left(\frac{g}{\cos\theta_W}\right)^2 (4(c_V^tc_A^t))\\
\beta_V^Z&=\frac{1}{4}\frac{1}{16\pi^2}\left(\frac{g}{\cos\theta_W}\right)^2 4((c_V^t)^2-(c_A^t)^2))\\
\beta_A^Z&=0 \qquad (6.51)
\end{aligned}$$

If we perform the same manipulations for the other four possible internal particles we find (remembering that β is trivially zero for charged bosons):

$$\begin{aligned}
\alpha_V^H &= \frac{g^2}{4}\left(\frac{m_t}{m_w}\right)^2 \frac{1}{16\pi^2}(1) \\
\alpha_A^H &= 0 \\
\beta_V^H &= \frac{g^2}{4}\left(\frac{m_t}{m_w}\right)^2 \frac{1}{16\pi^2}(-1) \\
\beta_A^H &= 0 \\
\alpha_V^{\phi_0} &= \frac{g^2}{4}\left(\frac{m_t}{m_w}\right)^2 \frac{1}{16\pi^2}(1) \\
\alpha_A^{\phi_0} &= 0 \\
\beta_V^{\phi_0} &= \frac{g^2}{4}\left(\frac{m_t}{m_w}\right)^2 \frac{1}{16\pi^2}(1) \\
\beta_A^{\phi_0} &= 0 \\
\alpha_V^{W_{+/-}} &= \frac{g^2}{8}\frac{1}{16\pi^2}(4) \\
\alpha_A^{W_{+/-}} &= \frac{g^2}{8}\frac{1}{16\pi^2}(4) \\
\alpha_V^{\phi_{+/-}} &= \frac{g^2}{8}\left(\frac{m_t}{m_w}\right)^2 \frac{1}{16\pi^2}(2) \\
\alpha_A^{\phi_{+/-}} &= \frac{g^2}{8}\left(\frac{m_t}{m_w}\right)^2 \frac{1}{16\pi^2}(2)
\end{aligned} \tag{6.52}$$

Internal Self Energy Corrections

We can also use the bubble 1PI functions derived above to evaluate the *internal* self energy corrections. These will again be bubble diagrams with an internal Z, H, ϕ_0, $W_{+/-}$ or $\phi_{+/-}$. For example, consider the diagram shown in fig(6.4) - the internal Z self energy correction to t-channel $gg \rightarrow t\bar{t}$.

The expression for this diagram derived from the Feynman rules is:

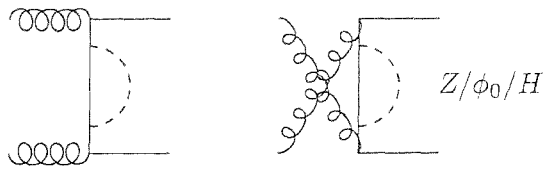

Figure 6.3: The bubbles may be inserted onto the internal top line of a t or u channel diagram. These will interfere with the s,t and u channel tree level diagrams.

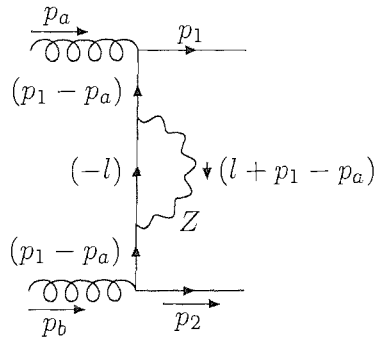

Figure 6.4: The internal Z self energy correction to $gg \to t\bar{t}$ in the t-channel. All quark propagators have mass m_t.

$$(-g_s^2 t^a t^b) \times \bar{u}(p_1)\gamma^\mu \epsilon_\mu(p_a) \left\{ \frac{i(p\!\!\!/_1 - p\!\!\!/_a + m_t)}{(p_1 - p_a)^2 - m_t^2} \right\}$$
$$\left[\int \frac{d^d l}{i\pi^2} \frac{i}{16\pi^2} \frac{g^2}{\cos^2\theta_W} \frac{1}{4} \frac{\gamma^\rho (c_V - c_A\gamma^5)(l\!\!\!/ - m_t)\gamma_\rho (c_V - c_A\gamma^5)}{(l^2 - m_t^2)((p_1 - p_a + l)^2 - m_z^2)} \right]$$
$$\left\{ \frac{i(p\!\!\!/_1 - p\!\!\!/_a + m_t)}{(p_1 - p_a)^2 - m_t^2} \right\} \gamma^\nu \epsilon_\nu(p_b) v(p_2) \tag{6.53}$$

We can rewrite the term in square brackets as:

$$\frac{-i}{16\pi^2} \frac{g^2}{\cos^2\theta_W} \frac{1}{4} \int \frac{d^d l}{i\pi^2} \left\{ \frac{\gamma^\rho (c_V - c_A\gamma^5)(m_t)\gamma_\rho (c_V - c_A\gamma^5)}{(l^2 - m_t^2)((p_1 - p_a + l)^2 - m_z^2)} \right.$$
$$\left. - \frac{\gamma^\rho (c_V - c_A\gamma^5)(l\!\!\!/)\gamma_\rho (c_V - c_A\gamma^5)}{(l^2 - m_t^2)((p_1 - p_a + l)^2 - m_z^2)} \right\}$$
$$= \frac{-i}{16\pi^2} \frac{g^2}{\cos^2\theta_W} \frac{1}{4} \{ \gamma^\rho (c_V - c_A\gamma^5)\gamma_\rho (c_V - c_A\gamma^5) m_t B_0(p^2)$$
$$- \gamma^\rho (c_V - c_A\gamma^5)(p\!\!\!/)\gamma_\rho (c_V - c_A\gamma^5) B_1(p^2) \} \tag{6.54}$$

(Where $p \equiv p_1 - p_a$.) From eq(6.48) and eq(6.49) we know that:

$$\gamma^\rho (c_V - c_A\gamma^5)\gamma_\rho (c_V - c_A\gamma^5) = 4(c_V^2 - c_A^2)$$
$$\gamma^\rho (c_V - c_A\gamma^5)(p\!\!\!/)\gamma_\rho (c_V - c_A\gamma^5) = [-2(c_V^2 + c_A^2) - 4c_V c_A\gamma^5]p\!\!\!/ \tag{6.55}$$

So we have:

$$\frac{-i}{16\pi^2}\frac{g^2}{\cos^2\theta_W}\frac{1}{4}\{4(c_V^2-c_A^2)m_t B_0(p^2)- \\ [-2(c_V^2+c_A^2)-4c_V c_A\gamma^5]\not{p}B_1(p^2)\} \tag{6.56}$$

Referring back to eq(6.51) this can be written as:

$$-i[\beta_V^Z m_t B_0(p^2)+\alpha_V^Z\not{p}B_1(p^2)+\alpha_A^Z\not{p}B_1(p^2)] \tag{6.57}$$

Therefore, we would calculate the amplitude in eq(6.53) using a Γ term of:

$$\Gamma = \\ (-g_S^2 t^a t^b)\gamma^\mu\epsilon_\mu(p_a)\left\{\frac{i(\not{p}_1-\not{p}_a+m_t)}{(p_1-p_a)^2-m_t^2}\right\} \\ -i[\beta_V^Z m_t B_0(p^2)+\alpha_V^Z\not{p}B_1(p^2)+\alpha_A^Z\not{p}B_1(p^2)] \\ \left\{\frac{i(\not{p}_1-\not{p}_a+m_t)}{(p_1-p_a)^2-m_t^2}\right\}\gamma^\nu\epsilon_\nu(p_b) \tag{6.58}$$

The same result would be reached for the W, H, ϕ_0 and $\phi_{+/-}$ cases where α and β would be defined as in eq(6.52).

Vertex Corrections

The weak vertex corrections that will contribute to the $gg \to t\bar{t}$ rate at $\alpha_S^2\alpha_W$ order are those shown in fig(6.5).

If we look at, for example, a general vector boson correction to the t-channel diagram we obtain an expression for Γ (this can easily be crossed to give the u-channel correction):

$$\Gamma = \frac{-i}{t-m_t^2}\int\frac{d^dl}{i\pi^2}c_0[\gamma^\kappa](A+B\gamma^5)(\not{l}+\not{p}_a+m_q)\gamma^\mu\epsilon_\mu^a(p_a) \\ (\not{l}+m_q)[\gamma_\kappa](A+B\gamma^5)(\not{p}_b-\not{p}_2+m_t)\gamma^\nu\epsilon_\nu^b(p_b)\times 2\frac{i}{16\pi^2} \tag{6.59}$$

The factor of two comes from allowing the correction to appear on either vertex.

Where

$$\int\frac{d^dl}{i\pi^2}\frac{1}{((l+p_a-p_1)^2-m_v^2)(l^2-m_q^2)((l+p_a)^2-m_q^2)}=\int\frac{d^dl}{i\pi^2}c_0=C_0.$$

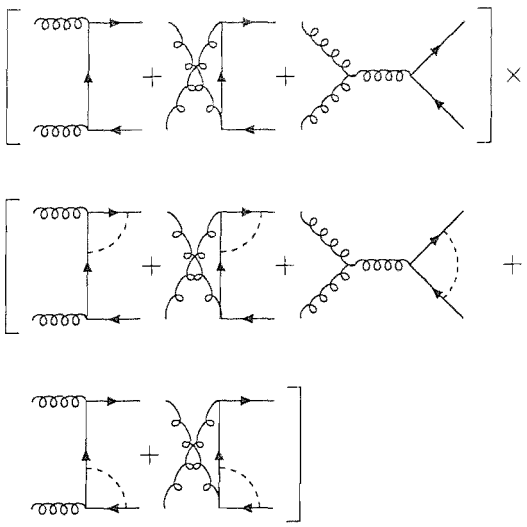

Figure 6.5: The interferences with virtual corrections that contribute to $gg \to t\bar{t}$. The internal boson can again be a Z, W, H or ϕ.

For the general vector boson correction to the s-channel diagram we have:

$$\Gamma = \frac{-i}{s}\int \frac{d^d l}{i\pi^2}[\gamma^\kappa](A + B\gamma^5)(\not{p}_a + \not{p}_b + \not{l} + m_q)\gamma_\mu$$
$$(\not{l} + m_q)[\gamma_\kappa](A + B\gamma^5)$$
$$(g^{\lambda\nu}(p_a^\mu - p_b^\mu) + g^{\nu\mu}(2p_b^\lambda + p_a^\lambda) + g^{\mu\lambda}(-2p_a^\nu - p_b^\nu))\epsilon_\lambda^a(p_a)\epsilon_\nu^b(p_b) \times \frac{i}{16\pi^2} \quad (6.60)$$

Here the triangle integral will be slightly different:

$$\int \frac{d^d l}{i\pi^2} \frac{1}{((l + p_a + p_b)^2 - m_q^2)(l^2 - m_q^2)((l + p_b)^2 - m_v^2)} = \int \frac{d^d l}{i\pi^2} c_0 = C_0.$$

In both cases A, B, m_q & m_v depend on whether we have a Z or W correction.

For a Z we have $A = \frac{g}{2\cos\theta_W} c_V, B = \frac{-g}{2\cos\theta_W} c_A, m_q = m_t, m_v = m_z$

For a W we have $A = \frac{g}{2\sqrt{2}}, B = \frac{-g}{2\sqrt{2}}, m_q = m_b, m_v = m_w$

The expressions for the same diagrams but with a scalar vertex correction can be

obtained from eq(6.59) and eq(6.60) by removing the gamma matrices that appear in square brackets.

For a H we have $A = \frac{g}{2}\frac{m_t}{m_w}, B = 0, m_q = m_t, m_v = m_H$

For a ϕ_0 we have $A = 0, B = \frac{ig}{2}\frac{m_t}{m_w}, m_q = m_t, m_v = m_Z$

For a $\phi_\pm$ we have $A = \frac{g}{2\sqrt{2}}\frac{m_t}{m_w}, B = \frac{g}{2\sqrt{2}}\frac{m_t}{m_w}, m_q = m_b, m_v = m_w$

To evaluate these diagrams we need to manipulate the Veltman and Passarino functions in much the same way as we did in the massless cases (explained in detail in the $b\bar{b}$ production chapter). This manipulation is only very slightly complicated by the inclusion of the top mass.

Box Corrections

We also need to consider box corrections to the $gg \rightarrow t\bar{t}$. These corrections need to be applied to the t and u channel tree level diagrams as shown in fig(6.6). For the t-channel diagram we have an expression for $\Gamma_{Z/W}$ (the string of gamma matrices as defined in section(6.2.1) for the Z or W box):

$$\Gamma_{Z/W} = \frac{1}{16\pi^2}\int \frac{d^d l}{i\pi^2} d_0 \gamma^\alpha (A + B\gamma^5)(\not{l} + \not{p}_a + \not{p}_b + m_{b/t})\gamma.\epsilon(p_a)$$
$$(\not{l} + \not{p}_b + m_{b/t})\gamma.\epsilon(p_b)(\not{l} + m_{b/t})\gamma_\alpha(A + B\gamma^5) \qquad (6.61)$$

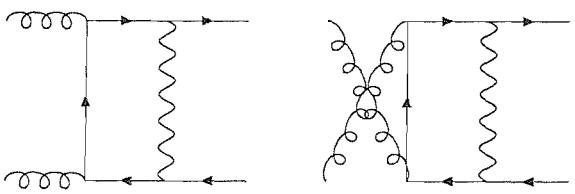

Figure 6.6: Box corrections in both the t and u channels. The internal weak particle can be a $Z, W_{+/-}, \phi_0, \phi_{+/-}$ or a Higgs. If the internal weak particle is a W or a $\phi_{+/-}$ then the internal fermion is a bottom quark otherwise the internal fermion is a top quark.

Where

$$\int \frac{d^dl}{i\pi^2} \frac{1}{[l^2 - m_{b/t}^2][(l+p_b)^2 - m_{b/t}^2][(l+p_a+p_b)^2 - m_{b/t}^2][(l-p_2)^2 - m_{z/w}^2]} = \int \frac{d^dl}{i\pi^2} d_0 = D_0,$$

$A_Z = g/2/\cos(\theta_W) g_V,$

$B_Z = -g/2/\cos(\theta_W) g_A,$

$A_W = g/2/\sqrt{2},$

$B_W = -g/2/\sqrt{2}$

For the scalar contribution we have:

$$\Gamma_{H/\phi_0/\phi_{+/-}} = -\frac{1}{16\pi^2} \int \frac{d^dl}{i\pi^2} d_0 (A + B\gamma^5)(\not{l} + \not{p}_a + \not{p} + m_{b/b/t})\gamma.\epsilon(p_a)$$
$$(\not{l} + \not{p}_b + m_{b/b/t})\gamma.\epsilon(p_b)(\not{l} + m_{b/b/t})(A + B\gamma^5) \qquad (6.62)$$

Where d_0 is defined as above and we also have: $A_H = g/2\ m_t/m_w,$

$B_H = 0,$

$A_{\phi_0} = 0,$

$B_{\phi_0} = ig/2\ m_t/m_w,$

$A_{\phi_{+/-}} = g/2/\sqrt{2}\ m_t/m_w,$

$B_{\phi_{+/-}} = g/2/\sqrt{2}\ m_t/m_w,$

Once again, to obtain the final result for these amplitudes we will need to manipulate the Veltman and Passarino functions in a similar fashion to the $b\bar{b}$ case.

Fermion Loop Corrections

Another contribution to the $gg \rightarrow t\bar{t}$ rate is the process where the two incoming gluons couple to an s-channel weak particle via a top quark triangle (as shown in fig(6.7)). We also can use the helicity amplitudes method to evaluate this interference. The expression we have for Γ (the string of gamma matrices between the Dirac spinors

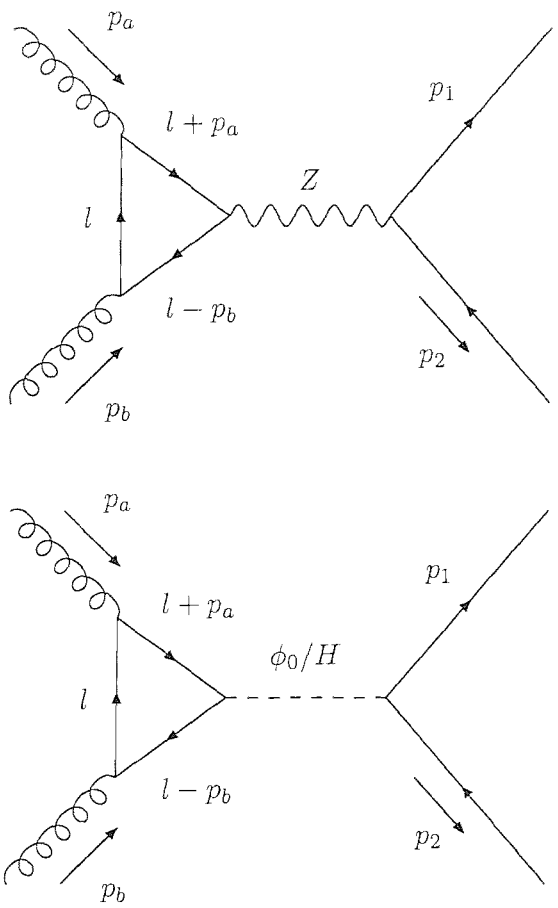

Figure 6.7: $gg \rightarrow t\bar{t}$ via a top loop

associated with the external top quarks) is:

$$\Gamma = \frac{g_S^2}{(p_a + p_b)^2 - m_Z^2} \int \frac{d^d l}{(2\pi)^d} \frac{\gamma^\mu (a + b\gamma^5)}{[l^2 - m_t^2][(l + p_a)^2 - m_t^2][(l - p_b)^2 - m_t^2]} \times \text{vert}_\mu \quad (6.63)$$

where

$$\text{vert}_\mu = \text{Tr}(\gamma^\rho \epsilon_\rho(p_a)(\not{l} + m_t)\gamma^\sigma \epsilon_\sigma(p_b)(\not{l} - \not{p}_b + m_t)\gamma_\mu(a + b\gamma^5)(\not{l} + \not{p}_a + m_t)) \quad (6.64)$$

Here we are looking at the case where a general vector boson is being exchanged - in actual fact the only vector boson that can be exchanged in this diagram is a Z-boson - the W-boson being disallowed by charge conservation. To modify the expression for the scalar exchanges we simply drop the two γ^μ matrices and select appropriate

substitutions for a and b. The only allowed scalar particles are the ϕ_0 or Higgs, again the $\phi_{+/-}$ exchanges are disallowed by charge.

The diagram with a gluon exchanged in the s-channel, whilst it is non-zero (Furry's theorem does not hold for three gluons), is not required for this calculation as the lowest order in α_S it can 'come in' at is α_S^3.

Note that for each exchanged weak particle we need to include two contributions - one where the top loop is running clockwise (as shown) and one where the top loop is running anti-clockwise.

6.3 $q\bar{q}$ to $t\bar{t}$

We now need to evaluate the diagrams that contribute to the four quark top production process. This process, unlike the gluon gluon case will include IR divergences as there are now bremsstrahlung contributions to the cross-section.

6.3.1 Helicity Amplitudes For $q\bar{q}$ To $t\bar{t}$

The helicity amplitudes method in the four quark case is very similar to that in the gluon gluon case. Because we are assuming that there are no bottom or top quarks in the initial state (as we did for $b\bar{b}$ production) all of the one loop interferences will be corrections to the interference between two tree-level s-channel diagrams (either gluon exchange squared or gluon exchange interfered with Z-boson exchange).

This means that we will have an outgoing massive fermion line which can be treated in the same way as in the gluon gluon case. However, this time rather than contract the free Lorentz index (or indices in the case of a box diagram) of the top quark line with the two incoming gluon polarisation vectors we contract them with the expression for

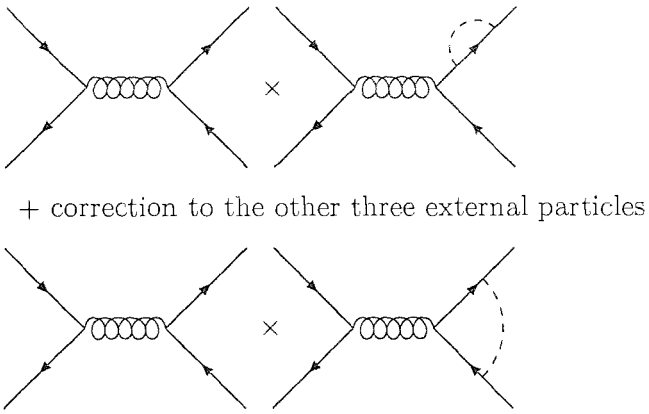

Figure 6.8: The IR finite loop correction interferences that contribute to $q\bar{q} \rightarrow t\bar{t}$. The correction (either bubble or vertex) to a final state top may be a Z, W, H, $\phi_{+/-}$ or ϕ_0. The correction to an initial state light quark will either be a W or a Z.

a massless fermion line (obtained for the $b\bar{b}$ calculation).

6.3.2 The IR Finite Loop Corrections To $q\bar{q}$ To $t\bar{t}$

In practise we find that the IR divergences are limited to the box diagrams so we will deal with them later.

The IR finite terms will be topologically identical to those in the $b\bar{b}$ case (see fig(6.8) with $m_b \rightarrow m_t$) with the addition of neutral Goldstone and Higgs corrections to the final state particles. These corrections did not apply in the massless case as the relevant couplings depend on the mass of the associated fermion. Note that the charged Goldstone did contribute in the $b\bar{b}$ case as emission of a ϕ_- turns a bottom quark into a top meaning that the top mass will appear in the coupling.

External Leg Self Energy Corrections

There will be two distinct sets of contributing diagrams to this part of the correction. Those where we have an external leg self energy correction to either of the final state top quarks and those where the correction is on one of the initial state light quarks.

In the case where the correction is on one of the top quarks we will have both a vector (W and Z boson) and a scalar (Goldstone and Higgs boson) contributions. The mechanics of calculating this term are almost identical to the case in the gluon gluon calculation where we had an external leg correction to the s-channel $gg \rightarrow t\bar{t}$ diagram given in section(6.2.2). We simply substitute a different tree level amplitude into eq(6.44 & 6.45).

When we have an external leg correction on one of the incoming quarks we only have a contribution from the vector boson as all of the scalar particle couplings are proportional to the mass of the quark and this is only non-negligible in the case of a top - as we are assuming that there are no bottom or top quarks in the initial state we will always be setting this mass to zero. In this case the corrections can be calculated exactly as they were in the massless quark cases so long as we include the top mass at the tree level.

Vertex Corrections

Again we will have two distinct contributions. One where we have a vertex correction to the final state top quarks and one where we have a vertex correction to the initial state light quarks.

The method of evaluating the correction on the final state particles is again analogous to the calculation performed to find the vertex corrections to the s-channel $gg \rightarrow t\bar{t}$ process described in section(6.2.2).

For the same reason as in the case of the external leg corrections we will only have

vector boson corrections to the incoming quarks and, once again, this means they can be calculated in a similar manner to in the massless quark calculations so long as we allow for the top mass in the final state.

6.3.3 The IR Divergent Loop Corrections To $q\bar{q}$ To $t\bar{t}$

Box Diagrams

The only IR divergent terms in $q\bar{q} \to t\bar{t}$ will be the four possible box diagrams (s-channel exchange of two gluons or a gluon and a Z-boson in both crossed and uncrossed topologies). Note that there will not be Higgs or Goldstone box corrections in the $q\bar{q}$ case as the couplings to the initial state quarks will be zero. There are also no W corrections here due to the very specific flavour combination being considered.

Once again the process of actually evaluating these interferences is very similar to that used in the $b\bar{b}$ case. We need to use the expressions obtained earlier for the massive helicity amplitudes and also use expressions for the Veltman & Passarino functions that include the top mass when applicable. After these changes the process is identical to the massless case.

The results in the massless case were sufficiently simple that we could compare the pole structure in the loop diagrams with that obtained during the subtraction procedure (see section(4.5) for this check in the massless case and section(6.6.1) for the integrated dipoles in the massive case) by hand to ensure that the divergences cancelled. This is impractical in the massive case due to the increased complexity of the expressions obtained. As a result we simply input both the VP functions and the endpoint terms in the subtraction method with the poles set explicitly to zero with the assumption that they will cancel.

6.4 Bremsstrahlung Corrections To $q\bar{q}$ To $t\bar{t}$

The bremsstrahlung topologies that contribute to this calculation are identical to those that contribute to the $b\bar{b}$ case (see fig(4.8)). Once again those terms where we interfere a final(initial) state emission with another final(initial) state emission are disallowed by colour.

With the exception of the obvious addition of the top mass to the calculation the process of evaluating the real corrections is exactly that described in the massless case.

The bremsstrahlung result must be combined with the sum of all contributing dipole terms (see section(6.5.1)) prior to integration - this renders the result finite and integrable.

6.5 The Subtraction Method With Massive Final State Particles

6.5.1 The Dipole Subtractions

For the case of massive external particles we use the subtraction method described in [8].

Analogously to the massless case we need to obtain a term $d\sigma^A$ such that,

$$[d\sigma^{REAL} - d\sigma^A] \tag{6.65}$$

is finite in both the soft and collinear limits.

In the soft limit the bremsstrahlung in the top production case is very similar to that in the massless case. Namely:

$$|\mathcal{M}_{a,b,1,2,3}(m_t^2)|^2 \rightarrow$$
$$-\frac{1}{\lambda^2}\mu^{2\epsilon}g_S^2\left(T_a\frac{p_a^\mu}{p_a.q}+T_b\frac{p_b^\mu}{p_b.q}+T_1\frac{p_1^\mu}{p_1.q}+T_2\frac{p_2^\mu}{p_2.q}\right)^2|\mathcal{M}_{a,b,1,2}(m_t^2)|^2 \tag{6.66}$$

Where $p_3 = \lambda q$ as $\lambda \to 0$. This expression is identical to eq(3.10) with the tree level matrix element squared replaced with the formula for the massive case.

The behaviour of the top-top bremsstrahlung in the collinear limit is a little more complicated.

For the case where we have two final state particles (p_i and p_3) going collinear the expression is:

$$\begin{aligned}
&|\mathcal{M}_{a,b,1,2,3}(m_t^2, p_i, \lambda_i)|^2 \to \\
&\mu^{2\epsilon} g_S^2 g_{i,+}^{final}(p_i, p_3) |\mathcal{M}_{a,b,1,2}(m_t^2, p_i + p_3, \lambda_i)|^2 \\
&+\mu^{2\epsilon} g_S^2 g_{i,-}^{final}(p_i, p_3) |\mathcal{M}_{a,b,1,2}(m_t^2, p_i + p_3, -\lambda_i)|^2
\end{aligned} \tag{6.67}$$

Where we define:

$$\begin{aligned}
g_S^2 g_{i,+}^{final}(p_i, p_3) &= \frac{1}{p_i \cdot p_3}\left[P_{i,i}(z_i) - \frac{m_t^2}{p_i \cdot p_3}\right] - g_S^2 g_{i,-}^{final}(p_i, p_3) \\
g_S^2 g_{i,-}^{final}(p_i, p_3) &= \frac{m_t^2}{2(p_i \cdot p_3)^2} \frac{(1 - z_i)^2}{z_i}
\end{aligned} \tag{6.68}$$

The second term in eq(6.67) is the 'spin flip' term. This term allows for the possibility that the emission of the collinear gluon flips the helicity of the final state quark that is emitting it. For example, if we are calculating a term with final state quark helicities λ_1 and λ_2 and are considering the case when the emitted gluon goes collinear with particle 1 then we will have two terms. One, the normal term, which is proportional to the tree level $|\mathcal{M}(\lambda_1, \lambda_2)|^2$ and a second, the spin flip term, which is proportional to the tree level $|\mathcal{M}(-\lambda_1, \lambda_2)|^2$. The final state quark in the spin flip term still has helicity λ_1 but the p_1 quark in the tree level is the quark prior to gluon emission and as such has the opposite helicity.

As we can safely make the assumption that the incoming particles are massless the

expression when the gluon (p_3) goes collinear with an initial state particle is very similar to the massless case:

$$|\mathcal{M}_{a,b,1,2,3}(m_t^2, p_a)|^2 \rightarrow$$
$$\mu^{2\epsilon} g_S^2 g_{i,+}^{initial}(p_a, p_3)|\mathcal{M}_{a,b,1,2}(m_t^2, x_a p_a)|^2 \tag{6.69}$$

Where:

$$g_{i,+}^{initial}(p_a, p_3) = \frac{1}{x_a p_a . p_3} P_{a,a}(x_a) \tag{6.70}$$

This term is identical to eq(3.20) with the massless tree level matrix element replaced with the expression for the top production case.

6.5.2 Final State State Emitter, Initial State Spectator

In the case where we have a final state emitter and an initial state spectator the dipole has the form:

$$\mathcal{D}_{i3}^{a} = -g_S \times (col) \times$$
$$\big[g_{ia,+}(p_i, p_a, p_3, x_{ia}, z_{ia})|\mathcal{M}(s, t, \lambda_a, \lambda_1, \lambda_2)|^2$$
$$g_{ia,-}(p_i, p_a, p_3, x_{ia}, z_{ia})|\mathcal{M}(s, t, \lambda_a, -\lambda_i, \lambda_j)|^2\big] \tag{6.71}$$

Where (col) is the colour factor.

Here the second term (proportional to $g_{ia,-}()$ is the 'helicity flip' term described above. This should exactly cancel with the equivalent term in eq(6.68) in the collinear limit. Note that in the soft limit $z_{ia} \rightarrow 1$ so $g_{ia,-}$ will vanish. This means that the helicity

flip term will not affect the cancellation with eq(6.66) in the soft limit.

$$g_{ia,+}(p_i,p_a,p_3,x_{ia},z_{ia}) = \frac{1}{x_{ia}p_i.p_3}\left[\frac{2}{2-x_{ia}-z_{ia}} - 1 - z_{ia} - \frac{m_t^2}{p_i.p_3}\right]$$
$$-g_{ia,-}(p_i,p_a,p_3,x_{ia},z_{ia})$$
$$g_{ia,-}(p_i,p_a,p_3,x_{ia},z_{ia}) = \frac{m_t^2}{2(p_i.p_3)^2x_{ia}^2}\frac{(1-z_{ia})^2}{z_{ia}} \tag{6.72}$$

Dipole $\mathcal{D}_{13}^a$

The dipole variables for the case where the emitter is particle 1 and the spectator is particle a.

$$(col) = -\frac{c_F c_A}{2}$$
$$x_{1a} = \frac{p_1.p_a + p_3.p_a - p_1.p_3}{p_1.p_a + p_3.p_a}$$
$$z_{1a} = \frac{p_1.p_a}{p_1.p_a + p_3.p_a}$$
$$t = -2p_2.p_b + m_t^2$$
$$s = 2x_{1a}p_a.p_b \tag{6.73}$$

Dipole $\mathcal{D}_{23}^a$

The dipole variables for the case where the emitter is particle 2 and the spectator is particle a.

$$(col) = \frac{c_F c_A}{2}$$
$$x_{2a} = \frac{p_2.p_a + p_3.p_a - p_2.p_3}{p_2.p_a + p_3.p_a}$$
$$z_{2a} = \frac{p_2.p_a}{p_2.p_a + p_3.p_a}$$
$$t = 2p_1.p_b - 2x_{2a}p_a.p_b + m_t^2$$
$$s = 2x_{2a}p_a.p_b \tag{6.74}$$

Dipole $\mathcal{D}_{13}^{b}$

The dipole variables for the case where the emitter is particle 1 and the spectator is particle b.

$$
\begin{aligned}
(col) &= \frac{c_F c_A}{2} \\
x_{1b} &= \frac{p_1.p_b + p_3.p_b - p_1.p_3}{p_1.p_b + p_3.p_b} \\
z_{1b} &= \frac{p_1.p_b}{p_1.p_b + p_3.p_b} \\
t &= 2p_2.p_a - 2x_{1b}p_a.p_b + m_t^2 \\
s &= 2x_{1b}p_a.p_b
\end{aligned}
\tag{6.75}
$$

Dipole $\mathcal{D}_{23}^{b}$

The dipole variables for the case where the emitter is particle 2 and the spectator is particle b.

$$
\begin{aligned}
(col) &= -\frac{c_F c_A}{2} \\
x_{2b} &= \frac{p_2.p_b + p_3.p_b - p_2.p_3}{p_2.p_b + p_3.p_b} \\
z_{2b} &= \frac{p_2.p_b}{p_2.p_b + p_3.p_b} \\
t &= -2p_1.p_a + m_t^2 \\
s &= 2x_{2b}p_a.p_b
\end{aligned}
\tag{6.76}
$$

It can be shown that, in the soft and collinear limits, these terms cancel the divergences shown in eq(6.66) and eq(6.68).

6.5.3 Initial State State Emitter, Final State Spectator

The dipoles associated with emission from the (massless) incoming quarks do not include a 'helicity flip' term and have the form:

$$\mathcal{D}_i^{a3} = -g_S \times (col) \times$$
$$g_{ai}(p_a, p_i, p_3, x_{ia}, z_{ia})|\mathcal{M}(s, t, \lambda_a, \lambda_1, \lambda_2)|^2 \tag{6.77}$$

Where g_{ai} is defined as:

$$g_{ai}(p_a, p_i, p_3, x_{ia}, z_{ia}) = \frac{1}{x_{ia} p_a.p_3}\left[\frac{2}{2 - x_{ia} - z_{ia}} - 1 - x_{ia}\right] \tag{6.78}$$

Dipole $\mathcal{D}_1^{a3}$

The dipole variables for the case where the emitter is particle 1 and the spectator is particle a.

$$(col) = -\frac{c_F c_A}{2}$$
$$x_{1a} = \frac{p_1.p_a + p_3.p_a - p_1.p_3}{p_1.p_a + p_3.p_a}$$
$$z_{1a} = \frac{p_1.p_a}{p_1.p_a + p_3.p_a}$$
$$t = -2p_2.p_b + m_t^2$$
$$s = 2x_{1a} p_a.p_b \tag{6.79}$$

Dipole $\mathcal{D}_2^{a3}$

The dipole variables for the case where the emitter is particle 2 and the spectator is particle a.

$$
\begin{aligned}
(col) &= \frac{c_F c_A}{2} \\
x_{2a} &= \frac{p_2 \cdot p_a + p_3 \cdot p_a - p_2 \cdot p_3}{p_2 \cdot p_a + p_3 \cdot p_a} \\
z_{2a} &= \frac{p_2 \cdot p_a}{p_2 \cdot p_a + p_3 \cdot p_a} \\
t &= 2p_1 \cdot p_b - 2x_{2a} p_a \cdot p_b + m_t^2 \\
s &= 2x_{2a} p_a \cdot p_b
\end{aligned}
\tag{6.80}
$$

Dipole $\mathcal{D}_1^{b3}$

The dipole variables for the case where the emitter is particle 1 and the spectator is particle b.

$$
\begin{aligned}
(col) &= \frac{c_F c_A}{2} \\
x_{1b} &= \frac{p_1 \cdot p_b + p_3 \cdot p_b - p_1 \cdot p_3}{p_1 \cdot p_b + p_3 \cdot p_b} \\
z_{1b} &= \frac{p_1 \cdot p_b}{p_1 \cdot p_b + p_3 \cdot p_b} \\
t &= 2p_2 \cdot p_a - 2x_{1b} p_a \cdot p_b + m_t^2 \\
s &= 2x_{1b} p_a \cdot p_b
\end{aligned}
\tag{6.81}
$$

Dipole $\mathcal{D}_2^{b3}$

The dipole variables for the case where the emitter is particle 2 and the spectator is particle b.

$$
\begin{aligned}
(col) &= -\frac{c_F c_A}{2} \\
x_{2b} &= \frac{p_2.p_b + p_3.p_b - p_2.p_3}{p_2.p_b + p_3.p_b} \\
z_{2b} &= \frac{p_2.p_b}{p_2.p_b + p_3.p_b} \\
t &= -2p_1.p_a + m_t^2 \\
s &= 2x_{2b}p_a.p_b
\end{aligned}
\tag{6.82}
$$

It can be shown that, in the soft and collinear limits respectively, these terms cancel the divergences shown in eq(6.66) and eq(6.69).

Rather than performing an analytical check it was confirmed that the dipoles cancel the soft and collinear divergences via a simple numerical check.

Note that, as in the $b\bar{b}$ case the remaining possible dipoles (all associated with initial-initial or final-final interferences) are all forbidden by colour.

6.6 The Integrated Dipoles

By integrating the dipole terms given in eq(6.73→6.82) over the single particle phase space we will obtain an expression analogous to that given in eq(3.103) for the massless case. Similarly to that result the expression will comprise of an x dependant part integrated over x and an x independent 'endpoint' term.

6.6.1 The Endpoint Terms

The endpoint terms are roughly analogous to the $I(\epsilon)$ terms in the massless case (eq(3.80) and onwards) - the x independent divergent parts of the integrated dipoles. Similarly to the massless case the divergences in these terms should exactly cancel the poles generated in the virtual corrections.

The expressions obtained for the endpoint terms are as follows:

The endpoint term for the case where the emitter is incoming particle a and the spectator is outgoing particle 1:

$$\left[\frac{g_S^2}{8\pi^2}\frac{c_F c_A}{2}\right]\left(G_+^{ai}(t)|\mathcal{M}(s,t,\lambda_a,\lambda_1)|^2 + G_-^{ai}(t)|\mathcal{M}(s,t,-\lambda_a,\lambda_1)|^2\right) \tag{6.83}$$

The case where the emitter is incoming particle a and the spectator is outgoing particle 2:

$$-\left[\frac{g_S^2}{8\pi^2}\frac{c_F c_A}{2}\right]\left(G_+^{ai}(u)|\mathcal{M}(s,t,\lambda_a,\lambda_2)|^2 + G_-^{ai}(u)|\mathcal{M}(s,t,-\lambda_a,\lambda_2)|^2\right) \tag{6.84}$$

Where the expressions for $G_{+/-}^{ai}$ are:

$$\begin{aligned} &G_+^{ai}(p^2) = \\ &\frac{1}{2}ln^2\left(\frac{\mu^2}{2m_t^2-p^2}\right)+\frac{\pi^2}{6}+2\left(Li_2\left(\frac{p^2}{2m_t^2-p^2}\right)-Li_2\left(\frac{m_t^2}{2m_t^2-p^2}\right)\right) \\ &+2ln\left(\frac{2m_t^2-p^2}{m_t^2-p^2}\right)ln\left(\frac{\mu^2 m_t^2}{(m_t^2-p^2)(2m_t^2-p^2)}\right)+\frac{3}{2}ln\left(\frac{\mu^2}{m_t^2-p^2}\right) \\ &-\frac{3}{2}+\frac{m_t^2(m_t^2-4p^2)}{4p^2}ln\left(1-\frac{p^2}{m_t^2}\right)+\frac{\pi^2}{3}+\frac{m_t^2}{2p^2} \\ &G_-^{ai}(p^2) = \frac{1}{2} \end{aligned} \tag{6.85}$$

Note that the fact that G_-^{ai} is independent of the Mandelstam variable means that the spin flip term will cancel between the a,1 term and the a,2 term (due to the minus sign

in the colour factor).

Also note that here we have dropped the divergent terms as these are assumed to cancel the divergent terms in the virtual corrections (in principle it is possible to demonstrate this as in the massless case however when we include the top mass the expressions become prohibitively complicated).

The case where the emitter is outgoing particle 1 and the spectator is incoming particle a:

$$\left[\frac{g_S^2}{8\pi^2}\frac{c_F c_A}{2}\right]\left(G_+^{ia}(t)|\mathcal{M}(s,t,\lambda_a,\lambda_1)|^2\right.$$
$$\left.+G_-^{ia}(t)|\mathcal{M}(s,t,\lambda_a,-\lambda_1)|^2\right) \tag{6.86}$$

The case where the emitter is outgoing particle 1 and the spectator is incoming particle b:

$$-\left[\frac{g_S^2}{8\pi^2}\frac{c_F c_A}{2}\right]\left(G_+^{ia}(u)|\mathcal{M}(s,t,\lambda_b,\lambda_1)|^2\right.$$
$$\left.+G_-^{ia}(u)|\mathcal{M}(s,t,\lambda_b,-\lambda_1)|^2\right) \tag{6.87}$$

Where the expressions for $G_{+/-}^{ia}$ are:

$$G_+^{ia}(p^2) =$$
$$ln\left(\frac{m_t^2}{\mu^2}\right)ln\left(2-\frac{p^2}{m_t^2}\right)+ln\left(\frac{\mu^2 m_t^2}{(m_t^2-p^2)^2}\right)$$
$$-2Li_2\left(\frac{p^2}{p^2-2m_t^2}\right)+\frac{1}{2}ln^2\left(2-\frac{p^2}{m_t^2}\right)$$
$$+\frac{(p^2-m_t^2)^2}{2p^2}ln\left(1-\frac{p^2}{m_t^2}\right)-\frac{\pi^2}{6}+1+\frac{m_t^2}{2p^2}$$
$$G_-^{ia}(p^2)=\frac{1}{2} \tag{6.88}$$

Note that again the spin flip term cancels across these two expressions as it still doesn't depend on the momenta.

6.6.2 The x Dependent Terms

The x dependent parts of the integrated dipoles are found to be as follows.

The case where the emitter is incoming particle a and the spectator is outgoing particle 1:

$$\begin{aligned}
&\left[\frac{g_S^2}{8\pi^2}\frac{c_F c_A}{2}\right]\times \\
&\left(\int_{x_0}^1 dx \int d\hat{\Phi}\frac{1}{x}G_+^{ai}(t,x)|\mathcal{M}(\hat{s},\hat{t},\lambda_a,\lambda_1)|^2\right. \\
&-\int_{x_0}^1 dx \int d\Phi G_+^{ai}(t,x)|\mathcal{M}(s,t,\lambda_a,\lambda_1)|^2 \\
&+\int_{x_0}^1 dx \int d\hat{\Phi}\frac{1}{x}G_-^{ai}(t,x)|\mathcal{M}(\hat{s},\hat{t},-\lambda_a,\lambda_1)|^2 \\
&\left.-\int_{x_0}^1 dx \int d\Phi G_-^{ai}(t,x)|\mathcal{M}(s,t,-\lambda_a,\lambda_1)|^2\right)
\end{aligned} \tag{6.89}$$

Here $\hat{s},\hat{t}$ are the Mandelstam variables scaled by x:

$$\begin{aligned}
\hat{s} &= 4(E_{cm}^x)^2 \\
\hat{t} &= m_t^2 - \frac{\hat{s}}{2} + 2E_{cm}^x p_{cm}^x cos\theta
\end{aligned} \tag{6.90}$$

Where E_{cm}^x and p_{cm}^x are the partonic centre of mass energy and momentum scaled by x.

Also $x_0 = m_t^2/E_{cm}^2$. This lower limit on the x integration ensures that the partonic energy is sufficient to produce the top pair. The case where the emitter is incoming particle a and the spectator is outgoing particle 2:

$$\begin{aligned}
&-\left[\frac{g_S^2}{8\pi^2}\frac{c_F c_A}{2}\right]\times \\
&\left(\int_{x_0}^1 dx \int d\hat{\Phi}\frac{1}{x}G_+^{ai}(u,x)|\mathcal{M}(\hat{s},\hat{t},\lambda_a,\lambda_2)|^2\right. \\
&-\int_{x_0}^1 dx \int d\Phi G_+^{ai}(u,x)|\mathcal{M}(s,t,\lambda_a,\lambda_2)|^2 \\
&+\int_{x_0}^1 dx \int d\hat{\Phi}\frac{1}{x}G_-^{ai}(u,x)|\mathcal{M}(\hat{s},\hat{t},-\lambda_a,\lambda_2)|^2 \\
&\left.-\int_{x_0}^1 dx \int d\Phi G_-^{ai}(u,x)|\mathcal{M}(s,t,-\lambda_a,\lambda_2)|^2\right)
\end{aligned} \tag{6.91}$$

Where $G^{ai}_{+/-}(p^2,x)$ are defined as:

$$
\begin{aligned}
&G^{ai}_{+}(p^2,x) = \\
&P_{aa}(x)\left(ln\left(\frac{m_i^2-p^2}{\mu^2}\right)+ln(1-z_i(x))-1\right) \\
&+(1+x)ln(1-x)-\frac{2}{1-x}ln(2-x-z_i(x)) \\
&G^{ai}_{-}(p^2,x) = 1-x
\end{aligned}
\tag{6.92}
$$

Once again the spin flip terms will cancel due to the fact that $G^{ai}_{-}(p^2,x)$ is independent of the momenta.

In the case where the emitter is outgoing particle 1 and the spectator is incoming particle a:

$$
\begin{aligned}
&\left[\frac{g_S^2}{8\pi^2}\frac{c_F c_A}{2}\right]\times \\
&\left(\int_{x_0}^1 dx\int d\hat{\Phi}\frac{1}{x}G^{ia}_{+}(t,x)|\mathcal{M}(\hat{s},\hat{t},\lambda_a,\lambda_1)|^2\right. \\
&-\int_{x_0}^1 dx\int d\Phi G^{ia}_{+}(t,x)|\mathcal{M}(s,t,\lambda_a,\lambda_1)|^2 \\
&+\int_{x_0}^1 dx\int d\hat{\Phi}\frac{1}{x}G^{ia}_{-}(t,x)|\mathcal{M}(\hat{s},\hat{t},\lambda_a,-\lambda_1)|^2 \\
&\left.-\int_{x_0}^1 dx\int d\Phi G^{ia}_{-}(t,x)|\mathcal{M}(s,t,\lambda_a,-\lambda_1)|^2\right)
\end{aligned}
\tag{6.93}
$$

In the case where the emitter is outgoing particle 1 and the spectator is incoming particle b:

$$
\begin{aligned}
&-\left[\frac{g_S^2}{8\pi^2}\frac{c_F c_A}{2}\right]\times \\
&\left(\int_{x_0}^1 dx\int d\hat{\Phi}\frac{1}{x}G^{ia}_{+}(u,x)|\mathcal{M}(\hat{s},\hat{t},\lambda_b,\lambda_1)|^2\right. \\
&-\int_{x_0}^1 dx\int d\Phi G^{ia}_{+}(u,x)|\mathcal{M}(s,t,\lambda_b,\lambda_1)|^2 \\
&+\int_{x_0}^1 dx\int d\hat{\Phi}\frac{1}{x}G^{ia}_{-}(u,x)|\mathcal{M}(\hat{s},\hat{t},\lambda_b,-\lambda_1)|^2 \\
&\left.-\int_{x_0}^1 dx\int d\Phi G^{ia}_{-}(u,x)|\mathcal{M}(s,t,\lambda_b,-\lambda_1)|^2\right)
\end{aligned}
\tag{6.94}
$$

Where the functions $G^{ia}_{+/-}(p^2,x)$ are defined as:

$$G^{ia}_{+}(p^2,x) =$$
$$\frac{z_i(x)-1}{2(1-x)}\left(3+z_i(x)-\frac{4m_t^2x}{(p^2m_t^2)(1-x)}\right)$$
$$+\frac{1}{1-x}2ln\left(\frac{2-x-z_i(x)}{1-x}\right)-G^{ia}_{-}(p^2,x)$$
$$G^{ia}_{-}(p^2,x)=\frac{m_t^2}{p^2-m_t^2}\frac{1}{1-x^2}\left[ln(z_1(x))+\frac{1}{2}(1-z_i(x))(3-z_1(x))\right] \quad (6.95)$$

(Where $z_1(x)=\frac{xm_t^2}{m_t^2-p^2(1-x)}$)

This time the spin flip term does depend on the momenta and as such will not cancel between eq(6.93) and eq(6.94)

6.7 Performing The Phase Space Integrals

6.7.1 Integrating Over The Two Body Phase Space

We will need two versions of the two body phase space - the first of these ($d\Phi$) is independent of x and is the measure we use for integrating the virtual corrections and some parts of the integrated dipoles (see section(6.6.2)). We will also need a measure that is shifted by x ($d\hat{\Phi}$) which we use as the measure when integrating the remainder of the integrated dipoles (the term integrated dipoles is referring to dipoles integrated over the phase space of the single emitted gluon - we now need to integrate them over the phase space of the remaining two particles).

We will begin by defining the x dependent part as the x independent part can be simply obtained by setting x to one.

We first set the value of s^{beam} (in what follows we will also refer to the partonic s denoted simply by s and also the partonic s scaled by x denoted by $\hat{s}$) , the energy of the beam. This will be determined by the collider energy (for example at LHC this will be in vicinity of 14TeV). From this we will also need the beam centre of mass

energy $E_{cm}^{beam} = \sqrt{s^{beam}}/2$. Another variable that is determined by the experiment that we are performing the calculation for is the maximum rapidity η_{max}. We will be integrating over the rapidity in the phase space integral but must restrict this so that we only consider events that can be picked up in the detector we are modelling. High η ($= -ln(tan(\theta/2))$ where θ is the scattering angle) corresponds to events where the jets are oriented along the beam pipe where they typically cannot be picked up by the detectors.

We also fix both the incoming and outgoing helicities for each run and need to run the Monte Carlo once for each possible combination of helicities.

We start with a phase space measure of:

$$d\hat{\Phi} = \frac{1}{(2\pi)^2}\int dx dx_1 dx_2 d(cos\theta) dE_{cm}^x d\phi \frac{p_{cm}^x}{2}\delta(x_1 x_2 x s - 2\sqrt{x_1 x_2 x s}E_{cm}^x) \qquad (6.96)$$

Here E_{cm}^x is the partonic centre of mass energy scaled by x, where $E_{cm}^x = \frac{\sqrt{x x_1 x_2 s^{beam}}}{2} = \sqrt{x}E_{cm}$.

p_{cm}^x is the partonic momentum, again scaled by x, $p_{cm}^x = \sqrt{(E_{cm}^x)^2 - m_t^2}$.

We use the x_2 integral to eliminate the delta function, ($\frac{d}{dx_2}(x_1 x_2 x s - 2\sqrt{x_1 x_2 x s}E_{cm}^x) = \frac{x x_1 s}{2}$) and we exchange the E_{cm}^x integral for an integral over E_{cm} ($dE_{cm}^x = \sqrt{x}E_{cm}$). Making these changes and performing the integral over ϕ we obtain:

$$d\hat{\Phi} = \frac{1}{2\pi}\int dE_{cm} dx_1 dx d(cos\theta)\frac{p_{cm}^x}{\sqrt{x}x_1 s} \qquad (6.97)$$

We now rewrite $\sqrt{x}$ as $\frac{E_{cm}^x}{E_{cm}}$ and change variables from $cos\theta$ to η. The Jacobian for this change of variables is $dcos\theta = -sin^2\theta d\eta$, however the θ integral runs from $0 \rightarrow \pi$ which corresponds to a rapidity integral of $+\infty \rightarrow -\infty$. We really want this to be the other way round so we add in a minus sign to the Jacobian ie: $dcos\theta = sin^2\theta d\eta$.

This leaves us with:

$$\frac{1}{2\pi}\int dE_{cm} dx_1 d_x d\eta \frac{p_{cm}^x E_{cm}}{E_{cm}^x x_1 s} sin^2\theta \qquad (6.98)$$

We also need to set the limits on these integrals to only include the physically allowed region.

The rapidity integral, as mentioned above, is defined to run from $-\eta_{max}$ to $+\eta_{max}$ as fixed by the collider being studied.

The scaled partonic centre of mass energy (E^x_{cm}) must at least equal the top mass - this means that, since x has a maximum value of 1, that the minimum allowed value of E_{cm} is also m_t. The maximum value is limited by the beam energy and is therefore $\frac{\sqrt{s^{beam}}}{2}$.

The allowed region of both the x_1 and x integrals are fixed by the value of E_{cm}. We already have $E_{cm} > m_t$ to produce a top pair so we know that $x > \frac{m_t^2}{E_{cm}^2}$ (the maximum value of x is of course 1).

The minimum value of x_1 is found by considering the equation $E_{cm} = \frac{\sqrt{x_1 x_2 s}}{2}$. The maximum value of x_2 is 1 so the minimum value of x_1 is $\frac{4E_{cm}^2}{s}$.

Therefore, the phase space measure and Jacobian we use is:

$$d\hat{\Phi} = \frac{1}{2\pi}\int_{m_t}^{E_{cm}^{beam}} dE_{cm} \int_{\frac{4E_{cm}}{s}}^{1} dx_1 \int_{\frac{m_t^2}{E_{cm}^2}}^{1} dx \int_{-\eta_{max}}^{+\eta_{max}} d\eta \frac{p^x_{cm} E_{cm}}{E^x_{cm} x_1 s} sin^2\theta \qquad (6.99)$$

We also need the unshifted phase space. This is obtained by setting x to one in the above equation:

$$d\Phi = \frac{1}{2\pi}\int_{m_t}^{E_{cm}^{beam}} dE_{cm} \int_{\frac{4E_{cm}}{s}}^{1} dx_1 \int_{\frac{m_t^2}{E_{cm}^2}}^{1} dx \int_{-\eta_{max}}^{+\eta_{max}} d\eta \frac{p_{cm}}{x_1 s} sin^2\theta \qquad (6.100)$$

We also need to include the flux factor and the appropriate parton distribution functions.

Note that the integral over x remains as we will still have an x dependence in the integrand.

At each iteration of the Monte Carlo we randomly generate a point in phase space within these bounds ie: an allowed set of values for (x, x_1, E_{cm}, η).

We will wish to generate a p_T distribution and so will have to bin the results according to their value of p_T. The terms proportional to $d\hat{\Phi}$ should be binned by $\hat{p_T}$ $(= \sqrt{(E^x_{cm})^2 - m_t^2} sin\theta)$ and those proportional to $d\Phi$ are binned by the unshifted p_T $(= \sqrt{(E_{cm})^2 - m_t^2} sin\theta)$.

6.7.2 Integrating Over The Three Body Phase Space

The three body phase space integral is somewhat simpler than the two body integral as none of the integrands will include integration over x or any shifted quantities.

The phase space we use is:

$$d\sigma = \frac{1}{(2\pi)^5} \frac{1}{16\hat{s}} |\mathcal{M}|^2 \frac{m_{12}^2 - 2m_t^2}{2m_{12}^2} \frac{\hat{s} - m_{12}^2}{2\hat{s}} dm_{12} d\Omega_1 d\Omega_3 \tag{6.101}$$

Where m_{12}^2 is the invariant mass squared of the top pair $(= (p_a + p_b - p_3)^2)$, $\hat{s}$ is s scaled by the Bjorken x's, Ω_1 is the scattering angle of particle 1 in the centre of mass frame and Ω_3 is the scattering angle of the gluon (particle 3) also in the centre of mass frame.

6.8 Results For $t\bar{t}$ Production

The NLO QCD corrections to $t\bar{t}$ production may be found in [26]

6.8.1 Comparison With The Single And Double Logarithm Calculation

As a check of the results it is possible to make a comparison with the results presented in [35] (also of some interest would be comparisons with [36]) where the single and double logarithms that contribute to the $t\bar{t}$ rate are calculated. We expect the double

logarithm contribution to be dominant at high energy so a check between our results and the logarithm result in the asymptotic limit should show some agreement.

gg to $t\bar{t}$

Fig(6.9) and fig(6.10) compare the correction to $gg \to t\bar{t}$ due to weak effects with the logarithmic correction for two different combinations of top helicities. The comparison is between the partonic matrix elements. Note that the $cos\theta$ selected is far away from the beam axis as we do not expect the logarithmic approximation to be very accurate at high rapidity.

The first obvious feature is that the correction to the cross section with a final state

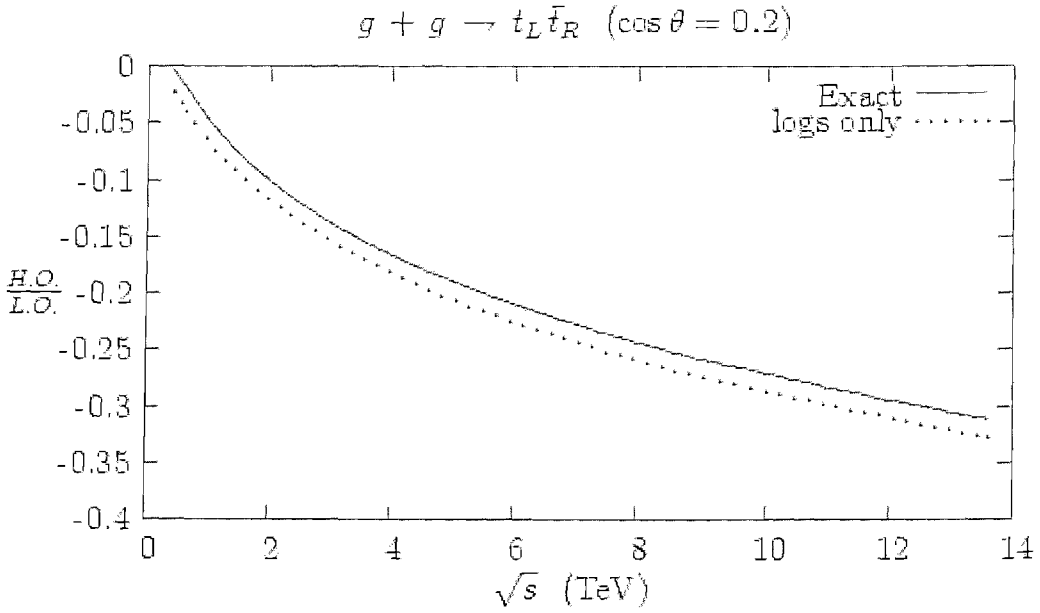

Figure 6.9: Plot showing the correction from NLO weak effects to $gg \to t\bar{t}$ (with a left handed top and right handed anti top) compared with the corrections predicted by large logarithms.

including a left handed top quark is larger than that to a final state including a right handed top quark. This is a consequence of the W coupling to a right handed particle being suppressed.

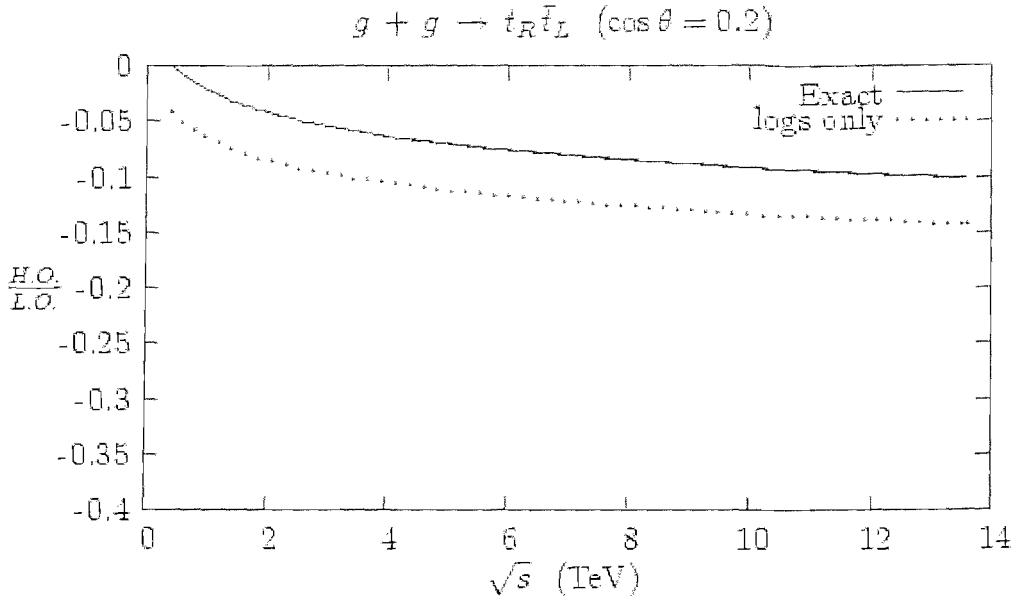

Figure 6.10: Plot showing the correction from NLO weak effects to $gg \to t\bar{t}$ (with a right handed top and left handed anti top) compared with the corrections predicted by a large logarithms.

The lowest $\sqrt{s}$ plotted is 400GeV and the agreement is good even at this low energy. The two methods seem to differ by a constant across the range of $\sqrt{s}$ in both helicity combinations but the agreement is close enough that we can be confident in the accuracy of the complete results.

$q\bar{q}$ to $t\bar{t}$

Fig(6.11) and fig(6.12) compare the correction to $q\bar{q} \to t\bar{t}$ due to NLO weak effects with the logarithm approximation. Once again $cos\theta$ has been taken such that the events are not along the beam pipe. Firstly it can be seen that the correction to the down-type initial state is somewhat stronger than that to the up-type interaction. This is due to the stronger vector coupling of the Z to down quarks compared to up quarks.

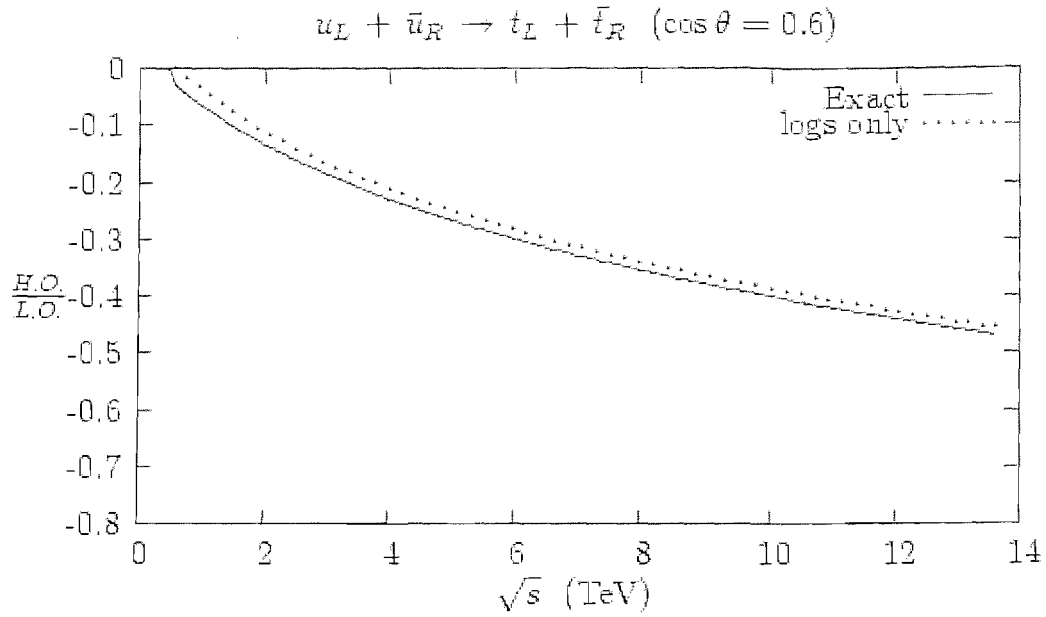

Figure 6.11: Plot showing the correction to $u\bar{u} \to t\bar{t}$ due to NLO weak effects compared to the large logarithm approximation of the same correction.

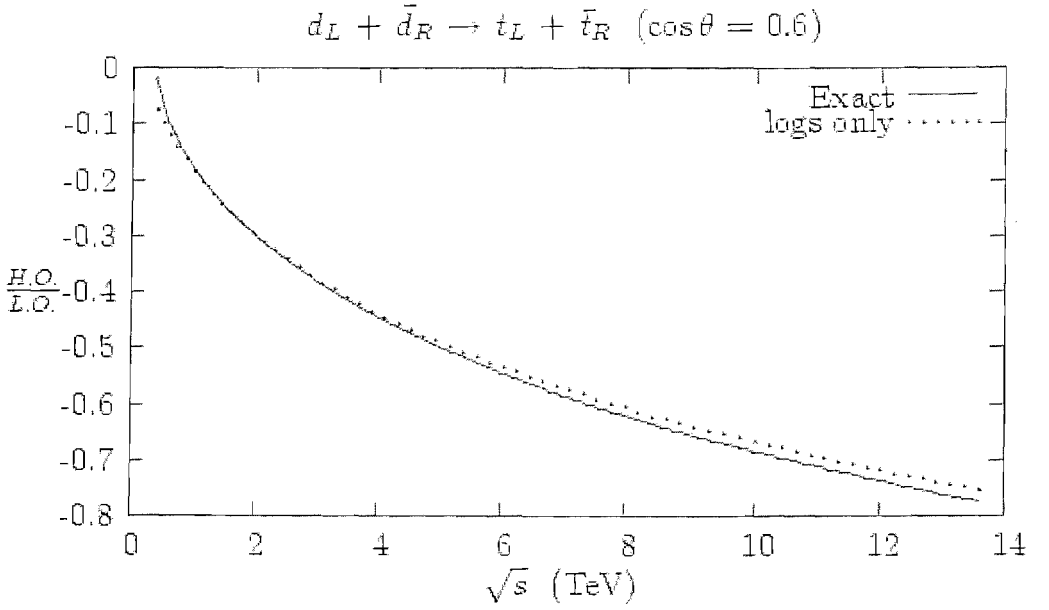

Figure 6.12: Plot showing the correction to $d\bar{d} \to t\bar{t}$ due to NLO weak effects compared to the large logarithm approximation of the same correction.

$$c_V^u = \frac{1}{2} - sin^2\theta_W \frac{2}{3}$$
$$c_V^d = -\frac{1}{2} + sin^2\theta_W \frac{1}{3} \tag{6.102}$$

Again the agreement between the logarithms and the complete calculation is very good and we can be confident in the accuracy of the complete calculation.

6.8.2 The Total Cross Section

gg to $t\bar{t}$

The results presented below (and in section(6.8.3)) are to be published in [37].

In this section we present the results obtained for the differential cross section for $gg \to t\bar{t}$ at LHC plotted against a number of different quantities (fig(6.13), fig(6.14), fig(6.15) and fig(6.16)). The $\alpha_S^2\alpha_W$ correction to the inclusive cross section (the integral of any of the curves in this section) is quite small but we find some of the differential cross sections to be significant.

The differential cross section against p_T (fig(6.13)) is 5% - 10% in regions where the cross-section should be large enough for the corrections to be visible.

We present the M_{tt} (the invariant mass of the top pair) distribution in fig(6.14) - here we see a correction with a very similar shape to that for $\frac{d\sigma}{dp_T}$ but at just over half the size.

Corrections to the E_t and rapidity spectrum are both small but it is worth noting that the cross-section remains large across the full range of these observables, thus we may expect accurate measurements of these cross-sections.

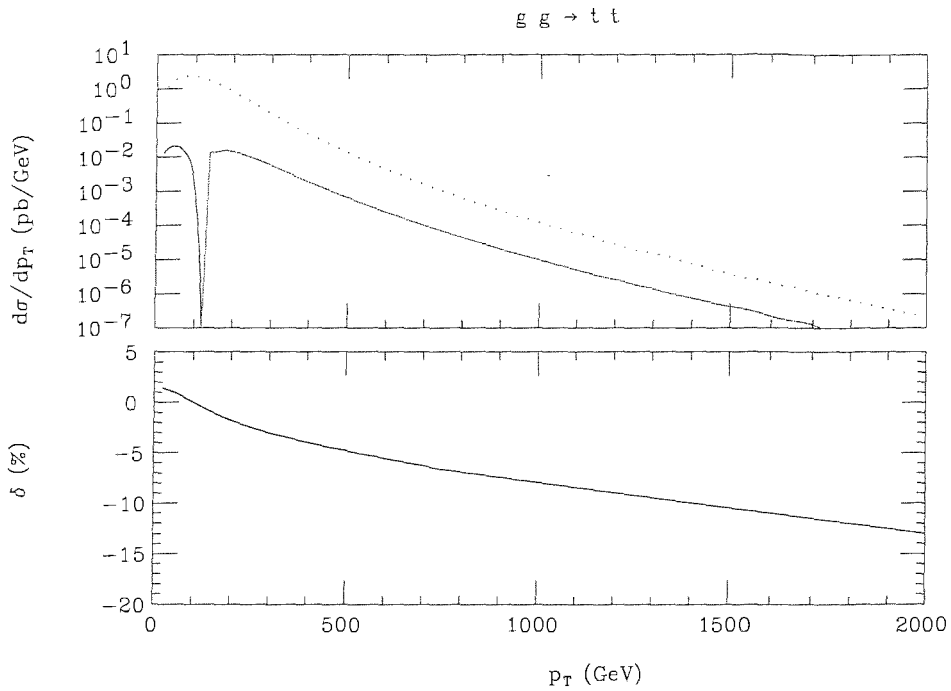

Figure 6.13: Presented here is the differential cross-section for $gg \to t\bar{t}$ plotted against p_T. In the upper frame the dotted line denotes the α_S^2 contribution and the black(grey) line denotes the positive(negative) correction due to $\alpha_S^2\alpha_W$. The lower frame shows the relative correction due to NLO weak effects.

$q\bar{q}$ to $t\bar{t}$

The calculation of the $q\bar{q} \to t\bar{t}$ has been recently published in [38] and [39].

Note that all results in this section are preliminary.

In fig(6.17) we see the differential cross section for $q\bar{q} \to t\bar{t}$ against transverse momentum. The results are also plotted as a correction to the full LO result ($\alpha_W^2 + \alpha_S^2$ note that there is no $\alpha_S\alpha_W$ correction due to the colour structure. This means that the LO weak correction is very small as it comes in at α_W^2 only.) Integrated over p_T to give an inclusive cross section these results show reasonable agreement with those in [38] [39].

The inclusive cross section at NLO weak for $q\bar{q} \to t\bar{t}$ calculated here is 0.0018 pb (0.0396 pb from the matrix element and -0.0378 pb from the integrated dipoles). This compares

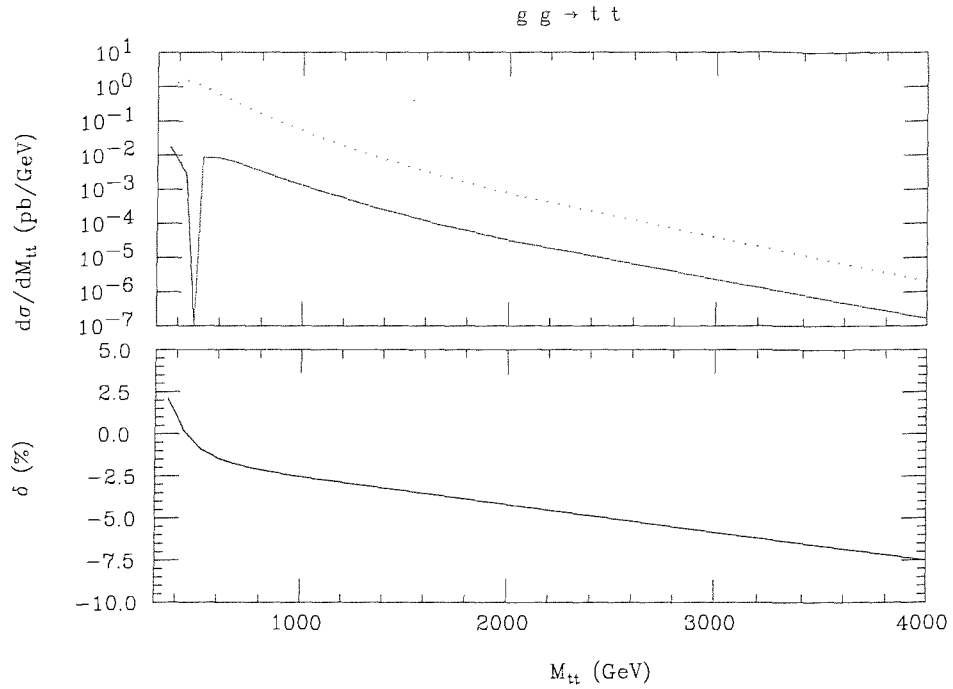

Figure 6.14: Presented above is the differential cross-section for $gg \rightarrow t\bar{t}$ plotted against the invariant mass of the top pair. In the upper frame the dotted line denotes the α_S^2 contribution and the black(grey) line denotes the positive(negative) correction due to $\alpha_S^2\alpha_W$. The lower frame shows the relative correction due to NLO weak effects.

reasonably well with the results of [38] (for m_H=150GeV).

Presented in fig(6.18) are the $q\bar{q}$ results for LHC. We see 10 to 15% corrections in the regions where the absolute value of the cross section is large. Here we obtain an inclusive cross section at NLO weak of -1.229 *pb* (-1.6459 *pb* from the matrix element and 0.4171 *pb* from the integrated dipoles). It is worth noting that this result is approximately 50% larger than that presented in [38] however, as mentioned above, work on our result is continuing.

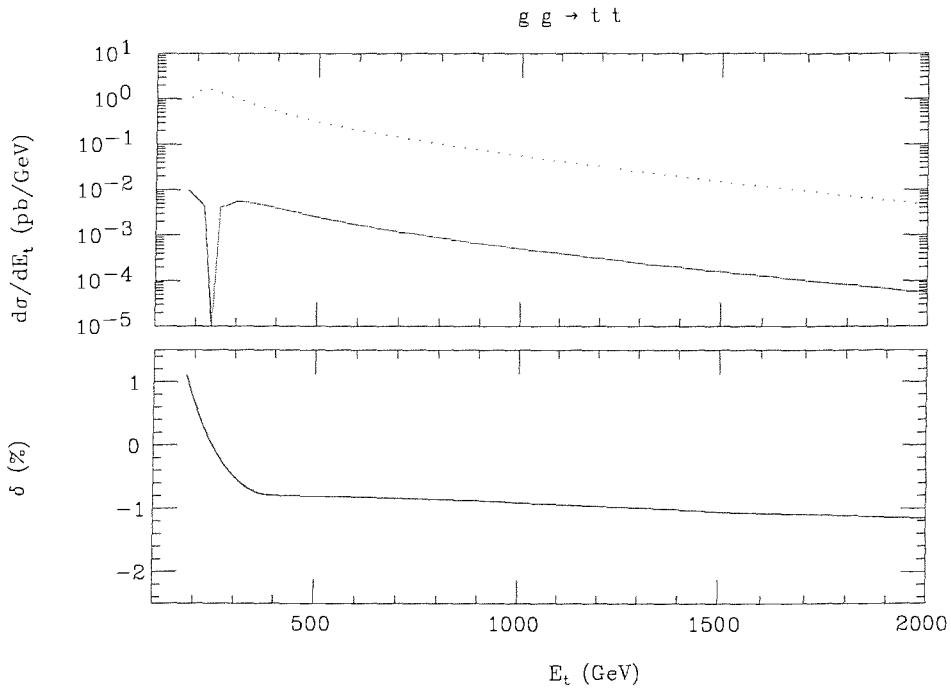

Figure 6.15: Presented above is the differential cross-section for $gg \to t\bar{t}$ plotted against the energy of the top quark. In the upper frame the dotted line denotes the α_S^2 contribution and the black(grey) line denotes the positive(negative) correction due to $\alpha_S^2\alpha_W$. The lower frame shows the relative correction due to NLO weak effects.

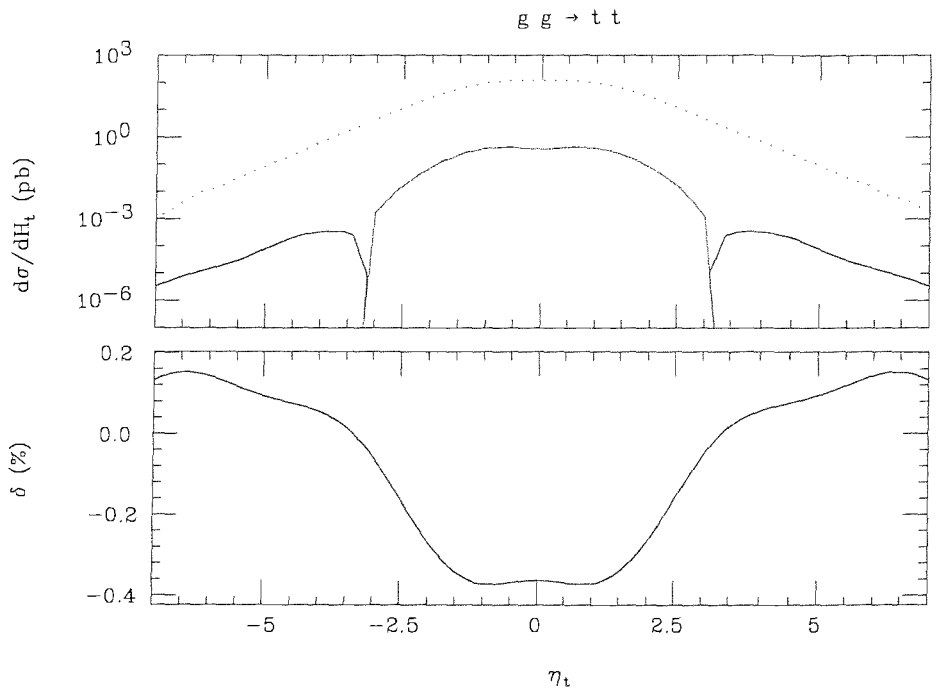

Figure 6.16: Presented above is the differential cross-section for $gg \rightarrow t\bar{t}$ plotted against rapidity. In the upper frame the dotted line denotes the α_S^2 contribution and the black(grey) line denotes the positive(negative) correction due to $\alpha_S^2\alpha_W$. The lower frame shows the relative correction due to NLO weak effects.

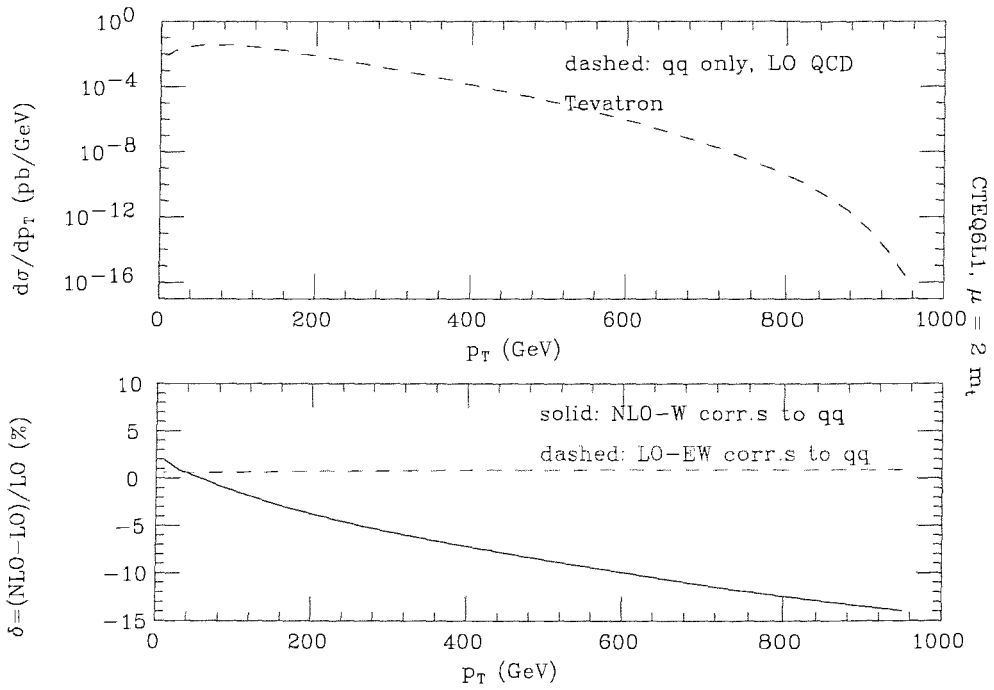

Figure 6.17: In the top frame we show the absolute value of the differential cross section at LO QCD plotted against p_T at the Tevatron. The lower frame shows the relative correction of LO (α_W^2) and NLO ($\alpha_S^2\alpha_W$) weak compared with the LO (α_S^2) result.

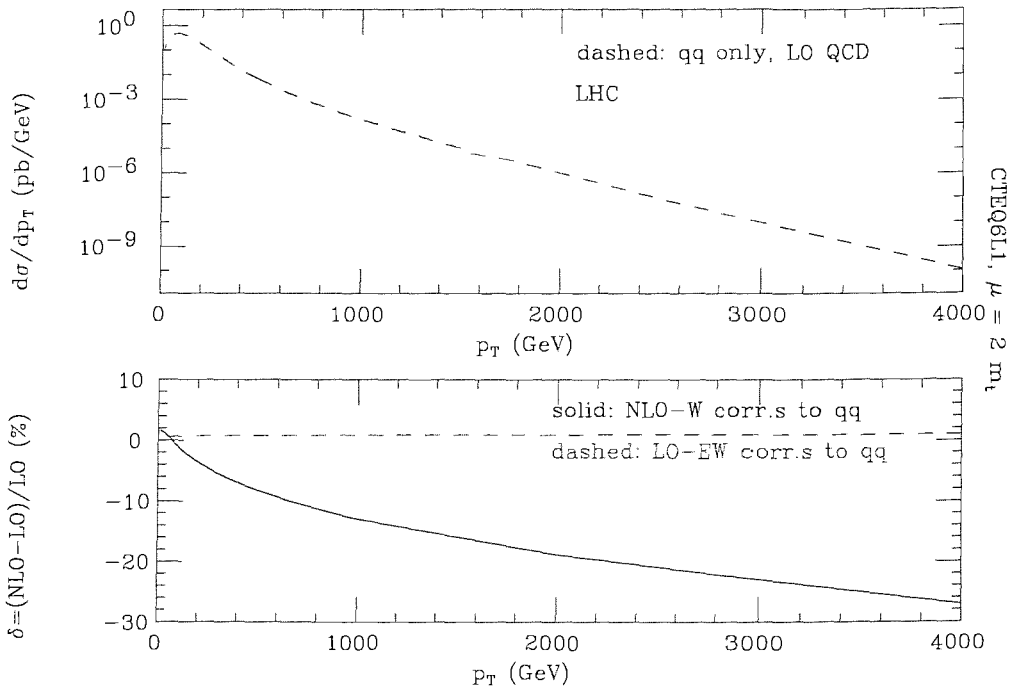

Figure 6.18: In the top frame we show the absolute value of the differential cross section at LO QCD plotted against p_T at the LHC. The lower frame shows the relative correction of LO (α_W^2) and NLO ($\alpha_S^2\alpha_W$) weak compared with the LO (α_S^2) result.

6.8.3 The Asymmetries

Presented below are the A_{LL}, A_L and A_{LL}^{PV} asymmetries. Note that to calculate these asymmetries we have imagined that the helicity of the top anti-top pair is directly measurable, however, as this is not the case, these are not realistic observables (to generate realistic observables we would have to follow the method outlined in section(6.1)). They should, however, give some indication of how significant realistic observables could be.

gg to $t\bar{t}$

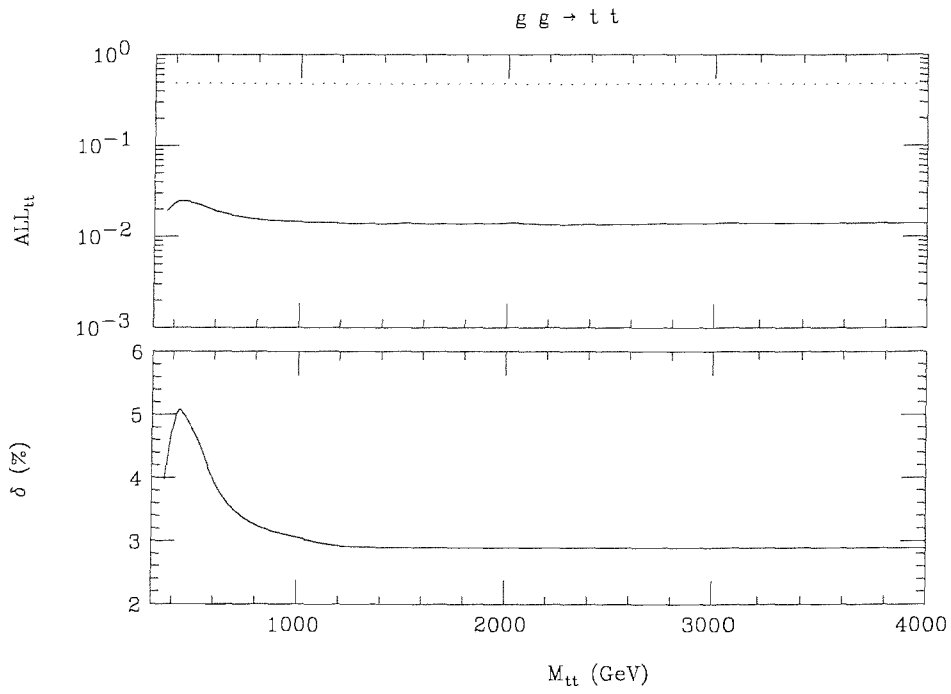

Figure 6.19: Presented here is A_{LL} plotted against the invariant mass of the top pair. In the upper frame the α_S^2 contribution is denoted by the dotted line and the $\alpha_S^2\alpha_W$ by the solid line. In the lower frame we have the relative correction due to NLO weak effects.

In fig(6.19) we see the correction to the non parity violating asymmetry, A_{LL}. As we saw in the $pp \rightarrow$ two jets case, the QCD contribution to this observable is large at LHC, however a 3%-5% correction to this from could be detectable.

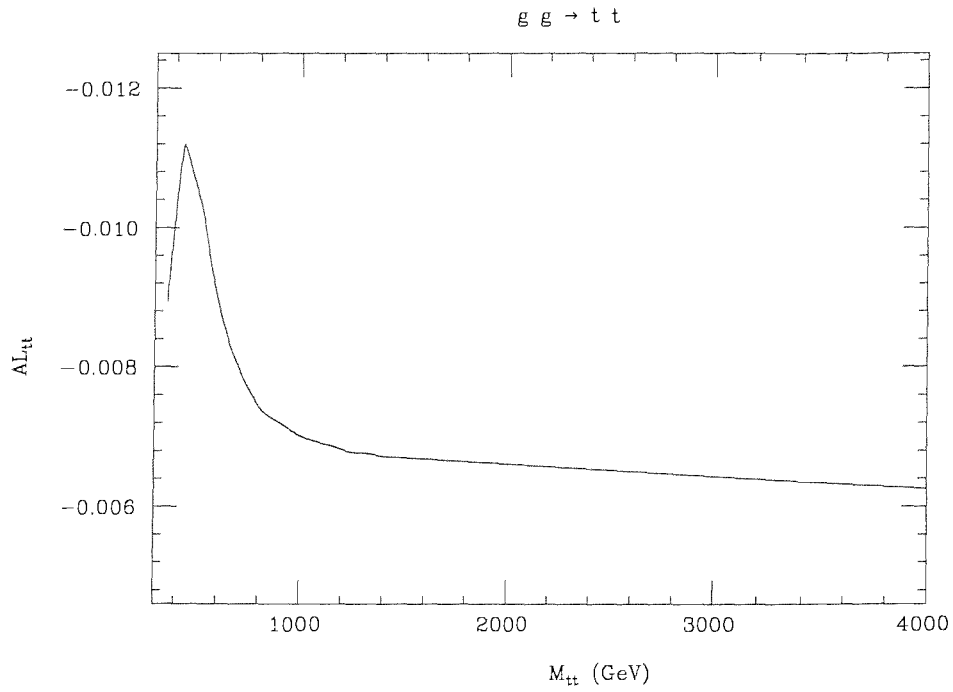

Figure 6.20: Presented here is the $\alpha_S^2\alpha_W$ calculation of A_L plotted against the invariant mass of the top pair. Note that there is no contribution to this asymmetry due to α_S^2 as it is a parity violating observable.

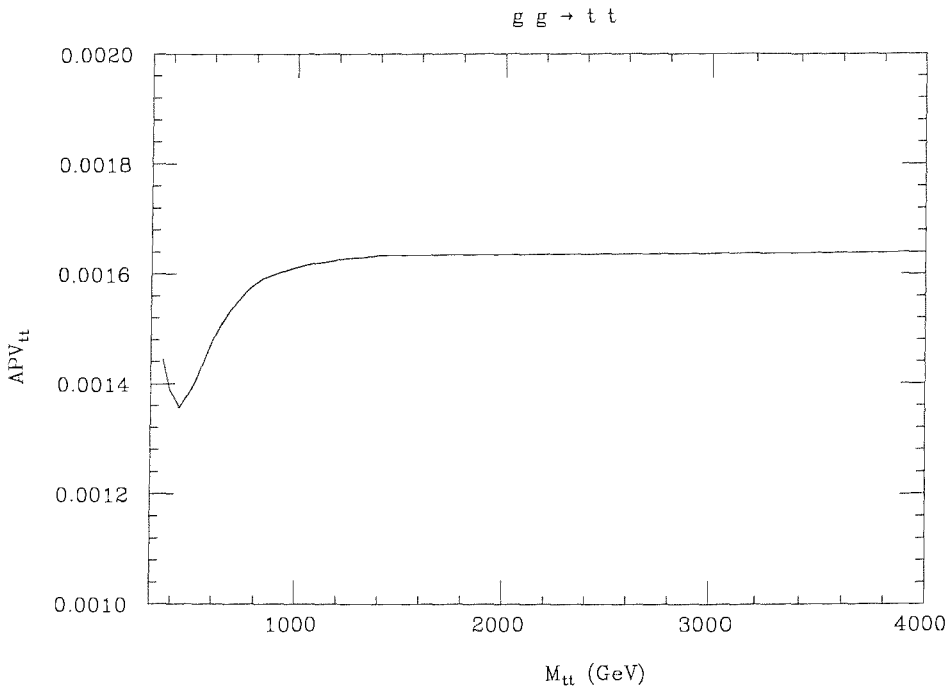

Figure 6.21: Presented here is the $\alpha_S^2\alpha_W$ calculation of A_L plotted against the invariant mass of the top pair. Note that there is no contribution to this asymmetry due to α_S^2 as it is a parity violating observable.

We may only plot the absolute values of the two parity violating observables (fig(6.20) and fig(6.21)) as there is no contribution from tree level QCD. These absolute values are not insignificant (especially that for A_L which remains somewhat above 0.5% over the entire p_T range) however it is difficult to make a determination as to their detectability without a proper treatment of the top quark decay.

Chapter 7

Conclusions.

7.1 $b\bar{b}$ Production

We studied the bottom anti-bottom production rate at both Tevatron and LHC. The correction to the total inclusive cross-sections at Tevatron were found to be very small (fractions of one percent) and undetectable. The correction to the inclusive cross-section at LHC was also found to be quite small (approximately -2% at high p_T) and currently swamped by QCD uncertainties, however following NNLO QCD calculations this level of accuracy may be required.

Also studied was the one loop weak contribution to the forward backward asymmetry at Tevatron, the contribution was found to be a not insignificant fraction of the one loop QCD correction.

7.2 pp To Two Jets

Following $b\bar{b}$ the full proton-(anti)proton to two jet cross section was calculated, again for Tevatron and LHC. This calculation yielded somewhat larger NLO weak corrections than in the $b\bar{b}$ rate at the inclusive level - as much as a -3% correction at Tevatron and

a -30% correction at LHC. The weak corrections at LHC are significantly larger than those at Tevatron (both in the two jet and $b\bar{b}$ cases) due to the former machines partonic centre of mass energy being typically above the threshold where Sudakov logarithmic enhancements become important.

Weak corrections to the polarised observables A_{LL}, A_L and A_{LL}^{PV} were also calculated for the full two jet case. At RHIC the absolute value of the non parity violating observable (A_{LL}) was found to be large and the weak correction to it to be as high as 60% (at $\sqrt{s}$ =600GeV). The absolute values of the parity violating observables (A_L and A_{LL}^{PV}) were found to be smaller but the weak corrections to them to be large (between -20% and -75%) across most of the p_T spectrum.

The same observables were calculated for a hypothetical polarised LHC. Here the absolute value of all the asymmetries was found to be smaller than at RHIC and the NLO weak correction to the parity conserving observable to be reduced (3%). The one loop weak corrections to the parity violating observables on the other hand were found to be very large indeed - -200% to -400% over most of the p_T range.

7.3 $t\bar{t}$ Production

Finally we performed the calculation for $t\bar{t}$ production. At the inclusive level $gg \rightarrow t\bar{t}$ corrections were found to be small but some of the differential cross sections ($\frac{d\sigma}{dp_T}$ for example) were found to generate measurable corrections in the region of -5 to -10%. $q\bar{q} \rightarrow t\bar{t}$ contributions were also calculated as a check of [38] and [39] with reasonable agreement in the case of the Tevatron. We also calculated some observables dependent on the helicity of the top pair (A_{LL}, A_L and A_{LL}^{PV}) where we make the assumption that we can measure the helicity of a produced top quark directly. In reality this is not the case and we actually need to look at the observables defined in [34]. This work has yet

to be carried out.

Appendix A

Veltman & Passarino Functions

The Veltman & Passarino functions [24] for the box diagram with two massless bosons (gluons) exchanged. For D_0, the scalar box integral, we have:

$$D_0 = \frac{1}{st}\left[\frac{4}{\epsilon^2} - \frac{2}{\epsilon} ln\left(\frac{|st|}{\mu^4}\right) + ln^2\left(\frac{|s|}{\mu^2}\right) + ln^2\left(\frac{|t|}{\mu^2}\right) - ln^2\left(\frac{|s|}{|t|}\right) - \pi^2\Theta(s) - \pi^2\Theta(t)\right] \quad \text{(A.1)}$$

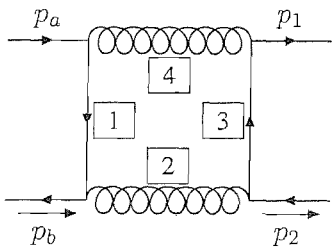

Figure A.1: The box diagram corresponding to D_0.

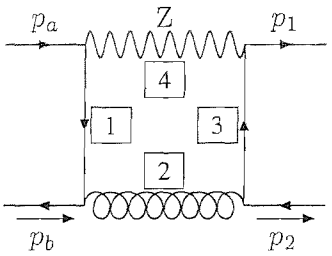

Figure A.2: The box diagram corresponding to D_0 for the case with one massive internal propagator.

$C_{0(i)}$ corresponds to the scalar triangle integral created by 'pinching off' propagator i in fig(A.1).

$$C_{0(3)} = \frac{1}{s}\left[\frac{1}{\epsilon^2} - \frac{1}{\epsilon} ln\left(\frac{|s|}{\mu^2}\right) + \frac{1}{2} ln^2\left(\frac{|s|}{\mu^2}\right) - \pi^2\Theta(s)\right] \tag{A.2}$$

$$C_{0(4)} = \frac{1}{t}\left[\frac{1}{\epsilon^2} - \frac{1}{\epsilon} ln\left(\frac{|t|}{\mu^2}\right) + \frac{1}{2} ln^2\left(\frac{|t|}{\mu^2}\right) - \pi^2\Theta(t)\right] \tag{A.3}$$

If we take care to shift the loop momentum then we also have $C_{0(1)} = C_{0(3)}$ and $C_{0(2)} = C_{0(4)}$. For the vector boxes we have:

$$C_{12(3)} = -\frac{1}{s}\left[-\frac{1}{\epsilon} - 2 + ln\left(\frac{|s|}{\mu^2}\right)\right] \tag{A.4}$$

$$C_{11(3)} = 2 \times C_{12(3)} \tag{A.5}$$

$$C_{12(4)} = -\frac{1}{t}\left[-\frac{1}{\epsilon} - 2 + ln\left(\frac{|t|}{\mu^2}\right)\right] \tag{A.6}$$

$$C_{11(4)} = 2 \times C_{12(4)} \tag{A.7}$$

The Veltman & Passarino functions for the box diagram with one gluon and one Z-boson exchanged. For D_0, the scalar box integral, we have:

$$D_0 =$$
$$\frac{1}{s(t-m_z^2)}\left[\frac{1}{\epsilon^2}-\frac{1}{\epsilon}ln\left(\frac{|s|}{\mu^2}\right)+2ln\left(\frac{m_z^2-t}{m_z^2}\right)\right.$$
$$+\frac{1}{2}ln^2\left(\frac{s}{\mu^2}\right)-\pi^2\Theta(s)+2ln\left(\frac{|s|}{\mu^2}\right)ln\left(\frac{|m_z^2-t|}{\mu^2}\right)-\pi^2\Theta(s)\Theta(t-m_z^2)$$
$$\left.-\frac{\pi^2}{6}-4Li_2\left(\frac{t}{t-m_z^2}\right)+Li_2\left(1+\frac{s}{m_z^2}\right)\right] \tag{A.8}$$

Again $C_{0(i)}$ corresponds to the scalar triangle integral created by 'pinching off' propagator i in fig(A.2).

$$C_{0(1)} =$$
$$\frac{1}{s}\left[\frac{1}{\epsilon^2}-\frac{1}{\epsilon}ln\left(\frac{|s|}{\mu^2}+\frac{1}{2}ln^2\left(\frac{|s|}{\mu^2}\right)\right)-\pi^2\Theta(S)\right] \tag{A.9}$$

$$C_{0(2)} =$$
$$\frac{1}{t}\left[-\frac{1}{\epsilon}ln\left(\frac{|m_z^2-t|}{m_z^2}\right)+\frac{1}{2}ln^2\left(\frac{|m_z^2-t|}{\mu^2}\right)\right.$$
$$\left.-\pi^2\Theta(t-m_z^2)-ln^2\left(\frac{m_z^2}{\mu^2}\right)-Li_2\left(\frac{t}{t-m_z^2}\right)\right] \tag{A.10}$$

$$C_{0(3)}=\frac{1}{s}\left[\frac{\pi^2}{6}-Li_2\left(1+\frac{s}{m_z^2}\right)\right] \tag{A.11}$$

$$C_{11(2)}=\frac{t-m_z^2}{t^2}ln\left(\frac{|m_z^2-t|}{m_z^2}\right)-\frac{1}{t}-C_{0(2)} \tag{A.12}$$

$$C_{12(2)} =$$
$$\frac{1}{t}\left[-\frac{1}{\epsilon}+ln\left(\frac{m_z^2}{\mu^2}\right)+\frac{2(t-m_z^2)}{t}ln\left(\frac{|m_z^2-t|}{m_z^2}\right)-3-(t-m_z^2)C_{0(2)}\right] \tag{A.13}$$

$$C_{11(3)} =$$
$$\frac{1}{s}\left[-2ln\left(\frac{|s|}{m_z^2}\right)-2+\frac{2m_z^2}{s}\frac{\pi^2}{6}-\frac{2m_z^2}{s}Li_2\left(1+\frac{s}{m_z^2}\right)\right] \tag{A.14}$$

$$C_{12(3)}=\frac{1}{2}C_{11(3)} \tag{A.15}$$

Appendix B

Prototype Diagrams For Massless Quark Interactions

The prototype diagrams required for the $q\bar{q} \rightarrow q\bar{q}$ are:

The s-channel tree level gluon exchange:

$$T_{s,g}(s,t,\lambda_1,\lambda_b) = g_S^2 \frac{1}{s}(s+2t-s\lambda_1\lambda_b) \tag{B.1}$$

The s-channel tree level Z exchange:

$$T_{s,Z}(s,t,\lambda_1,\lambda_b) = \frac{g^2}{4\cos^2(\theta_W)}(c_V^1+\lambda_1 c_A^1)(c_V^b-\lambda_b c_A^b)\frac{1}{s-m_Z^2+i\Gamma_Z m_Z}(s+2t-s\lambda_1\lambda_b) \tag{B.2}$$

The s-channel tree level W exchange:

$$T_{s,W}(s,t,\lambda_1,\lambda_b) = \frac{g^2}{8}(1+\lambda_1)(1-\lambda_b)\frac{1}{s-m_W^2+i\Gamma_W m_W}(s+2t-s\lambda_1\lambda_b) \tag{B.3}$$

A box diagram amplitude with two gluons exchanged in the s-channel:

$$
\begin{aligned}
&B_{s,gg}(s,t,\lambda_1,\lambda_b) = \\
&g_S^4 \frac{1}{16\pi^2} \times \frac{1}{s}(s+2t-\lambda_1\lambda_b) \times \left[\frac{-4}{\epsilon^2} + \frac{4}{\epsilon} ln\left(\frac{|t|}{\mu^2}\right)\right] \\
&+g_S^4 \frac{1}{16\pi^2} \times \left[\pi^2 \lambda_1\lambda_b \frac{s}{u} + \pi^2\left(4\frac{t}{s} - \frac{s}{u}\right) + 2\lambda_1\lambda_b ln\left(\frac{s}{t}\right)\right. \\
&+\left(2+\frac{s}{u}\right)\lambda_1\lambda_b ln^2\left(\frac{s}{t}\right) + \left(-2-\frac{s}{u}\right) ln^2\left(\frac{s}{t}\right) \\
&-4\lambda_1\lambda_b ln\left(\frac{s}{t}\right) ln\left(\frac{-s}{\mu^2}\right) + \left(4+8\frac{t}{s}\right) ln\left(\frac{s}{t}\right) ln\left(\frac{-s}{\mu^2}\right) \\
&\left.-2ln\left(\frac{s}{t}\right) + 2\lambda_1\lambda_b ln^2\left(\frac{-s}{\mu^2}\right) + \left(-2-4\frac{t}{s}\right) ln^2\left(\frac{-s}{\mu^2}\right)\right]
\end{aligned}
\tag{B.4}
$$

A box diagram amplitude with one gluon and one Z or W boson exchanged in the s-channel:

$$B_{s,gZ/gW}(s,t,\lambda_1,\lambda_b) =$$

$$C_{Z/W} \times$$

$$\left\{ \frac{1}{16\pi^2} \left[-\frac{2}{\epsilon^2} + \frac{2}{\epsilon} ln\left(\frac{|t|}{\mu^2}\right) + \frac{4}{\epsilon}\frac{m_{Z/W}^2}{s} ln\left(\left|1-\frac{s}{m_{Z/W}^2}\right|\right)\right]\right.$$

$$\frac{1}{(s-m_{Z/W}^2+i\Gamma_{Z/W}m_{Z/W})}(s+2t-\lambda_1\lambda_b)$$

$$+\frac{1}{32\pi^2}\frac{1}{(s-m_{Z/W}^2+i\Gamma_{Z/W}m_{Z/W})}\left[ln\left(1-\frac{s}{m_{Z/W}^2}\right)\lambda_1\lambda_b\left(-8m_{Z/W}^2+4\frac{m_{Z/W}^2}{s}+4s\right)\right.$$

$$+ln\left(1-\frac{s}{m_{Z/W}^2}\right)\left(8m_{Z/W}^2-4\frac{m_{Z/W}^2}{s}-4s\right)+8m_{Z/W}^2 ln^2\left(1-\frac{s}{m_{Z/W}^2}\right)\lambda_1\lambda_b$$

$$+ln^2\left(1-\frac{s}{m_{Z/W}^2}\right)\left(-16m_{Z/W}^2\frac{t}{s}-8m_{Z/W}^2\right)+ln\left(\frac{-t}{m_{Z/W}^2}\right)\lambda_1\lambda_b(4m_{Z/W}^2-4s)$$

$$+ln\left(\frac{-t}{m_{Z/W}^2}\right)(-4m_{Z/W}^2+4s)$$

$$+ln\left(\frac{-t}{m_{Z/W}^2}\right)ln\left(1-\frac{s}{m_{Z/W}^2}\right)\lambda_1\lambda_b\left(8m_{Z/W}^2\frac{s}{u}+8m_{Z/W}^2-4\frac{m_{Z/W}^4}{u}-4\frac{s^2}{u}\right)$$

$$+ln\left(\frac{-t}{m_{Z/W}^2}\right)ln\left(1-\frac{s}{m_{Z/W}^2}\right)\left(-8m_{Z/W}^2\frac{s}{u}-8m_{Z/W}^2+4\frac{m_{Z/W}^4}{u}+4\frac{s^2}{u}-16t\right)$$

$$+ln\left(\frac{-t}{m_{Z/W}^2}\right)ln\left(1+\frac{t}{m_{Z/W}^2}\right)\lambda_1\lambda_b\left(-8m_{Z/W}^2\frac{s}{u}-8m_{Z/W}^2+4\frac{m_{Z/W}^4}{u}+4s+4\frac{s^2}{u}\right)$$

$$+ln\left(\frac{-t}{m_{Z/W}^2}\right)ln\left(1+\frac{t}{m_{Z/W}^2}\right)\left(8m_{Z/W}^2\frac{s}{u}+8m_{Z/W}^2-4\frac{m_{Z/W}^4}{u}-4s-4\frac{s^2}{u}+8t\right)$$

$$+ln^2\left(\frac{-t}{m_{Z/W}^2}\right)2s\lambda_1\lambda_b+(-2s-4t)ln^2\left(\frac{-t}{m_{Z/W}^2}\right)$$

$$+ln\left(\frac{-t}{m_{Z/W}^2}\right)ln\left(\frac{m_{Z/W}^2}{\mu^2}\right)4s\lambda_1\lambda_b+ln\left(\frac{-t}{m_{Z/W}^2}\right)ln\left(\frac{m_{Z/W}^2}{\mu^2}\right)(-4s-8t)$$

$$+ln\left(\frac{m_{Z/W}^2}{\mu^2}\right)ln\left(1-\frac{s}{m_{Z/W}^2}\right)\lambda_1\lambda_b(8m_{Z/W}^2)$$

$$\left.+ln\left(\frac{m_{Z/W}^2}{\mu^2}\right)ln\left(1-\frac{s}{m_{Z/W}^2}\right)\left(-16\frac{m_{Z/W}^2 t}{s}-8m_{Z/W}^2\right)+ln^2\left(\frac{m_{Z/W}^2}{\mu^2}\right)2s\lambda_1\lambda_b\right.$$

$$
\begin{aligned}
&+ln^2\left(\frac{m_{Z/W}^2}{\mu^2}\right)(-2s-4t)\\
&+Li_2\left(\frac{s}{m_{Z/W}^2}\right)\lambda_1\lambda_b\left(8m_{Z/W}^2\frac{s}{u}+16m_{Z/W}^2-4\frac{m_{Z/W}^4}{u}-4\frac{s^2}{u}\right)\\
&+Li_2\left(\frac{s}{m_{Z/W}^2}\right)\left(-16m_{Z/W}^2\frac{t}{s}-8m_{Z/W}^2\frac{s}{u}-16m_{Z/W}^2+4\frac{m_{Z/W}^4}{u}+4\frac{s^2}{u}-16t\right)\\
&+Li_2\left(\frac{-t}{m_{Z/W}^2}\right)\lambda_1\lambda_b\left(-8m_{Z/W}^2\frac{s}{u}-8m_{Z/W}^2+4\frac{m_{Z/W}^4}{u}+4s+4\frac{s^2}{u}\right)\\
&+Li_2\left(\frac{-t}{m_{Z/W}^2}\right)\left(8m_{Z/W}^2\frac{s}{u}+8m_{Z/W}^2-4\frac{m_{Z/W}^4}{u}-4s+8t-4\frac{s^2}{u}\right)\Bigg]\Bigg\}
\end{aligned}
\tag{B.5}
$$

Where:

$$
\begin{aligned}
C_Z &= g_S^2\frac{g^2}{4cos^2(\theta_W)}(c_V^1+\lambda_1 c_A^1)(c_V^b-\lambda_b c_A^b)\\
C_W &= g_S^2\frac{g^2}{8}(1+\lambda_1)(1-\lambda_b)
\end{aligned}
\tag{B.6}
$$

A gluon QED type vertex correction to s-channel gluon exchange:

$$
\begin{aligned}
&V_{s,gvge}^{qed}(s,t,\lambda_1,\lambda_b)=\\
&g_S^4\frac{1}{16\pi^2}\left[-\frac{2}{\epsilon^2}-\frac{3}{\epsilon}+\frac{2}{\epsilon}ln\left(\frac{s}{\mu^2}\right)\right]\frac{1}{s}(s+2t-\lambda_1\lambda_b)\\
&+g_S^4\frac{1}{16\pi^2}\Bigg[ln^2\left(\frac{-s}{\mu^2}\right)\left(-1-2\frac{t}{s}+\lambda_1\lambda_b\right)\\
&ln\left(\frac{-s}{\mu^2}\right)\left(3+6\frac{t}{s}-3\lambda_1\lambda_b\right)-7-14\frac{t}{s}+7\lambda_1\lambda_b\Bigg]
\end{aligned}
\tag{B.7}
$$

A gluon vertex correction to s-channel Z or W boson exchange:

$$
\begin{aligned}
&V_{s,gvZ/We}^{qed}(s,t,\lambda_1,\lambda_b)=\\
&C_{Z/W}\times\\
&\frac{1}{16\pi^2}\left[-\frac{2}{\epsilon^2}-\frac{3}{\epsilon}+\frac{2}{\epsilon}ln\left(\frac{s}{\mu^2}\right)\right]\frac{1}{s-m_{Z/W}^2+i\Gamma_{z/W}m_{Z/W}}(s+2t-\lambda_1\lambda_b)\\
&+\frac{1}{16\pi^2}\Bigg[ln^2\left(\frac{-s}{\mu^2}\right)\left(-1-2\frac{t}{s}+\lambda_1\lambda_b\right)\\
&ln\left(\frac{-s}{\mu^2}\right)\left(3+6\frac{t}{s}-3\lambda_1\lambda_b\right)-7-14\frac{t}{s}+7\lambda_1\lambda_b\Bigg]\frac{s}{s-m_{Z/W}^2+i\Gamma_{Z/W}m_{Z/W}}
\end{aligned}
\tag{B.8}
$$

Where C_Z and C_W are as defined above.

A gluon QCD type vertex correction to s-channel gluon exchange:

$$
\begin{aligned}
&V^{qcd}_{s,gvge}(s,t,\lambda_1,\lambda_b) = \\
&g_S^2\frac{1}{16\pi^2}\left[-\frac{1}{\epsilon}\right]\frac{1}{s}(s+2t-\lambda_1\lambda_b) \\
&+g_S^2\frac{1}{16\pi^2}\left[\ln\left(\frac{-s}{\mu^2}\right)\left(-1-2\frac{t}{s}+\lambda_1\lambda_b\right)+1+2\frac{t}{s}-\lambda_1\lambda_b\right]
\end{aligned}
\tag{B.9}
$$

The fermion self energy correction to s-channel gluon exchange:

$$
\begin{aligned}
&SE^{int}_{s,ferm}(s,t,\lambda_1,\lambda_b) = \\
&g_S^4\frac{1}{16\pi^2}\times N \\
&\left[\frac{4}{3}ln\left(\frac{-s}{\mu^2}\right)(1-\lambda_1\lambda_b)+\frac{8}{3}ln\left(\frac{-s}{\mu^2}\right)\frac{t}{s}\right]
\end{aligned}
\tag{B.10}
$$

Where N is the number of active flavours for the internal quarks - a flavour is 'active' if $\sqrt{s}>$ two times the mass of the quark flavour. Note that since the internal particles need not be real the contribution is only suppressed beneath threshold rather than ruled out entirely - however setting the contribution to zero below threshold is a good approximation.

The gluon self energy correction to to s-channel gluon exchange:

$$
\begin{aligned}
&SE^{int}_{s,g}(s,t,\lambda_1,\lambda_b) = \\
&g_s^4\frac{1}{16\pi^2}\times \\
&\left[-\frac{5}{3}ln\left(\frac{-s}{\mu^2}\right)(1-\lambda_1\lambda_b)-\frac{10}{3}ln\left(\frac{-s}{\mu^2}\right)\frac{t}{s}\right]
\end{aligned}
\tag{B.11}
$$

The Z or W vertex correction to s-channel gluon exchange:

$$
\begin{aligned}
&V^{qed}_{s,Z/Wvge}(s,t,\lambda_1,\lambda_b) = \\
&D_{Z/W}\times\frac{1}{16\pi^2}\times \\
&(2B_0+sC_{11}+sC_{12}+4C_{24})-(C_{12}-C_{11})s
\end{aligned}
\tag{B.12}
$$

Where, when the vertex is attached to the out going quarks we have:

$$D_Z = g_S^2 \frac{g^2}{4cos^2(\theta_W)}(c_V^1 + c_A^1 \lambda_1)^2$$
$$D_W = g_S^2 \frac{g^2}{8}(1+\lambda_1)^2 \tag{B.13}$$

And when the vertex is attached to the incoming quarks we have:

$$D_Z = g_S^2 \frac{g^2}{4cos^2(\theta_W)}(c_V^b + c_A^b \lambda_b)^2$$
$$D_W = g_S^2 \frac{g^2}{8}(1+\lambda_b)^2 \tag{B.14}$$

The $\phi_{+/-}$ vertex correction to s-channel gluon exchange:

$$V_{s,\phi vge}^{qed}(s,t,\lambda_1,\lambda_b) =$$
$$g_S^2 \frac{g^2}{8}(1+\lambda_1)^2 \times \frac{1}{16\pi^2} \times$$
$$\frac{m_t^2}{2m_W^2}(-2B_0 - sC_{11} - sC_{12} + 4C_{24}) - \frac{m_t^2}{2M_W^2}(C_{12} - C_{11})s \tag{B.15}$$

This expression is for the case where the vertex is attached to the final state quarks which is in fact the only contribution. The ϕ vertex will only contribute if the external quarks associated with it are bottoms - in which case the internal quark will be a top making the ϕ coupling significant.

Z and W external leg self energy corrections to s-channel gluon exchange.

$$SE_{s,Z/W}^{ext}(s,t,\lambda_1,\lambda_b) =$$
$$E_{Z/W} \times \frac{1}{32\pi^2} \times$$
$$(4B_1 + 2)\frac{1}{s}(s + 2t - \lambda_1\lambda_b) \tag{B.16}$$

Where:

$$E_Z = g_S^2 \frac{g^2}{4cos^2(\theta_W)} 2((c_V^1 + c_A^1\lambda_1)^2 + (c_V^b + c_A^b\lambda_b)^2)$$
$$E_W = g_S^2 \frac{g^2}{8} 2((1+\lambda_1)^2 + (1+\lambda_b)^2) \tag{B.17}$$

The $\phi_{+/-}$ self energy correction to s-channel gluon exchange.

$$SE^{ext}_{s,\phi}(s,t,\lambda_1,\lambda_b) =$$
$$E_\phi \times \frac{1}{32\pi^2} \times$$
$$-2\frac{m_t^2}{m_Z^2} B_1 \frac{1}{s}(s+2t-\lambda_1\lambda_b) \tag{B.18}$$

Where:

$$E_\phi = g_S^2 \frac{g^2}{8} 2((1+\lambda_1)^2 + (1+\lambda_b)^2) \tag{B.19}$$

The ϕ self energy only contributes if the quark it is attached to is a bottom - in this case the internal quark in the loop is a top meaning that the ϕ coupling is not negligible.

For a given s-channel amplitude $A_s(s,t,\lambda_1,\lambda_b)$ the crossing relation to the t and u channels are:

$$A_t = A_s(t,s,\lambda_1,\lambda_2)$$
$$A_u = A_s(u,t,\lambda_1,-\lambda_2) \tag{B.20}$$

For a given s-channel box amplitude $B_s(s,t,\lambda_1,\lambda_b)$ the crossed box amplitude in the s,t and u channels are given by:

$$B_{s,X} = B_s(s,u,\lambda_1,-\lambda_b)$$
$$B_{t,X} = B_s(t,u,\lambda_1,-\lambda_2)$$
$$B_{u,X} = B_s(u,t,\lambda_1,-\lambda_2) \tag{B.21}$$

Bibliography

[1] R.K. Ellis et al., SLAC-REPRINT-2001-056, FERMILAB-PUB-01-197 (2001) (Chapter 9 and all references therin)

[2] S. Frixione and M.L. Mangano, Nucl. Phys. B **483** 321 (1997)

[3] P. Nason, G. Ridolfi, O. Schneider, G.F. Tartarelli and P. Vikas (conveners), in proceedings of the workshop on 'Standard Model Physics (and more) at the LHC', Geneva 1999 (Pg. 231-304 and references therein)

[4] T. Affolder et al.[CDF collaboration], Phys. Rev. **D64** (2001) 032001 [Erratum-ibid. **D65** (2002) 039903]

[5] For example: D. Stump, J. Huston, J. Pumplin, W.K. Tung, H.L. Lai, S. Kuhlmann and J.F. Owens, JHEP **0310** (2003) 046

[6] A. Bodek and U. Baur, Eur. Phys. J. bf C21, 607 (2001)

[7] S. Catani and M.H. Seymour, Nucl. Phys. B **485** 291 (1997) [Erratum-ibid. **B510** 503 (1997)]

[8] S. Dittmaier, Nucl. Phys. B **565** 69 (2000)

[9] E.W.N. Glover, Nucl. Phys. Proc. Suppl. **116** 3 (2003) (and references therein)

[10] C. Bourrely, J.P. Guillet, J. Soffer, Nucl. Phys. **B361** 72 (1991)

[11] J.M. Virey, P. Taxil, Nucl. Phys. Proc. Suppl. **105** 150 (2002)

[12] S.D. Bass, A. De Roeck, Nucl. Phys. Proc. Suppl. **105** 1 (2002)

[13] M. Dittmar, A. Nicollerat, A. Djouadi, Phys. Lett. **B583** 111 (2004)

[14] J.H. Kühn, G. Rodrigo, Phys. Rev. **D59** 054017 (1999)

[15] M. Melles, Phys. Rept. **375** 219 (2003)

[16] A. Denner, arXiv:hep-ph/0110155

[17] M. Ciafaloni, P. Ciafaloni, D. Comelli, Phys. Rev. Lett. **84** 4810 (2000), Nucl. Phys. **B589** 359 (2000)

[18] For example: Y.L. Dokshitzer, V.A. Khoze, A.H. Mueller, S.I. Troian, Gif-sur-Yvette, France: Ed. Frontieres (1991)

[19] G. Bunce, N. Saito, J. Soffer, W. Vogelsang, Ann. Rev. Nucl. Part. Sci. **50** 525 (2000)

[20] J. Pumplin, D.R. Stump, J. Huston, H.L. Lai, P. Nadolsky, W.K. Tung, JHEP **0207** 012 (2002)

[21] T. Gehrmann, W.J. Stirling, Phys. Rev. **D53** 6100 (1996)

[22] M. Gluck, E. Reya, M. Stratmann, W. Vogelsang, Phys. Rev. **D63** 095005 (2001)

[23] J.A.M. Vermaseren, preprint NIKHEF-00-032 [math-ph/0010025]

[24] G. Passarino, M. Veltman, Nucl. Phys. **B160** 151 (1979)

[25] E. Maina, S. Moretti, M.R. Nolten, D.A. Ross, Phys. Lett. **B570** 205 (2003)

[26] P. Nason, S. Dawson, R.K. Ellis, Nucl. Phys. **B303** 607 (1998) & Nucl. Phys. **B327** 49 (1989), W. Beenakker, H. Kuijf, W.L. van Neerven, J, Smith, Phys. Rev. D 40 54 (1989), W. Beenakker, W.L. van Neerven, R. Meng, G.A. Schuler, J. Smith, Nucl. Phys. **B351** 507 (1991), M.L. Mangano, P. Nason, G. Ridolfi, Nucl. Phys. **B373** 295 (1992)

[27] G.Peter Lepage, CLNS-80/447, (1980)

[28] S. Moretti, M.R. Nolten, D.A. Ross, arXiv:hep-ph/0503152

[29] http://www-cdf.fnal.gov/physics/new/inclusive

[30] R.K. Ellis, J.C. Sexton, Nucl. Phys. **B269** 445 (1986)

[31] S.D. Ellis, Z. Kunszt, Davison E. Soper, Phys. Rev. Lett. **64** 2121 (1990)

[32] W.T. Giele, E.W.N. Glover, David A. Kosower, Phys. Rev. Lett. **73** 2019 (1994)

[33] S. Moretti, M.R. Nolten, D.A. Ross, arXiv:hep-ph/0509254

[34] W. Bernreuther, A. Brandenburg, Z.G. Si, P. Uwer, arXiv:hep-ph/0410197, Nucl. Phys. **B690** 81 (2004), Acta Phys. Polon. **B34** 4477 (2003) arXiv:hep-ph/0209202, Int. J. Mod. Phys. **A18** 1357 (2003), Phys. Rev. Lett. **87** 242002 (2001), Phys. Lett. **B509** 53 (2001), P. Uwer, Phys. Lett. B **609** 271 (2005), A. Brandenburg, Z.G. Si, P. Uwer, Phys. Lett. B **539** 235 (2002), W. Bernreuther, A. Brandenburg, P. Uwer, Phys. Lett. B **368** 153 (1996)

[35] M. Beccaria, S. Bentvelsen, M. Cobal, F.M. Renard, C. Verzegnassi, Phys. Rev. **D71** 073003 (2005)

[36] M. Beccaria, F.M. Renard, C. Verzegnassi, Phys. Rev. **D72** 093001 (2005)

[37] *Weak Corrections To Gluon-induced top-antitop Hadro-production*, S. Moretti, M.R. Nolten, D.A. Ross, No hep-ph number at time of writing.

[38] J.H. Kühn, A. Scharf P.Uwer, Eur. Phys. J. **C45** 139 (2006)

[39] W. Bernreuther, M. Fucker, Z.G. Si, arXix:hep-ph/0509210